Hormonal Regulation and Transcriptional Targets of *RORA*, a Novel Candidate Gene for Autism Spectrum Disorder

by Tewarit Sarachana

B.S. in Medical Technology, May 2005, Chulalongkorn University
M.S. in Genomics and Bioinformatics, January 2009, The George Washington University

A Dissertation submitted to

The Faculty of
Columbian College of Arts and Sciences
of The George Washington University
in partial fulfillment of the requirements
for the degree of Doctor of Philosophy

August 31, 2012

Dissertation directed by

Valerie W. Hu
Professor of Biochemistry and Molecular Biology

The Columbian College of Arts and Sciences of The George Washington University certifies that Tewarit Sarachana has passed the Final Examination for the degree of Doctor of Philosophy as of August 13, 2012. This is the final and approved form of the dissertation.

Hormonal Regulation and Transcriptional Targets of *RORA*, a Novel Candidate Gene for Autism Spectrum Disorder

Tewarit Sarachana

Dissertation Research Committee:

Valerie W. Hu, Professor of Biochemistry and Molecular Biology, Dissertation Director

Anthony S. LaMantia, Professor of Pharmacology and Physiology, Committee Member

Sidney W. Fu, Research Professor of Medicine, Committee Member

© Copyright 2012 by Tewarit Sarachana
All rights reserved

Dedication

Growing up in a poor family with a single mother who had to sell a variety of foods on the street and tailor clothes for little money to look after her three children all by herself made graduate education seem like an impossible dream for me. Undeniably, I would not have come this far without continuous help, support, and encouragement from many people in my life. I wish to dedicate this Ph.D. dissertation with my highest appreciation to these people who made this seemingly impossible dream come true for me.

I gratefully dedicate this dissertation first and foremost to His Majesty King Bhumibol Adulyadej of Thailand who granted me a Bhumibol scholarship every year when I was an undergraduate student. That prestigious royal scholarship not only helped defray part of tuition fees that my family could not afford, but also encouraged me to hold on to education through tough times in my life. I also appreciatively dedicate this dissertation to all Thai citizens who pay taxes, part of which are allocated for scholarships to support education of students from low-income families across the country, including me.

Moreover, without selfless support, encouragement, and kind words from people around me, I could have given up this dream, and for this reason, I wish to dedicate this Ph.D. dissertation to the most wonderful group of people in my life: my mother, Maleerat Kijjareonseree, who is always willing to sacrifice her happiness for me, my two elder sisters, Kusuma Sarachana and Hamemaporn Sarachana, who sacrificed their dream of higher education so that I could pursue mine, my best friends, Depicha Jindatip and Pornpun Supavonwong, as well as friends at the Thai Chef Sushi Bar restaurant, who provide emotional support through my graduate education. Lastly, this dissertation is

thankfully dedicated to Natthapon Premjit, my life partner of thirteen years who insists to stay beside and support me through all the ups and downs of my life.

Acknowledgments

I, the author, appreciatively acknowledge first and foremost Dr. Valerie W. Hu, my dissertation research mentor, for her guidance, wonderful support, encouragement, and patience, through this project. It is also with the utmost gratitude to acknowledge the Research Advisory and Examination Committee (Dr. Anthony S. LaMantia, Dr. Norman H. Lee, Dr. Sidney W. Fu, and Dr. Ray C. Wu) for their helpful advice to improve the experimental designs and the interpretation of the research outcomes. I also wish to thank the families of the brain donors for their invaluable gift to autism research and the Autism Tissue Program (San Diego, CA) for making tissue arrays and frozen human brain tissues available for this work, through the laboratory of Dr. Janine LaSalle (University of California, Davis) and the Harvard Brain Tissue Resource Center (Harvard University), to whom I am also grateful. I gratefully acknowledge Dr. Anastas Popratiloff (Director, Center for Microscopy and Image Analysis, The George Washington University School of Medicine and Health Sciences) for providing training on the confocal fluorescence microscope and helpful advice on image analysis. The assistance of Minyi Xu with time-course and dose-response studies, the assistance of Biruk Bekele (a summer high school intern) with image analysis, the assistance of Brendan Belovarac with AR/ERα siRNA transfection, and the assistance of Jing Jing and Yi Hong with RNA isolation from human brain tissues are also thankfully acknowledged. Last, but not least, I wish to thank the Institute for Biomedical Sciences (IBS), The George Washington University, for giving me a wonderful opportunity to study in this excellent Ph.D. program, as well as the Office of the Commission on Higher Education of the Royal Thai Government, Thailand, for

providing a Higher Educational Strategic Scholarship for Frontier Research Network to do master's and Ph.D. studies in the United States.

Abstract of Dissertation

Hormonal Regulation and Transcriptional Targets of *RORA*,
a Novel Candidate Gene for Autism Spectrum Disorder

Autism spectrum disorder (ASD or autism) is a pervasive neurodevelopmental disorder characterized by deficits in social understanding and interactions, aberrant language development and/or usage, and stereotyped, repetitive behaviors. Autism is inexplicably biased towards males by a ratio of at least 4:1, with no clear understanding of whether or how sex hormones may play a role in autism susceptibility. Here, we show that dihydrotestosterone (DHT) and 17β-estradiol oppositely regulate expression of a novel autism candidate gene, the retinoic acid-related orphan receptor alpha (*RORA*), in the human neuronal cell line SH-SY5Y. DHT acts through androgen receptor (AR) which may interact with the corepressor protein SUMO-1 to suppress *RORA* expression, whereas estradiol enhances *RORA* expression through estrogen receptor alpha (ERα) which interacts with the coactivator protein NCOA5. Moreover, we extensively identify transcriptional targets of RORA in human neuronal cells using whole-genome promoter array analysis. Several potential transcriptional targets of RORA are then selected for experimental validation by independent chromatin immunoprecipitation-quantitative polymerase chain reaction (qPCR) expression analyses and shRNA-mediated knockdown analyses. We demonstrate that RORA indeed regulates expression of several genes whose functions have been associated with autism. These validated RORA targets are *A2BP1, CYP19A1, HSD17B10, ITPR1, NLGN1,* and *NTRK2*. Quantitative reverse transcriptase-PCR analysis of brain tissues from individuals with autism, as well as sex- and age-matched unaffected

individuals, reveals that expression of these targets is aberrant in the brain of individuals with autism who exhibit reduced *RORA* expression. Interestingly, the transcript levels of selected targets, especially *CYP19A1*, correlate positively with *RORA* transcript levels in the human brain tissues. Co-immunoprecipitation and sequential chromatin immunoprecipitation analyses performed in neuronal cells show that RORA interacts with NCOA1 and NCOA5 in the human neuronal cell line, and that RORA can form a complex with NCOA5 to modulate *CYP19A1* expression. Using confocal immunofluorescence microscopic analysis of tissue arrays containing postmortem specimens from the frontal cortex of individuals with autism and age-matched controls, we further show that the protein levels of RORA and aromatase, a protein encoded by the gene *CYP19A1* which is the key enzyme converting androgens to estrogens, are significantly reduced in the brain of individuals with autism relative to that of sex- and age-matched controls. Aromatase protein levels also correlate positively with RORA protein levels in the brain tissues, suggesting that aromatase expression may be regulated by RORA in the human brain. Findings from this dissertation indicate that *RORA* has the potential to be under feedback regulation by both androgen and estrogen through one of its transcriptional targets, aromatase, and further suggest a mechanism for introducing sex bias in autism.

Table of Contents

Dedication iv

Acknowledgments vi

Abstract of Dissertation viii

List of Figures xi

List of Tables xiiii

List of Abbreviations xiv

Chapter 1: Introduction 1

Chapter 2: Literature Review 6

Chapter 3: Materials and Methods 47

Chapter 4: Results 62

Chapter 5: Discussion 108

References 126

Appendices 178

List of Figures

Figure 1…….19

Figure 2…….20

Figure 3…….23

Figure 4…….24

Figure 5…….27

Figure 6…….28

Figure 7…….30

Figure 8…….32

Figure 9…….37

Figure 10……...46

Figure 11……...64

Figure 12……...67

Figure 13……...70

Figure 14……...73

Figure 15……...76

Figure 16……...80

Figure 17……...83

Figure 18……...91

Figure 19……...92

Figure 20……...95

Figure 21……...97

Figure 22……...99

Figure 23……103

Figure 24……105

Figure 25……106

Figure 26……111

List of Tables

Table 1…….....13

Table 2……..86

Table 3……..87

Table 4……..88

Table 5……102

Supplemental Table 1..…….……..178

Supplemental Table 2.…….……...179

Supplemental Table 3.…….……...180

Supplemental Table 4…….……182

Supplemental Table 5…….……....183

List of Abbreviations

1.	A2BP1	Ataxin 2 binding protein 1
2.	Acsl4	Acyl-CoA synthetase long-chain family member 4
3.	ADHD	Attention deficit hyperactivity disorder
4.	AF2	Activation function 2
5.	AGRE	Autism Genetic Resource Exchange
6.	Akt2	V-akt murine thymoma viral oncogene homolog 2
7.	AR	Androgen receptor
8.	ARbs	Androgen receptor binding site
9.	AS	Asperger's syndrome
10.	ASD	Autism spectrum disorder
11.	ASTN2	Astrotactin 2
12.	AT	Adenine and thymine
13.	BA9/10	Brodmann area 9 -10
14.	BCA	Bicinchoninic acid assay
15.	BDNF	Brain-derived neurotrophic factor
16.	BMAL1	Brain and muscle ARNT-like 1
17.	Calb1	Calbindin 1, 28kDa
18.	Cals1	Callose synthase 1
19.	CBP	cAMP response element-binding (CREB)-binding protein
20.	Cd36	Trombospondin receptor
21.	ChIP-on-chip	Chromatin immunoprecipitation, followed by microarray

22.	ChIP-PET	Chromatin immunoprecipitation, followed by paired-end tag
23.	ChIP-reChIP	Sequential chromatin immunoprecipitation
24.	ChIP-seq	Chromatin immunoprecipitation, followed by sequencing
25.	CIA	Coactivator independent of AF-2 function
26.	Cidea	Cell death-inducing DFFA-like effector a
27.	Cidec	Cell death-inducing DFFA-like effector c
28.	c-myc	Myelocytomatosis viral oncogene homolog
29.	CNS	Central nervous system
30.	CNTN4	Contactin 4
31.	CNTNAP	Contactin associated protein
32.	CNV	Copy number variation
33.	Co-IP	Co-immunoprecipitation
34.	COX-2	Cyclooxygenase 2
35.	CpG	Cytosine, followed by guanine
36.	CYP19A1	Cytochrome P450, family 19, subfamily A, polypeptide 1
37.	DAPI	4′, 6′-diamidino-2-phynylindole dihydrochloride
38.	DBD	DNA binding domain
39.	DCX	Doublecortin
40.	DHT	Dihydrotestosterone
41.	DMEM	Dulbecco’s modified Eagle’s medium
42.	DSS	Disuccinimidyl suberate
43.	E2	Estradiol
44.	EDTA	Ethylenediaminetetraacetic acid

45.	Elk-1	E twenty-six (ETS)-like transcription factor 1
46.	EQ	Empathy quotient
47.	ERbs	Estrogen receptor binding site
48.	ERα	Estrogen receptor alpha
49.	ERβ	Estrogen receptor beta
50.	F12	Ham's nutrient mixture F-12
51.	FHL2	Four and a half LIM domains protein 2
52.	FISH	Fluorescent in situ hybridization
53.	FMR1	Fragile X mental retardation 1
54.	FOX1	Multicopper ferroxidase (RBFOX1)
55.	FOXP3	Forkhead box P3
56.	FRAX	Fragile X syndrome
57.	GAPDH	Glyceraldehyde 3-phosphate dehydrogenase
58.	GLI	Gliotactin
59.	GR	Glucocorticoid receptor
60.	Grm1	Glutamate receptor, metabotropic 1
61.	GWAS	Genome-wide association study
62.	Hif1a	Hypoxia inducible factor 1, alpha subunit
63.	HRE	Hormone response element
64.	hRORA1	Human retinoic acid receptor-related orphan receptor 1
65.	HRP	Horseradish peroxidase
66.	HSD17B10	Hydroxysteroid (17-beta) dehydrogenase 10
67.	IL-1β	Interleukin-1 beta

68.	IL-6	Interleukin-6
69.	IL-8	Interleukin-8
70.	IPA	Ingenuity Pathway Analysis
71.	IPTG	Isopropyl-β-D-thio-galactoside
72.	IQ	Intelligence quotient
73.	ITPR1	Inositol 1,4,5-trisphosphate receptor, type 1
74.	Ki67	Antigen identified by monoclonal antibody Ki-67
75.	LB	Lysogeny broth
76.	LBD	Ligand binding domain
77.	LCL	Lymphoblastoid cell line
78.	LOD	Logarithm (base 10) of odds
79.	LXRa	Liver X receptor alpha
80.	MAP2	Microtubule-associated protein 2
81.	MCF7	Michigan Cancer Foundation – 7 breast cancer cell line
82.	MeCP2	Methyl-CpG-binding protein 2
83.	MEM	Modified Eagle's medium
84.	Mogat1	Monoacylglycerol O-acyltransferase 1
85.	MyoD	Myogenic differentiation 1
86.	NCOA1	Nuclear receptor coregulator 1
87.	NCOA2	Nuclear receptor coactivator 2
88.	NCOA5	Nuclear receptor coactivator 5
89.	NeuN	Neuronal nuclear antigen A60 (RBFOX3)

90.	NFκB	Nuclear factor of kappa light polypeptide gene enhancer in B-cells
91.	NIX1	Neuronal interacting factor X 1
92.	NLGN1	Neuroligin 1
93.	NRXN1	Neurexin 1
94.	NT3	Neurotransmitter transporter 3
95.	NT4	Neurotransmitter transporter 4
96.	NTRK2	Neurotrophic tyrosine kinase, receptor, type 2
97.	p300	Adenovirus type 5 early region 1A(E1A)-binding protein, 300kDa
98.	Pcp2	Purkinje cell protein 2
99.	Pcp4	Purkinje cell protein 4
100.	PDD-NOS	Pervasive developmental disorder-not otherwise specified
101.	PGC-1α	Peroxisome proliferator-activated receptor gamma coactivator 1 alpha
102.	PLYKELF	Proline – Leucine - Tyrosine - Lysine - Glutamic acid - Leucine - Phenylalanine
103.	PMSF	Phenylmethylsulfonylfluoride
104.	pS2	Phosphate starvation-induced protein 2
105.	Ptch	Patched receptor
106.	PVDF	Polyvinylidene difluoride
107.	qPCR	Quantitative polymerase chain reaction

108.	RAR	Retinoic acid-related
109.	REV-ERB	Nuclear receptor subfamily 1, group D, member 2
110.	RIP140	Receptor interacting protein 140
111.	RORA	Retinoic acid receptor-related orphan receptor alpha
112.	RORAbs	RORA binding site
113.	RORE	Retinoic acid receptor-related orphan receptor binding element
114.	RT	Reverse transcription
115.	RXR	Retinoid X receptor
116.	RZRα	Retinoic acid receptor-related orphan receptor alpha
117.	S.E.M.	Standard error of mean
118.	SHANK3	SH3 and multiple ankyrin repeat domains 3
119.	SHBG	Sex hormone binding globulin
120.	Shh	Sonic hedgehog
121.	shRNA	Short RNA
122.	SH-SY5Y	Human neuroblastoma cell line
123.	siRNA	Silencing RNA
124.	Slc1a6	Solute carrier protein 1, member 6
125.	SNP	Single-nucleotide polymorphism
126.	SQ	Systemizing quotient
127.	SREBP-1c	Sterol regulatory element-binding protein 1c
128.	SUMO-1	SMT3 suppressor of mif two 3 homolog 1
129.	TBST	Tris-Buffered Saline and Tween 20
130.	Th17	T helper 17 cells

131.	TIP30	HIV-1 Tat interactive protein 2, 30kDa
132.	TNFα	Tumour necrosis factor alpha
133.	TSC	Tuberous sclerosis complex
134.	TSC1	Tuberous sclerosis complex 1
135.	TSC2	Tuberous sclerosis complex 2
136.	WT	Wildtype
137.	X-Gal	5-bromo-4-chloro-indolyl-β-D-galactopyranoside

Chapter 1: Introduction

Autism spectrum disorder (ASD or autism) is a neurodevelopmental disorder with a prevalence of ~1:88 that is characterized by deficits in social understanding and interactions, aberrant communication, and repetitive, stereotyped behaviors, often with restricted interests(American Psychiatric Association & American Psychiatric Association. Task Force on DSM-IV, 2000; F. R. Volkmar et al., 1994). Autism is inexplicably biased towards males by a ratio of at least 4:1, prompting theories that fetal or perinatal exposure to elevated levels of male hormones may increase susceptibility towards autism (Baron-Cohen, Knickmeyer, & Belmonte, 2005). Despite some evidence linking elevated fetal testosterone levels in amniotic fluid to autistic symptomatology (Auyeung et al., 2009; Auyeung, Taylor, Hackett, & Baron-Cohen, 2010) and increasing rightward asymmetry of the corpus callosum (Chura et al., 2010) known to be aberrant in autism (Just, Cherkassky, Keller, Kana, & Minshew, 2007), and our own studies which have identified deregulated genes involved in androgen biosynthesis as well as higher testosterone levels in lymphoblastoid cell lines from individuals with autism (V. W. Hu et al., 2009), no sex hormone-sensitive candidate genes for autism have been reported. At present, there is still no clear understanding of the molecular mechanisms through which the sex hormones may play a role in autism susceptibility.

We have recently identified a novel autism candidate gene, retinoic acid-related (RAR) orphan receptor-alpha (RORA) (Nguyen, Rauch, Pfeifer, & Hu, 2010), which is a ligand-dependent nuclear receptor transcription factor. In brief, our studies have demonstrated: a) reduced expression of RORA in lymphoblastoid cell lines (LCL) derived

from individuals with autism (V. W. Hu, Frank, Heine, Lee, & Quackenbush, 2006; V. W. Hu, Sarachana et al., 2009); b) increased methylation and reduced protein of RORA in the LCL (Nguyen et al., 2010); and c) decreased expression of RORA protein in the prefrontal cortex and the cerebellum of individuals with autism (Nguyen et al., 2010). Together, these results link molecular changes in RORA in peripheral cells to molecular pathology in the brain of individuals with autism. These findings are particularly relevant to autism as RORA is involved in several key processes negatively impacted in autism, including Purkinje cell differentiation (Boukhtouche et al., 2006; Hadj-Sahraoui et al., 2001), cerebellar development (Gold, Gent, & Hamilton, 2007; Harding, Atkins, Jaffe, Seo, & Lazar, 1997), protection of neurons against oxidative stress (Boukhtouche, Vodjdani et al., 2006), suppression of inflammation (Delerive et al., 2001), and regulation of circadian rhythm (Sato et al., 2004). Behavioral studies on the RORA-deficient *staggerer* mouse, primarily used as a model to study ataxia and dystonia (Gold et al., 2007), further show that RORA is also associated with restricted behaviors reminiscent of autism, such as perseverative tendencies (Lalonde & Strazielle, 2008), limited maze patrolling (Goodall & Gheusi, 1987), anomalous object exploration (Lalonde, Botez, & Boivin, 1987a), as well as deficits in spatial learning (Lalonde, 1987a). Although there are currently no reported studies on the social behaviors of *staggerer* mice, it is clear that RORA is associated with at least some of the symptomatology and pathology of autism.

RORA is known to bind DNA as a monomer or as a homodimer to hormone response elements (HREs) upstream of several genes to modulate expression of those genes, suggesting that RORA is a hormone-dependent orphan nuclear receptor. Nevertheless, which and how endogenous hormones regulate RORA remain unknown.

Interestingly, loss of neurons in male mice with loss-of-function mutation in the *Rora* gene (called *staggerer* mice) has been found to occur much earlier in life in comparison to female *staggerer* mice (Doulazmi et al., 1999; Janmaat et al., 2011), indicating that males are more susceptible than females to pathological conditions associated with RORA deficiency. This observation suggests that the pathology of RORA deficiency is sex-related, leading us to investigate the role of sex hormones in the regulation of *RORA*.

In *staggerer* mice, Rora deficiency has been reported to cause aberrant expression of several genes involved in Purkinje cell differentiation (e.g., *Shh*), calcium-mediated signaling (e.g., *Itpr1, Calb1, Cals1, Pcp4*), as well as excitatory neurotransmission at glutamatergic synapses of Purkinje cells in the cerebellum (e.g., *Slc1a6, Grm1, Pcp2*) (Gold et al., 2003). In mouse skeletal muscles, Rora influences genes associated with lipid and carbohydrate metabolism (e.g., *Acsl4, Cd36, Hif1a*), LXR nuclear receptor signaling (e.g.. *LXRa, Srebp-1c*) , and Akt and AMPK signaling (e.g., *Akt2*) (Raichur et al., 2010). Liver tissues of Rora-deficient mice have been shown to exhibit altered expression of several genes involved in triglyceride synthesis and storage (e.g., *Cidec, Cidea, Mogat1*) (Kang et al., 2011). However, little is known about transcriptional targets of RORA in humans, particularly in the central nervous system (CNS). We therefore sought to extensively identify transcriptional targets of RORA in human neuronal cells, as well as in the human brain. Since *RORA* expression has been shown to be down-regulated in individuals with autism, we also investigated expression of RORA targets in the brain tissues of individuals diagnosed with autism, as well as those from sex- and age-matched unaffected individuals, to determine whether expression of RORA targets are also aberrant in the brain of individuals who are affected by the disorder.

Purpose and Significance

The dissertation research presented here aims to determine whether and how *RORA* is regulated by the sex hormones, as well as to identify molecular mechanisms involved in sex hormone regulation of *RORA*. Moreover, we utilize high-throughput, whole-genome promoter analysis to comprehensively identify transcriptional targets of RORA in human neuronal cells. Potentially direct transcriptional targets of RORA whose functions are known to be negatively impacted in individuals with autism are then selected for further validation by independent chromatin immunoprecipitation-qPCR and shRNA-mediated knockdown analyses to examine how aberrant *RORA* expression influences expression of downstream targets relevant to the known pathobiology of autism. Furthermore, we investigate expression of RORA targets in brain tissues from individuals with autism, as well as from sex- and age-matched unaffected individuals to examine whether expression of RORA targets is also altered in the autistic brain.

Hypotheses

We hypothesize that male and female sex hormones differentially regulate expression of *RORA* which, in turn, regulates a number of genes whose functions have been associated with autism. We also postulate that RORA reduction will lead to aberrant expression of its transcriptional targets in RORA-deficient human neuronal cells, as well as in the brain of individuals with autism who display RORA deficiency. Finally, we predict coregulator protein involvement in the hormone-induced changes in *RORA* expression as well as in RORA-mediated regulation of its transcriptional targets.

This dissertation, for the first time, describes a functionally relevant, hormonally responsive candidate gene for autism and offers a better understanding of molecular mechanisms involved in sex hormone regulation of RORA, which could lead to an explanation for the sex bias in autism. Moreover, this is the first study that comprehensively investigates transcriptional targets of this orphan nuclear receptor in human CNS. Findings from this dissertation could provide novel targets for future therapies to correct or ameliorate aberrant neurobiological functions in individuals with autism, especially those who exhibit RORA deficiency.

Chapter 2: Literature Review

Autism spectrum disorder: core features

Autism spectrum disorder (ASD or autism) is a neurodevelopmental disorder that typically becomes noticeable within the first three years of life and is defined by a pattern of qualitative abnormalities in reciprocal social interaction, communication, and restricted interests often with repetitive behaviors (American Psychiatric Association & American Psychiatric Association. Task Force on DSM-IV, 2000; Moldin & Rubenstein, 2006; F. Volkmar, Chawarska, & Klin, 2005; F. R. Volkmar et al., 1994). Difficulties in social interaction distinguish autism from other developmental disorders (Rapin & Tuchman, 2008). Individuals with autism are less likely to exhibit social understanding, approach other people spontaneously, imitate and respond to emotions, and take turns with other people (Sigman, Dijamco, Gratier, & Rozga, 2004). They often show less attention to social stimuli, have less eye contact, and do not have the ability to use simple movements (i.e., gestures) to effectively express themselves (F. R. Volkmar & Chawarska, 2008). Deficits in communication observed in individuals with autism may be both verbal and non-verbal. Most individuals with autism are delayed in their acquisition of both receptive and expressive language (Philofsky, Hepburn, Hayes, Hagerman, & Rogers, 2004). Many children with autism have delayed onset of babbling, unusual gestures, and do not develop enough natural speech to meet their daily communication needs (Noens, van Berckelaer-Onnes, Verpoorten, & van Duijn, 2006). Other common deficits in communication associated with autism include echolalia (repeating others' words out of context), pronoun

reversal, and excessive repetition of phrases (Kanner, 1968; Landa, 2007; Tager-Flusberg & Caronna, 2007).

Another behavioral area widely known to be a major characteristic of autism is restricted interests and repetitive behaviors. Common restricted and repetitive behaviors associated with autism can be categorized into five types: stereotypic and perseverative behavior, sameness and ritualistic behavior, compulsive behavior, restricted interests, and self-injury (Lam & Aman, 2007). Stereotypic and perseverative behavior is abnormal and excessive repetition of an action or phrase over time (e.g. body rocking and hand flapping). Ritualistic behavior involves unvarying pattern of daily activities (e.g. wearing the same clothes or watching the same movies everyday). Compulsive behavior is often manifested by the obsessive intent to follow rules (e.g. arranging objects in stacks or lines). Restricted interest is having unusual preoccupations and circumscribed interests so intense that they interfere with social interactions and other behaviors (e.g., preoccupation with the wheels on toy vehicles). Self-injury in autism includes movements that can injure the person (e.g. head banging, skin picking, and hand biting). Although there is no single abnormal repetitive behavior shown to be specific to autism, an elevated pattern of occurrence and the severity of repetitive behaviors are known to characterize and predict severity of the disorder (Bodfish, Symons, Parker, & Lewis, 2000).

Other associated features and comorbid diagnoses

In addition to the core behavioral features, a number of other abnormalities have been reported in association with autism. Mental retardation is among those found to be associated with a considerable subset of individuals with this disorder. Bertrand and

colleagues (2001) reported that approximately 50% of children with autism achieved IQ scores in the range of mental retardation (i.e., IQ score < 70) (Bertrand et al., 2001). This finding was supported by several recent studies, including ones from Chakrabarti and Fombonne, in which they have reported that the percentage of individuals with autism who have abnormal IQ could be as high as 70% (S. Chakrabarti & Fombonne, 2001; S. Chakrabarti & Fombonne, 2005).

Sensory and motor abnormalities are also frequently reported in individuals with autism. Many children with autism have aberrant responsiveness to sensory stimuli (e.g. abnormally sensitive to certain textures or surfaces) (Rogers, Hepburn, & Wehner, 2003) or exhibit an increased or lowered pain threshold (Charman & Baird, 2002; Filipek et al., 2000). Up to 33% of individuals with autism were reported to have delayed motor development (Mayes & Calhoun, 2003). Motor impairments frequently associated with autism include gait disturbances (Kielinen, Rantala, Timonen, Linna, & Moilanen, 2004; Vilensky, Damasio, & Maurer, 1981), problems with balance and coordination (Ghaziuddin & Butler, 1998; V. Jones & Prior, 1985), and postural abnormalities (Minshew, Sung, Jones, & Furman, 2004).

Several studies have demonstrated that the rate of autism in individuals with epilepsy is much higher than in the general population, especially when epilepsy coexists with mental retardation (C. Gillberg, 2005; Steffenburg, Gillberg, & Steffenburg, 1996; Steffenburg, Steffenburg, & Gillberg, 2003). Conversely, the rate of epilepsy in autism varies widely from 5-44% (Tuchman & Rapin, 2002), likely due to the heterogeneity in clinical phenotypes and genetics (Ballaban-Gil & Tuchman, 2000). If only classic autism is considered, the rate of epilepsy was reported to be approximately 20% in early childhood

(Olsson, Steffenburg, & Gillberg, 1988; F. R. Volkmar & Nelson, 1990) and about 25 – 40% in adults (Danielsson, Gillberg, Billstedt, Gillberg, & Olsson, 2005; C. Gillberg, 1984; Rutter, 1970).

Other comorbid conditions reported in individuals with autism include macrocephaly (Bailey et al., 1998; Kemper & Bauman, 1993a; Piven et al., 1995; Piven, Arndt, Bailey, & Andreasen, 1996), ataxia (Ahsgren et al., 2005), attention deficit hyperactivity disorder (ADHD) (Goldstein & Schwebach, 2004), depression (Ghaziuddin, Ghaziuddin, & Greden, 2002), bipolar disorder (Stahlberg, Soderstrom, Rastam, & Gillberg, 2004; Wozniak et al., 1997), anxiety (Muris, Steerneman, Merckelbach, Holdrinet, & Meesters, 1998), obsessive compulsive symptoms (Russell, Mataix-Cols, Anson, & Murphy, 2005), Tourette syndrome (Baron-Cohen, Scahill, Izaguirre, Hornsey, & Robertson, 1999), and schizophrenia (Konstantareas & Hewitt, 2001; F. R. Volkmar & Cohen, 1991).

Autism is a major public health challenge

The prevalence of autism is phenomenally rising every year. Epidemiological surveys of autism, combining different forms of autism (i.e. classic autism, PDD-NOS, and Asperger's syndrome), reveal that the prevalence of autism has dramatically increased from an average of one child in every 14,000 in 1970 (Treffert, 1970) to approximately one in every 88 children in 2012 (Baio, 2012). Although an increase in the prevalence of autism is partly due to improved diagnosis and awareness, careful research shows that the actual prevalence of autism is also increased (Baio, 2012; Hertz-Picciotto & Delwiche, 2009). Currently, more children are diagnosed with autism than with AIDS, diabetes, and cancer

combined (Autism Speaks, 2012). It is estimated that autism currently costs the nation over 137 billion dollars a year and the figure is predicted to be dramatically increasing (Autism Speaks, 2012). At present, however, there is still no molecular detection or cure for autism. Thus, it is clear that autism is a major public health challenge which requires more scientific research from all aspects of research, including basic science, clinical, and translational. A better understanding of this neurodevelopmental disorder could eventually lead to development of strategies that allow not only for early diagnosis and novel therapies, but also prevention of autism.

Sex differences in autism

The prevalence of autism in males is much higher than in females, with ratios of 4-5 to 1 for classic autism, as reported in most epidemiological studies (S. Chakrabarti & Fombonne, 2001; Moldin & Rubenstein, 2006), and as high as 11 to 1 in some research samples (C. Gillberg, Cederlund, Lamberg, & Zeijlon, 2006). In the United States, 1 out of 54 boys and 1 out of 252 girls are diagnosed with autism (Baio, 2012). The specific factors responsible for the higher prevalence of autism in males remain unclear.

The Empathizing-Systemizing theory and the Extreme Male Brain theory, are thought to be involved in the male bias in autism. The Empathizing-Systemizing theory focuses on the distinction between the cognitive domains of empathy (the drive to identify another person's thoughts and feelings and respond with an appropriate emotion) and systemizing (the drive to analyze and construct rule-based systems) (Baron-Cohen, 2009; Beacher et al., 2012). In the general population, typical females show higher levels of empathy compared with systemizing, whereas typical males show the reverse profile

(Baron-Cohen, 2009). The Extreme Male Brain theory extends the Empathizing-Systemizing theory to autism (Baron-Cohen, Richler, Bisarya, Gurunathan, & Wheelwright, 2003; Baron-Cohen & Wheelwright, 2004). On the Empathy Quotient (EQ) typical females score higher than typical males who, in turn, score higher than those with autism (Baron-Cohen & Wheelwright, 2004). On the other hand, the reverse pattern is exhibited for scores on the Systemizing Quotient (SQ) (Auyeung et al., 2006; Baron-Cohen et al., 2003; Wheelwright et al., 2006). These findings and additional evidence from studies on the social-emotional behaviors of individuals (**Table 1**) show that people with autism have an extreme male psychological profiles (reviewed in Baron-Cohen et al., 2011) (Baron-Cohen et al., 2011). It is noteworthy that the Extreme Male Brain theory does not state that all psychological sex differences will be exaggerated in autism, only those associated with empathy and systemizing. However, neither of these theories offers insight into the molecular basis of autism.

Other biological theories involved in the sex bias of autism include the X Chromosome theory, the Y Chromosome theory, and the Reduced Autosomal Penetrance theory. The X Chromosome theory focuses on the possibility that mutations or other genetic or epigenetic dysregulations on X chromosome are responsible for autism, thus females are less susceptible because there is additional X chromosome. On the other hand, the Y Chromosome theory proposes that dysregulations on Y chromosome causes autism, thus males are more susceptible than females to have autism. A problem for these theories is that the majority of linkage and association studies of autism have failed to find regions of interest on the sex chromosomes (Baron-Cohen et al., 2011). The Reduced Autosomal Penetrance theory proposes that dominant de novo mutations on the autosomes that have

reduced penetrance in females are responsible for the sex bias of autism. However, this theory does not provide an explanation why the penetrance should be reduced in females (Baron-Cohen et al., 2011). Clearly, further studies are needed to elucidate to what extent these theories can explain the heightened prevalence of autism in males.

Table 1. A summary of the psychological evidence for the Extreme Male Brain theory.

(Adapted from (Baron-Cohen et al., 2011))

Psychological Measure	Autism>Male>Female	Female>Male>Autism
Adolescent AQ	✓	
Adult Autism Spectrum Quotient (AQ)	✓	
Adult Systemizing Quotient (SQ)	✓	
Child AQ	✓	
Child SQ	✓	
Childhood Autism Spectrum Test (CAST)	✓	
Embedded Figures Test	✓	
Intuitive Physics Test	✓	
Social Responsiveness Scale	✓	
Quantitative Checklist for Autism in Toddlers (Q-CHAT)	✓	
Adult Empathy Quotient (EQ)		✓
Child EQ		✓
Faux Pas Test		✓
Friendship and Relationship Questionnaire (FQ)		✓
Reading the Mind in the Eyes		✓
Social Stories Questionnaire (SSQ)		✓

There is evidence that some of the mechanisms causing autism may involve endogenous sex steroids associated with typical sex differences. Fetal or perinatal exposure to elevated levels of androgens, including testosterone, may increase susceptibility towards autism (Baron-Cohen et al., 2005; Baron-Cohen et al., 2011). Currently, evidence suggesting that fetal testosterone may play a role in autism includes the following findings (Baron-Cohen et al., 2005). (i) Fetal testosterone is associated with low ratios of second-to-fourth digit length (S. Lutchmaya, Baron-Cohen, Raggatt, Knickmeyer, & Manning, 2004), and a low digit-length ratio is in turn associated with autism-spectrum conditions (Manning, Baron-Cohen, Wheelwright, & Sanders, 2001). (ii) Females with congenital adrenal hyperplasia, a genetic condition that elevates fetal testosterone, manifest more autism-like traits than their unaffected sisters (Knickmeyer et al., 2006). (iii) Within normal development, fetal testosterone is inversely correlated with behaviors associated with diagnostic symptoms for autism. These traits include eye contact, vocabulary development, social functioning, and narrow interests (Knickmeyer, Baron-Cohen, Raggatt, & Taylor, 2005; S. Lutchmaya, Baron-Cohen, & Raggatt, 2002; S. Lutchmaya & Baron-Cohen, 2002). (iv) There is preliminary evidence of somatic hypermasculinization in autism (Tordjman, Ferrari, Sulmont, Duyme, & Roubertoux, 1997). (v) There is precocious puberty in boys with autism (Baron-Cohen et al., 2005). (vi) Serotonin levels (Belmonte et al., 2004) and BDNF levels, both mediated by fetal testosterone are elevated in autism (Wisniewski, 1998). (vii) Our recent gene expression study of siblings discordant for diagnosis of autism has identified deregulated genes involved in androgen biosynthesis as well as higher testosterone levels in lymphoblastoid cell lines (LCL) derived from the siblings with autism (V. W. Hu et al., 2009). Although these observations suggest that

testosterone may be associated with risk of autism, the mechanisms linking elevated androgen levels to heightened autism susceptibility remains unknown.

Moreover, testosterone can be converted to estradiol, a form of estrogen, by an enzyme called aromatase. Expression of aromatase is detectable in the fetal brain during the second trimester of pregnancy (usually 14-20 weeks of gestation), the same period when serum testosterone peaks in male fetuses (Price, Aitken, & Simpson, 1992). Thus, many of the effects of testosterone in shaping the male brain are in fact due to estrogens converted from testosterone by the enzyme aromatase during this period of gestation, although the precise molecular mechanisms through which estradiol impact neural development are unknown (Purves et al., 2012). Moreover, the association between estrogen and the susceptibility of autism has never been investigated. Further studies are therefore needed to elucidate the precise molecular mechanisms through which both androgen and estrogen may play a role in autism etiology or susceptibility.

Etiology of autism

Many studies have attempted to identify the underlying neuropathological conditions and genetic abnormalities that might directly contribute to the etiology of autism; nevertheless, the etiological basis of idiopathic autism remains unclear. Currently, only approximately 10 to 15% of autistic cases are found to be etiologically related to known neurological or genetic disorders (Barton & Volkmar, 1998; Rutter, Bailey, Bolton, & Le Couteur, 1994), and only 3 to 9% are believed to have detectable cytogenetic abnormalities (Fombonne, Du Mazaubrun, Cans, & Grandjean, 1997; Wassink, Piven, & Patil, 2001). Fragile X Syndrome (FRAX), for instance, is among the syndromic autism

spectrum disorders with a known genetic basis. The causative condition contributing to the syndrome is a mutation in the *FMR1* gene on the X chromosome which results in triplet repeat (CGG) expansion in the gene. The CGG repeats lead to hypermethylation ultimately resulting in transcriptional silencing of *FMR1* which is critical for normal neuronal development (Hornstra, Nelson, Warren, & Yang, 1993; Sutcliffe et al., 1992). Up to 44% of Fragile X patients are reported to exhibit some autistic characteristics (Philofsky et al., 2004). However, fewer than 5% of autism patients have Fragile X (Bailey et al., 1993; Klauck et al., 1997; Piven, Gayle, Landa, Wzorek, & Folstein, 1991; Wassink et al., 2001). Similar to Fragile X syndrome, up to 61% of tuberous sclerosis complex (TSC) patients have autistic features (Curatolo, Porfirio, Manzi, & Seri, 2004), but less than 3% of autistic individuals have been reported to develop TSC (I. C. Gillberg, Gillberg, & Ahlsen, 1994; Smalley, 1998). Mutations in the TSC genes, *TSC1* and *TSC2*, result in widespread development of benign tumors in multiple organ systems including the central nervous system (CNS) (Gomez, 1995). The CNS manifestations of TSC include seizures, epilepsy, mental retardation, and behavioral disorders commonly associated with autism (Cross, 2005; Sparagana & Roach, 2000; Webb, Fryer, & Osborne, 1991). Rett's Syndrome is another autism-associated disorder induced by mutation in a single gene, *MeCP2* (methyl-CpG-binding protein 2). *MeCP2* encodes a chromatin-associated protein controlling gene expression by binding to CpG sites where it recruits transcriptional silencers and histone deacetylase, resulting in transcriptional repression (P. L. Jones et al., 1998; Lewis et al., 1992; Meehan, Lewis, & Bird, 1992; Nan et al., 1998). Mutations in *MeCP2* therefore lead to failure to deacetylate histones and repress gene expression. Despite the success in identification of these genetic disorders in individuals with syndromic autism (reviewed by

(Benvenuto, Moavero, Alessandrelli, Manzi, & Curatolo, 2009)), 80-90% of autism cases remain idiopathic.

Biomarkers for Autism

With regard to identifying genes associated with idiopathic autism, there have been several previous studies performing genome-wide scans for autism genetic linkages. As a result, susceptibility loci have been identified on almost every chromosome, especially chromosomes 2q, 3q, 7q, 15q, 16p, and 17q. No single region, however, has been found to be highly significant and consistently reproducible, and no genetic variation or mutation within these regions has been found to be able to fully explain the etiology of autism. Copy number variations (CNV) have been associated with autism as well. Glessner and colleagues (2009) conducted a whole-genome CNV study on a cohort of 859 individuals with autism and 1,409 healthy children of European ancestry who were genotyped with approximately 550,000 SNP markers. Positive findings were evaluated in an independent cohort of 1,336 autism cases and 1,110 controls of European ancestry. They identified genes previously reported to be associated with autism, including *NRXN1* and *CNTN4*. Several new susceptibility genes encoding neuronal cell-adhesion molecules, including NLGN1 and ASTN2, were enriched in CNVs in autism cases compared to controls (Glessner et al., 2009). However, no CNV was found to be highly significant. Moreover, numerous candidate genes for autism have been identified. Some of the well-described genes are *NLGN* (Lise & El-Husseini, 2006), *SHANK3* (Durand et al., 2007), *NRXN1* (Kim et al., 2008), and *CNTNAP* (Arking et al., 2008), which together focus attention on synaptic

connections and functions. However, no autism candidate gene identified by these studies has provided an explanation for the male bias in autism.

RORA as a novel candidate gene for autism

We have recently identified retinoic acid-related (RAR) orphan receptor-alpha (*RORA*) as a novel candidate gene for autism (Nguyen et al., 2010). *RORA*, also known as *NR1F1*, is a member of the thyroid hormone receptor-like (NR1) subfamily of nuclear hormone receptors and can bind as a monomer or as a homodimer to hormone response elements upstream of several genes to regulate the transcription of those genes. Gene expression profiling analysis of lymphoblastoid cell lines (LCLs) revealed significant reduction of the transcript levels of *RORA* in cells from individuals with autism relative to cells from controls (V. W. Hu, Sarachana et al., 2009). Using large-scale methylation profiling by CpG island microarray and methylation-specific PCR analysis of LCLs derived from monozygotic twins discordant for diagnosis of autism and their non-autistic siblings, we found that the CpG island in the promoter region of *RORA* is significantly hypermethylated in LCLs from individuals with autism relative to controls (Nguyen et al., 2010). The protein levels of RORA were significantly reduced in LCLs from individuals with autism relative to non-autistic siblings. Moreover, immunohistochemical analyses of tissue arrays containing slices of the cerebellum **(Figure 1)** and the frontal cortex **(Figure 2)** of individuals with autism and age- and sex-matched controls revealed decreased expression of RORA proteins in the autistic brain.

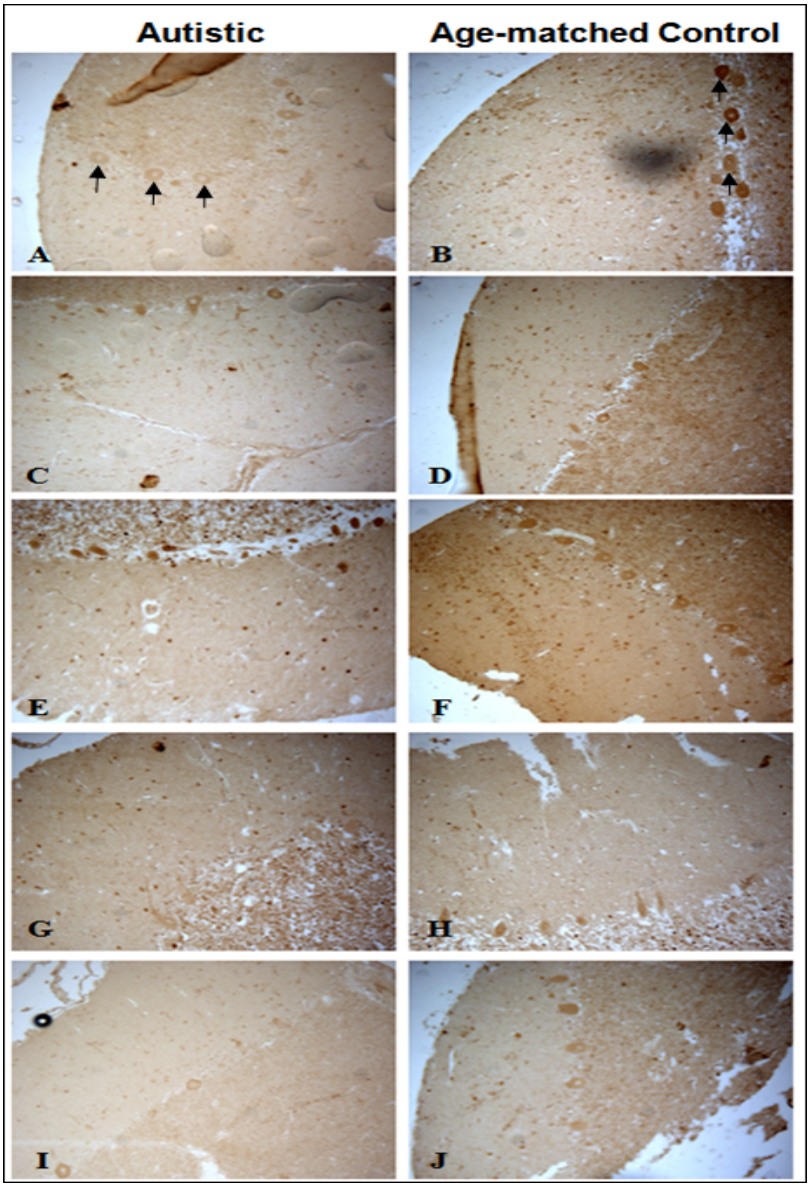

Figure 1. Immunohistochemical staining for RORA protein in the cerebellum (From (Nguyen et al., 2010)). Immunohistochemistry analysis for RORA protein was performed using a standard avidin-biotin complex method of detection. Representative images (X20) were taken from the autism tissue array, which contained tissue cores from 5 autistic brains (A, C, E, G, I) and age-matched controls (B, D, F, H, J). Samples E, F, G, H were from female donors.

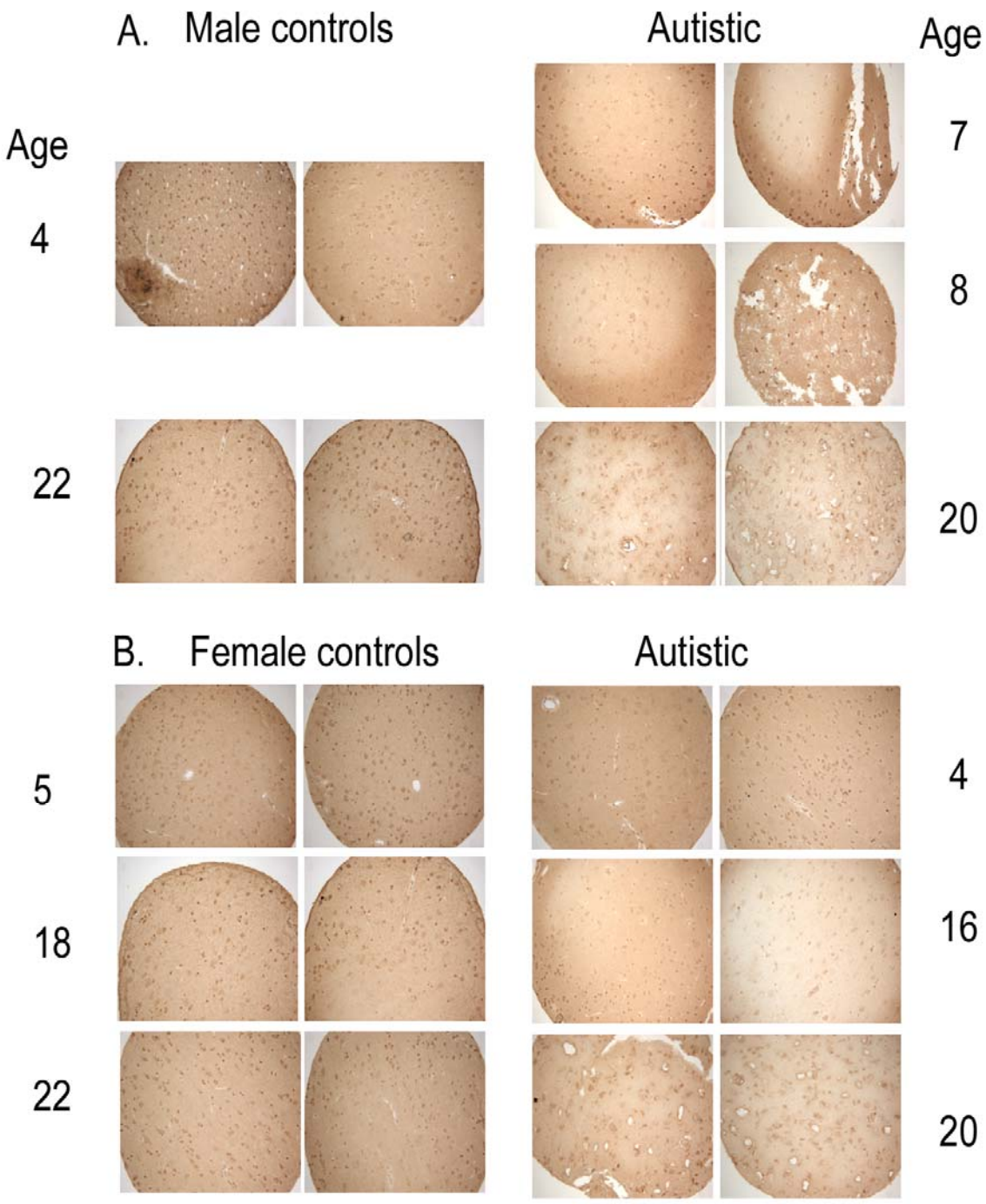

Figure 2. Immunohistochemical staining for RORA protein in the frontal cortex

(From (Nguyen et al., 2010)).

RORA structure and functions

RORA (NR1F1, RORα, or RZRα) is a member of the retinoic acid-related (or retinoid-related) orphan receptor (ROR) group of the thyroid hormone receptor-like nuclear receptor subfamily (Becker-Andre, Andre, & DeLamarter, 1993; Giguere et al., 1994; Giguere, Beatty, Squire, Copeland, & Jenkins, 1995; Jetten, 2009). *RORA* is highly conserved across mammalian species and zebrafish, and ROR orthologs have also been identified in several lower species, including *Drosophila melanogaster*, *Caenorhabditis elegans*, and *Manduca sexta* (Jetten, 2009). The human gene spans a ~741 kb genomic region on chromosome15q22.2 and is transcribed into four isoforms, referred to as *RORA1-4*, whereas only isoform 1 and 4 have been found in mice (**Figure 3**). All isoforms have a central well-conserved DNA binding domain (DBD), a variable N-terminal domain, a non-conserved hinge region, and a C-terminal ligand binding domain (LBD; **Figure 4**).

The DBD contains a loop between the last two cysteines within the first zinc finger in DBD (called P-box), which interacts with the core motif in the major groove, and the C-terminal extension, which interacts with the 5'-AT-rich region of the RORA binding elements in the adjacent minor groove. The LBD of RORA, like other nuclear receptors, is thought to be involved in ligand binding, nuclear localization, receptor dimerization, and coregulator interaction (Jetten, 2009). Major regions in RORA LBD include typical 12 canonical α-helices (H1-12), two additional helices (H2' and H11'), and the activation function 2 (AF2) in H12 consisting of PLYKELF, which is 100%-conserved among ROR nuclear receptors (J. A. Kallen et al., 2002; Stehlin et al., 2001; Stehlin-Gaon et al., 2003). Mutations in the H12 region abolishes the ROR transactivation activity and results in a dominant negative ROR (Kurebayashi et al., 2004; Lau, Bailey, Dowhan, & Muscat, 1999).

H10 is thought to be responsible for homo- and heterodimerization (J. A. Kallen et al., 2002; Stehlin et al., 2001; Stehlin-Gaon et al., 2003).

The ligand binding pocket of RORA was calculated to be 722 Å (J. A. Kallen et al., 2002; Stehlin et al., 2001; Stehlin-Gaon et al., 2003). X-ray crystallography and mass spectrometry analysis suggested that cholesterol and its derivatives, including cholesterol sulfate and 7-dehydrocholesterol (provitamin D3), may be natural ligands of RORA (Bitsch et al., 2003; J. Kallen, Schlaeppi, Bitsch, Delhon, & Fournier, 2004; J. A. Kallen et al., 2002). Kallen and colleagues (2002) found that RORA transcriptional activity could be modulated by changes in intracellular cholesterol level or mutation of residues involved in cholesterol binding (J. A. Kallen et al., 2002). However, further studies are required to determine whether cholesterol and its derivatives function as genuine physiological ligands of RORA.

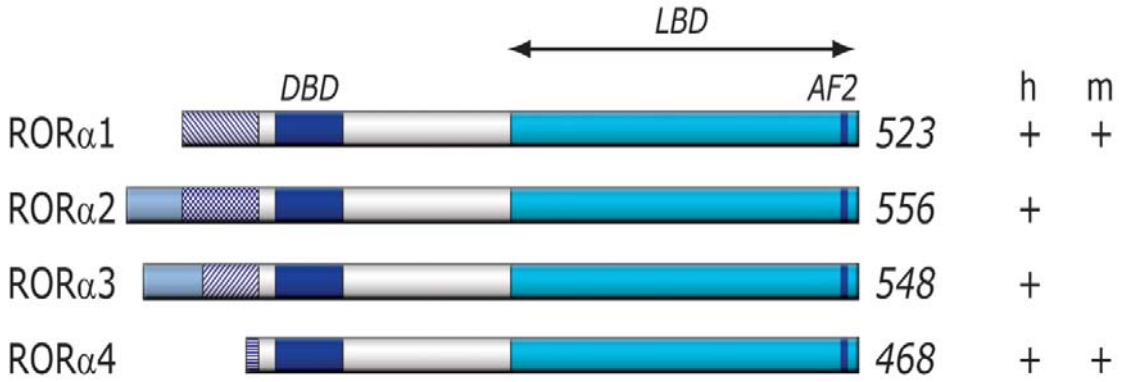

Figure 3. Schematic representation of various RORA isoforms. The DNA binding domain (DBD) and ligand binding domain (LBD), and activation function 2 (AF2) are indicated. The variable regions at the N-terminus of each ROR generated by alternative promoter usage and/or alternative slicing are indicated by patterned boxes on the left. The numbers on the right refer to the total number of amino acids in RORA. The different RORA isoforms identified in human and mouse are shown on the right (+/-). Adapted from (Jetten, 2009).

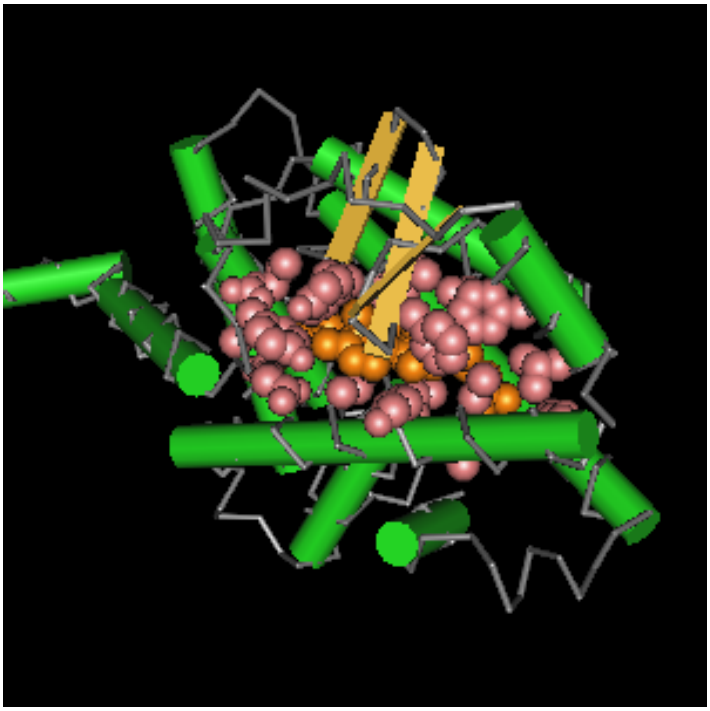

Figure 4. Ligand binding domain of RORA. The ligand binding domain of human RORA (green) is shown in complex with cholesterol sulfate (pink and orange) at 4 Å (J. A. Kallen et al., 2002).

Nuclear receptors in the ROR group regulate gene transcription by binding to specific DNA response elements (ROREs) consisting of the consensus (A/G)GGTCA core motif in the regulatory region of target genes (**Figure 5**) (Schrader, Danielsson, Wiesenberg, & Carlberg, 1996). RORA binds RORE motifs as a monomer or homodimer and do not form heterodimers with other RORs or retinoid-X receptors (RXRs) (Carlberg, Hooft van Huijsduijnen, Staple, DeLamarter, & Becker-Andre, 1994). In addition to RORA, some RORE motifs can be recognized by the transcriptional repressor REV-ERB (Burris, 2008; Giguere et al., 1995), thus REV-ERB can inhibit RORA-mediated transcriptional activation by competing with RORA for RORE binding.

Once transcriptionally active, RORA forms a hydrophobic cleft and a charge clamp involving a conserved Lys residue in H3 and a conserved Glu in H12 (J. A. Kallen et al., 2002; Stehlin et al., 2001; Stehlin-Gaon et al., 2003). The charge clamp then functions as an interaction interface for LXXLL motifs in coactivators and related motifs in corepressors (Harris, Lau, Chen, & Muscat, 2002). RORA-coactivator complexes induce histone acetylation, resulting in decompaction of chromatin and increased transcription of target genes (**Figure 6**) (Glass & Rosenfeld, 2000; McKenna & O'Malley, 2002; Wolf, Heitzer, Grubisha, & DeFranco, 2008; Xu, 2005). RORA-corepressor complexes, on the other hand, result in histone deacetylation, causing compaction of chromatin and, in turn, suppression of gene transcription (Horlein et al., 1995; X. Hu & Lazar, 2000; Nagy et al., 1999). Several nuclear receptor coactivators and corepressors have been shown to interact with RORA to positively or negatively regulate transcription of RORA targets. Coactivators found within RORA protein complexes include NCOA1, NCOA2, PGC-1α, p300, and CBP (Atkins et al., 1999; Gold et al., 2003; Harding et al., 1997; Harris et al.,

2002; Lau et al., 1999). Corepressors reported to interact with RORA include NCOR1, NCOR2, RIP140, NIX1, and FOXP3 (Du, Huang, Zhou, & Ziegler, 2008; Greiner et al., 2000; Harding et al., 1997).

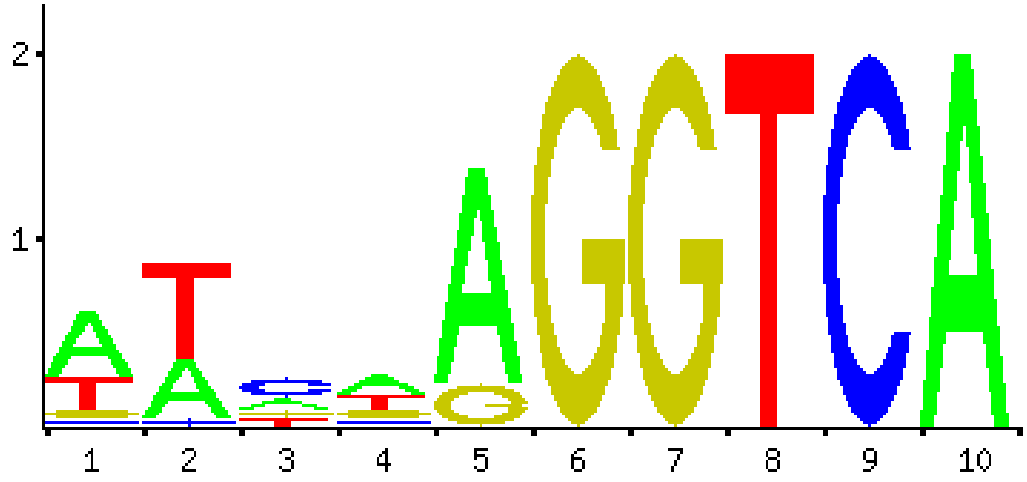

Figure 5. Pictogram representation of the consensus motif for RORA. The diagram shows the frequency of each nucleotide at each position of the consensus using 25 functional RORA binding elements in the JASPAR database (Bryne et al., 2008). The height of each letter is proportional to its frequency.

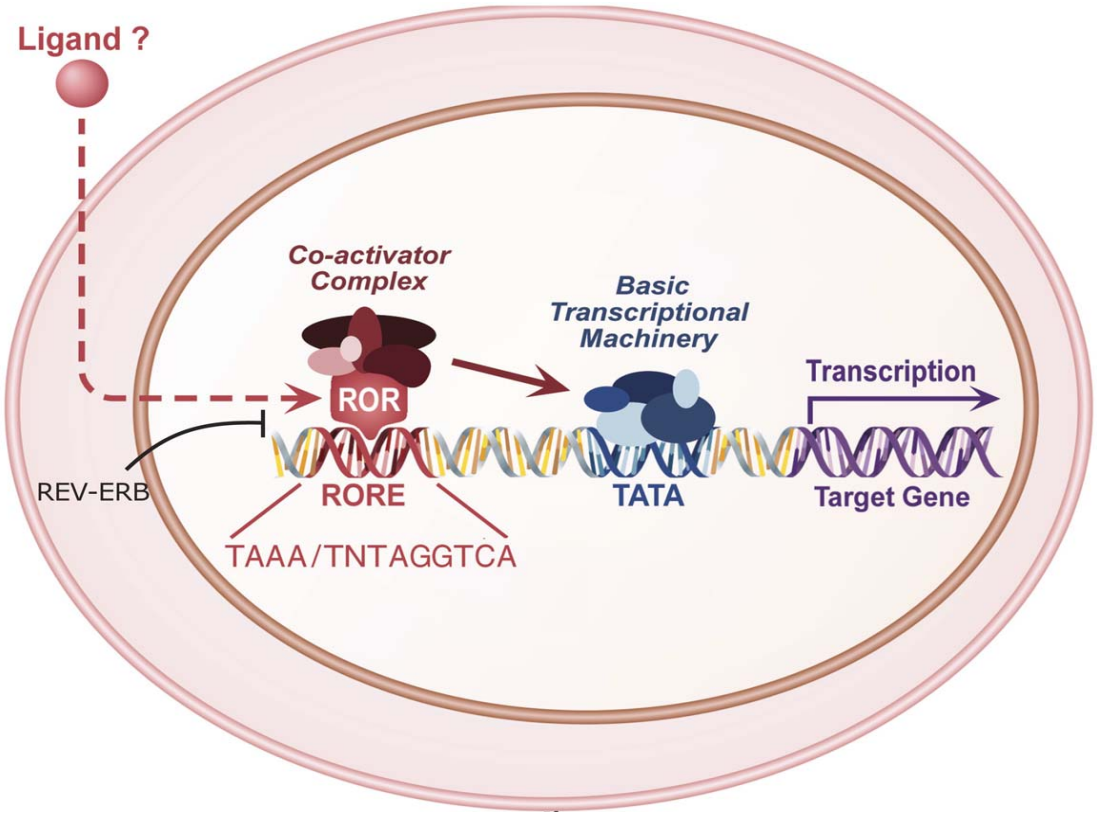

Figure 6. Mechanism of RORA action. RORA binds ROR binding elements in regulatory regions of target genes and recruits a coactivator protein complex and subsequently basic transcriptional machinery, which in turn leads to activation of transcription of target genes. (Jetten, 2009).

RORA is ubiquitously expressed in a variety of tissues, including bone marrow, blood, lymph node, brain, muscle, kidney, liver, skin, and testis (**Figure 7**) (Shmueli et al., 2003; Su et al., 2004; Yanai et al., 2005). In the brain, *RORA* is highly expressed in the Purkinje cells, stellate cells, and basket cells in the cerebellum (**Figure 8**) (Ino, 2004). Most of studies have focused on the role of RORA in the development of the cerebellum. However, medium to high *RORA* expression was also reported in other regions of the brain, including the thalamus, cerebral cortex (mainly in the layer IV), dorsal cochlear nucleus, suprachiasmatic nucleus, superior colliculus, spinal trigeminal nucleus, and retina (Ino, 2004), suggesting that RORA may be involved in a variety of neurological functions beyond those exclusive to cerebellum.

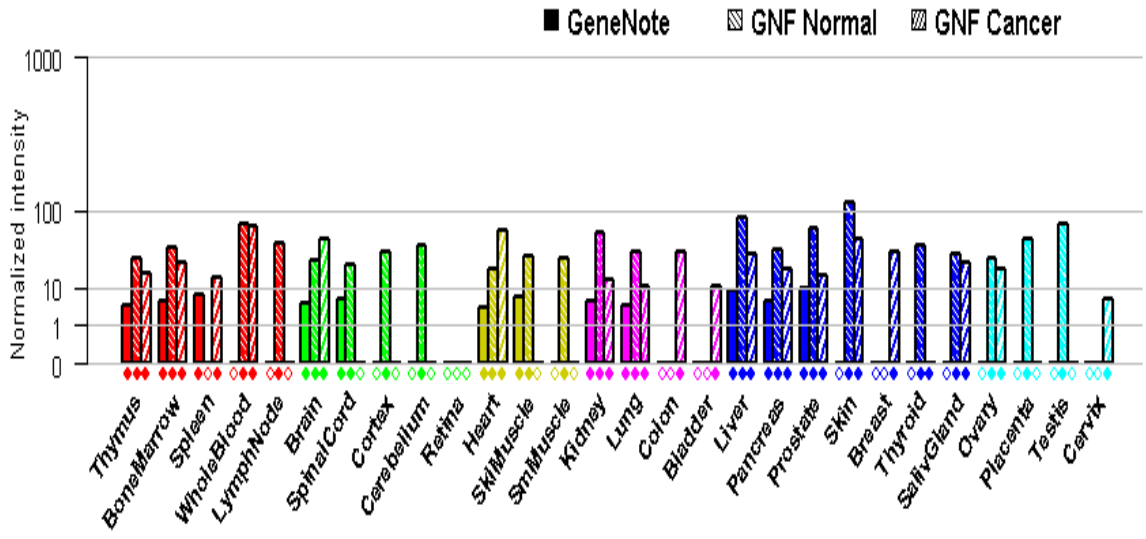

Figure 7. RORA expression in human tissues. *RORA* mRNA expression data in human tissues were provided by the GeneNote database in which normalized gene expression levels in each tissue were obtained from three experiments (Shmueli et al., 2003; Su et al., 2004; Yanai et al., 2005). According to the GeneNote database, the GeneNote experiment (first column in each tissue) used 12 normal human tissues hybridized against Affymetrix GeneChips HG-U95A-E microarrays. The GNF Normal experiment (middle column in each tissue) used 22 normal human tissues hybridized against HG-U133A. The GNF Cancer experiment (last column in each tissue) used 18 NCI60 cancer cell lines hybridized against HG-U133A. The diamonds along the x-axis of each graph hint that the tissue/cell line expression values are available for the gene. Empty diamonds indicate that either there is no such tissue for a specific microarray platform, or the gene has no matching probe sets on the microarray. Filled diamonds along the x-axis without data shown in the graph indicate that after normalization there is no meaningful *RORA* expression data for that

tissue. Normalized intensities are drawn on a root scale, which is an intermediate between log and linear scales. The Affymetrix MAS5 algorithm was used for array processing.

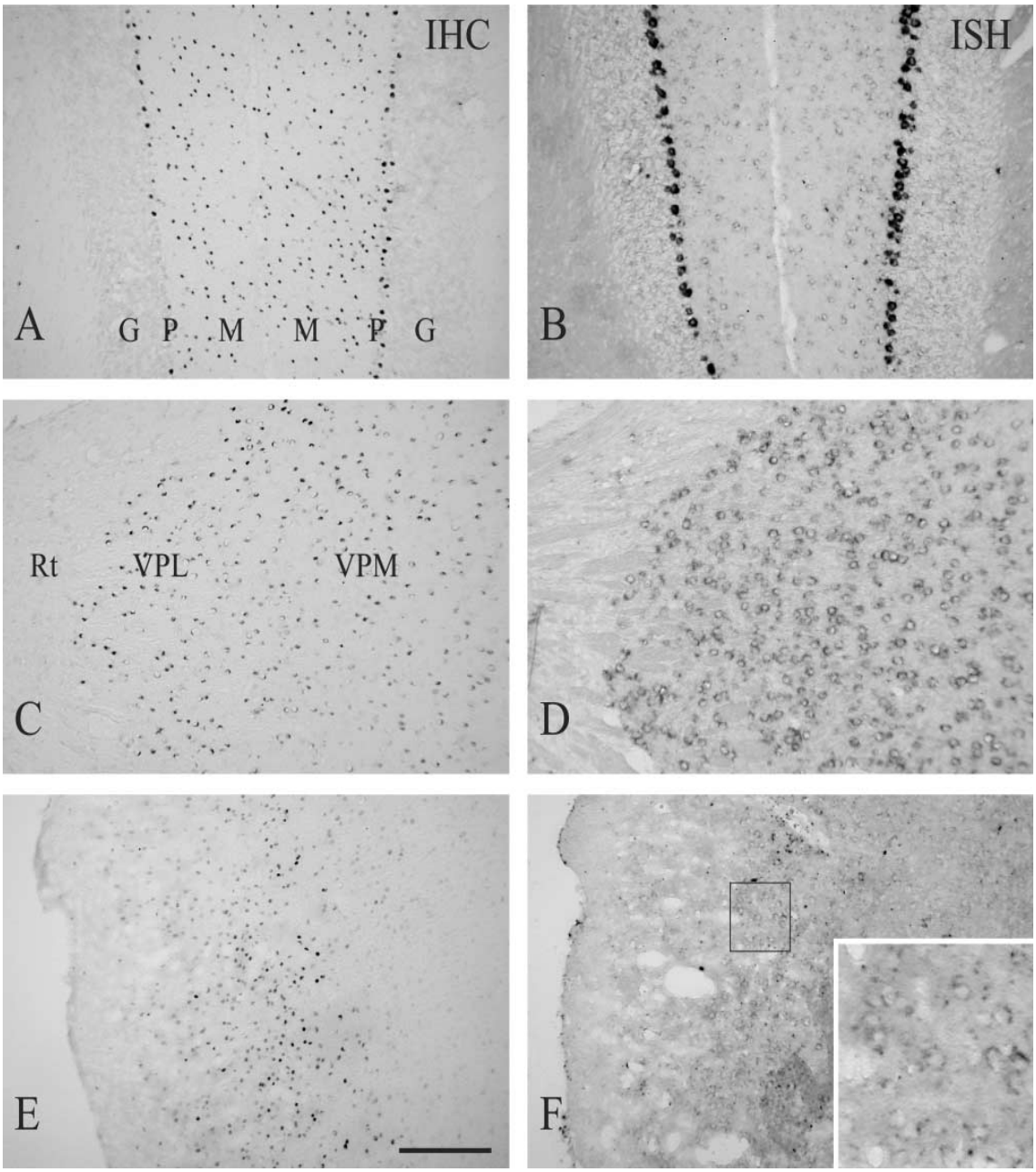

Figure 8. RORA expression in adult mouse cerebellum, thalamus, and cerebral cortex (Ino, 2004). Parasagittal sections of the cerebellum (A,B), and coronal sections of the thalamus showing the reticular, ventral posterolateral, and ventral posteromedial thalamic nuclei (C,D) and the cerebral cortex (E,F). RORA was detected by immunohistochemistry (IHC; A,C,E) and by *in situ* hybridization (ISH; B,D,F). In the cerebellum, RORA-positive

cells were observed in the Purkinje cell and molecular layers but not in the granule cell layer (A). Strong hybridization signal was observed in Purkinje cells and, with lower intensity, in cells of the molecular layer (B). Both RORA protein and mRNA were detected in the ventral posterolateral and ventral posteromedial thalamic nuclei but not in the reticular thalamic nucleus (C,D). In the cerebral cortex, intense RORA immunoreactivity was observed in layer VI (E). Inset in F shows a higher-magnification view of the area indicated by the box. M, molecular layer; P, Purkinje cell layer; G, granule cell layer; Rt, reticular thalamic nucleus; VPL, ventral posterolateral thalamic nucleus; VPM, ventral posteromedial thalamic nucleus. Bar = 200 μm.

In mice, *Rora* expression can be detected as early as embryonic day 12, just after Purkinje cell precursors exit the mitotic cycle and migrate along radial glia from the ventricular zone to form a cerebellar plate-like structure (Gold et al., 2003; Gold et al., 2007; Goldowitz & Hamre, 1998; Jetten & Joo, 2006; Jetten, 2009). A natural mutant mouse strain for *Rora*, called *staggerer*, carries a 6.4 kb intragenic insertion resulting in the deletion of the fifth exon, encoding the beginning of the LBD, and a frameshift that causes a premature stop codon (Gold et al., 2007; Hamilton et al., 1996). *Staggerer* mice exhibit extensive neurodegeneration in the cerebellum resulting in severe ataxia (Gold et al., 2007). The number of Purkinje cells in wild-type (WT) and homozygous *staggerer* ($Rora^{sg/sg}$) mice appears to be similar at E17.5 (Doulazmi et al., 2001; Vogel, Sinclair, Qiu, & Fan, 2000). However, by postnatal day 5, the number of Purkinje cells is greatly reduced and dendritogenesis is impaired in surviving cells. This is accompanied by a lack of parallel fiber input and a persistence of multiple climbing fiber innervations (Boukhtouche et al., 2006; Janmaat et al., 2009; Jetten, 2009; Mariani & Changeux, 1980; Mariani, 1982). Gold and colleagues (2003) have shown that Rora deficiency causes aberrant expression of several genes involved in calcium-mediated signal transduction and glutamatergic signaling in Purkinje cells (Figure 7). The genes that show Rora-dependent expression include *Shh* (sonic hedgehog), *Pcp4* (a calmodulin inhibitor), *Itpr1* (IP3 receptor and calmodulin target), *Cals1* (an Itpr1 binding partner), *Calb1* (a calcium buffer), *Slc1a6* (gene encoding EAAT4, the major glutamate transporter of Purkinje cells), and *Spnb3* (brain-specific β-spectrin III, which anchors EAAT4 to the cytoskeleton) (Gold et al., 2003). Chromatin immunoprecipitation analysis revealed that Rora is associated with ROREs in the promoter region of several genes down-regulated in Purkinje cells of *staggerer* mice, including *Pcp2,*

Pcp4, Itpr1, Shh, and *Slc1a6* (Gold et al., 2003), suggesting that these genes are directly regulated by Rora. It is interesting to note that the most consistent neurological abnormalities reported in individuals with autism is marked Purkinje cell loss in the cerebellum as determined by histopathological examinations, as well as atrophy of the cerebellar folia as determined by *in vivo* imaging (Bailey et al., 1998; Courchesne, Yeung-Courchesne, Press, Hesselink, & Jernigan, 1988; Courchesne, 1991; Courchesne, Press, & Yeung-Courchesne, 1993; Courchesne, 1995; Heh et al., 1989; Kemper & Bauman, 1993b; Kern, 2003; Murakami, Courchesne, Press, Yeung-Courchesne, & Hesselink, 1989; Ritvo et al., 1986; Williams, Hauser, Purpura, DeLong, & Swisher, 1980). A recent study on tuberous sclerosis complex, a genetic disorder caused by mutation of either *TSC1* or *TSC2* with high rates of autism comorbidity, also showed that reduced Purkinje cell numbers caused by *TSC1* mutation results in autistic-like behaviors, including abnormal social interaction, repetitive behavior and vocalizations, as well as decreased Purkinje cell excitability (Tsai et al., 2012).

In addition to Purkinje cells, the granule cell layer of the cerebellum is also negatively affected in *staggerer* mice. The number of granule cells in *staggerer* mice is slightly reduced at birth, and reduction is more pronounced during the first weeks after birth (Jetten, 2009). In adult Rora-deficient mice, the granular layer is very thin and depleted of granule cells (Doulazmi et al., 1999; Doulazmi et al., 2001; Dussault, Fawcett, Matthyssen, Bader, & Giguere, 1998; Gold et al., 2007; Hamilton et al., 1996; Herrup & Mullen, 1979; Herrup & Mullen, 1981; Jetten, 2009; Landis & Reese, 1977; Landis & Sidman, 1978; Sidman, Lane, & Dickie, 1962; Steinmayr et al., 1998; Yoon, 1972). Studies using WT:*staggerer* chimeras indicated that the depletion of cerebellar granule cells in

Rora$^{sg/sg}$ mice is related to abnormalities inherent to Rora$^{sg/sg}$ Purkinje cells (Herrup & Mullen, 1979; Herrup & Mullen, 1981; Jetten, 2009). Gold and colleagues (2003) found that *Shh* expression is reduced in Purkinje cells of *staggerer* mice and recombinant *Shh* is sufficient to stimulate proliferation of granule cell precursor proliferation in *staggerer* cerebellar slice cultures (Gold et al., 2003). These findings suggest that diminished proliferation of granule cell precursors may be a consequence of reduced *Shh* expression in Purkinje cells (**Figure 9**; (Jetten, 2009)). The morphology of the cerebellar cortex in young heterozygous (Rora$^{sg/+}$) mice appears normal, but an accelerated loss of Purkinje and granule cells was observed upon aging (Doulazmi et al., 1999; Hadj-Sahraoui et al., 2001; Zanjani, Mariani, Delhaye-Bouchaud, & Herrup, 1992).

Recent studies have expanded the role of Rora beyond the cerebellum. The cerebrum of homozygous *staggerer* Rora$^{sg/sg}$ mice was reported to be much smaller than that of WT mice (Yi et al., 2010). Immunohistochemistry analysis of Ki67, DCX, and NeuN, which are cell proliferation, neuronal differentiation and mature neuron markers, respectively, revealed that neuronal differentiation and maturation are aberrant while cell proliferation is not affected in the dentate gyrus of *staggerer* mice relative to WT controls (Yi et al., 2010), suggesting that Rora plays an important role in differentiation and maturation of neurons in the dentate gyrus.

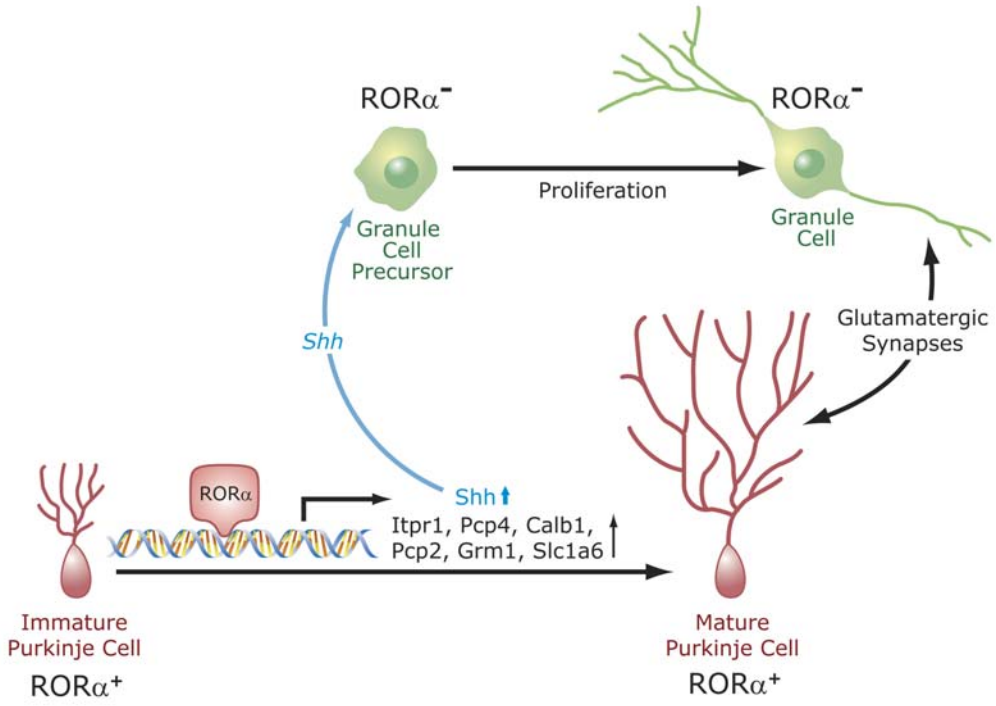

Figure 9. Regulation of Purkinje cell maturation and cerebellar development by RORA (Jetten, 2009)**.** RORA regulates the expression of several genes in Purkinje cells. *RORA* becomes highly expressed in postmitotic Purkinje cells and regulates their maturation, particularly dendritic differentiation. Dendritogenesis and the expression of several genes, including *Shh, Itpr1, Pcp4, Calb1, Pcp2,* and *Slc1a6*, normally expressed in mature Purkinje cells, are inhibited in Rora-deficient mice. The transcription of several of these genes is under direct control of Rora. Shh released by Purkinje cells interacts with Patched (Ptch) receptors on granule cell precursors, leading to activation of GLI transcription factors and the subsequent induction of proliferation-promoting genes. Reduced *Shh* expression in Purkinje cells from Rora-deficient mice is a major factor in the cerebellar atrophy observed in these mice. Cerebellar granule cells and Purkinje cells mutually interact (e.g., glutamatergic synapses). From (Jetten, 2009).

Boukhtouche and colleagues (2006) investigated a role of Rora in oxidative stress-induced neuronal apoptosis (Boukhtouche, Vodjdani et al., 2006). Overexpression of human Rora1 by transient transfection of a plasmid encoding hRora1 or by infecting cultures with a lentiviral-derived vector encoding hRora1 provided a significant increase in the survival rate of cortical neurons exposed to the pro-apoptotic stimuli β-amyloid peptide, c_2-ceramide, and H_2O_2. Cortical neurons overexpressing hRora1 were shown to have an increase in the levels of antioxidant enzymes, specifically glutathione peroxidase 1 and peroxiredoxin 6, and a significant decrease in the levels of reactive oxygen species relative to control cortical neurons without overexpression of Rora1. Knockdown of the antioxidant enzymes inhibited the neuroprotective effect of Rora against apoptosis induced by the pro-apoptotic stimuli. These observations indicate that overexpression of Rora leads to an increase in the levels of these antioxidant enzymes, resulting in a reduction in the accumulation of reactive oxygen species in cortical neurons. It was concluded that Rora mediates neuroprotection against oxidative stress-induced apoptosis, at least in part, through glutathione peroxidase 1 and peroxiredoxin 6 (Boukhtouche, Vodjdani et al., 2006). It is noteworthy that oxidative stress has been strongly associated with autism. Both increased levels of pro-oxidants and decreased levels of anti-oxidants were proposed to be involved in the etiology and the susceptibility of the disorder (Chauhan & Chauhan, 2006). Individuals with autism were reported to display decreased activity of glutathione peroxidase in plasma (Yorbik, Sayal, Akay, Akbiyik, & Sohmen, 2002) and in erythrocytes (Pasca et al., 2006; Yorbik et al., 2002), reduced levels of total glutathione and lower redox ratio of reduced form of glutathione to oxidized form of glutathione in plasma (James et al., 2004), and decreased catalase (Zoroglu et al., 2004) and superoxide dismutase activity in

erythrocytes (Chauhan & Chauhan, 2006; Yorbik et al., 2002). Given that RORA is involved in cellular protection against oxidative stress, aberrant expression of RORA in individuals with autism may result in oxidative stress-related abnormalities observed in autism.

RORA is also a functional component of the mammalian circadian clock by serving as an activator of BMAL1, a key transcriptional activator necessary for core oscillator function (Sato et al., 2004). The nuclear receptor is required for normal Bmal1 expression and consolidation of daily locomotor activity and is regulated by the core clock in the suprachiasmatic nucleus. Expression of *RORA* shows a rhythmic pattern with a peak at Circadian Time 6-8 in the suprachiasmatic nucleus in the brain and a weak circadian oscillation of RORA was also reported in liver, kidney, retina, and lung (Akashi & Takumi, 2005; Kamphuis, Cailotto, Dijk, Bergen, & Buijs, 2005; Tosini, Davidson, Fukuhara, Kasamatsu, & Castanon-Cervantes, 2007; Ueda et al., 2002; X. Yang et al., 2006). Behavioral analyses revealed that Rora-deficient *staggerer* mice have aberrant locomotor activity and unstable rhythmicity (Akashi & Takumi, 2005; Sato et al., 2004), further indicating that Rora is required for maintaining normal circadian rhythm. Interestingly, our recent transcriptomic analysis of LCLs from individuals with autism revealed that, in addition to RORA, as many as 14 other genes involving in regulation of circadian rhythm showed aberrant expression in cells from individuals with autism with language impairment (V. W. Hu, Sarachana et al., 2009). Moreover, children with autism are frequently reported to have disturbed sleep-wake patterns and abnormal hormone profiles, including melatonin, which is considered as a good marker for circadian rhythm because it is not easily influenced by environmental or social factors (Glickman, 2010). Interestingly,

overall reduced amplitude in melatonin rhythm, including diminished nocturnal values, has been reported in individuals with autism (Glickman, 2010; Kulman et al., 2000; Nir et al., 1995).

Rora is also known to have anti-inflammatory effects. *Staggerer* mutant mice also exhibit abnormal innate immunity characterized by an increased susceptibility to inflammatory stimuli (Kopmels et al., 1990; Kopmels, Mariani, Taupin, Delhaye-Bouchaud, & Wollman, 1991; Kopmels et al., 1992; Stapleton et al., 2005). When stimulated by the macrophage activators lipopolysaccharide, N-acetylmuramyl-L-alanyl-D-isoglutamine, or murabutide, macrophages of *staggerer* mice produce significantly higher levels of IL-1β, IL-6, and TNFα, in comparison with stimulated macrophages of WT mice, suggesting that macrophages of *staggerer* mice are in a state of general hyperexcitability (Kopmels et al., 1990; Kopmels et al., 1991; Kopmels et al., 1992). It was also reported that *staggerer* mice display a higher degree of lipopolysaccharide-induced lung inflammation and increased levels of IL-1β, IL-6, and macrophage inflammatory protein-2 than WT mice, suggesting enhanced susceptibility of *staggerer* mice to lipopolysaccharide-induced lung inflammation (Stapleton et al., 2005). Ectopic expression of Rora has been demonstrated to inhibit TNFα-induced IL-6, IL-8, and COX-2 expression. This anti-inflammatory effect of Rora is mediated through inhibition of the NFκB pathway. Rora negatively interferes with the NFκB signaling pathway by positively regulating the expression of IκBα, a negative regulator of the NFκB pathway, and reducing p65 translocation (Delerive et al., 2001). In the brain, Rora exerts bi-directional regulation of IL-6 in resting and reactive astrocytes. In resting astrocytes, Rora directly transactivates IL-

6 expression, whereas it indirectly inhibits IL-6 expression through the NFκB pathway in activated astrocytes (Journiac et al., 2009). These observations suggest that Rora may function as a negative regulator of inflammation. Recent studies have established an association between autism and inflammation. Neurogliosis and inflammatory reactions were reported in the cerebral cortex, white matter, and cerebellum of individuals with autism (Pardo, Vargas, & Zimmerman, 2005; Vargas, Nascimbene, Krishnan, Zimmerman, & Pardo, 2005; Zimmerman et al., 2005). Interestingly, expression of NFκB-p65 has been shown to be significantly increased in neurons, astrocytes, and microglia in the brain of people with autism relative to matched controls (Young, Campbell, Lynch, Suckling, & Powis, 2011). Moreover, cytokine and chemokine profiling analysis also revealed increased levels of analytes, including IL-1β, in individuals with autism (Suzuki et al., 2011).

Staggerer mice also develop muscular dystrophy. Lau and colleagues (1999) have shown that expression of a dominant-negative Rora lacking LBD delays the morphological differentiation of myotubes and induction of muscle-specific genes, including *MyoD* and myogenin, transcription factors critical for myotubule differentiation (Lau et al., 1999). In addition to aforementioned functions, Rora is also associated with development of both T and B lymphocytes (Dzhagalov, Giguere, & He, 2004; Dzhagalov, Zhang, & He, 2004), differentiation of T helper 17 (Th17) cells (X. O. Yang et al., 2008), hypoxia (Chauvet, Bois-Joyeux, Berra, Pouyssegur, & Danan, 2004), angiogenesis (Besnard et al., 2001), endoplasmic reticulum stress (Joo, Liao, Collins, Grissom, & Jetten, 2007; Zhu, McAvoy, Kuhn, & Smith, 2006), and lipid and cholesterol metabolism (Lau et al., 2008; Wada et al., 2008).

Behavioral analyses of staggerer mice

Research has also indicated functional abnormalities in Rora-deficient *staggerer* mice, including reactions to novelty (Lalonde, 1987b; Lalonde, Botez, & Boivin, 1987b; Lalonde, Manseau, & Botez, 1988; Misslin, Cigrang, & Guastavino, 1986), spatial learning (Bensoula et al., 1995; Caston, Chianale, & Mariani, 2004; Lalonde, Filali, Bensoula, Monnier, & Guastavino, 1996), cold adaptation (Bertin, Guastavino, & Portet, 1990; Guastavino, Bertin, & Portet, 1991), olfactory bulb characteristics (Deiss, Dubois, Lalonde, & Strazielle, 2001; Michel, Monnier, Guastavino, Propper, & Math, 2000), and reproductive behaviors (Bulloch, Hamburger, & Loy, 1982; Guastavino & Larsson, 1992; Guastavino, Boufares, & Crusio, 2005). *Staggerer* mice were reported to have abnormal patterns of maze patrolling (Goodall & Gheusi, 1987). The mutant mice had a reduction in the total ambulatory activity in a maze, unsurprisingly due to postural and gait abnormalities caused by disruption of cerebellar architecture. However, a behavioral study by Goodall and Gheusi (1987) revealed more interesting findings involving qualitative aspects of the maze patrolling by *staggerer* mice. Measuring the distribution of the subjects' visits to different maze locations and varying the configuration and the amount of familiarization with the maze, the authors found that the mutant mice, relative to normal mice, confined their ambulatory activity to a smaller number of different locations, which were more intensively visited (Goodall & Gheusi, 1987). *Staggerer* mice displayed a pronounced tendency to return to the place that was most recently visited, compared to a tendency by normal mice to avoid that location, suggesting that *staggerer* mice have a reduced tendency to pursue an initiated trajectory or altered novelty reactions. Abnormal

reactions to novelty of *staggerer* mice were also reported by several other studies (Lalonde, 1987b; Lalonde, Botez, & Boivin, 1987b; Lalonde et al., 1988; Misslin et al., 1986). Frederic and colleagues (2006) compared the stress response of *staggerer* and WT mice to novelty as well as their diurnal cycles of adrenocorticotropic hormone and corticosterone secretion. They found that *staggerer* mice displayed an enhanced endocrine response to novelty stress and lacked the diurnal shift in corticosterone under non-stressed conditions (Frederic, Chianale, Oliver, & Mariani, 2006), suggesting that *staggerer* mice exhibit abnormal reactions to novelty.

Using left-right and light-dark discrimination tests in a water-filled T-maze, Lalonde and Strazielle (2008) found that the acquisition rate of *staggerer* mice was slowed down during light-dark, but not left-right discrimination learning. The mutant mice were impaired in reversal training in both tasks, but not impaired in passive avoidance learning. (Lalonde & Strazielle, 2008). Spontaneous alternation and maze learning tests also showed that *staggerer* mutants did not alternate spontaneously and had deficits in the acquisition of maze learning (Lalonde et al., 1988). These observations indicate that *staggerer* mice are affected in spatial learning and have perseverative tendencies reminiscent of autism.

RORA and sex hormones

Disturbances in several reproductive functions have been reported in *staggerer* mice. Both male and female reproductive capacity are highly abnormal (Guastavino & Larsson, 1992; Guastavino, Larsson, & Jaisson, 1992; Guastavino, Larsson, Allain, & Jaisson, 1993). Although few *staggerer* males were reported to be sexually active, often showing a constant penile erection (Guastavino et al., 1992; Guastavino et al., 2005), male

staggerer mice generally do not mate partially due to motor disturbances associated with cerebellar abnormalities. However, some of their reproductive traits could be restored by environmental modifications (Feron & Baudoin, 1995; Feron & Baudoin, 1997). Social experience and probable sensory motor stimulation produced by the post-weaning cohabitation with several non-mutant mice could improve interactive behaviors of *staggerer* males when encountering sexually receptive non-mutant females (Feron & Baudoin, 1997). About 2 out of 3 *staggerer* females could reproduce (Guastavino et al., 2005) but they showed delayed onset of puberty, abnormalities in estrous cycle (Larsson, Guastavino, & Ly, 1986), a marked acceleration of the reproductive aging process (Guastavino & Larsson, 1992), reduced number of oocytes in the ovaries, and production of smaller litters (Guastavino et al., 2005). These observations suggest that Rora may also play a role in reproductive function and/or regulation rather than be restricted to cerebellar or CNS development.

In heterozygous *staggerer* mice, Purkinje cell loss is associated with sex (**Figure 10**). Heterogenous *staggerer* males displayed a significant reduction of Purkinje cells by 1-3 months, whereas loss of the cells began at 9-13 months in female *staggerer* mice (Doulazmi et al., 1999; Janmaat et al., 2011). These findings indicate that males are more susceptible to and/or females are more protected from Purkinje cell loss triggered by Rora deficiency, suggesting the influence of sex on the pathology of Rora deficiency. Interestingly, Janmaat and colleagues (2011) found that plasma concentrations of 17β-estradiol and progesterone, were reduced in $Rora^{+/sg}$ mice relative to WT controls. In fact, plasma concentrations of 17β-estradiol correlated directly with Purkinje cell numbers in both sexes of $Rora^{+/sg}$ and WT mice (Janmaat et al., 2011), suggesting that 17β-estradiol

may play an important role in Purkinje cell survival in both Rora-deficient and normal mice. Using computational approaches to analyze three public available chromatin immunoprecipitation (ChIP)-based datasets: ChIP-seq, ChIP-PET, and ChIP-on-chip datasets, Gu and colleagues (2010) identified ERα-associated hierarchical transcriptional regulatory networks in the breast cancer cell line MCF7. Interestingly, RORA was among transcription factors identified to be associated with ERα in all three ChIP datasets (Gu et al., 2010). Moreover, elevated expression of *RORA1* has been reported to enhance 17β-estradiol-induced transcriptional activation of ERα in MCF7 cells (Dong et al., 2010). These observations suggest an association of *RORA* and sex hormones, especially estradiol.

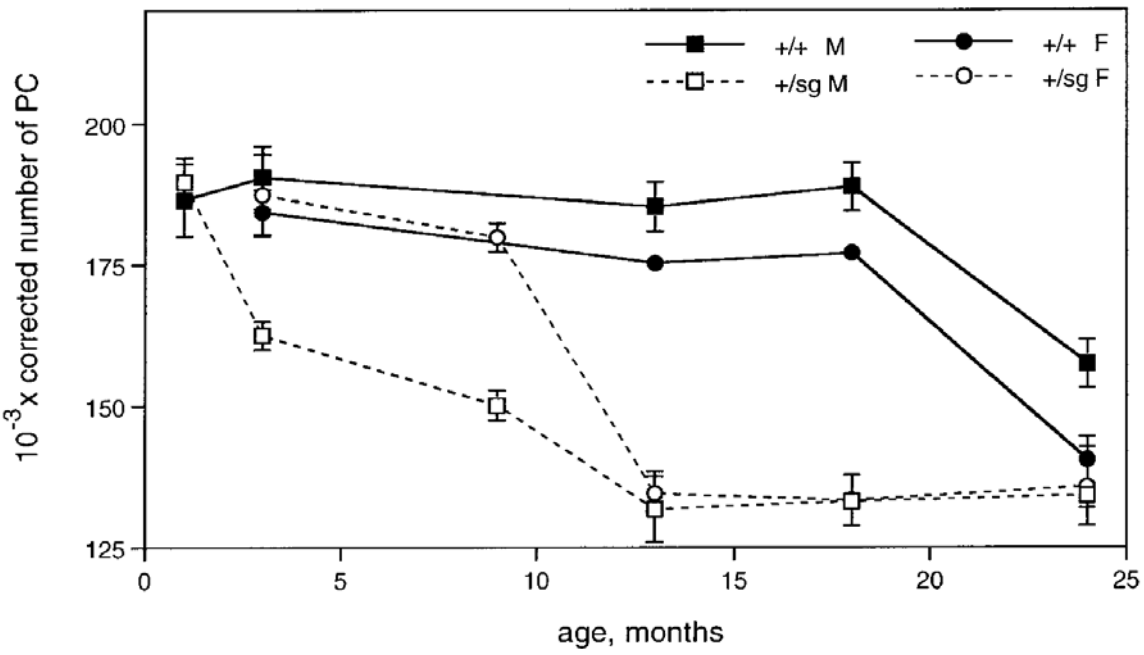

Figure 10. Changes in the number of Purkinje cells throughout mouse lifespan. The number of Purkinje cells in WT (+/+) and *Rora*$^{+/sg}$ (+/sg) males (M) and females (F) from 1 to 24 months were measured. Values are mean ± S.E.M. Values in WT males remained higher than in WT females. In WT, a significant deficit in cell number is observed only in 24-month-old animals of both genders. As compared to age-and gender-matched WT, a deficit exists at 13 months and afterwards in female *Rora*$^{+/sg}$, whereas it is already present in 3- and 9-month-old male *Rora*$^{+/sg}$. At 24 months, no difference is observed between WT females and *Rora*$^{+/sg}$ of either gender. Adapted from (Doulazmi et al., 1999).

Chapter 3: Materials and Methods

Cell culture

The human neuroblastoma cells SH-SY5Y (ATCC, Manassas,VA) were cultured in 1:1 Modified Eagle's Medium (MEM) and Ham's F12 media (MediaTech, Manassas, VA) supplemented with 15% (v/v) fetal bovine serum (Atlanta Biologicals, Lawrenceville, GA) and 1% penicillin/streptomycin (P/S; MediaTech). Cells were maintained at 37°C with 5% CO_2, and split 1:2 every 3–4 days when the cells reached ~80% confluency. For harvesting, the cells were treated with trypsin-EDTA (MediaTech) for 2–3 min to release them from the surface of the culture flask. Complete growth medium was then added to the flask containing suspension cells to inactivate trypsin. Cells were transferred to a sterile centrifuge tube and pelleted by spinning at 800 rpm for 5 min at 4°C and gently washed twice with ice-cold PBS.

Frozen human brain tissues

Frozen post-mortem prefrontal cortex (BA9/10) tissues from individuals with autism (n = 3) and from sex- and age-matched typically developing individuals (n = 3) were obtained through the Autism Tissue Program (San Diego, CA). All frozen brain tissues were from male donors and were preserved by the Harvard Brain Tissue Resource Center, Harvard Medical School. The list of human brain tissues is shown in **Supplemental Table 1**.

Hormone treatment

For hormone treatment, SH-SY5Y cells were cultured in culture flasks until the cultures became ~80% confluent. Confluent cells were carefully washed twice with phenol red-free 1:1 DMEM/F12 media (MediaTech) supplemented with 15% charcoal dextran-treated serum (Atlanta Biologicals) and 1% P/S, and then cultured in the phenol red-free medium for 24 hrs. Lyophilized 4,5α-dihydrotestosterone (DHT; Sigma-Aldrich, St. Louis, MO) and 17β-estradiol (E2; Sigma-Aldrich) were diluted with molecular biology grade absolute ethanol (Fisher Scientific, Pittsburgh, PA) to make 1μM DHT or 1μM E2 stock solutions. The stock solutions were further diluted with prewarmed complete phenol red-free culture medium to the desired final concentrations for hormone treatment and carefully added to the confluent cells. Cells were incubated in the hormone-supplemented phenol red-free medium for the desired treatment time at 37°C with 5% CO_2.

Prediction of transcription factor binding elements

Putative binding sites of AR and ERα in the human *RORA1* promoter region and putative binding sites of RORA in the promoter regions of *A2BP1, CYP19A1, HSD17B10, ITPR1, NLGN1*, and *NTRK2* were predicted using PROMO 3.0 (Farre et al., 2003; Messeguer et al., 2002), JASPAR (Bryne et al., 2008), and SABiosciences EpiTect ChIP Search Portal (SABiosciences; http://www.sabiosciences.com/chipqpcrsearch.php) programs. For each target gene, a total of 3-4 predicted transcription factor binding sites were selected for chromatin immunoprecipitation analyses.

Chromatin immunoprecipitation

Chromatin immunoprecipitation (ChIP) for ChIP-qPCR analysis of AR/ERα binding elements in the *RORA* promoter region and ChIP-on-chip analysis was performed using the Millipore EZ-ChIP Chromatin Immunoprecipitation Kit (Millipore, Billerica, MA) according to the manufacturer's protocol. Briefly, the human neuronal cell line SH-SY5Y was cultured in complete growth medium in a T-175 flask until ~80% confluency (approximately 1.5×10^7 cells). The medium was then substituted with phenol red-free medium and the confluent cells were treated with 1nM DHT or 1nM E2 for 2 hrs following the aforementioned hormone treatment procedure. The medium was then carefully removed without disturbing the cells. The hormone-treated cells were fixed with 37% formaldehyde for exactly 10 min to crosslink chromatin. The crosslinking reaction was terminated by addition of 10% glycine, then ice-cold PBS supplemented with protease inhibitor cocktail was added to the culture flask to wash and chill the cells. The crosslinked cells were dislodged from the flask by scraping gently with a cell scraper and then transferred to a pre-chilled centrifuge tube. Crosslinked cells were pelleted and stored at -80°C until use.

Nuclear extraction was performed using the Active Motif Nuclear Extract Kit (Active Motif, Carlsbad, CA) according to the manufacturer's protocol. Nuclear pellets were resuspended in SDS Lysis Buffer and sonicated on wet ice to shear crosslinked chromatin to 200-1,000 bp using a Heat Systems-Ultrasonics W-380 sonicator (Heat Systems-Ultrasonics/Misonix, Farmingdale, NY) set to 30% of maximum output power for 20 × 10 seconds with 1 min interval. Sonicated chromatin was divided into several aliquots for immunoprecipitation reactions and stored at -80°C until use. Each immunoprecipitation

reaction was conducted using 1μg of mouse monoclonal anti-AR (AR-441), mouse monoclonal anti-ERα (ERα D-12), or normal mouse IgG antibody (Santa Cruz Biotechnology, Santa Cruz, CA). Immunoprecipitated chromatin was then reverse-crosslinked by adding 5 M NaCl to the final concentration of 0.2 M and incubated at 65°C overnight. DNA from the immunoprecipitated chromatin was isolated and purified using Millipore DNA purification columns (Millipore).

Because the sonicator was dysfunctional after the laboratory was moved, chromatin immunoprecipitation for subsequent ChIP experiments, including ChIP-qPCR analysis of RORA binding elements in the promoter region of RORA targets and sequential chromatin immunoprecipitation (ChIP-reChIP) analysis, was conducted using the ChIP-IT Express Enzymatic Kit (Active Motif) following the manufacturer's instructions. Briefly, confluent SH-SY5Y cells (approximately 1.5×10^7 cells in a T-175 flask) were fixed with 10% formaldehyde and the fixation reaction was stopped by adding 10% glycine. The cells were washed with 10 ml ice-cold PBS for 5 seconds, then 6 ml ice-cold PBS supplemented with 0.5 mM (final concentration) PMSF supplied in the kit was added to the culture flask to wash and chill the cells. The crosslinked cells were transferred from the flask to a pre-chilled centrifuge tube by scraping gently with a cell scraper. Crosslinked cells were pelleted and stored at -80°C until use.

Cells were homogenized using a dounce homogenizer with a tight pestle to release the nucleus. Optimal cell lysis was assessed under a phase contrast microscope using a hemocytometer. The cell lysate was transferred to a 1.7 ml microcentrifuge tube and centrifuged for 10 minutes at 5,000 rpm (2,400 RCF) in a 4°C microcentrifuge to pellet nuclei. Chromatin was then isolated from the nuclear pellets and sheared into 150-1,000bp

by incubating with 10U/ml (final concentration) Enzymatic Shearing Cocktail (Active Motif) at 37°C for exactly 10 min. The enzymatic shearing reaction was stopped by adding EDTA to a final concentration of 10mM EDTA and chilling the reaction tube on ice for 10 min. Optimal shearing was assessed by agarose gel electrophoresis. For each chromatin immunoprecipitation reaction, enzymatically-sheared chromatin containing ~7-25 μg chromatin DNA was immunoprecipitated using 1ug antibody and 25ul Protein G Magnetic Beads (Active Motif). The list of antibodies for ChIP analysis is shown in **Supplemental Table 2**. Immunoprecipitated chromatin was reverse-crosslinked and DNA was isolated and purified from the chromatin using the ChIP DNA Purification Kit (Active Motif).

Sequential chromatin immunoprecipitation

Sheared, formaldehyde-crosslinked chromatin was prepared using the ChIP-IT-Express Enzymatic Kit (Actif Motif). Sequential chromatin immunoprecipitation (ChIP-reChIP) was conducted using the Re-ChIP-IT Kit (Actif Motif) according to the manufacturer's protocol. Briefly, 1μg of mouse anti-AR, anti-ERα, anti-RORA, or IgG antibody was used to immunoprecipitate sheared chromatin. The immunoprecipitated chromatin was then washed to remove the first antibody on the chromatin. The second antibody against each coregulator protein or IgG antibody (1μg) was then added to the tube to re-immunoprecipitate the chromatin. DNA from re-immunoprecipitated chromatin was isolated and purified using the ChIP DNA Purification Kit (Active Motif). The list of antibodies for sequential ChIP is shown in **Supplemental Table 2**.

ChIP-on-chip analysis

Chromatin was isolated from SH-SY5Y cells and sonicated per the aforementioned chromatin immunoprecipitation procedure. Sheared chromatin was immunoprecipitated with 1μg rabbit anti-RORA1 or normal rabbit IgG antibody (Santa Cruz Biotechnology). Immunoprecipitated DNA was purified using Millipore DNA purification columns (Millipore) and amplified using the Whole Genome Amplification 2 Kit (Sigma Aldrich). The amplification product of each immunoprecipitation reaction was purified and hybridized on Affymatrix GeneChip Human Promoter 1.0R microarrays (n = 3 arrays/each ChIP reaction; Affymetrix, Santa Clara, CA). Probes significantly enriched in RORA-immunoprecipitated DNA relative to IgG-immunoprecipitated DNA were identified using the Partek Genomics Suite software (Partek, St. Louis, MO).

Real-time, quantitative PCR analysis

Real-Time qPCR analysis was conducted using an ABI Prism 7300 Sequence Detection System (Applied Biosystems, Foster City, CA) to determine the enrichment of each AR/ERα/RORA binding element in immunoprecipitated or sequentially-immunoprecipitated DNA. Primers for qPCR analysis were designed using Primer3 software (http://frodo.wi.mit.edu/; (Rozen & Skaletsky, 2000)) and synthesized by Integrated DNA Technologies (IDT; Coralville, IA). Input DNA was diluted into five 10-fold serial dilutions and included in qPCR analysis. Relative enrichment values of AR/ERα/RORA binding elements in each sequentially-immunoprecipitated chromatin were calculated using standard curves obtained from the enrichment of respective

AR/ERα/RORA binding elements in the 10-fold serial dilutions of input DNA. The list of primers is shown in **Supplemental Table 3**.

siRNA-mediated knockdown of AR and ERα

Knockdown of AR or ERα was conducted using Lipofectamine RNAiMAX transfection agent (Invitrogen, Carlsbard, CA) according to the manufacturer's protocol. Briefly, SH-SY5Y cells were cultured in complete growth medium without antibiotics in a 6-well culture plate. When cells were ~50% confluent, the medium was substituted with phenol red-free culture medium without antibiotics and the cells were further incubated for 24 hrs. AR- or ERα siRNA (150 pmol) was diluted in 250 µl phenol red-free Opti-MEM I Reduced Serum Medium (Invitrogen). Lipofectamine RNAiMAX (7.5 µl) was diluted in 250 µl phenol red-free Opti-MEM I Reduced Serum Medium in a separate tube. Then, the diluted siRNA and the diluted Lipofectamine RNAiMax were combined. The siRNA-Lipofectamine complex was incubated at room temperature for 5 min and added to the cells to a final siRNA concentration of 10nM. The cells were incubated for 24 hrs and then treated with 1nM DHT, 1nM E2, or ethanol, for 2 hrs according to the aforementioned hormone treatment procedure before harvesting for subsequent analysis. The list of siRNAs is shown in **Supplemental Table 2**.

shRNA transfection

SH-SY5Y cells were cultured in a 6-well culture plate containing complete growth medium without antibiotics (approximately $2.5x10^5$ cells per well) until cells were ~70% confluent. For each well, the cells were transfected with 2.5µg RORA1 shRNA (Santa

Cruz Biotechnology) or 2.5µg negative control shRNA (Santa Cruz Biotechnology) using Lipofectamine LTX and PLUS reagent (Invitrogen) according to the manufacturer's protocol. Briefly, shRNA (2.50 µg) was diluted in 500 µl of Opti-MEM I Reduced Serum Medium (Invitrogen) and 1.25 µl of PLUS reagent was added to the diluted shRNA solution. Lipofectamine LTX (25 µl) was then added to the shRNA-PLUS solution, incubated for 25 min at room temperature to form shRNA-Lipofectamine LTX-PLUS complexes, and added to the cells. The cells were then incubated with the shRNA-Lipofectamine LTX-PLUS complexes at 37°C and 5% CO_2 for 24 hrs before harvesting. The list of shRNAs is shown in **Supplemental Table 2**.

Quantitative RT-PCR analysis

Quantitative RT-PCR analyses were performed as described [8]. Total RNA from the cells was isolated using TRIzol (Invitrogen) and purified using the RNeasy Mini Kit (Qiagen) following the manufacturers' instructions. Human brain tissues were homogenized in the Bullet Blender Homogenizer (Next Advance, Averill Park, NY) using nuclease-free glass beads, and total RNA was isolated from homogenized tissues using RNeasy Mini Kit (Qiagen). A total of 1µg purified total RNA was used for cDNA synthesis using iScript cDNA Synthesis Kit (BioRad, Hercules, CA) according to the manufacturer's protocols. The reaction was incubated at 25°C for 5 min, followed by 42°C for 30 min, and ending with 85°C for 5 min. After reverse transcription, the cDNA reaction mixture was diluted to a volume of 50µl with nuclease-free water and used as a template for qPCR analyses. Real-time PCR analyses were conducted using an ABI Prism 7300 Sequence Detection System (Applied Biosystems, Foster City, CA). Primers for qRT-PCR analyses designed by

Primer3 are listed in **Supplemental Table 3**. The relative quantity of transcripts in each sample was calculated using standard curves obtained from relative quantity of 18S RNA transcript in 10-fold serial dilutions of that sample.

Cloning

DNA was isolated from SH-SY5Y cells using the DNeasy Blood and Tissue Kit (Qiagen, Valencia, CA) according to the manufacturer's protocols. The promoter regions of *RORA* were then amplified by a PCR method tailored for long stretches of nucleotides using the GoTaq Long PCR Master Mix (Promega, Madison, WI) and DNA primers tagged with SfiI restriction sites at the 5' end (Integrated DNA Technologies, Coralville, IA) according to the manufacturer's protocols. Primers for PCR cloning are listed in **Supplemental Table 3**. Briefly, a total of 0.5 μg of purified human genomic DNA isolated from SH-SY5Y cells was combined with the GoTaq Long PCR Master Mix and 10μM (final concentration) of each DNA primer. The thermal cycling condition was set as follows: 95°C for 2 min, 30 cycles of 92°C for 30 sec and 65°C for 15 min, followed by 72°C for 10 min. PCR products were analyzed by gel electrophoresis using 1% agarose. The bands with expected sizes were excised from the gel and purified using the Wizard SV Gel and PCR Clean-Up System (Promega).

Purified PCR products with different sizes were then separately inserted into pGEM-T Easy vector (Promega) containing lacZ and ampicillin-resistant genes following the manufacturer's instructions. The vector containing each PCR product was transformed into JM109 High-Efficiency Competent *E.coli* cells (Promega) by heat-shocking at exactly 42°C in a water bath for 50 sec. Transformed bacteria were spread on duplicate LB agar

plates containing 100μg/ml ampicillin, 0.5mM IPTG, and 80μg/ml X-Gal, and incubated at 37°C overnight for blue-white screening. Well-isolated white colonies were selected and further cultured in LB medium supplemented with 125μg/ml ampicillin at 37°C for 12-16 h with shaking at 250 rpm.

Plasmid DNA was purified from bacteria using Wizard Plus SV Minipreps DNA Purification System (Promega) according to the manufacturer's protocol. Presence of *RORA* promoter in the plasmid was validated by long PCR analysis using GoTaq Long PCR Master Mix (Promega), followed by gel electrophoresis. *RORA* promoter inserts were then released from the pGEM-T Easy plasmids using SfiI restriction enzyme and purified by gel electrophoresis. The luciferase vector pGL4.20[luc2/Puro] (Promega) containing firefly luciferase, puromycin-resistant, and ampicillin-resistant genes was prepared by digestion with the SfiI restriction enzyme and dephosphorylation using TSAP Thermosensitive Alkaline Phosphatase (Promega) to prevent self-recircularization of the linearized vector during ligation. *RORA* promoter inserts were then ligated into the dephosphorylated luciferase vector using LigaFast Rapid DNA Ligation System (Promega) and transformed into the JM109 High-Efficiency Competent E.coli. Transformed bacteria were cultured on LB agar plate containing 125μg/ml ampicillin. Colonies of bacteria were harvested and further cultured in LB medium containing 125μg/ml ampicillin overnight. Luciferase plasmids containing the *RORA* promoter regions were then purified from the transformed bacteria using Wizard Plus SV Minipreps DNA Purification System. Presence of *RORA* promoter insert was confirmed by long PCR analysis.

Dual-luciferase reporter assays

The pGL4.20[luc2/Puro] vector containing a specific *RORA* promoter region was mixed with the pGL4.74[hRluc/TK] vector containing *Renilla reniformis* luciferase gene with a ratio of 50:1 in phenol red-free Opti-MEM I reduced serum medium (Invitrogen). The FuGENE HD Transfection Reagent (Promega) was then added to the medium containing the vectors to obtain a ratio of 3:1 (i.e., 3 μl transfection agent for 1 μg DNA). The mixture was added to a 96-well plate containing SH-SY5Y cells (~2×10^4 cells/well) and incubated at 37°C, 5% CO_2, for 48 h. The transfected cells were treated with 10 nM DHT, 10 nM E2, or ethanol control for 2 h, then dual-luciferase reporter assays were performed using Dual-Luciferase Reporter Assay System (Promega) according to the manufacturer's protocol. Briefly, lysis buffer was added to the 96-well plates containing hormone-treated transfected cells and complete lysis of cells was assessed under an inverted microscope. Cell lysates were collected and transferred to Cellstar 96-well plate (BioExpress, Kaysville, UT). A Veritas Microplate Luminometer (Turner Biosystems, Sunnyvale, CA) was used for development of firefly and Renilla luminescences as well as for measurement of both firefly and Renilla luciferase activity signals. Firefly luciferase luminescence in each well was normalized by Renilla luciferase luminescence in the same well.

Co-immunoprecipitation analysis

The SH-SY5Y cells were cultured in complete growth medium until the confluency was approximately 70-80% and hormone treatment was conducted as mentioned above. Co-immunoprecipitation assays were then conducted using Pierce Crosslink Magnetic

IP/Co-IP Kit (Thermo Scientific, Rockford, IL) according to the manufacturer's protocol. Briefly, the medium was removed from the flask containing cells. Then, cells were washed with ice-cold PBS containing phosphatase and deacetylase inhibitors and whole-cell lysis buffer was added directly into the flask. Protein A/G magnetic beads for immunoprecipitation were treated with anti-NCOA1, anti-NCOA5, anti-SUMO-1, anti-FHL2, or IgG antibody, and the antibody-bound magnetic beads were crosslinked with 20μM disuccinimidyl suberate (DSS). The list of antibodies used is shown in **Supplemental Table 2**. The crosslinked magnetic beads were mixed with SH-SY5Y whole-cell extract and incubated overnight at 4°C. The magnetic beads were then collected and protein complexes bound to the beads were eluted. Eluted immunoprecipitated proteins were analyzed to determine the enrichment of AR, ERα, or RORA protein by western blot analysis.

BCA assays

Protein concentration was determined by BCA assays using Pierce BCA Protein Assay Kit (Thermo Scientific) according to the manufacturer's directions for microplate method. Briefly, the sample was mixed with BCA reagent containing bicinchoninic acid (BCA) and cupric sulfate and incubated at 37°C for 30 min. To determine protein concentration in an unknown sample, serial dilutions of albumin (25 – 2,000 μg/ml) were included in the analysis and used for creating a standard curve. The absorbance of each sample was measured at 562 nm using a Synergy HT Multi-Mode microplate reader (BioTek, Winooski, VT). The protein concentration in each unknown sample was

calculated using standard curves obtained from absorbance values of the serial dilutions of albumin standards.

Western blot analysis

A total of 20-30μg of immunoprecipitated protein was mixed with 5X Thermo Scientific Lane Marker Non-Reducing Sample Buffer (Thermo Scientific) containing 0.3M Tris-HCl, 5% SDS, 50% glycerol, and pink tracking dye. The sample was boiled for 5 min and loaded onto a Mini-PROTEAN TGX precast polyacrylamide gel (Biorad, Hercules, CA). Electrophoresis was conducted at 200V using 1X Tris-glycine buffer containing 25mM Tris base, 190mM glycine, and 0.1% SDS, as a running buffer. Proteins on the gel were then transferred to PVDF membrane and blocking was performed for 1 h at 4°C using 5% (w/v) non-fat dry milk (Biorad) in TBST buffer containing 2.42g Trizma-HCl, 8g NaCl, and 1X Tween20. Protein detection was conducted by incubating the PVDF membrane with anti-AR, anti-ERα, anti-RORA, or anti-RORA1 antibody (1:200 in 1% milk/TBST) at 4°C overnight. The membrane was washed and treated with donkey secondary antibody conjugated with horseradish peroxidase (HRP; Santa Cruz Biotechnology; 1:2,500) for 1h at room temperature. Protein visualization was performed using a chemiluminescence method by incubating the membrane in chemiluminescence substrates (PerkinElmer, Waltham, MA). Protein signals on the membrane were detected using ChemiDoc XRS+ Imager (Biorad).

Confocal immunofluoresecence analysis

Human tissue arrays from Dr. Janine LaSalle's laboratory (University of California, Davis) were obtained through the Autism Tissue Program (San Diego, CA). Each array contains 600 μm diameter x 5 μm thick sections in triplicate from the BA9 region of the prefrontal cortex from individuals with autism and sex- and age-matched controls as well as from individuals with a variety of developmental disorders as previously described (Nagarajan, Hogart, Gwye, Martin, & LaSalle, 2006). Confocal immunofluorescence analysis of RORA and aromatase was performed using the Alexa Fluor-conjugated secondary antibody method of detection. Briefly, a tissue array was deparaffinized in xylene and rehydrated using a dilution series of 100%, 95% and 75% ethanol. The array slide was then subjected to heat-induced antigen retrieval by incubation in Tris-EDTA buffer (10 nM Tris Base, 1 mM EDTA, 0.05% Tween 20, pH 9.0) at 95°C for 25 minutes.

Rabbit polyclonal antibody (1:50 final dilution) against RORA (4 μg/ml, Santa Cruz Biotechnology: sc-28612), goat polyclonal antibody (1:50 dilution) against aromatase (4 μg/ml, Santa Cruz Biotechnology: sc-14245), and mouse monoclonal antibody (1:100 dilution) against MAP2 (5 μg/ml, Invitrogen) were pooled and added to the tissue array in a humidified chamber. After overnight incubation at 4°C, unbound primary antibodies were removed by washing the slide 3 times with PBS. Alexa Fluor 488-conjugated donkey anti-mouse (1:200 final dilution), Alexa Fluor 546-conjugated donkey anti-goat (1:200), and Alexa Fluor 647-conjugated donkey anti-rabbit (1:200) secondary antibodies (Invitrogen) were pooled and added to the slide for 45 min at room temperature. The slide was washed and incubated with 4′, 6′-diamidino-2-phynylindole dihydrochloride (DAPI) for 5 min at room temperature to counterstain the nuclei, mounted using ProLong Gold antifade reagent

(Invitrogen), and incubated in the dark at room temperature for 24 hrs before imaging. The fixed slide was imaged using a Zeiss LSM 710 confocal microscope (Carl Zeiss, Thornwood, NY) with a 60X objective lens. The images were collected using ZEN 2009 software (Carl Zeiss). The same laser power and other scanning parameters were maintained for all specimens.

Tissue images were coded with numbers and letters and analyzed in blind fashion using Volocity software (PerkinElmer, Waltham, MA). For each specimen, 40–50 prefrontal cortical neurons identified by distinct expression of MAP2 fluorescence and nuclear staining were selected for quantification of RORA and aromatase fluorescence intensities. The mean fluorescence intensity values from all neurons in each specimen were averaged and normalized by background subtraction.

Statistical analysis

Paired Student *t* test was used for statistical significance of differences in numerical data. All of the statistical tests were 2-sided. *P* value of less than 0.05 was considered to be statistically significant.

Chapter 4: Results

Male and female sex hormones oppositely regulate *RORA* expression in human neuroblastoma cells

Because RORA is a hormone-dependent transcription factor that is involved in a variety of functions impacted in autism, we sought to investigate the effects of both male and female sex hormones on *RORA* expression. Inasmuch as estrogen is known to have neuroprotective effects on the brain and RORA has been reported to be neuroprotective against oxidative stress (Boukhtouche, Vodjdani et al., 2006) and inflammation (Delerive et al., 2001), we first treated the human neuroblastoma cell line SH-SY5Y with different concentrations of 17β-estradiol, and measured RORA expression by qRT-PCR analyses. The estradiol treatment significantly enhanced RORA expression, and the greatest upregulation (15-fold) of *RORA* was observed when the cells were treated with 1 nM estradiol (**Figure 11A**). We also conducted a time-course experiment to investigate changes in *RORA* expression at different time points after estradiol exposure. The time-course study revealed that *RORA* expression was highest at 2 hrs after estradiol treatment, and the upregulation of *RORA* could be observed as long as 24 hrs after the treatment (**Figure 11B**).

To determine whether androgen also influences *RORA* expression, dose-effect and time-course experiments using dihydrotestosterone (DHT) were performed in the same manner as the aforementioned estradiol treatment. Interestingly, in contrast to estradiol treatment, DHT treatment caused a decrease in *RORA* expression compared with mock

treatment (**Figure 11C**). A time-course study showed that the greatest suppression of *RORA* was observed between 2 and 4 hrs, and downregulation of *RORA* could be observed as long as 24 hrs after DHT treatment (**Figure 11D**). This unexpected result (that is, decrease in *RORA* expression) led us to investigate whether or not *RORA* might be a transcriptional target of both estrogen receptor (ER) and androgen receptor (AR) by chromatin immunoprecipitation (ChIP)-PCR analyses.

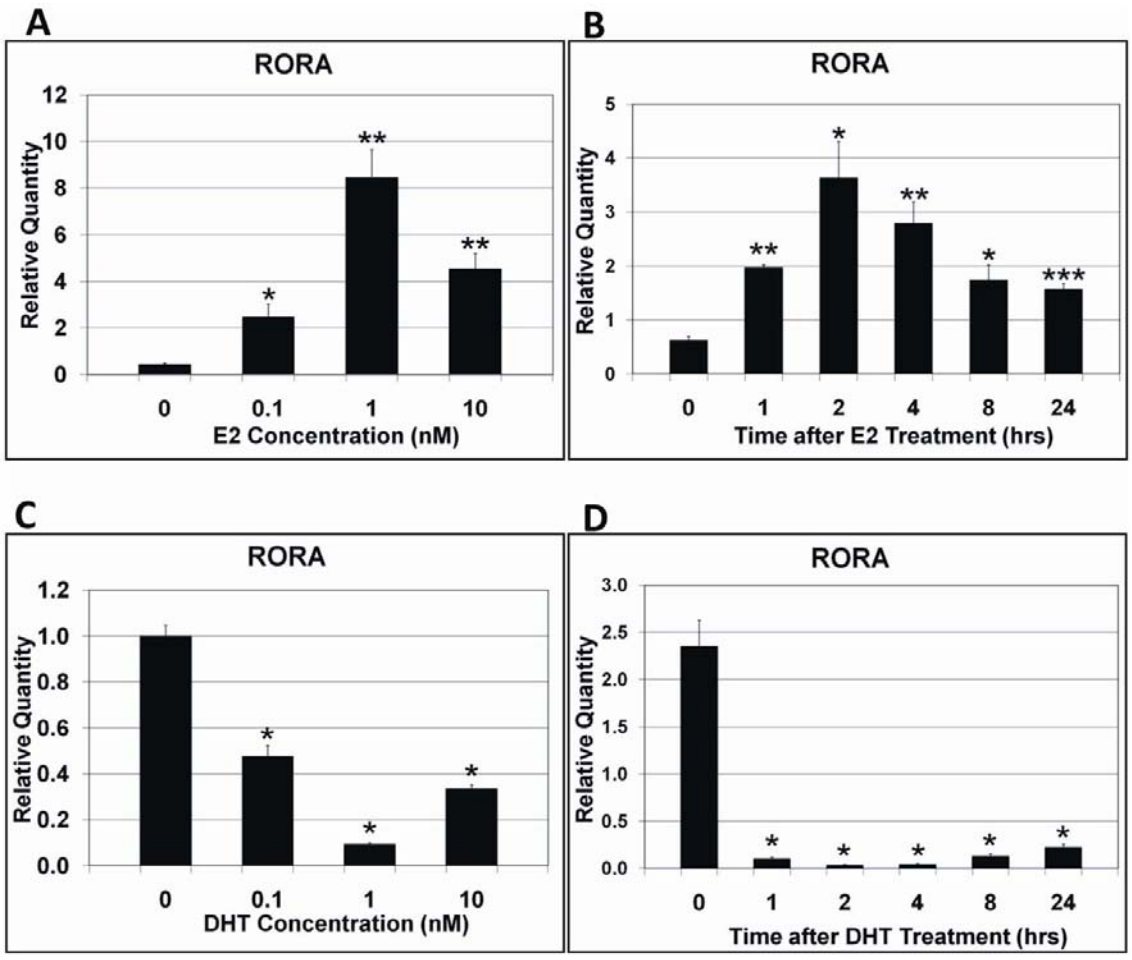

Figure 11. Effect of sex hormones on *RORA* expression in SH-SY5Y cells. (A) Dose-response to estradiol. The cells were treated with 0.1, 1, or 10 nM 17β-estradiol (E2) for 2 hrs and *RORA* expression was measured by qRT-PCR analyses (n = 3 per treatment group). (B) Time-course of response to estradiol. The cells were treated with 1 nM 17β-estradiol and qRT-PCR analyses (n = 3 per time point) were conducted to determine *RORA* expression at different times after hormone addition. (C) Dose-response to DHT. The cells were treated with 0.1, 1, or 10 nM DHT for 2 hrs and *RORA* expression was measured by RT-qPCR analyses (n = 3 per treatment group). (D) Time-course of response to DHT. The cells were treated with 10 nM DHT and qRT-PCR analyses (n = 3 per time point) were

conducted to determine *RORA* expression at different times after hormone addition. Error bars indicate S.E.M. (*P < 0.05, **P < 0.01, ***P < 0.005, versus mock-treatment control). (Adapted from (Sarachana, Xu, Wu, & Hu, 2011b); courtesy of Minyi Xu)

RORA is a transcriptional target of androgen and estrogen receptors

DHT and estradiol are known to exert their transcriptional regulatory functions through androgen receptor (AR) and estrogen receptor alpha (ERα), respectively. To investigate whether *RORA* might be a direct transcriptional target of either AR or ERα, we first identified potential binding sites for AR and ERα within 10 kb upstream of the *RORA* transcription start site using JASPAR, PROMO 3.0, and SABioscience ChampionChIP Real-Time PCR databases (Bryne et al., 2008; Farre et al., 2003; Messeguer et al., 2002). Three potential AR binding sites (namely ARbs-I-III) and four potential ERα binding sites (namely ERbs-I-IV) were selected for ChIP-qPCR analyses (**Figure 12A**). The list of all potential binding sites and their genomic locations is shown in **Supplemental Table 4**. Neuroblastoma cells, treated with 1 nM DHT or 1 nM estradiol, were employed for the ChIP assays using anti-AR or anti-ERα antibody, respectively. Interestingly, the enrichment of the AR binding sites in anti-AR-IP DNA was significantly increased when the cells were treated with DHT, compared with mock treatment (**Figure 12B**). The highest enrichment was observed in the ARbs-I region. Similarly, we found a significant increase in enrichment of the ERα binding sites in anti-ERα-IP DNA when the cells were treated with estradiol (**Figure 12C**). The ERbs-II site exhibited the greatest enrichment (~70-fold), compared with the other potential ER binding sites. These data indicate that *RORA* is likely a direct transcriptional target of both AR and ERα, with DHT and estradiol treatment significantly increasing the binding of AR and ER, respectively, to the *RORA* promoter region.

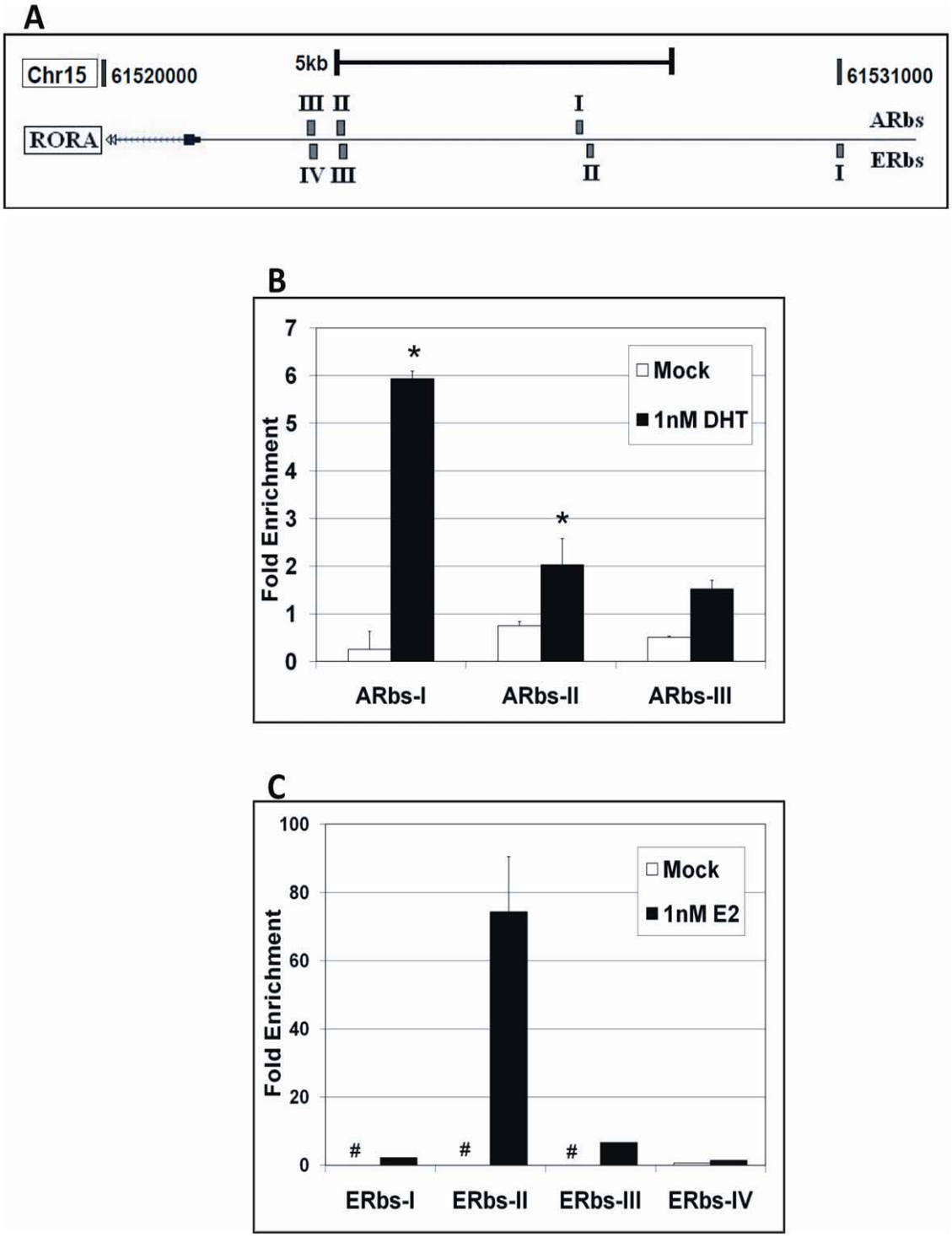
A
Chr15
61520000
5kb
61531000
III II
I
ARbs
RORA
IV III
II
I
ERbs
B
Fold Enrichment
Mock
1nM DHT
*
*
ARbs-I
ARbs-II
ARbs-III
C
Fold Enrichment
Mock
1nM E2
#
#
#
ERbs-I
ERbs-II
ERbs-III
ERbs-IV

Figure 12. *RORA* is a transcriptional target of both AR and ER. (A) Schematic diagram showing the upstream region of the *RORA* gene (edited from the UCSC Genome Browser). Potential AR and ER binding sites are labeled (ARbs = AR potential binding site, ERbs = ER potential binding site). (B) Chromatin Immunoprecipitation followed by qPCR (ChIP-qPCR) analyses of AR potential binding sites on the *RORA* gene promoter region. Sonicated chromatin from SH-SY5Y cells treated with 1 nM DHT for 2 hrs was immunoprecipitated (IP) using anti-AR or IgG antibody. Parallel samples were mock-treated with the hormone delivery vehicle, ethanol. The enrichment of each AR binding site in anti-AR-IP DNA was determined by qPCR analyses (n = 3), and normalized to the enrichment in IgG-IP DNA (control). Error bars indicate S.E.M. (*$P < 0.01$ versus mock-treatment control). (C) ChIP-qPCR analyses of ERα potential binding sites on the *RORA* gene promoter region. Sonicated chromatin from SH-SY5Y cells treated with 1 nM 17β-estradiol (or vehicle) for 2 hrs was immunoprecipitated using anti-ERα or control IgG antibody. The enrichment of each ERα binding site in anti-ERα-IP DNA was determined by qPCR analyses (n = 3), and normalized to the enrichment in IgG-IP DNA. Error bars indicate S.E.M. (#Undetectable amount of ERα binding sites in the mock-treatment control). (Adapted from (Sarachana, Xu, Wu, & Hu, 2011b))

AR and ERα are required for sex hormone regulation of *RORA*

Androgen and estrogen are also able to regulate their transcriptional targets through AR- and ERα-independent mechanisms. To determine whether androgen and estrogen require AR and ERα, respectively, to regulate *RORA* expression, we performed siRNA-mediated knockdowns of AR and ERα in the human neuronal cells SH-SY5Y and examined the effect of AR and ERα knockdowns on *RORA* expression in the presence of sex hormones. SH-SY5Y cells were transfected with AR siRNA, ERα siRNA, or vehicle control, and treated with 1nM DHT, 1nM E2, or ethanol. *RORA* expression was determined by RT-qPCR analysis. Interestingly, when AR was knockdown, the suppressing effect of DHT on *RORA* expression was completely diminished (**Figure 13A**), indicating that AR is required for DHT regulation of *RORA*. On the other hand, when ERα was knockdown, the enhancing effect of E2 on *RORA* expression was significantly reduced although not completely diminished (**Figure 13B**), indicating that ERα is required for effective E2 regulation of *RORA*.

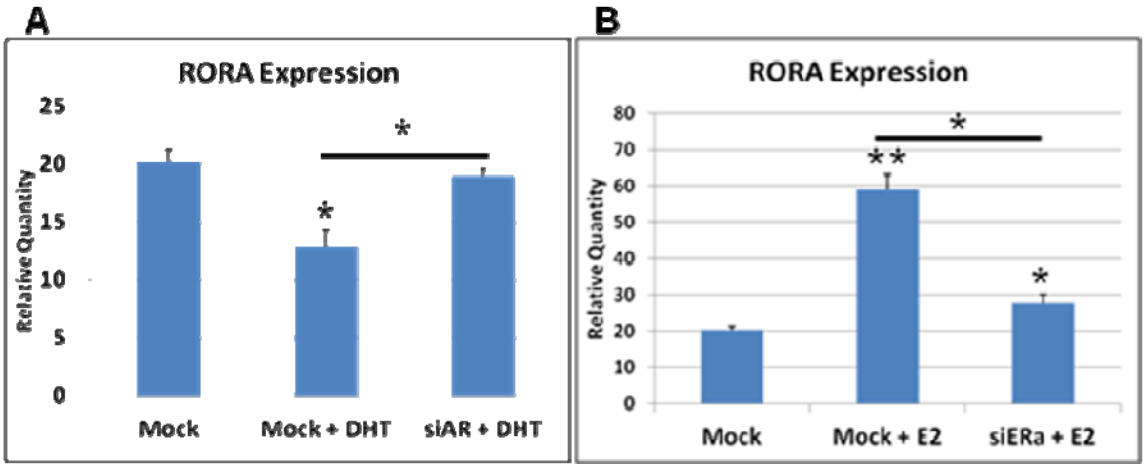

Figure 13. siRNA-mediated knockdowns of AR and ERα. SH-SY5Y cells were transfected with AR siRNA (siAR), ERα siRNA (siERα), or vehicle control (Mock) for 24 h, then treated with 1 nM DHT, 1 nM E2, or ethanol for 2 h. Quantitative RT-qPCR analysis (n = 3) of the hormone-treated, transfected cells was conducted to determine *RORA* expression. Relative *RORA* quantity in each sample was calculated using a standard curve obtained from *18S* expression levels in ten-fold serial dilutions of that sample. Error bars indicate S.E.M. Asterisks above each bar indicate statistical significance of difference relative to vehicle control-transfected, ethanol-treated cells (Mock). Asterisks above the horizontal line between two bars indicate statistical significance of difference relative to vehicle control-transfected, hormone-treated cells (Mock + DHT/ Mock + E2). *P < 0.05, **P < 0.01.

Identification of AR and ERα coregulators involved in sex hormone regulation of *RORA*

AR and ERα need to interact with coregulator proteins to suppress or activate expression of their transcriptional targets. Although a number of AR- and ERα coregulator proteins have been identified elsewhere, it is unknown which coregulators are involved in sex hormone regulation of *RORA*. Since now we have demonstrated that AR and ERα are required for regulation of *RORA* expression by male and female sex hormones, respectively. We therefore sought to identify coactivator proteins required for modulation of *RORA* by AR and ERα.

In our previous gene expression profiling study, we found a number of coregulators differentially regulated in lymphoblastoid cell lines derived from individuals with autism relative to sex-matched typically developing individuals. Among those deregulated AR/ER coregulators were NCOA1, NCOA5, SUMO-1, and FHL2. To determine whether these coregulators interact with AR and ERα in human neuronal cells, we conducted co-immunoprecipitation analysis using whole-cell lysates of SH-SY5Y cells treated with 1 nM DHT or 1 nM E2. Protein complexes in the lysates were immunoprecipitated using anti-NCOA1, anti-NCOA5, anti-SUMO-1, anti-FHL2, or IgG antibody. Western blot analysis was then conducted to determine the enrichment of AR and ERα in the immunoprecipitated protein samples. Interestingly, we found an increase in the enrichment of AR protein in protein samples immunoprecipitated with NCOA1, NCOA5, SUMO-1, and FHL2 relative to IgG antibody (**Figure 14A**), indicating that AR intereacts with these coregulators in the human neuronal cell line SH-SY5Y. On the other hand, we found an increase in the enrichment of ERα protein in protein samples immunoprecipitated

with NCOA5 and FHL2 (**Figure 14B**), indicating that ERα interacts with these two coregulators in the human neuronal cell line SH-SY5Y.

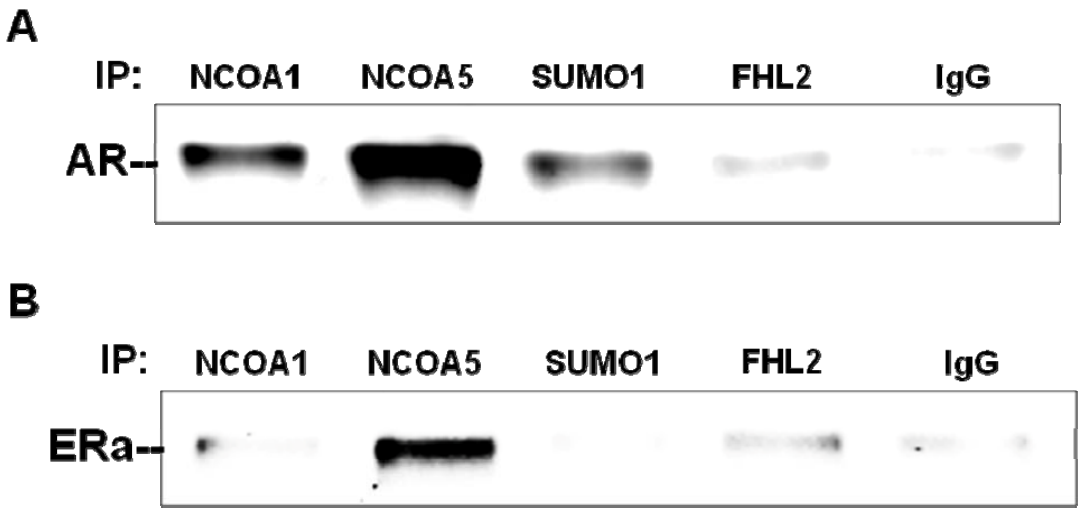

Figure 14. Co-immunoprecipitation analysis of AR/ERα coregulators. Whole-cell lysates of SH-SY5Y cells were prepared and immunoprecipitated with anti-NCOA1, anti-NCOA5, anti-SUMO-1, anti-FHL2, or IgG antibody. The immunoprecipitated proteins were then used for western blot analysis to determine the enrichment of AR (A) and ERα (B).

AR and ERα require different coregulator proteins to regulate different transcriptional targets. To examine whether these coregulators are involved in regulation of RORA in human neuronal cells, sequential chromatin immunoprecipitation of SH-SY5Y cell lysates was conducted using anti-AR or anti-ERα antibody, followed by an anti-coregulator antibody. The enrichment of AR/ERα binding sites in RORA promoter region in each re-immunoprecipitated chromatin sample was then determined by qPCR analysis. None of the AR binding elements was found to be statistically significantly enriched in the re-immunoprecipitated chromatin samples due to variability (**Figure 15A**). However, we found an increase in the average enrichment of ARbs-I in the chromatin sample immunoprecipitated with AR, followed by SUMO-1 (**Figure 15A**). A modest increase in the average enrichment of ARbs-II and ARbs-III was also observed in the chromatin samples re-immunoprecipitated with FHL2 and SUMO-1, respectively. Because there is a high degree of variability in the enrichment of ARbs-I in SUMO-1 re-immunoprecipitated chromatin, which is probably due to low expression of AR in the SH-SY5Y cells, we conducted an independent sequential chromatin immunoprecipitation, followed by conventional PCR and gel electrophoresis analysis to confirm binding of AR and SUMO-1 proteins to the AR binding site in RORA promoter region. An increase in the enrichment of ARbs-I was found in chromatin sample immunoprecipitated with AR, followed by SUMO-1, relative to IgG-immunoprecipitated chromatin (**Figure 15B**), indicating that AR is likely to interact with SUMO-1 coregulator protein at the AR binding element ARbs-I in *RORA* promoter region.

A pronounced increase in the enrichment of the ERα binding sites ERbs-I and ERbs-IV was found in chromatin samples immunoprecipitated with ERα, followed by

NCOA5 and by FHL2, respectively, whereas a modest increase in the enrichment of ERbs-II was also observed in chromatin samples immunoprecipitated with ERα, followed by NCOA5 (**Figure 15C**). This finding indicates that ERα interacts with NCOA5 and FHL2 in *RORA* promoter region.

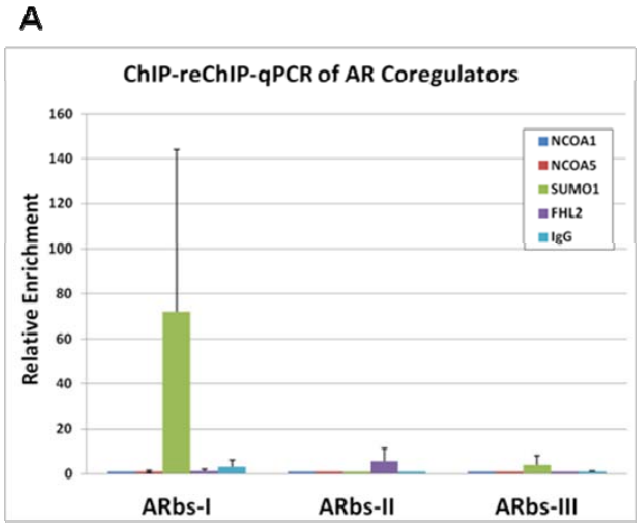

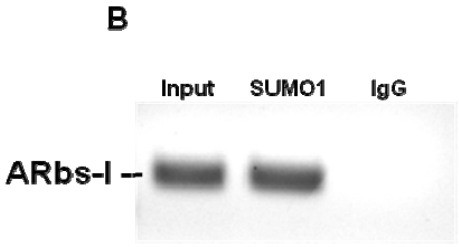

C

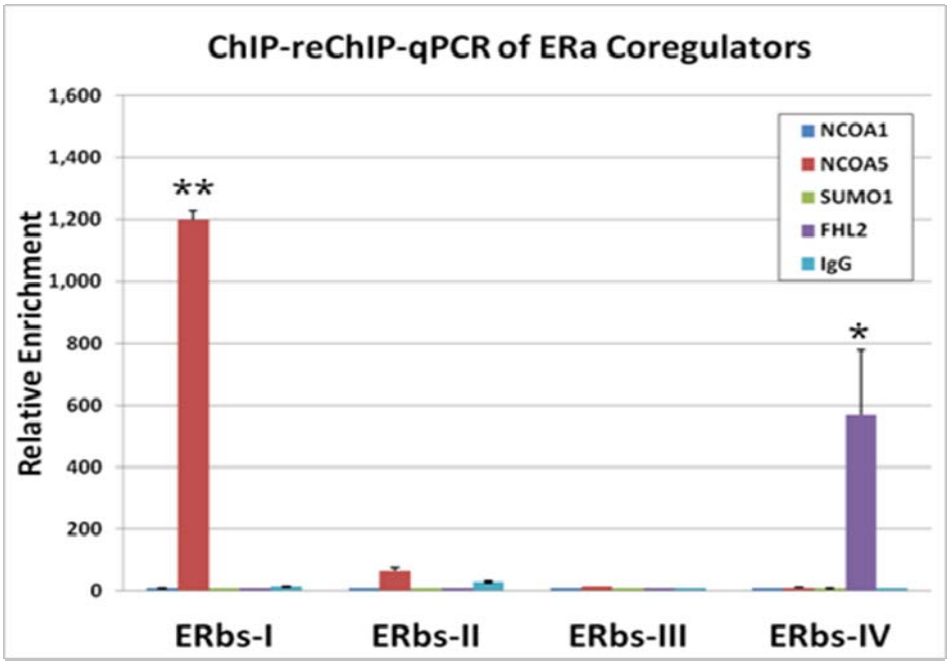

Figure 15. ChIP-reChIP analysis of AR/ERα coregulators. A) SH-SY5Y cells were treated with 1 nM DHT and whole-cell lysates were prepared and immunoprecipitated with anti-AR or IgG antibogy. The immunoprecipitated chromatin-antibody complex was then dissociated and washed to get rid of the antibody. The immunoprecipitated chromatin was then re-immunoprecipitated using anti-NCOA1, anti-NCOA5, anti-SUMO-1, anti-FHL2, IgG antibody, or no-second antibody negative control. The enrichment of AR binding sites in *RORA* promoter region in each re-immunoprecipitated chromatin sample was then determined using qPCR analysis (n = 3) and normalized with the enrichment in no-second antibody control. B) ChIP-PCR analysis of input chromatin, chromatin immunoprecipitated with AR, followed by SUMO-1, or IgG, followed by IgG. C) ChIP-reChIP analysis of ERα

binding sites in *RORA* promoter was conducted in the same manner as AR using SH-SY5Y cells treated with 1nM E2. Error bar indicates S.E.M., ** p-value < 0.01, * p-value < 0.05.

Androgen and estrogen require distal AR/ERα binding sites to oppositely modulate *RORA* promoter activity.

To confirm that androgen and estrogen regulate *RORA* expression by modulating *RORA* promoter activity, as well as to determine whether and which AR/ERα binding elements are required for opposite regulation of *RORA* expression by the sex hormones, we conducted dual luciferase reporter assays using firefly luciferase vectors containing *RORA* promoter region with different AR/ERα binding sites and a negative control Renilla

luciferase vector (**Figure 16**). First, we isolated genomic DNA from the human neuronal cells SH-SY5Y and amplified upstream regions of human *RORA* gene containing different AR/ERα binding sites using PCR amplification technique. PCR primers were designed to specifically amplify -1992 to -48 (ARbs-III and ERbs-IV), -2344 to -48 (ARbs-II-III and ERbs-III-IV), -6000 to -48 (ARbs-I-III and ERbs-II-IV), and -10055 to -48 (ARbs-I-III and ERbs-I-IV) upstream regions of human *RORA1* gene. Different PCR products were then separately inserted into pGEM-T-Easy vectors for blue/white screening assays and subcloned into the firefly luciferase vector pGL4.20. Each firefly luciferase vector containing *RORA* promoter insert was then co-transfected with Renilla negative control luciferase vector into the human neuronal cell line SH-SY5Y. The transfected cells were treated with 10 nM DHT, 10 nM E2, or ethanol for 2 h, then the activity of firefly and Renilla luciferase enzymes was measured using automatic dual luciferase reporter assays. Luminescence signal from firefly luciferase in each reaction was normalized with signal from Renilla luciferase in the same reaction to account for the variability between transfection experiments.

Interestingly, the activity of firefly luciferase gene was clearly oppositely regulated by DHT and E2 only when the gene was driven by entire *RORA* promoter region (-10055 to -48) containing ARbs-I-III and ERbs-I-IV (**Figure 16**). Consistent with the RT-qPCR analysis of hormone-treated SH-SY5Y cells (**Figure 11**), DHT significantly suppressed *RORA* promoter-driven luciferase activity (p-value < 0.05), whereas E2 enhanced it by over 2.5 fold (p-value < 0.05). When the ERbs-I was deleted, the enhancing effect of E2 on *RORA* promoter activity was completely diminished. In fact, without the ERbs-I, the luciferase activity was significantly suppressed by E2. This finding indicates that the ERbs-

I is critical for the upregulation of *RORA* transcription by estrogen. Without ERbs-I, E2 has a negative effect on *RORA* promoter activity.

In the presence of all AR binding sites in *RORA* promoter region, the luciferase activity was significantly suppressed by DHT (**Figure 16**). When only ARbs-I was deleted, the suppressing effect of DHT on luciferase activity was completely diminished. In fact, without the ARbs-I only, the luciferase activity was significantly enhanced by DHT (p-value < 0.01). However, when both ARbs-I and –II were deleted, the suppressing effect of DHT on *RORA* promoter-driven luciferase activity was restored. This finding indicates that DHT suppresses *RORA* promoter activity through ARbs-I and ARbs-III, but enhanced the promoter activity through ARbs-II. In the presence of ARbs-II, ARbs-I is required for DHT-mediated suppression of *RORA*.

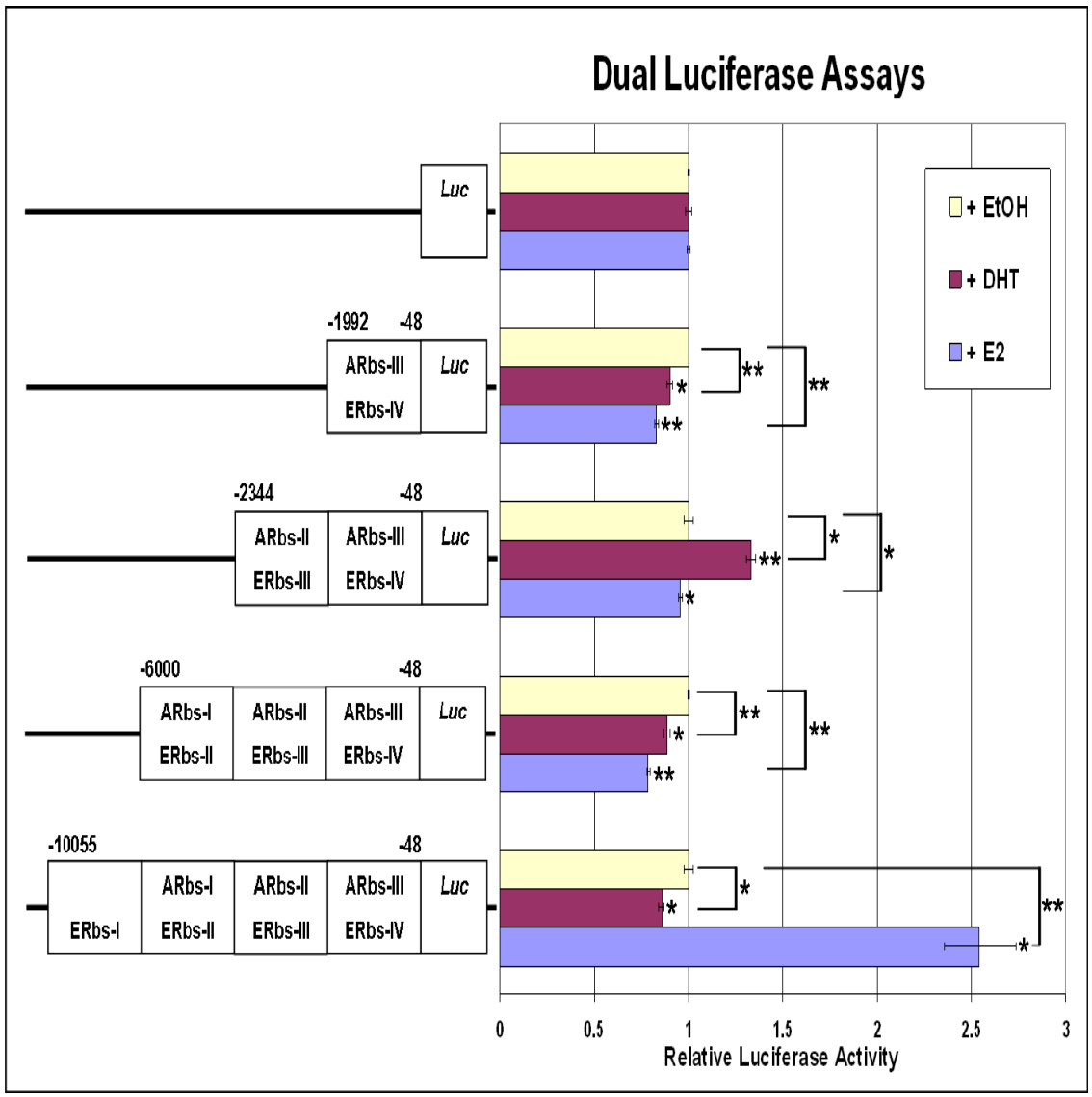

Figure 16. Dual luciferase reporter assays of SH-SY5Y cells transfected with *RORA* promoter luciferase vectors. AR/ERα binding sites in *RORA* promoter region were PCR-amplified and cloned into the pGEM-T-Easy vector for blue/white screening assays. Each *RORA* promoter insert containing different AR/ERα binding sites in the pGEM-T-Easy vector was then subcloned into the firefly luciferase vector pGL4.20 and co-transfected into SH-SY5Y cells with the Renilla negative control luciferase vector pGL4.24. The transfected cells were treated with 10nM DHT, 10nM E2, or ethanol and dual luciferase

reporter assays (n = 3/each group) were performed to determine *RORA* promoter activity. Firefly luminescence signal of each reaction was automatically detected and normalized by Renilla luciferase signal in the same reaction. To allow for comparison across transfection experiments, the firefly/Renilla luminescence ratios in hormone-treated groups were further normalized by firefly/Renilla luminescence ratio in ethanol-treated cells within the same transfection group, and also normalized by firefly/Renilla luminescence ratio in the empty vector transfection group. Error bars indicate SEM. The asterisks adjacent to each bar indicate statistical significance of difference relative to cells transfected with empty luciferase vector. The asterisks between the bars indicate the statistical significance of difference versus ethanol-treated cells within the same transfection group (*p-value < 0.05, ** p-value < 0.01).

Regulation of *RORA* by sex hormones is mediated by SUMO-1 and NCOA5.

To determine whether SUMO-1 and NCOA5 are required for regulation of *RORA* by androgen and estrogen, respectively, siRNA-mediated knockdowns of SUMO-1 and NCOA5 were conducted in SH-SY5Y cells. The transfected cells were then treated with 1nM DHT, 1nM E2, or the vehicle control ethanol. *RORA* expression in siRNA-transfected cells was measured using RT-qPCR analysis. Interestingly, the suppressing effect of DHT on *RORA* expression was completely diminished in SUMO-1 siRNA-transfected cells (**Figure 17A**), indicating that SUMO-1 is involved in *RORA* suppression mediated by androgen. On the other hand, the enhancing effect of E2 on *RORA* expression was significantly reduced in NCOA5 siRNA-transfected cells (**Figure 17B**), indicating that NCOA5 is required for effective *RORA* upregulation mediated by estrogen.

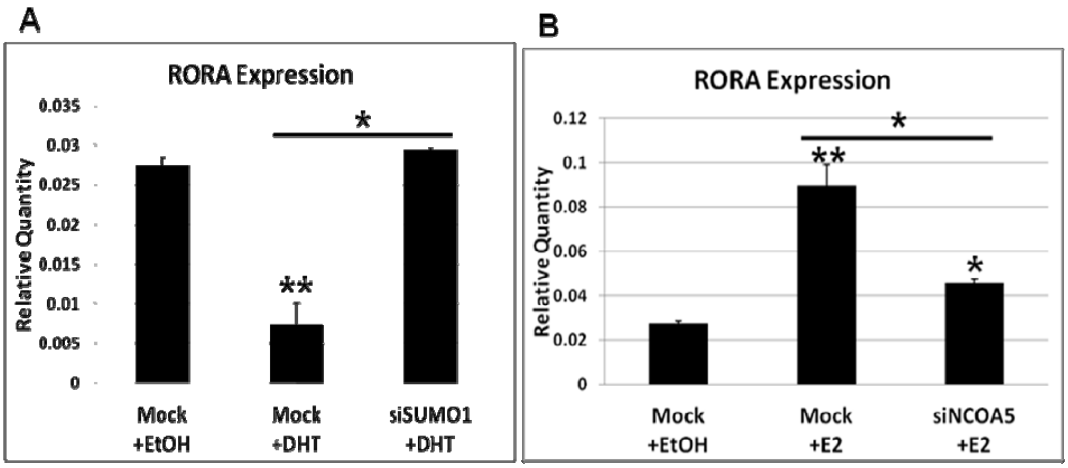

Figure 17. siRNA-mediated knockdowns of SUMO-1 and NCOA5. A) SH-SY5Y cells were transfected with SUMO-1 siRNA or vehicle control for 24 h and treated with 1nM DHT or ethanol for 2 h. *RORA* expression was then measured by RT-qPCR analysis (n = 3). B) NCOA5 knockdown was performed in the same manner as SUMO-1 using 1 nM E2. Error bars indicate S.E.M. Asterisks above each bar indicate statistical significance of difference relative to vehicle control-transfected, ethanol-treated cells (Mock + EtOH). Asterisks above the horizontal line between two bars indicate statistical significance of difference versus the hormone-treated, vehicle control-transfected cells (Mock + DHT or Mock + E2). *P < 0.05, **P < 0.01.

Identification of RORA transcriptional targets using whole-genome promoter array analysis

There is evidence that mouse Rora regulates a number of transcriptional targets whose functions are known to be aberrant in individuals with autism, including differentiation and survival of neurons, calcium-mediated signaling, and glutamatergic synapses. However, transcriptional targets of RORA in humans, especially in nervous tissues, have not been investigated. To comprehensively identify potential transcriptional targets of RORA, chromatin immunoprecipitation, followed by high-throughput promoter microarray (ChIP-on-chip) analysis was conducted using Affymetrix GeneChip Human Promoter 1.0R arrays containing 4.6 million probes tiled through over 25,500 human promoter regions. Nuclear lysates of the human neuronal cells SH-SY5Y were incubated with anti-RORA1 or IgG antibody. DNA was then isolated and purified from the immunoprecipitated chromatin and hybridized onto Affymetrix GeneChip Human Promoter 1.0R arrays (n = 3/group). The microarray was scanned using Affymetrix GeneChip Scanner 3000 and Partek Genomics Suite software was utilized to identify DNA probes significantly enriched in RORA-immunoprecipitated DNA samples relative to IgG-immunoprecipitated samples.

The ChIP-on-chip analysis revealed that a total of 2,764 probes were significantly enriched in RORA-immunoprecipitated chromatin relative to IgG-immunoprecipitated chromatin (ANOVA; p-value < 0.05). Among these, a total of 1,338 probes in promoter regions of 1,274 genes were significantly enriched with log2 ratio > 0.3. To prioritize genes for further confirmation, biological network and pathway analysis of these genes with log2 ratio > 0.3 was conducted using the Ingenuity Pathway Analysis (IPA) program

(www.ingenuity.com). IPA analysis revealed as many as 349 genes to be associated with neurological functions and disorders (**Table 2**). Interestingly, neurological functions known to be negatively impacted in individuals with autism, including neuronal adhesion, synapse density, and neurogenesis, were also identified to be significantly associated with this set of RORA potential transcriptional targets (**Table 3**). Several diseases known to be co-morbid disorders of autism, including movement disorder, encephalopathy, bipolar disorder, amyotrophic lateral sclerosis, schizophrenia, mental retardation, and neurodegeneration, were also highlighted (**Table 4**).

Table 2. Top biological functions associated with potential RORA transcriptional targets. Biological functions and disorders associated with 1,274 potential transcription targets of RORA identified by ChIP-on-chip analysis with log2enrichment > 0.3 were predicted by IPA program. All p-values were calculated using Fisher's exact test.

Category	p-value	# Genes
Top Disorders		
Genetic Disorder	5.91E-18 - 2.70E-02	570
Neurological Disorder	9.31E-12 - 2.61E-02	349
Cardiovascular Disorder	1.02E-11 - 2.42E-02	236
Immunological Disorder	1.20E-11 - 2.45E-02	266
Skeletal and Muscular Disorders	4.35E-11 - 2.60E-02	287
Top Development and Functions		
Immune Cell Trafficking	1.36E-04 - 2.76E-02	90
Organismal Development	2.61E-04 - 2.70E-02	167
Hematological System Development and Function	3.72E-04 - 2.76E-02	127
Tissue Development	6.02E-04 - 2.51E-02	218
Nervous System Development and Function	7.37E-04 - 2.50E-02	90

Table 3. Top nervous system development and functions associated with potential RORA transcriptional targets. Neurological functions associated with 1,274 potential transcription targets of RORA identified by ChIP-on-chip analysis with log2 enrichment > 0.3 were predicted by IPA program. All p-values were calculated using Fisher's exact test.

Neurological Functions	p-value	Genes	# Genes
Adhesion of neuronal cells	7.37E-04	CDK5R1, CNTN4, CSNK2B, GLI2, LAMB2, NCAM2, NLGN1	7
Neuromuscular junctions	2.69E-03	CSNK2B, SOD1	2
Loss of neurons	3.09E-03	ADRBK1, CDK5R1, GFRA2, IKBKB, ITPR1, MAOB, NTRK2, SHC3, SOD1, SOD2, THRB, TTR	12
Neurogenesis	1.02E-02	AKTIP, ANKRD6, APBA2, ARHGEF10, ATN1, ATP2B2, BCL11B, BCR, CACNA1F, CD40LG, CD44, CDK5R1, CNTN4, CRKL, CTNND2, CUX1, CXCL5, CYP19A1, DSCAM, E2F1, EPHB1, FGF1, FKBP4, FOXA2, GDF5, GFRA2, GLI2, HOXB1, IKBKB, IL1B, ITGB5, LPPR5, LRRK2, MARK2, MEIS1, NAPA, NCAM2, NDN, NF2, NFATC2, NINJ1, NLGN1, NTRK2, PAX3, PDIA3, PECAM1, PIAS2, PLAT, PTPN11, RAP1GAP, RHOG, RND1, SERPINE2, SH2B1, SHC3, SIP1, SMN1/SMN2, SOD2, SPR, TACC2, TCF3, TESK1, TFAM, THBS2, THRB, USH1C, VCL, ZHX2	68
Development of cortical lamina	1.51E-02	CDK5R1, NTRK2	2
Density of synapse	1.68E-02	CTNND2, MALAT1, NTRK2	3
Foliation of cerebellum	2.42E-02	CDK5R1, GLI2	2
Myelination of nerves	2.50E-02	ARHGEF10, IL1B, NTRK2, THRB	4

Table 4. Top neurological diseases and disorders. Neurological disorders associated with 1,274 potential transcription targets of RORA identified by ChIP-on-chip analysis with log2enrichment > 0.3 were predicted by IPA program. All p-values were calculated using Fisher's exact test.

Neurological Diseases	**p-value**	**# Genes**
Amyotrophic lateral sclerosis	1.20E-03	53
Bipolar disorder	1.50E-03	87
Alzheimer's disease	2.35E-03	77
Dementia	2.74E-03	78
Movement disorder	3.31E-03	102
Neurodegeneration	4.80E-03	80
Schizophrenia	5.86E-03	49
Encephalopathy	6.28E-03	94
Mental retardation	1.35E-02	10

Confirmation of RORA transcriptional targets in human neuronal cells

To confirm binding of RORA protein in the promoter region of potential transcriptional targets identified by the ChIP-on-chip analysis, we selected 6 potential RORA transcriptional targets for confirmation and further functional analyses. These selected potential targets of RORA are *ITPR1*, *CYP19A1*, *A2BP1*, *HSD17B10*, *NLGN1*, and *NTRK2*. *ITPR1* has been well-identified to be a direct transcriptional target of RORA in mouse Purkinje neurons (Gold et al., 2003). *CYP19A1*, encoding aromatase which is the critical enzyme converting androgens to estrogens, has been shown to be regulated by RORA in the human breast cancer cell line MCF7 (Odawara et al., 2009), but the regulation of aromatase by RORA in neuronal cells has not been investigated. The other selected genes have never been reported to be regulated by RORA elsewhere, thus likely to be novel transcriptional targets of RORA. Pathway analysis of these 5 genes using Pathway Studio 7.0 program revealed an association of these genes with several neurological disorders, including autism and ataxia, as well as autism-related neurological functions, including synaptogenesis, synaptic transmission, long-term potentiation, differentiation, learning, and memory (**Figure 18**), suggesting that these RORA transcriptional targets may play an important role in some pathobiological conditions of autism.

To confirm that RORA protein binds to the promoter region of these potential transcriptional targets, we conducted chromatin immunoprecipitation using anti-RORA1 or IgG antibody, followed by qPCR analysis to determine the enrichment of RORA binding sites in the promoter region of *A2BP1*, *CYP19A1*, *HSD17B10*, *ITPR1*, *NLGN1*, and *NTRK2*. We found that RORA binding sites in the promoter region of these potential targets were significantly enriched in chromatin samples immunoprecipitated by anti-

RORA1 antibody relative to IgG-immunoprecipitated chromatin (**Figure 19**), indicating that RORA protein indeed binds to the promoter of *A2BP1*, *CYP19A1*, *HSD17B10*, *ITPR1*, *NLGN1*, and *NTRK2*.

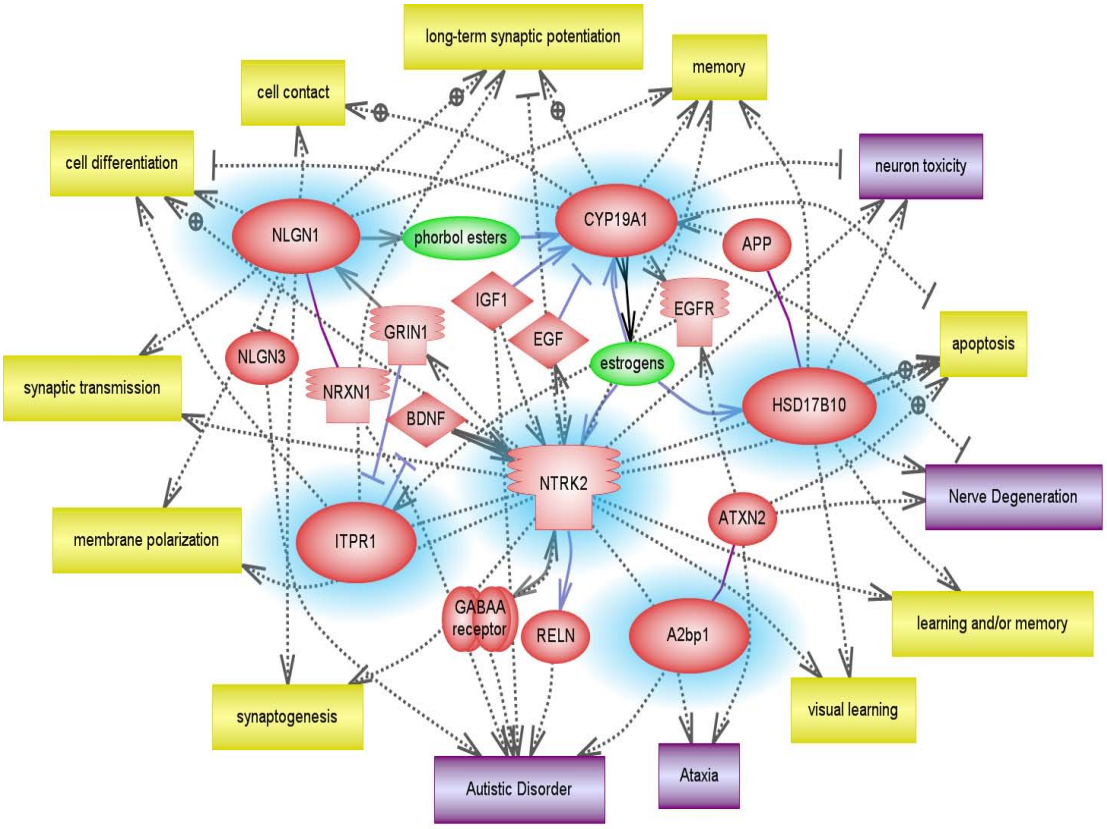

Figure 18. Pathway analysis of selected potential transcriptional targets of RORA. Biological network was created using Pathway Studio 7.0 program to identify biological functions and disorders associated with potential RORA transcriptional targets (i.e. *ITPR1*, *CYP19A1*, *A2BP1*, *HSD17B10*, *NLGN1*, and *NTRK2*) selected for confirmation (highlighted in blue).

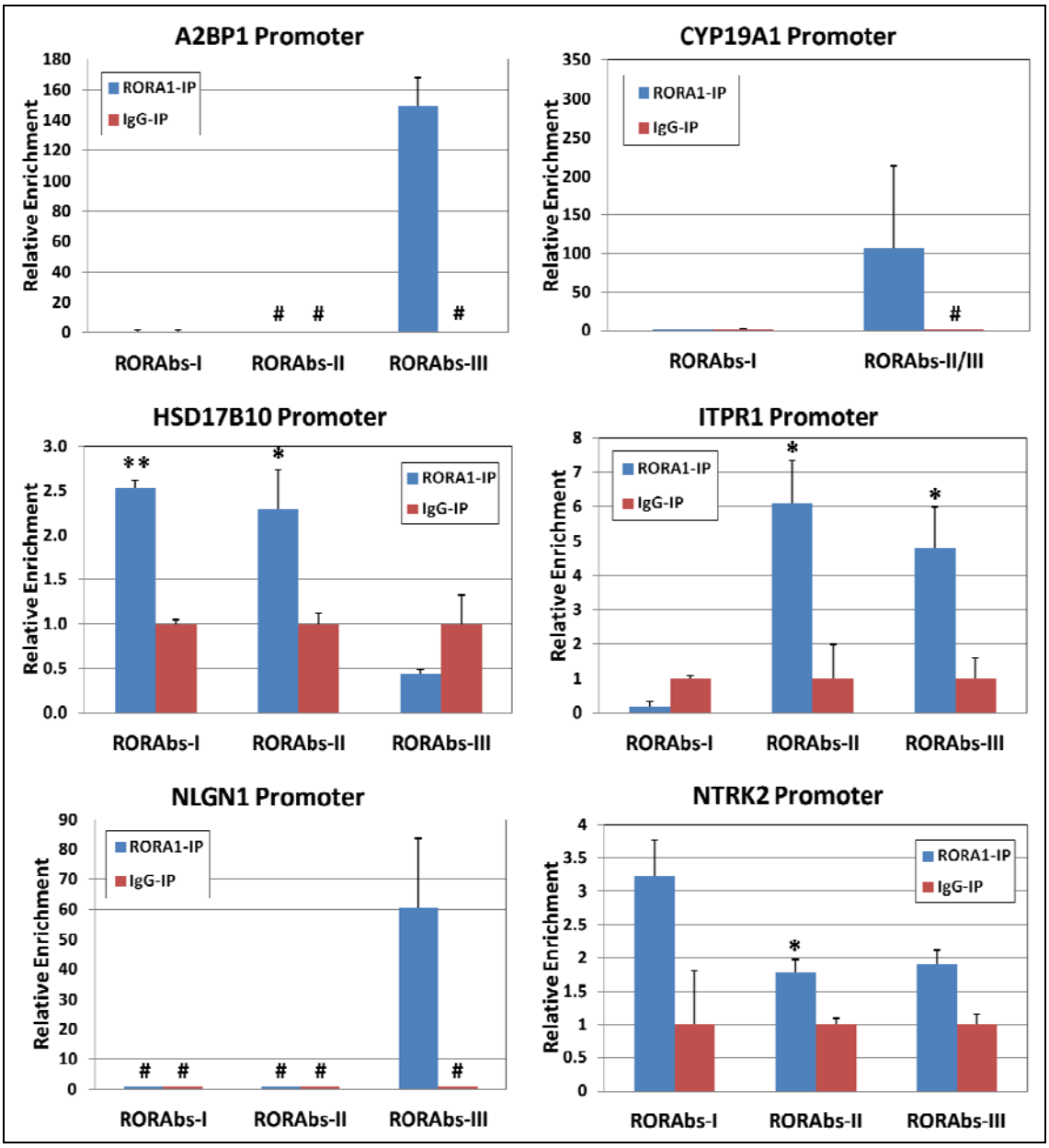

Figure 19. ChIP-qPCR of RORA transcriptional targets. Chromatin immunoprecipitation (ChIP) followed by qPCR analysis was conducted to determine whether RORA protein binds to *A2BP1*, *CYP19A1*, *HSD17B10*, *ITPR1*, *NLGN1*, and *NTRK2* promoters. Chromatin was isolated from SH-SY5Y cells and immunoprecipitated with anti-RORA1 or IgG antibody. DNA was purified from the immunoprecipitated

chromatin and real-time qPCR analysis (n = 3) was performed to determine the enrichment of each RORA binding element in the promoter region of the selected potential RORA targets. Error bars indicate S.E.M. (* p-value < 0.05; ** p-value < 0.01; # = Undetectable).

RORA reduction causes aberrant expression of selected potential transcriptional targets in human neuronal cells

To further validate that RORA regulates expression of *A2BP1*, *CYP19A1*, *HSD17B10*, *ITPR1*, *NLGN1*, and *NTRK2*, and examine whether reduction of *RORA* expression leads to aberrant expression of these selected RORA transcriptional targets, shRNA-mediated knockdown of RORA was performed in SH-SY5Y cells using RORA1 shRNA and RT-qPCR analysis was conducted to measure expression of *RORA1* and the potential targets. Expression of *RORA1* in SH-SY5Y cells was significantly down-regulated by approximately 50% compared with cells transfected with negative control shRNA, indicating that shRNA-mediated knockdown of RORA1 was successful. Interestingly, expression of all selected RORA transcriptional targets was significantly reduced (**Figure 20**), indicating that expression of these genes is regulated by RORA and that these genes indeed are RORA transcriptional targets in human neuronal cells.

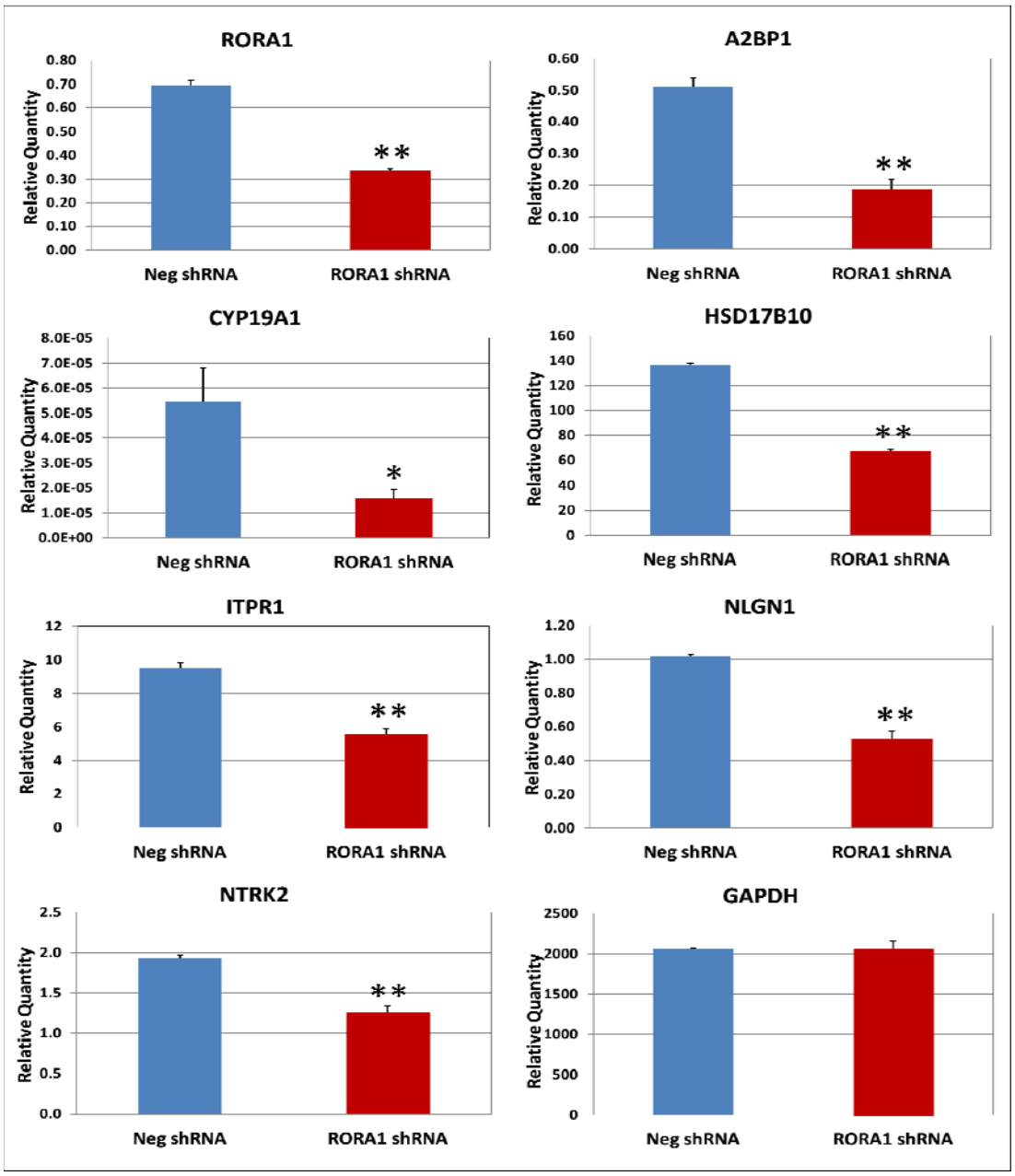

Figure 20. RT-qPCR analysis of RORA shRNA-transfected SH-SY5Y cells. SH-SY5Y cells were transfected with RORA1 shRNA or negative control shRNA for 24 h and RT-qPCR analysis (n = 3) was performed to determine expression of *RORA1* and potential transcriptional targets in the transfected cells. *GAPDH* was included as a negative control. Error bars indicate S.E.M. (* p-value < 0.05; ** p-value < 0.01).

Identification of RORA coregulators involved in regulation of *CYP19A1*

Like AR and ERα, RORA interacts with coregulator proteins to regulate transcription of target genes. In fact, several nuclear receptor coregulators are known to interact with both RORA and the sex hormone receptors. To determine whether RORA interacts with the nuclear receptor coregulators NCOA1, NCOA5, SUMO-1, and FHL2 in human neuronal cells, co-immunoprecipitation, followed by western blot analysis was performed. Whole-cell lysates of SH-SY5Y cells were prepared and immunoprecipitated with anti-NCOA1, anti-NCOA5, anti-SUMO-1, anti-FHL2, or IgG antibody. Immunoprecipitated proteins were analyzed by western blot analysis to determine the enrichment of RORA in each protein sample. Co-immunoprecipitation analysis showed that RORA protein is enriched in protein samples immunoprecipitated with NCOA1 and NCOA5 (**Figure 21**), indicating that RORA interacts with these coregulators in the human neuronal cell line SH-SY5Y.

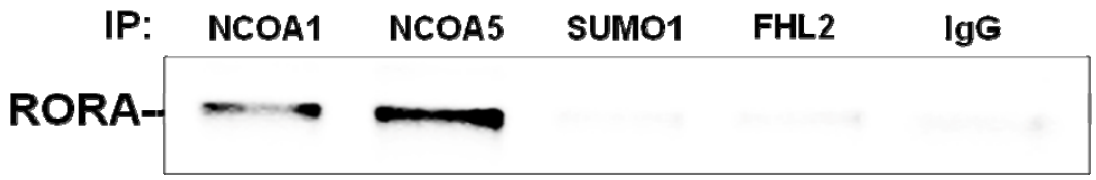

Figure 21. Co-immunoprecipitation analysis of RORA coregulators. Whole-cell lysates of SH-SY5Y cells were prepared and immunoprecipitated with anti-NCOA1, anti-NCOA5, anti-SUMO-1, anti-FHL2, or IgG antibody. The immunoprecipitated proteins were then used for western blot analysis to determine the enrichment of RORA protein.

To determine whether these coregulators are also involved in regulation of *CYP19A1* gene, we conducted sequential chromatin immunoprecipitation using anti-RORA or IgG antibody, followed by re-chromatin immunoprecipitation using anti-NCOA1, anti-NCOA5, anti-SUMO-1, anti-FHL2, or IgG antibody. The enrichment of each RORA potential binding site (RORAbs) in *CYP19A1* promoter (**Figure 22A**) in the re-immunoprecipitated chromatin was determined by qPCR analysis. RORAbs-II and III are located adjacent to each other and cannot be analyzed separately by qPCR analysis, thus shown as "RORAbs-II/III). Neither RORAbs-I nor RORAbs-II/III was statistically significantly enriched in RORA-immunoprecipitated chromatin. However, an increase in the average enrichment of RORAbs-I in the promoter region of *CYP19A1* was observed the chromatin sequentially immunoprecipitated by anti-RORA, followed by anti-NCOA5 (**Figure 22B**), indicating that RORA may interact with NCOA5 at this RORA binding site in the promoter region of *CYP19A1*.

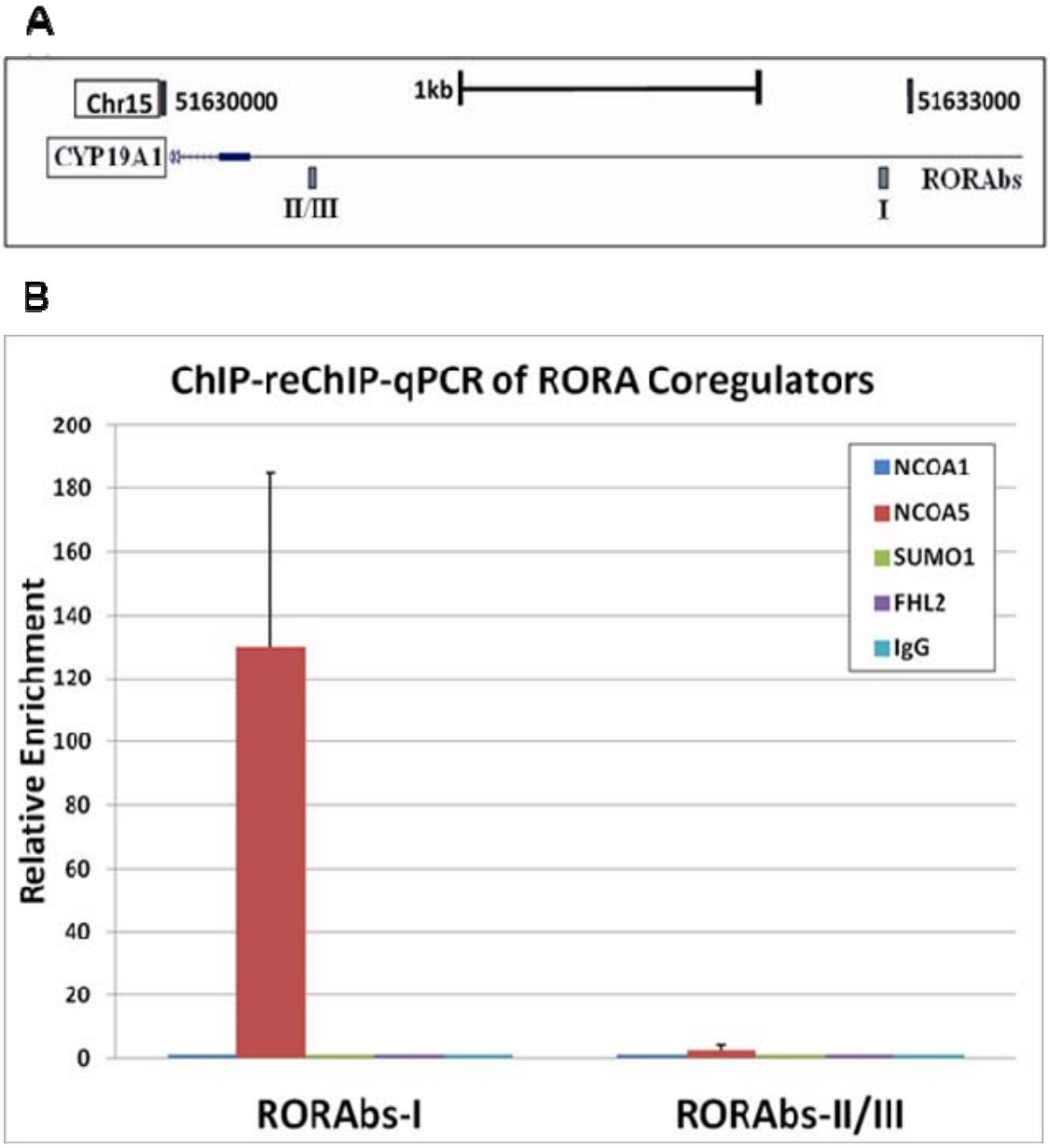

Figure 22. ChIP-reChIP analysis of RORA coregulators binding to *CYP19A1* promoter region. Sequential chromatin immunoprecipitation (ChIP-reChIP) followed by qPCR analysis was conducted to determine whether NCOA1, NCOA5, SUMO-1, or FHL2 interact with RORA in *CYP19A1* promoter region. Chromatin was isolated from SH-SY5Y cells and first immunoprecipitated with anti-RORA. The RORA-immunoprecipitated

chromatin was washed to dissociate and get rid of anti-RORA, then free chromatin was re-immunoprecipitated with anti-NCOA1, anti-NCOA5, anti-SUMO-1, anti-FHL2, IgG control, or no-second antibody control. Real-time qPCR analysis (n = 3) was performed to determine the enrichment of each RORA binding site in *CYP19A1* promoter region. The relative enrichment was calculated using standard curves obtained from relative enrichment of each RORA binding site in 10-fold serial dilutions of input and normalized with the relative enrichment of RORA binding site in no-second antibody control. Error bars indicate S.E.M. (# = Undetectable).

Expression of RORA transcriptional targets is aberrant in the brain of individuals with autism

Reduction of RORA has been consistently reported in several independent cohorts using the lymphoblastoid cell lines, the prefrontal cortex, and the cerebellum of individuals with autism. To examine whether RORA reduction observed in the brain of individuals with autism could lead to aberrant expression of RORA transcriptional targets identified in this study, RT-qPCR analysis of frozen post-mortem prefrontal cortex tissues from individuals with autism (n = 3) and sex- and age-matched controls (n = 3) was performed. We found that *RORA* expression was significantly reduced in all three brain tissue samples from individuals with autism (**Table 5**). Interestingly, transcript levels of *A2BP1*, *CYP19A1*, *HSD17B10*, *ITPR1*, and *NLGN1* were also significantly decreased in all three brain tissues from autism. *NTRK2* transcript levels were significantly down-regulated in two autistic brain tissues, but show increased expression in the other sample.

Correlation analysis was performed to determine whether transcript levels of confirmed transcriptional targets were correlated with *RORA* transcript levels (**Figure 23**). It is interesting to note that *CYP19A1* transcript levels exhibited a strong positive correlation with *RORA* transcript levels (R^2-value = 0.954). Transcript levels of *A2BP1* and *NLGN1* also showed a moderate positive correlation with *RORA* (R^2-value = 0.366 and 0.368, respectively), whereas *HSD17B10*, *ITPR1*, and *NTRK2* showed low or no correlation with *RORA* transcript levels (R^2-value = 0.238, 0.039, and 0.119, respectively).

Table 5. RT-qPCR analysis of post-mortem brain tissues from individuals with autism. Total RNA was isolated and purified from frozen post-mortem prefrontal cortex tissues from individuals with autism (n = 3) and sex- and age-matched controls (n = 3). RT-qPCR analysis (n = 3) was performed to measure expression of *RORA* and confirmed transcriptional targets. The transcript levels of each gene were calculated using standard curves obtained from relative *18S* expression in 10-fold serial dilutions of each sample. The numbers highlighted in green color indicate down-regulation of genes in autism brain tissues relative to respective matched controls, whereas the number highlighted in red indicates up-regulation. Samples from individuals with autism were indicated by "A_" and samples from controls were indicated by "C_". The four-letter numbers in sample names indicate brain tissue identity numbers from the Autism Tissue Program.

Sample ID	Log_2 ratio of autistic/control (p-value)						
	RORA	A2BP1	CYP19A1	HSD17B10	ITPR1	NLGN1	NTRK2
A_5144/C_5251	-1.663 (0.002)	-2.392 (5.3E-05)	-1.705 (0.049)	-3.033 (4.8E-05)	-0.851 (0.035)	-2.907 (7.4E-05)	-2.563 (8.0E-04)
A_5173/C_5873	-0.597 (0.008)	-3.483 (0.003)	-1.039 (0.020)	-1.621 (1.1E-05)	-3.173 (8.8E-06)	-2.508 (2.0E-04)	-1.271 (3.0E-05)
A_6337/C_5718	-4.453 (0.013)	-1.929 (1.3E-05)	-6.266 (0.022)	-0.280 (0.022)	-0.302 (0.040)	-0.463 (0.002)	0.444 (4.0E-04)

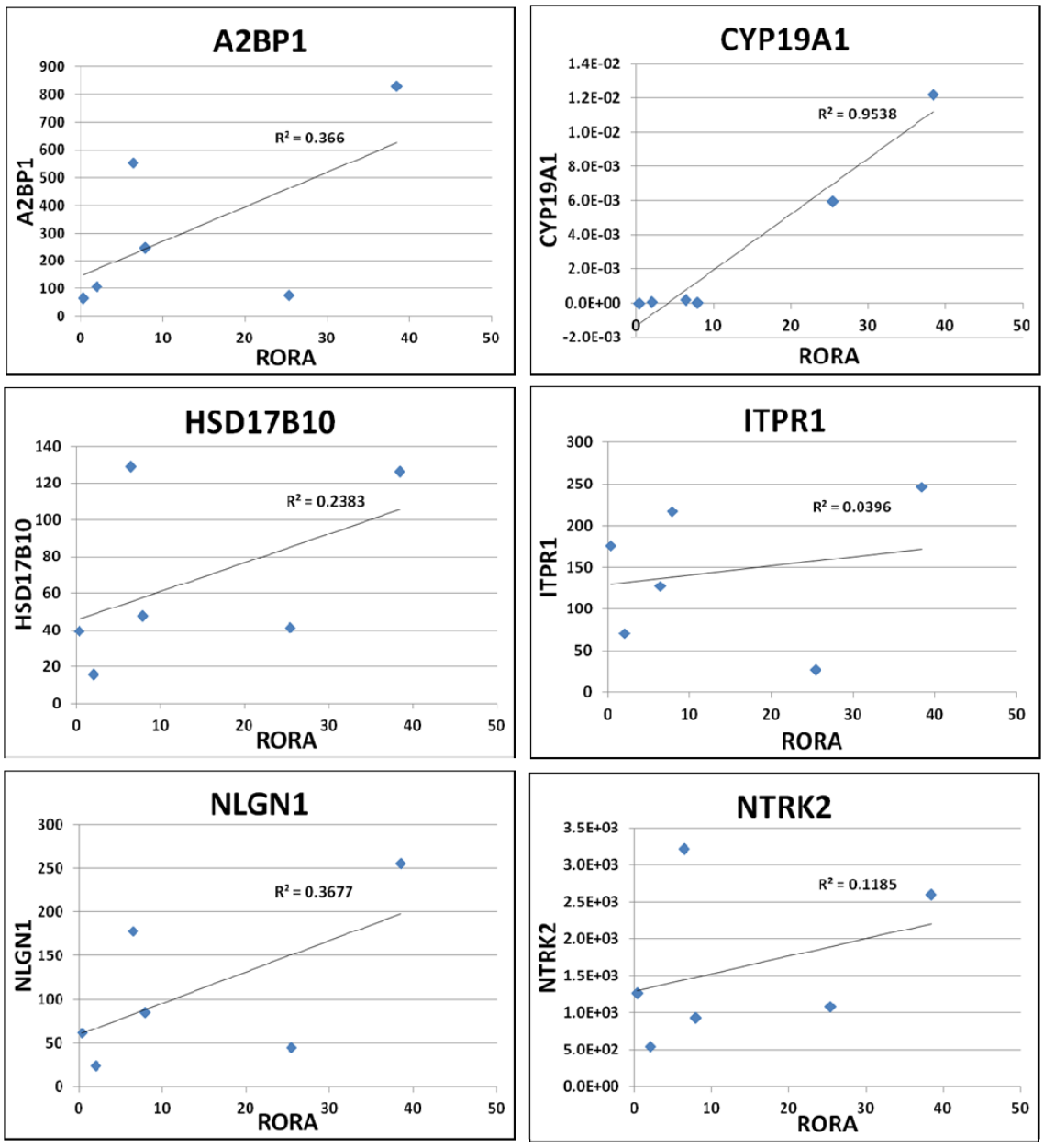

Figure 23. Correlation analysis of transcript levels of *RORA* and confirmed transcriptional targets in human brain tissues. Transcript levels of *RORA* and confirmed transcriptional targets in human prefrontal cortex tissues (autism = 3; control = 3) determined by RT-qPCR analysis (n = 3) were used for correlation analysis. Each dot represents a brain tissue sample.

To determine whether the level of aromatase, a protein enzyme encoded by *CYP19A1* gene, is also decreased and correlated with RORA protein level in the brain of individuals with autism, confocal immunofluorescence analysis of a tissue array containing postmortem frontal cortex from autistic individuals (n =12) and sex- and age-matched controls (n=22) was conducted. The tissue array was co-immunolabeled for RORA, aromatase, and the neuronal marker MAP2, and counter-stained with DAPI to visualize the nucleus of the cells (**Figure 24**). Neurons (n = 40-50/sample) were identified by distinct staining of the neuronal marker MAP2 and the nuclear staining DAPI. Immunofluorescence signals of RORA and aromatase in each neuron were measured and normalized by background subtraction using immunofluoresecence signals in no-cell areas. Average RORA and aromatase expression in each prefrontal cortical neuron were calculated and compared between sample groups.

Interestingly, both RORA and aromatase proteins were significantly reduced in prefrontal cortical neurons of individuals with autism relative to sex- and age-matched controls (p-values = 0.017 and 0.010, respectively; **Figure 25A, B**). Immunofluorescence levels of MAP2 and DAPI were not significantly changed in tissue samples from individuals with autism (p-values = 0.147 and 0.166, respectively). Moreover, immunofluorescence levels of aromatase were also correlated with immunofluorescence levels of RORA with a high, positive correlation (R^2-value = 0.915; **Figure 25C**).

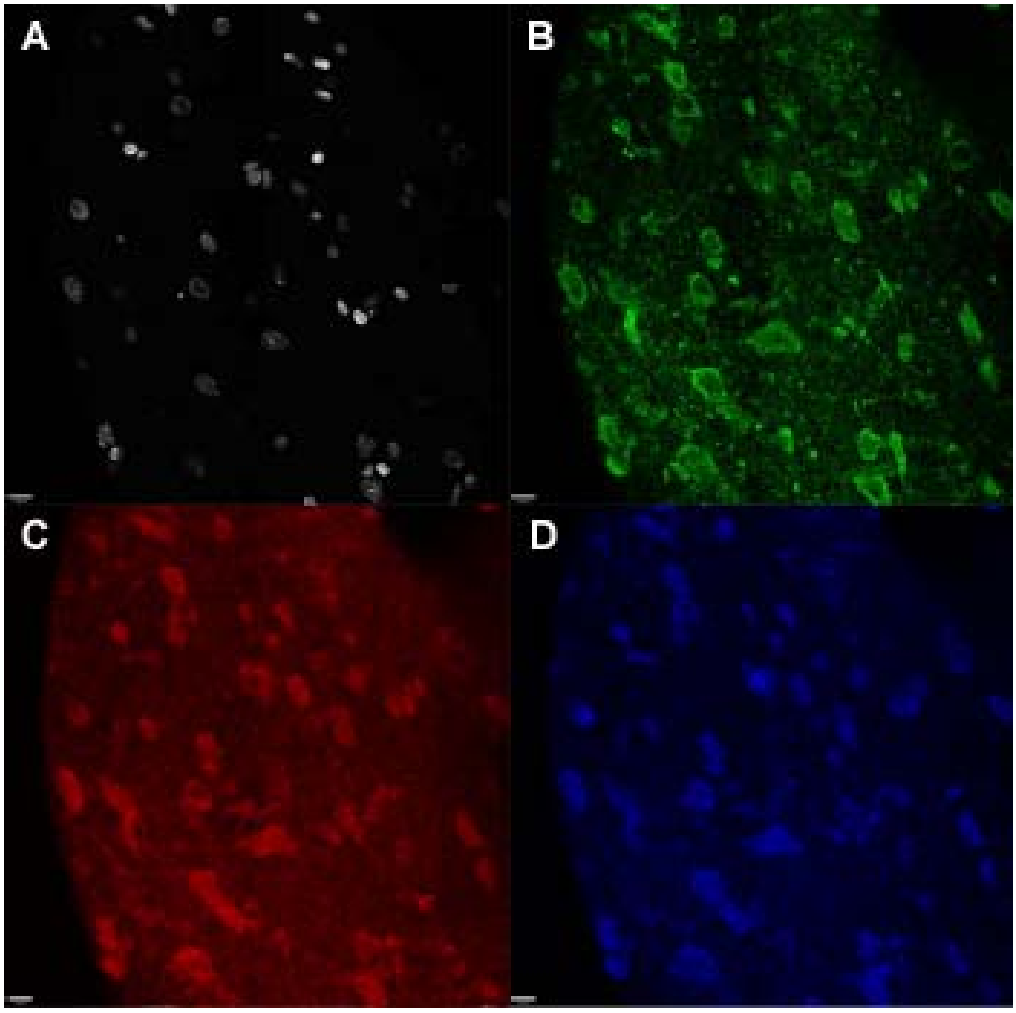

Figure 24. Confocal immunofluorescence analysis of tissue array. Representative confocal immunofluoresecence images of a brain tissue on the tissue array stained for A) nuclei, B) MAP2, C) Aromatase, and D) RORA. Figure from (Sarachana, Xu, Wu, & Hu, 2011).

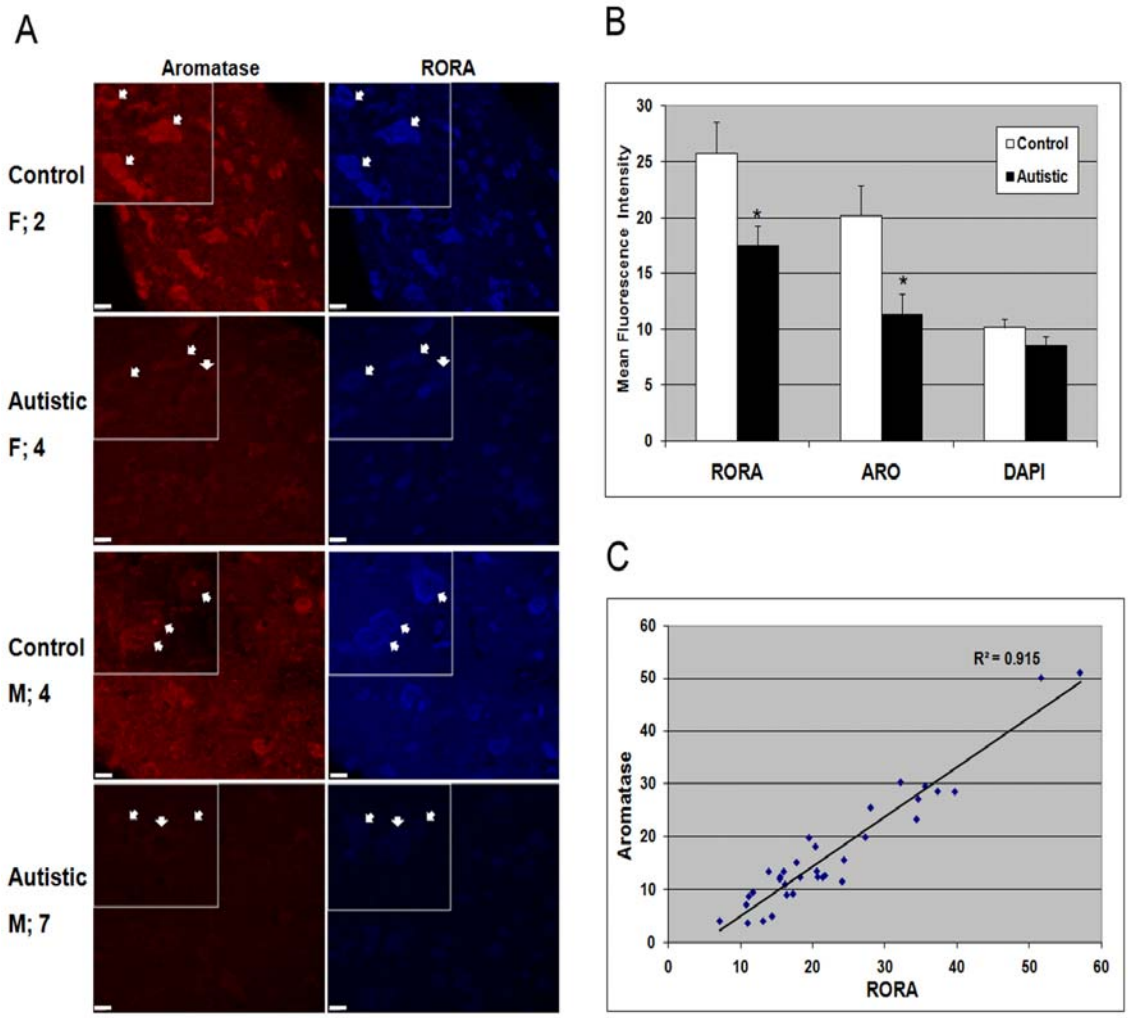

Figure 25. RORA and aromatase proteins are decreased in postmortem brain tissues from individuals with autism. A tissue array containing postmortem prefrontal cortex specimens from 12 autistic individuals and 22 age- and sex-matched controls was co-immunolabeled for aromatase (red), RORA (blue), and MAP2, and counterstained with DAPI to reveal nuclei. (A) Representative images from confocal immunofluorescence analyses of the prefrontal cortex tissue array. Arrows mark neurons in the prefrontal cortex. Scale bars, 20 μm. F: female; M: male; numbers indicate the respective ages of the subjects from whom the brain tissues were obtained. (B) Quantitative analyses of confocal

fluorescence images of RORA, aromatase, and DAPI. Prefrontal cortex neurons expressing MAP2 protein were selected according to its green immunofluorescence, and fluorescence signal intensity for RORA, aromatase (ARO), and DAPI, in the neurons were extracted using image analysis software and normalized by background subtraction. For each sample, ~40–50 neurons were selected for quantification of RORA and aromatase fluorescence in a "sample blind" fashion such that the identities of the samples were unknown to the person performing the analyses. Error bars indicate S.E.M. (*p-value < 0.05 versus the control samples). (C) Correlation analysis of RORA and aromatase protein expression in the prefrontal cortical neurons. Adapted from (Sarachana, Xu, Wu, & Hu, 2011).

Chapter 5: Discussion

The results of this study indicate that the expression of *RORA* is inversely modulated by male and female sex hormones, with DHT and estradiol increasing the binding of AR and ERα , respectively to the *RORA* promoter region. Interestingly, DHT represses the expression of *RORA*, whereas estradiol enhances *RORA* expression. We further demonstrate that the AR corepressor SUMO-1 is involved in DHT-mediated repression of *RORA*, likely by interacting with AR in the *RORA* promoter region, while estradiol-mediated overexpression of *RORA* requires the coactivator NCOA5 which interacts with ERα in the *RORA* promoter region. We also show that RORA, in turn, directly regulates expression of several targets, including *A2BP1*, *CYP19A1*, *HSD17B10*, *ITPR1*, *NLGN1*, and *NTRK2*, in the SH-SY5Y neuronal cell line and expression of these RORA targets is aberrant in the prefrontal cortex tissues from individuals with autism. Interestingly, the transcript and protein levels of aromatase, an enzyme encoded by *CYP19A1* which is critical for estrogen biosynthesis from testosterone, are significantly reduced and strongly correlated with the transcript and protein levels of RORA in the prefrontal cortex tissues.

RORA and the sex bias of autism

This study is the first to provide a molecular mechanism in which male and female sex hormones may play a role in the sex bias in autism. The potential of *RORA* to be under both negative regulation by AR and positive regulation by ERα, together with the possibility that RORA regulates aromatase expression in the brain, suggests that RORA

may be important for maintaining the balance between male and female sex hormones in the brain through reciprocal, an inverse regulatory mechanism as illustrated in **Figure 26**, which summarizes the principal findings of this study. We propose that reduction of RORA observed in individuals with autism, probably due to hypermethylation of the *RORA* promoter region (Nguyen et al., 2010) and/or aberrant expression of AR/ER coregulator proteins (V. W. Hu, Sarachana et al., 2009), is exacerbated by a feedback mechanism involving decreased aromatase level, which further causes accumulation of its substrate, testosterone, and reduction of its product, estradiol. Increased testosterone and reduced estradiol levels, in turn, exhibit inverse feedback regulation of *RORA* expression, causing further reduction of *RORA*.

This proposed molecular mechanism provides a plausible explanation for aberrant concentrations of sex hormones and altered reproductive functions observed in Rora-deficient mice (e.g., reduced concentrations of estradiol, abnormalities in estrous cycle, and reduced number of oocytes (Guastavino & Larsson, 1992; Guastavino et al., 2005), as well as in some individuals with autism (e.g., increased levels of androgens, elevated rates of androgen-related disorders in women with autism, and irregular menstrual cycle (Ingudomnukul, Baron-Cohen, Wheelwright, & Knickmeyer, 2007; Ruta, Ingudomnukul, Taylor, Chakrabarti, & Baron-Cohen, 2011)). Moreover, the findings from this study also suggest that males are more susceptible to RORA deficiency in comparison to females, partially because the presence of higher estradiol concentrations in females may exhibit a neuroprotective effect against RORA deficiency through ERα-mediated transcriptional regulation of *RORA*. This is consistent with the observations in previous studies in which loss of neurons (specifically Purkinje cells) in male Rora-deficient mice was found to occur

much earlier in life in comparison with female Rora-deficient mice (Doulazmi et al., 1999; Janmaat et al., 2011). Since RORA plays critical roles in several autism-related neurological functions (e.g., differentiation and survival of neurons, neuroprotection against both oxidative stress and inflammation), this finding also provides a plausible explanation for the heightened prevalence of autism in males. Interestingly, RORA and ER share a consensus binding site on DNA (AGGTCA) and consequently common target genes. The existence of shared gene targets may further explain why females are less susceptible to autism. That is, estrogens may not only protect females against autism by increasing the level of *RORA* expression, but also by inducing shared target genes of RORA through ER, thus compensating in part for RORA deficiency.

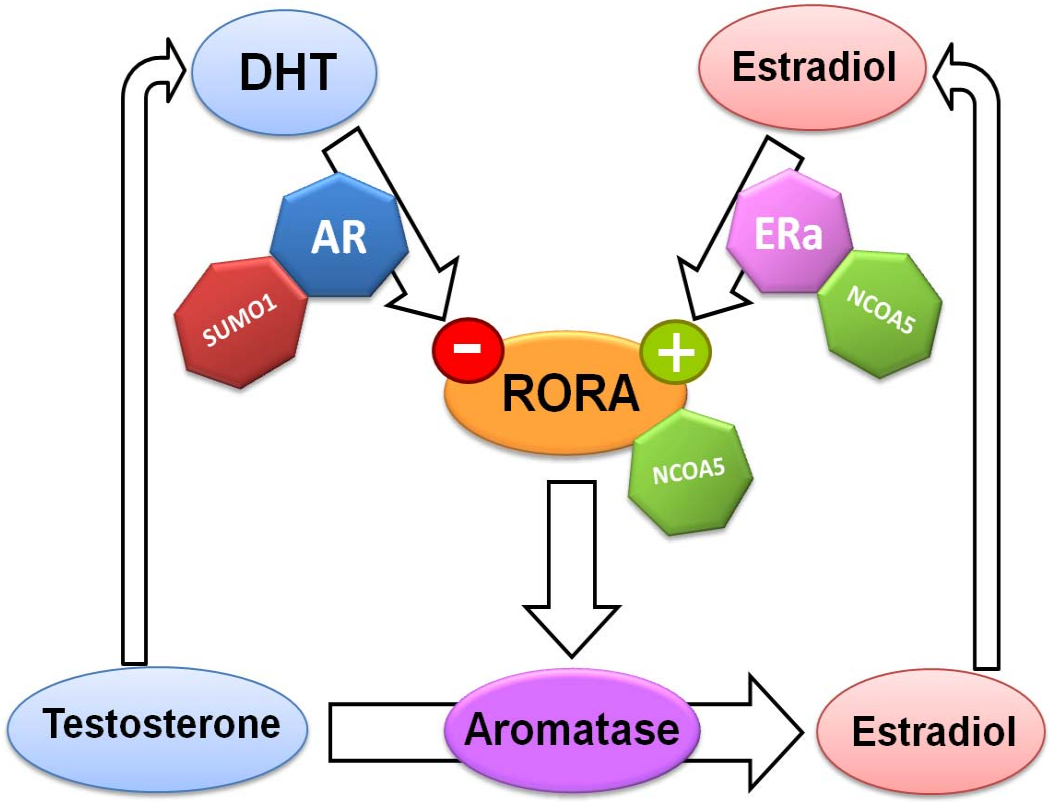

Figure 26. A model for reciprocal hormonal effects on *RORA*. The schematic illustrates a mechanism through which the observed reduction in RORA in autistic brain may lead to increased testosterone levels through downregulation of aromatase. Through AR/SUMO-1 complex, testosterone negatively modulates *RORA*, whereas estrogen upregulates *RORA* through ERα/NCOA5 complex. RORA, in turn, positively regulates expression of aromatase, probably by interacting with NCOA5.

Roles of coregulators in autism

Autism is believed to be a complex disorder involving dysregulation of multiple genes. Global changes in gene expression profiles observed in several recent studies suggest the operation of molecular "master switches" which can activate or suppress multiple genes at once (V. W. Hu et al., 2006; V. W. Hu et al., 2009; V. W. Hu, Sarachana et al., 2009; Voineagu et al., 2011). Coregulators are potential regulators of gene expression that can operate in this fashion because they have the potential to modulate transcriptional regulation activity of several nuclear receptors in the cells. Dysregulation of coregulators can result in aberrant expression of a number of target genes and, in turn, results in a variety of abnormalities in cellular functions.

Our previous gene expression profiling study revealed that, in addition to *RORA*, several coregulators (e.g., *NCOA1*, *NCOA5*, *SUMO-1*, and *FHL2*) are also dysregulated in LCLs from individuals with autism (V. W. Hu, Sarachana et al., 2009). The transcript levels of SUMO-1 and NCOA5 are significantly increased and decreased, respectively, in LCLs from individuals with autism relative to controls. SUMO-1, the Small Ubiquitin-related MOdifier 1, functions in a manner similar to ubiquitin in that it is bound to target proteins as part of a post-translational modification system. However, unlike ubiquitin which targets proteins for proteasomal degradation, this protein is involved in a variety of cellular processes, such as nuclear transport, transcriptional regulation, apoptosis, and protein stability (Johnson, 2004). SUMO-1 is expressed in all tissues with highest abundance in the testis, brain, lung, and spleen (Zhang et al., 2008). Poukka and colleagues have demonstrated that SUMO-1 covalently modifies AR at the N-terminal domain and inhibits the activity of AR (Poukka, Karvonen, Janne, & Palvimo, 2000). The molecular

mechanisms through which SUMO-1 suppresses transcription of AR targets (including *RORA*) have not been elucidated, but it might involve chromatin modifications, including histone deacetylation, histone demethylation, histone methylation, and/or nucleosomal remodeling, which have been demonstrated to play an important role in SUMO-dependent corepression of other transcription factors (Ayyanathan et al., 2003; Ivanov et al., 2007; Kuo et al., 2005; Lin et al., 2006; Ouyang & Gill, 2009; Ouyang, Shi, Valin, Xuan, & Gill, 2009; Stielow et al., 2008).

Another coregulator significantly dysregulated in individuals with autism is NCOA5, also known as CIA (Coactivator Independent of AF-2 function) (V. W. Hu, Sarachana et al., 2009). NCOA5 is abundantly expressed in the heart, brain, lung, kidney, and spleen (Sauve et al., 2001). Unlike other coregulators, NCOA5 does not require the ligand-dependent activation function-2 (AF2) domain of the target nuclear receptors to interact with nuclear receptors and mediate transcriptional regulation. Using yeast two-hybrid screen, Sauve and colleagues (2001) identified NCOA5 as a novel ER coactivator. They showed that NCOA5 formed complexes with ERα and ERβ in a ligand-independent manner *in vitro* and enhanced ERα transcriptional activity (Sauve et al., 2001). In the presence of estradiol, NCOA5 interacts with ERα on the promoter of *pS2* gene and increases transcriptional activity of the gene. In addition to ER coactivator activity, NCOA5 was reported to possess corepressor activity as well (Jiang et al., 2004; Sauve et al., 2001). Jiang and colleagues (2004) found that liganded ERα recruited NCOA5 and TIP30 to the promoter of *c-myc* gene to repress ERα-mediated *c-myc* transcription (Jiang et al., 2004). These findings suggest that transcriptional activity mediated by NCOA5 is

target-dependent. Nevertheless, the precise mechanisms by which NCOA5 enhances or represses transcription remain unknown and deserve further study.

Interestingly, this study shows that SUMO-1 is involved in DHT-mediated repression of *RORA*, whereas NCOA5 is required for estradiol-mediated overexpression of *RORA* and may be involved in regulation of aromatase expression by RORA. Co-immunoprecipitation and sequential chromatin immunoprecipitation analyses in this study revealed that AR and ERα interacts with the AR coregulator SUMO-1 and the ER coregulator NCOA5, respectively, in the *RORA* promoter region. Moreover, siRNA-mediated knockdown of these coregulator proteins significantly reduced the inverse regulatory effects of the sex hormones on *RORA* expression. Knockdown of SUMO-1 completely abolished DHT-mediated repression of *RORA* expression, whereas knockdown of NCOA5 significantly diminished the enhancement of *RORA* expression induced by estradiol. These findings indicate that SUMO-1 acts as an AR corepressor while NCOA5 acts as an ERα coactivator to regulate *RORA* expression and that SUMO-1 and NCOA5 are involved in inverse modulation of *RORA* expression by the sex hormones.

To identify specific chromosomal locations required for the sex hormone regulation of *RORA*, we performed luciferase dual reporter assays using luciferase vectors in which *RORA* promoter was inserted upstream of firefly luciferase gene such that the transcription of luciferase was regulated by the *RORA* promoter. The luciferase reporter assays revealed that distal AR- and ERα-binding sites (as far as ~10kb upstream) were required for the inverse regulation of *RORA* by the sex hormones. Interestingly, the results from luciferase assays seem to support the findings from sequential chromatin immunoprecipitation analysis of AR- and ERα coregulators. The ChIP-reChIP analysis showed that SUMO-1 is

likely to interact with AR at the ARbs-I and, with a lower degree of enrichment, at the ARbs-III in the promoter region of *RORA*. The coregulator FHL2, thought to be a coactivator of AR (Muller et al., 2000), seems to interact with AR at the ARbs-II. The luciferase assays revealed that, in the presence of ARbs-II, but absence of ARbs-I, the DHT-mediated repression of *RORA* promoter activity was lost. In fact, the addition of DHT increased the activity of the *RORA* promoter containing only ARbs-II and –III, suggesting that FHL2-mediated transcriptional coactivation through ARbs-II may overcome SUMO-1-mediated corepression through ARbs-III. However, it should be noted that the changes in the *RORA* promoter activity mediated by DHT were modest, albeit significant, probably because the expression of AR in the SH-SY5Y cell line which is derived from a female donor may be low. Thus, future studies may include the use of AR-overexpressed neuronal cell line to clearly elucidate the effect of DHT-mediated regulation of *RORA* promoter activity.

The ChIP-reChIP analysis of ERα coregulators showed that NCOA5 interacted with ERα at the ERbs-I and, with a lower degree of enrichment, the ERbs-II in the promoter of *RORA*. The coregulator FHL2, thought to be a corepressor of ERα (Xiong et al., 2010), preferentially interacted with ERα at the ERbs-IV. Using luciferase reporter assays, we demonstrated that the ERbs-I is required for estradiol-mediated transcriptional activation of *RORA*. Without ERbs-I, the addition of estradiol resulted in transcriptional repression of *RORA* promoter activity, likely due to the transcriptional corepression by FHL2 at ERbs-IV. However, we cannot rule out the roles of other nuclear receptor coregulators not studied here. Thus future studies are needed to elucidate a role of

additional coregulator proteins interacting with AR and ERα on the *RORA* promoter region to regulate the transcription of *RORA* gene.

These results suggest that reduction of RORA and aromatase in autism may be aggravated by the dysregulation of these coregulator proteins. Moreover, it is interesting that RORA not only shares binding consensus with ER, but is also likely to share some coregulators, including NCOA5, suggesting the possibility that some transcriptional regulatory functions of RORA may be partially compensated by ERα.

RORA directly regulates other genes associated with autism

Like other nuclear receptor transcription factors, RORA potentially regulates a number of target genes at once. Reduction of RORA, as observed in individuals with autism, may trigger changes in expression of several target genes involved in a variety of cellular functions associated with autism. Using high-throughput, whole-genome promoter microarray analysis, we identify promoter regions potentially regulated by the orphan nuclear receptor RORA in the human genome. Instead of using t-test analysis with multiple sample corrections which is a conventional statistical analysis for gene expression microarray data, we used ANOVA which has been shown to be useful for ChIP-on-chip analysis to prioritize potential target genes for further confirmation (Song et al., 2009). Interestingly, the promoter region of as many as 1,274 genes throughout the human genome may be regulated by RORA. Biological network and pathway analysis revealed that these potential transcriptional targets of RORA are significantly associated with nervous system development and functions in which RORA is known to play an important role. These neurological functions include development of cortex and cerebellum, adhesion

of neuronal cells, neurogenesis, and synaptic density, all of which have been associated with autism (Amaral, Schumann, & Nordahl, 2008; Bourgeron, 2009; Carper & Courchesne, 2005; Courchesne & Pierce, 2005; Kelleher & Bear, 2008; Wegiel et al., 2010). It is also noteworthy that neurological disorders known to be co-morbid disorders with autism, including bipolar disorder (Stahlberg et al., 2004; Wozniak et al., 1997), schizophrenia (Konstantareas & Hewitt, 2001; F. R. Volkmar & Cohen, 1991), movement disorder (Ghaziuddin & Butler, 1998; V. Jones & Prior, 1985; Kielinen et al., 2004; Minshew et al., 2004; Vilensky et al., 1981), and mental retardation (Bertrand et al., 2001; S. Chakrabarti & Fombonne, 2001; S. Chakrabarti & Fombonne, 2005), were also identified to be associated with these potential targets of RORA.

A well-established RORA target (i.e. *ITPR1*) and five novel potential RORA targets in nervous system tissues (i.e. *A2BP1*, *CYP19A1*, *HSD17B10*, *NLGN1*, and *NTRK2*) were selected for confirmation using independent ChIP-qPCR analysis, and further functionally validated using shRNA-mediated knockdown of *RORA*. Using independent chromatin immunoprecipitation assays, we found that the promoter regions of all selected targets were significantly enriched in the chromatin immunoprecipitated with RORA. Knockdown of RORA using shRNA revealed that the reduction of *RORA* expression also resulted in aberrant expression of these targets, confirming that the selected targets are actual transcriptional targets of RORA.

Pathway analysis using Pathway Studio, a gene network prediction software that uses text-mining to scan the PubMed database, revealed associations of these confirmed RORA targets with autism as well as autism-related neurological functions and disorders, including synaptogenesis and synaptic functions, synaptic plasticity, learning, memory, and

nerve degeneration. It is interesting to note that ataxia which is known to be a neurological disorder caused by RORA deficiency as well as a comorbid disorder of autism, was also identified to be associated with these RORA targets, suggesting that these selected targets are also relevant to pathological conditions associated with RORA deficiency.

To minimize false-positive associations identified by the text-mining program, we also downloaded the research articles that proposed the link between these genes and autism from the PubMed database and verified by independent review of the literature that these RORA targets were reliably associated with autism. A2BP1 (ataxin 2-binding protein 1), also known as FOX1, is an RNA-binding protein that regulates tissue-specific alternative splicing. Several studies, both genetic and gene expression analyses, have established the link between this gene and autism. Using FISH and qPCR analyses, Martin and colleagues (2007) found a cryptic deletion of *A2BP1* gene in a female with autism, epilepsy, and global development delay. Reduction of *A2BP1* transcript level was also observed in the lymphocytes of this individual, suggesting that the deletion causes aberrant expression of this gene in this autism case. By genotyping 27 SNPs across this gene in 206 parent-child trios, they identified two regions exhibiting a nominal association with autism ($p \leq 0.008$) (Martin et al., 2007). Moreover, a recent noise-reduction GWAS (GWAS-NR) analysis of two autism GWAS datasets (with 597 and 696 families) from the Autism Genetic Resource Exchange (AGRE) revealed 1,535 significant linkage disequilibrium blocks overlapping 431 genes (Hussman et al., 2011). Interestingly, regions in *A2BP1* gene were identified among the most significant linkage disequilibrium blocks ($p = 3.6E-05$). Furthermore, Voineagu and colleagues (2011) also conducted transcriptomic analysis of post-mortem frontal and temporal cortex tissues from 19 individuals with autism and 17

controls using microarrays. They found that *A2BP1* expression was significantly reduced in both frontal and temporal cortex tissues from individuals with autism relative to controls. Using high-throughput RNA sequencing and semi-quantitative RT-PCR analyses, they also demonstrated that splicing of A2BP1-dependent alternative exons in the brain of individuals with autism was dysregulated (Voineagu et al., 2011), suggesting that aberrant expression of *A2BP1* results in dysregulation of alternative splicing in autism. Findings from several CNV studies (Autism Genome Project Consortium et al., 2007; Bucan et al., 2009; Gai et al., 2012; Pinto et al., 2010; Sanders et al., 2011; Sebat et al., 2007) and linkage studies (Buxbaum et al., 2004; International Molecular Genetic Study of Autism Consortium (IMGSAC), 1998; International Molecular Genetic Study of Autism Consortium (IMGSAC), 2001; Lauritsen et al., 2006; McCauley et al., 2005) have also reported that *A2BP1* is associated with autism.

CYP19A1 encodes aromatase, a key enzyme converting androstenedione to estrone and converting testosterone to estradiol. Aromatase promotes regulatory effects on several neurological processes, including cell survival, neuronal differentiation, synaptic function and plasticity, and protection of oxidative stress (Azcoitia et al., 2001; Garcia-Segura, Veiga, Sierra, Melcangi, & Azcoitia, 2003; Garcia-Segura, 2008; Kretz et al., 2004; Lepore, Gadau, Mura, Zedda, & Farina, 2009; Lepore et al., 2011; Liu, Hurn, Roselli, & Alkayed, 2007; Saldanha, Duncan, & Walters, 2009; Zhou et al., 2010), all of which have been associated with autism (Chauhan & Chauhan, 2006; Herbert, 2011; McGinnis, 2004; Wegiel et al., 2010). CYP19A1 has been associated with autism by genetic studies. Allen-Brady and colleagues (2010) conducted genome-wide screen of 70 families (192 individuals with autism and 461 unaffected relatives) and identified three regions shown to

be highly significant in the linkage analysis. Interestingly, one of the three regions is 15q21.1-15q22.2 (heterogeneity LOD = 5.31) where the *CYP19A1* gene is located (Allen-Brady et al., 2010). Moreover, Chakrabarti and colleagues (2009) studied SNPs in 68 candidate genes for autism to identify common genetic variations associated with autistic traits and Asperger syndrome, a high-functioning subgroup of autism. A case-control association analysis of individuals with Asperger syndrome (n = 174) revealed regions in 14 genes, including *CYP19A1*, that showed a nominally significant association with Asperger syndrome (B. Chakrabarti et al., 2009).

HSD17B10 encodes 3-hydroxyacyl-CoA dehydrogenase type-2, a mitochondrial enzyme involved in mitochondrial integrity and oxidation of fatty acids and steroids. It is noteworthy that mitochondrial dysfunction has been reported in individuals with autism (Giulivi et al., 2010; Oliveira et al., 2005). Reduced expression of *HSD17B10* causes X-linked mental retardation, choreoathetosis, language impairment, and abnormal behavior (Lenski et al., 2007; Ofman et al., 2003; Reyniers et al., 1999). Using chromosome microarray analysis, Edens and colleagues (2011) reported duplications involving Xp11.22-p11.23, a region where *HSD17B10* gene is located, in two females with autism and epilepsy (Edens, Lyons, Duron, Dupont, & Holden, 2011).

ITPR1 (inositol 1,4,5-triphosphate receptor type 1) is a ligand-gated ion channel activated by cytosolic calcium and inositol triphosphate. This receptor is localized on intracellular membranes, including endoplasmic reticulum, and mediates the mobilization of intracellular calcium ion stores. Mutations of this gene cause spinocerebellar ataxia type 15 and have been associated with autism. Transcriptomic analysis of frontal and temporal cortex tissues from 16 individuals with autism and 16 controls revealed down-regulation of

ITPR1 (Voineagu et al., 2011). Bremer and colleagues (2010) used high-resolution whole genome array-based comparative genomic hybridization (array-CGH) to screen 223 individuals with autism to identify gene dose alterations associated with autism susceptibility. They found regions in chromosome 3p25.3, where *ITPR1* is located, significantly enriched in individuals with autism (Bremer et al., 2011). Another CNV study by Sanders and colleagues (2011) using 1,124 families, each of which comprised of a single proband, unaffected parents and, in most families, an unaffected sibling, revealed as many as 234 CNV regions in several genes, including *ITPR1*, to be associated with autism (Sanders et al., 2011). Moreover, Levy and colleagues (2011) studied genomic copy-number variation in a large cohort of families with a single affected child and at least one unaffected sibling. Among significant regions identified to be *de novo* CNVs were regions containing the *ITPR1* gene (Levy et al., 2011).

NLGN1 encodes neuroligin-1, a neuronal cell surface protein. NLGN1 is involved in formation and remodeling of synapses in the CNS (Scheiffele, Fan, Choih, Fetter, & Serafini, 2000), a neurological function impacted in individuals with autism. Glessner and colleagues (2009) conducted a whole-genome CNV analysis of 859 individuals with autism and 1,409 typically developing children of European ancestry who were genotyped with ~550,000 SNP markers to comprehensively identify CNVs conferring susceptibility to autism. Positive findings were evaluated in an independent cohort of 1,336 individuals with autism and 1,110 controls of European ancestry. Interestingly, a CNV region in *NLGN1* gene was significantly enriched in individuals with autism ($p = 0.010$) (Glessner et al., 2009). Moreover, Ylisaukko-oja and colleagues (2005) conducted family-based association analysis of 100 families with autism and found a modest significant association at a region

in *NLGN1* gene (rs1488545, p = 0.002) (Ylisaukko-oja et al., 2005). A high-density SNP, genome-wide linkage study also showed that the chromosomal region 3q26.31-q27.3 was significantly associated with autism (nonparametric linkage = 4.85) (Allen-Brady et al., 2009). Deletion of this gene was also reported to cause impaired spatial memory and increased repetitive behavior (Blundell et al., 2010).

NTRK2 (neurotrophic tyrosine kinase receptor type 2) is a catalytic receptor for several neurotrophins, including BDNF, NT4, and NT3. NTRK2 is involved in neuronal differentiation and survival. Correia and colleagues (2010) performed genetic association analysis of 146 children with autism and 50 typically developing controls to identify regions in *NTRK2* gene that are associated with autism susceptibility. Interestingly, 6 SNPs and multiple haplotypes in the *NTRK2* gene were identified to be associated with autism (pSNPs = 0.004 - 0.039; pHaplotypes = 5×10^{4} – 0.042). They also found that BDNF levels were significantly increased in children with autism relative to controls ($p < 0.0001$), supporting a role of NTRK2/BDNF signaling as a susceptibility factor for the disorder (Correia et al., 2010).

Using RT-qPCR analysis, we also showed that the transcript levels of selected transcriptional targets of RORA were also dysregulated in postmortem brain tissues from individuals with autism. Interestingly, the transcript levels of *CYP19A1*, *A2BP1*, and *NLGN1* were positively correlated with the transcript level of *RORA*, suggesting that expression of these genes may be regulated by RORA in the prefrontal cortex. Although the other 3 RORA targets were also significantly reduced in the autistic brain samples relative to that in the controls (with the exception of *NTRK2* which increased in the autistic sample of 1 matched pair), the correlation with decrease with *RORA* transcript level was

modest or very low. Confocal immunofluorescence analysis of a tissue array containing prefrontal cortex tissues from an independent set of subjects revealed significant reduction of both RORA and CYP19A1 (aromatase) in individuals with autism relative to controls. The immunofluorescence levels of MAP2 and DAPI were not significantly changed in brain tissues from individuals with autism, indicating that decreased levels of RORA and aromatase proteins are specific to the disorder, and not because neurons are broadly compromised by neurodegenerative processes in the brain of individuals with autism. It is interesting to note that the levels of aromatase protein were strongly correlated with the levels of RORA protein in this independent cohort, thus supporting our hypothesis that RORA may regulate aromatase expression in the human prefrontal cortex.

The fact that RORA can regulate several genes that have been directly associated with autism in previous studies by other groups suggests that RORA may serve as an upstream regulator that controls other autism candidate genes, and further supports the possibility that the dysregulation of RORA is involved in the etiology and/or the susceptibility of autism.

Potential pitfalls and future directions

In this study, we utilized DHT, a biologically active form of androgen that cannot be converted to estrogen, to study the effect of male sex hormone on *RORA* expression. Thus, the effect of DHT on *RORA* expression observed in this study is likely to be a direct effect of androgen, not an indirect effect of estrogen being converted from androgen. However, although the inverse effects of dihydrotestosterone and estradiol were observed in the SH-SY5Y neuroblastoma cell line which is a widely used neuronal cell model, this

line may not replicate all responses of neurons in the brain in which there are also other aromatizable forms of androgens available. Thus, it would also be important to study the effects of sex hormones on *RORA* expression and interactions *in vivo* using an appropriate animal model in which the concentration of androgens and estrogens can be carefully examined, especially in the brain. Moreover, androgens and estrogens circulating in the bloodstream are bound mostly to the sex hormone binding globulin (SHBG) and serum albumin. Only a small amount of circulating sex hormones is unbound from proteins and biologically active. The levels of the sex hormone binding proteins which influence the bioavailability of sex hormones as well as the concentrations of free sex hormones should be taken into consideration in future *in vivo* studies as well. Furthermore, we focused on the prefrontal cortex region which has been implicated in autism-related executive functions, including planning complex cognitive behavior, personality expression, decision making and moderating social behavior, and is known to be highly affected in autism (Courchesne et al., 2011; Y. Yang & Raine, 2009). However, it would also be interesting to investigate the proposed mechanism in sexually dimorphic neuroanatomical structures, including the anteroventral paraventricular nucleus (AVPV) and the sexually dimorphic nucleus of the preoptic area (SDN-POA) in the hypothalamus.

A number of coregulator proteins have been shown to be involved in the modulation of nuclear receptor transactivation or transrepression. In this study, we focus only on the coregulator proteins whose expression was found to be most aberrant in LCLs from individuals with autism. In cells, however, each nuclear receptor is likely to interact with more than one protein to regulate expression of its transcriptional targets. Thus, it would be interesting to identify other proteins that form a complex to regulate

transcriptional activity of AR and ERα on *RORA* expression, as well as proteins regulating the activity of *RORA* on expression of its transcriptional targets. It would be also interesting to examine expression of nuclear receptors and coregulators in the brain of individuals with autism.

Both ERα and ERβ are known to be ubiquitously expressed in the human brain from early prenatal stages to adult life. However, we focus only on ERα in this study because there is evidence that ERα may be more important in biological functions associated with autism, including early cortical development processes (Gonzalez et al., 2007), regulation of transcriptional targets in the cortex (Delaunay, Pettersson, Tujague, & Gustafsson, 2000; Gonzalez et al., 2007), neuroprotection against cytotoxicity (Spampinato et al., 2012) and ischemia (Dubal et al., 2001), and social discrimination (Choleris et al., 2006). However, the mechanisms through which ERβ may be involved in regulation of RORA also deserve further study since ERβ is also known to be highly expressed in cortex, amygdala, and cerebellum, where AR is also highly expressed (Purves et al., 2012). Moreover, ERβ may be important for development of future therapies for RORA deficiency because ERβ is known to have little or no expression in the breast or uterus, thus selective activation of ERβ may provide the beneficial effects of estrogen in the brain without undesired effects in reproductive organs.

References

Ahsgren, I., Baldwin, I., Goetzinger-Falk, C., Erikson, A., Flodmark, O., & Gillberg, C. (2005). Ataxia, autism, and the cerebellum: A clinical study of 32 individuals with congenital ataxia. *Developmental Medicine and Child Neurology, 47*(3), 193-198.

Akashi, M., & Takumi, T. (2005). The orphan nuclear receptor RORalpha regulates circadian transcription of the mammalian core-clock Bmal1. *Nature Structural & Molecular Biology, 12*(5), 441-448. doi: 10.1038/nsmb925

Allen-Brady, K., Miller, J., Matsunami, N., Stevens, J., Block, H., Farley, M., . . . Coon, H. (2009). A high-density SNP genome-wide linkage scan in a large autism extended pedigree. *Molecular Psychiatry, 14*(6), 590-600. doi: 10.1038/mp.2008.14

Allen-Brady, K., Robison, R., Cannon, D., Varvil, T., Villalobos, M., Pingree, C., . . . Coon, H. (2010). Genome-wide linkage in utah autism pedigrees. *Molecular Psychiatry, 15*(10), 1006-1015. doi: 10.1038/mp.2009.42

Amaral, D. G., Schumann, C. M., & Nordahl, C. W. (2008). Neuroanatomy of autism. *Trends in Neurosciences, 31*(3), 137-145. doi: 10.1016/j.tins.2007.12.005

American Psychiatric Association, & American Psychiatric Association. Task Force on DSM-IV. (2000). *Diagnostic and statistical manual of mental disorders: DSM-IV-TR* (4th , text revision ed.). Washington, DC: American Psychiatric Association.

Arking, D. E., Cutler, D. J., Brune, C. W., Teslovich, T. M., West, K., Ikeda, M., . . . Chakravarti, A. (2008). A common genetic variant in the neurexin superfamily

member CNTNAP2 increases familial risk of autism. *American Journal of Human Genetics, 82*(1), 160-164. doi: 10.1016/j.ajhg.2007.09.015

Atkins, G. B., Hu, X., Guenther, M. G., Rachez, C., Freedman, L. P., & Lazar, M. A. (1999). Coactivators for the orphan nuclear receptor RORalpha. *Molecular Endocrinology (Baltimore, Md.), 13*(9), 1550-1557.

Autism Genome Project Consortium, Szatmari, P., Paterson, A. D., Zwaigenbaum, L., Roberts, W., Brian, J., . . . Meyer, K. J. (2007). Mapping autism risk loci using genetic linkage and chromosomal rearrangements. *Nature Genetics, 39*(3), 319-328. doi: 10.1038/ng1985

Autism Speaks. (2012). *Facts about autism.* Retrieved 7/9, 2012, from http://www.autismspeaks.org/what-autism/facts-about-autism

Auyeung, B., Baron-Cohen, S., Ashwin, E., Knickmeyer, R., Taylor, K., & Hackett, G. (2009). Fetal testosterone and autistic traits. *British Journal of Psychology (London, England : 1953), 100*(Pt 1), 1-22. doi: 10.1348/000712608X311731

Auyeung, B., Baron-Cohen, S., Chapman, E., Knickmeyer, R., Taylor, K., & Hackett, G. (2006). Foetal testosterone and the child systemizing quotient. *European Journal of Endocrinology, 155*, S123-S130.

Auyeung, B., Taylor, K., Hackett, G., & Baron-Cohen, S. (2010). Foetal testosterone and autistic traits in 18 to 24-month-old children. *Molecular Autism, 1*(1), 11. doi: 10.1186/2040-2392-1-11

Ayyanathan, K., Lechner, M. S., Bell, P., Maul, G. G., Schultz, D. C., Yamada, Y., . . . Rauscher, F. J.,3rd. (2003). Regulated recruitment of HP1 to a euchromatic gene induces mitotically heritable, epigenetic gene silencing: A mammalian cell culture model of gene variegation. *Genes & Development, 17*(15), 1855-1869. doi: 10.1101/gad.1102803

Azcoitia, I., Sierra, A., Veiga, S., Honda, S., Harada, N., & Garcia-Segura, L. M. (2001). Brain aromatase is neuroprotective. *Journal of Neurobiology, 47*(4), 318-329.

Bailey, A., Bolton, P., Butler, L., Le Couteur, A., Murphy, M., Scott, S., . . . Rutter, M. (1993). Prevalence of the fragile X anomaly amongst autistic twins and singletons. *Journal of Child Psychology and Psychiatry, and Allied Disciplines, 34*(5), 673-688.

Bailey, A., Luthert, P., Dean, A., Harding, B., Janota, I., Montgomery, M., . . . Lantos, P. (1998). A clinicopathological study of autism. *Brain : A Journal of Neurology, 121 (Pt 5)*(Pt 5), 889-905.

Baio, J. (2012). Prevalence of autism spectrum disorders - autism and developmental disabilities monitoring network, 14 sites, united states, 2008. *Centers for Disease Control and Prevention Morbidity and Mortality Weekly Report, 61*(3)

Ballaban-Gil, K., & Tuchman, R. (2000). Epilepsy and epileptiform EEG: Association with autism and language disorders. *Mental Retardation and Developmental Disabilities Research Reviews, 6*(4), 300-308. doi: 2-R

Baron-Cohen, S. (2009). Autism: The empathizing-systemizing (E-S) theory. *Annals of the New York Academy of Sciences, 1156*, 68-80. doi: 10.1111/j.1749-6632.2009.04467.x

Baron-Cohen, S., Knickmeyer, R. C., & Belmonte, M. K. (2005). Sex differences in the brain: Implications for explaining autism. *Science (New York, N.Y.), 310*(5749), 819-823. doi: 10.1126/science.1115455

Baron-Cohen, S., Lombardo, M. V., Auyeung, B., Ashwin, E., Chakrabarti, B., & Knickmeyer, R. (2011). Why are autism spectrum conditions more prevalent in males? *PLoS Biology, 9*(6), e1001081. doi: 10.1371/journal.pbio.1001081

Baron-Cohen, S., Richler, J., Bisarya, D., Gurunathan, N., & Wheelwright, S. (2003). The systemizing quotient: An investigation of adults with asperger syndrome or high-functioning autism, and normal sex differences. *Philosophical Transactions of the Royal Society of London.Series B, Biological Sciences, 358*(1430), 361-374. doi: 10.1098/rstb.2002.1206

Baron-Cohen, S., Scahill, V. L., Izaguirre, J., Hornsey, H., & Robertson, M. M. (1999). The prevalence of gilles de la tourette syndrome in children and adolescents with autism: A large scale study. *Psychological Medicine, 29*(5), 1151-1159.

Baron-Cohen, S., & Wheelwright, S. (2004). The empathy quotient: An investigation of adults with asperger syndrome or high functioning autism, and normal sex differences. *Journal of Autism and Developmental Disorders, 34*(2), 163-175.

Barton, M., & Volkmar, F. (1998). How commonly are known medical conditions associated with autism? *Journal of Autism and Developmental Disorders, 28*(4), 273-278.

Beacher, F. D., Radulescu, E., Minati, L., Baron-Cohen, S., Lombardo, M. V., Lai, M. C., . . . Critchley, H. D. (2012). Sex differences and autism: Brain function during verbal fluency and mental rotation. *PloS One, 7*(6), e38355. doi: 10.1371/journal.pone.0038355

Becker-Andre, M., Andre, E., & DeLamarter, J. F. (1993). Identification of nuclear receptor mRNAs by RT-PCR amplification of conserved zinc-finger motif sequences. *Biochemical and Biophysical Research Communications, 194*(3), 1371-1379.

Belmonte, M. K., Cook, E. H.,Jr, Anderson, G. M., Rubenstein, J. L., Greenough, W. T., Beckel-Mitchener, A., . . . Tierney, E. (2004). Autism as a disorder of neural information processing: Directions for research and targets for therapy. *Molecular Psychiatry, 9*(7), 646-663. doi: 10.1038/sj.mp.4001499

Bensoula, A. N., Guastavino, J. M., Lalonde, R., Portet, R., Bertin, R., & Krafft, B. (1995). Spatial navigation of staggerer and normal mice during juvenile and adult stages. *Physiology & Behavior, 58*(5), 823-825.

Benvenuto, A., Moavero, R., Alessandrelli, R., Manzi, B., & Curatolo, P. (2009). Syndromic autism: Causes and pathogenetic pathways. *World Journal of Pediatrics : WJP, 5*(3), 169-176. doi: 10.1007/s12519-009-0033-2

Bertin, R., Guastavino, J. M., & Portet, R. (1990). Effects of cold acclimation on the energetic metabolism of the staggerer mutant mouse. *Physiology & Behavior, 47*(2), 377-380.

Bertrand, J., Mars, A., Boyle, C., Bove, F., Yeargin-Allsopp, M., & Decoufle, P. (2001). Prevalence of autism in a united states population: The brick township, new jersey, investigation. *Pediatrics, 108*(5), 1155-1161.

Besnard, S., Silvestre, J. S., Duriez, M., Bakouche, J., Lemaigre-Dubreuil, Y., Mariani, J., . . . Tedgui, A. (2001). Increased ischemia-induced angiogenesis in the staggerer mouse, a mutant of the nuclear receptor roralpha. *Circulation Research, 89*(12), 1209-1215.

Bitsch, F., Aichholz, R., Kallen, J., Geisse, S., Fournier, B., & Schlaeppi, J. M. (2003). Identification of natural ligands of retinoic acid receptor-related orphan receptor alpha ligand-binding domain expressed in Sf9 cells--a mass spectrometry approach. *Analytical Biochemistry, 323*(1), 139-149.

Blundell, J., Blaiss, C. A., Etherton, M. R., Espinosa, F., Tabuchi, K., Walz, C., . . . Powell, C. M. (2010). Neuroligin-1 deletion results in impaired spatial memory and increased repetitive behavior. *The Journal of Neuroscience : The Official Journal of the Society for Neuroscience, 30*(6), 2115-2129. doi: 10.1523/JNEUROSCI.4517-09.2010

Bodfish, J. W., Symons, F. J., Parker, D. E., & Lewis, M. H. (2000). Varieties of repetitive behavior in autism: Comparisons to mental retardation. *Journal of Autism and Developmental Disorders, 30*(3), 237-243.

Boukhtouche, F., Janmaat, S., Vodjdani, G., Gautheron, V., Mallet, J., Dusart, I., & Mariani, J. (2006). Retinoid-related orphan receptor alpha controls the early steps of purkinje cell dendritic differentiation. *The Journal of Neuroscience : The Official Journal of the Society for Neuroscience, 26*(5), 1531-1538. doi: 10.1523/JNEUROSCI.4636-05.2006

Boukhtouche, F., Vodjdani, G., Jarvis, C. I., Bakouche, J., Staels, B., Mallet, J., . . . Brugg, B. (2006). Human retinoic acid receptor-related orphan receptor alpha1 overexpression protects neurones against oxidative stress-induced apoptosis. *Journal of Neurochemistry, 96*(6), 1778-1789. doi: 10.1111/j.1471-4159.2006.03708.x

Bourgeron, T. (2009). A synaptic trek to autism. *Current Opinion in Neurobiology, 19*(2), 231-234. doi: 10.1016/j.conb.2009.06.003

Bremer, A., Giacobini, M., Eriksson, M., Gustavsson, P., Nordin, V., Fernell, E., . . . Schoumans, J. (2011). Copy number variation characteristics in subpopulations of patients with autism spectrum disorders. *American Journal of Medical Genetics.Part B, Neuropsychiatric Genetics : The Official Publication of the International Society of Psychiatric Genetics, 156*(2), 115-124. doi: 10.1002/ajmg.b.31142; 10.1002/ajmg.b.31142

Bryne, J. C., Valen, E., Tang, M. H., Marstrand, T., Winther, O., da Piedade, I., . . . Sandelin, A. (2008). JASPAR, the open access database of transcription factor-binding profiles: New content and tools in the 2008 update. *Nucleic Acids Research, 36*(Database issue), D102-6. doi: 10.1093/nar/gkm955

Bucan, M., Abrahams, B. S., Wang, K., Glessner, J. T., Herman, E. I., Sonnenblick, L. I., . . . Hakonarson, H. (2009). Genome-wide analyses of exonic copy number variants in a family-based study point to novel autism susceptibility genes. *PLoS Genetics, 5*(6), e1000536. doi: 10.1371/journal.pgen.1000536

Bulloch, K., Hamburger, R. N., & Loy, R. (1982). Nest-building behavior in two cerebellar mutant mice: Staggerer and weaver. *Behavioral and Neural Biology, 36*(1), 94-97.

Burris, T. P. (2008). Nuclear hormone receptors for heme: REV-ERBalpha and REV-ERBbeta are ligand-regulated components of the mammalian clock. *Molecular Endocrinology (Baltimore, Md.), 22*(7), 1509-1520. doi: 10.1210/me.2007-0519

Buxbaum, J. D., Silverman, J., Keddache, M., Smith, C. J., Hollander, E., Ramoz, N., & Reichert, J. G. (2004). Linkage analysis for autism in a subset families with obsessive-compulsive behaviors: Evidence for an autism susceptibility gene on chromosome 1 and further support for susceptibility genes on chromosome 6 and 19. *Molecular Psychiatry, 9*(2), 144-150. doi: 10.1038/sj.mp.4001465

Carlberg, C., Hooft van Huijsduijnen, R., Staple, J. K., DeLamarter, J. F., & Becker-Andre, M. (1994). RZRs, a new family of retinoid-related orphan receptors that

function as both monomers and homodimers. *Molecular Endocrinology (Baltimore, Md.), 8*(6), 757-770.

Carper, R. A., & Courchesne, E. (2005). Localized enlargement of the frontal cortex in early autism. *Biological Psychiatry, 57*(2), 126-133. doi: 10.1016/j.biopsych.2004.11.005

Caston, J., Chianale, C., & Mariani, J. (2004). Spatial memory of heterozygous staggerer (rora(+)/Rora(sg)) versus normal (rora(+)/Rora(+)) mice during aging. *Behavior Genetics, 34*(3), 319-324. doi: 10.1023/B:BEGE.0000017875.78571.a6

Chakrabarti, B., Dudbridge, F., Kent, L., Wheelwright, S., Hill-Cawthorne, G., Allison, C., . . . Baron-Cohen, S. (2009). Genes related to sex steroids, neural growth, and social-emotional behavior are associated with autistic traits, empathy, and asperger syndrome. *Autism Research : Official Journal of the International Society for Autism Research, 2*(3), 157-177. doi: 10.1002/aur.80

Chakrabarti, S., & Fombonne, E. (2001). Pervasive developmental disorders in preschool children. *JAMA : The Journal of the American Medical Association, 285*(24), 3093-3099.

Chakrabarti, S., & Fombonne, E. (2005). Pervasive developmental disorders in preschool children: Confirmation of high prevalence. *The American Journal of Psychiatry, 162*(6), 1133-1141. doi: 10.1176/appi.ajp.162.6.1133

Charman, T., & Baird, G. (2002). Practitioner review: Diagnosis of autism spectrum disorder in 2- and 3-year-old children. *Journal of Child Psychology and Psychiatry, and Allied Disciplines, 43*(3), 289-305.

Chauhan, A., & Chauhan, V. (2006). Oxidative stress in autism. *Pathophysiology : The Official Journal of the International Society for Pathophysiology / ISP, 13*(3), 171-181. doi: 10.1016/j.pathophys.2006.05.007

Chauvet, C., Bois-Joyeux, B., Berra, E., Pouyssegur, J., & Danan, J. L. (2004). The gene encoding human retinoic acid-receptor-related orphan receptor alpha is a target for hypoxia-inducible factor 1. *The Biochemical Journal, 384*(Pt 1), 79-85. doi: 10.1042/BJ20040709

Choleris, E., Ogawa, S., Kavaliers, M., Gustafsson, J. A., Korach, K. S., Muglia, L. J., & Pfaff, D. W. (2006). Involvement of estrogen receptor alpha, beta and oxytocin in social discrimination: A detailed behavioral analysis with knockout female mice. *Genes, Brain, and Behavior, 5*(7), 528-539. doi: 10.1111/j.1601-183X.2006.00203.x

Chura, L. R., Lombardo, M. V., Ashwin, E., Auyeung, B., Chakrabarti, B., Bullmore, E. T., & Baron-Cohen, S. (2010). Organizational effects of fetal testosterone on human corpus callosum size and asymmetry. *Psychoneuroendocrinology, 35*(1), 122-132. doi: 10.1016/j.psyneuen.2009.09.009

Correia, C. T., Coutinho, A. M., Sequeira, A. F., Sousa, I. G., Lourenco Venda, L., Almeida, J. P., . . . Vicente, A. M. (2010). Increased BDNF levels and NTRK2 gene association suggest a disruption of BDNF/TrkB signaling in autism. *Genes, Brain,*

and Behavior, 9(7), 841-848. doi: 10.1111/j.1601-183X.2010.00627.x; 10.1111/j.1601-183X.2010.00627.x

Courchesne, E. (1991). Neuroanatomic imaging in autism. *Pediatrics, 87*(5 Pt 2), 781-790.

Courchesne, E. (1995). New evidence of cerebellar and brainstem hypoplasia in autistic infants, children and adolescents: The MR imaging study by hashimoto and colleagues. *Journal of Autism and Developmental Disorders, 25*(1), 19-22.

Courchesne, E., Mouton, P. R., Calhoun, M. E., Semendeferi, K., Ahrens-Barbeau, C., Hallet, M. J., . . . Pierce, K. (2011). Neuron number and size in prefrontal cortex of children with autism. *JAMA : The Journal of the American Medical Association, 306*(18), 2001-2010. doi: 10.1001/jama.2011.1638

Courchesne, E., & Pierce, K. (2005). Why the frontal cortex in autism might be talking only to itself: Local over-connectivity but long-distance disconnection. *Current Opinion in Neurobiology, 15*(2), 225-230. doi: 10.1016/j.conb.2005.03.001

Courchesne, E., Press, G. A., & Yeung-Courchesne, R. (1993). Parietal lobe abnormalities detected with MR in patients with infantile autism. *AJR.American Journal of Roentgenology, 160*(2), 387-393.

Courchesne, E., Yeung-Courchesne, R., Press, G. A., Hesselink, J. R., & Jernigan, T. L. (1988). Hypoplasia of cerebellar vermal lobules VI and VII in autism. *The New*

England Journal of Medicine, 318(21), 1349-1354. doi: 10.1056/NEJM198805263182102

Cross, J. H. (2005). Neurocutaneous syndromes and epilepsy-issues in diagnosis and management. *Epilepsia, 46 Suppl 10*, 17-23. doi: 10.1111/j.1528-1167.2005.00353.x

Curatolo, P., Porfirio, M. C., Manzi, B., & Seri, S. (2004). Autism in tuberous sclerosis. *European Journal of Paediatric Neurology : EJPN : Official Journal of the European Paediatric Neurology Society, 8*(6), 327-332. doi: 10.1016/j.ejpn.2004.08.005

Danielsson, S., Gillberg, I. C., Billstedt, E., Gillberg, C., & Olsson, I. (2005). Epilepsy in young adults with autism: A prospective population-based follow-up study of 120 individuals diagnosed in childhood. *Epilepsia, 46*(6), 918-923. doi: 10.1111/j.1528-1167.2005.57504.x

Deiss, V., Dubois, M., Lalonde, R., & Strazielle, C. (2001). Cytochrome oxidase activity in the olfactory system of staggerer mutant mice. *Brain Research, 910*(1-2), 126-133.

Delaunay, F., Pettersson, K., Tujague, M., & Gustafsson, J. A. (2000). Functional differences between the amino-terminal domains of estrogen receptors alpha and beta. *Molecular Pharmacology, 58*(3), 584-590.

Delerive, P., Monte, D., Dubois, G., Trottein, F., Fruchart-Najib, J., Mariani, J., . . . Staels, B. (2001). The orphan nuclear receptor ROR alpha is a negative regulator of

the inflammatory response. *EMBO Reports, 2*(1), 42-48. doi: 10.1093/embo-reports/kve007

Dong, C., Yuan, L., Dai, J., Lai, L., Mao, L., Xiang, S., . . . Hill, S. M. (2010). Melatonin inhibits mitogenic cross-talk between retinoic acid-related orphan receptor alpha (RORalpha) and ERalpha in MCF-7 human breast cancer cells. *Steroids, 75*(12), 944-951. doi: 10.1016/j.steroids.2010.06.002

Doulazmi, M., Frederic, F., Capone, F., Becker-Andre, M., Delhaye-Bouchaud, N., & Mariani, J. (2001). A comparative study of purkinje cells in two RORalpha gene mutant mice: Staggerer and RORalpha(-/-). *Brain Research.Developmental Brain Research, 127*(2), 165-174.

Doulazmi, M., Frederic, F., Lemaigre-Dubreuil, Y., Hadj-Sahraoui, N., Delhaye-Bouchaud, N., & Mariani, J. (1999). Cerebellar purkinje cell loss during life span of the heterozygous staggerer mouse (rora(+)/Rora(sg)) is gender-related. *The Journal of Comparative Neurology, 411*(2), 267-273.

Du, J., Huang, C., Zhou, B., & Ziegler, S. F. (2008). Isoform-specific inhibition of ROR alpha-mediated transcriptional activation by human FOXP3. *Journal of Immunology (Baltimore, Md.: 1950), 180*(7), 4785-4792.

Dubal, D. B., Zhu, H., Yu, J., Rau, S. W., Shughrue, P. J., Merchenthaler, I., . . . Wise, P. M. (2001). Estrogen receptor alpha, not beta, is a critical link in estradiol-mediated protection against brain injury. *Proceedings of the National Academy of Sciences of the United States of America, 98*(4), 1952-1957. doi: 10.1073/pnas.041483198

Durand, C. M., Betancur, C., Boeckers, T. M., Bockmann, J., Chaste, P., Fauchereau, F., . . . Bourgeron, T. (2007). Mutations in the gene encoding the synaptic scaffolding protein SHANK3 are associated with autism spectrum disorders. *Nature Genetics, 39*(1), 25-27. doi: 10.1038/ng1933

Dussault, I., Fawcett, D., Matthyssen, A., Bader, J. A., & Giguere, V. (1998). Orphan nuclear receptor ROR alpha-deficient mice display the cerebellar defects of staggerer. *Mechanisms of Development, 70*(1-2), 147-153.

Dzhagalov, I., Giguere, V., & He, Y. W. (2004). Lymphocyte development and function in the absence of retinoic acid-related orphan receptor alpha. *Journal of Immunology (Baltimore, Md.: 1950), 173*(5), 2952-2959.

Dzhagalov, I., Zhang, N., & He, Y. W. (2004). The roles of orphan nuclear receptors in the development and function of the immune system. *Cellular & Molecular Immunology, 1*(6), 401-407.

Edens, A. C., Lyons, M. J., Duron, R. M., Dupont, B. R., & Holden, K. R. (2011). Autism in two females with duplications involving Xp11.22-p11.23. *Developmental Medicine and Child Neurology, 53*(5), 463-466. doi: 10.1111/j.1469-8749.2010.03909.x; 10.1111/j.1469-8749.2010.03909.x

Farre, D., Roset, R., Huerta, M., Adsuara, J. E., Rosello, L., Alba, M. M., & Messeguer, X. (2003). Identification of patterns in biological sequences at the ALGGEN server: PROMO and MALGEN. *Nucleic Acids Research, 31*(13), 3651-3653.

Feron, C., & Baudoin, C. (1995). Social isolation partially restores reproduction of male staggerer mutant mice. *Physiology & Behavior, 58*(1), 107-110.

Feron, C., & Baudoin, C. (1997). Post-weaning social factors promote motor and social behaviors in staggerer mice. *Behavioural Processes, 41*(2), 171.

Filipek, P. A., Accardo, P. J., Ashwal, S., Baranek, G. T., Cook, E. H.,Jr, Dawson, G., . . . Volkmar, F. R. (2000). Practice parameter: Screening and diagnosis of autism: Report of the quality standards subcommittee of the american academy of neurology and the child neurology society. *Neurology, 55*(4), 468-479.

Fombonne, E., Du Mazaubrun, C., Cans, C., & Grandjean, H. (1997). Autism and associated medical disorders in a french epidemiological survey. *Journal of the American Academy of Child and Adolescent Psychiatry, 36*(11), 1561-1569. doi: 10.1016/S0890-8567(09)66566-7

Frederic, F., Chianale, C., Oliver, C., & Mariani, J. (2006). Enhanced endocrine response to novel environment stress and lack of corticosterone circadian rhythm in staggerer (rora sg/sg) mutant mice. *Journal of Neuroscience Research, 83*(8), 1525-1532. doi: 10.1002/jnr.20843

Gai, X., Xie, H. M., Perin, J. C., Takahashi, N., Murphy, K., Wenocur, A. S., . . . White, P. S. (2012). Rare structural variation of synapse and neurotransmission genes in autism. *Molecular Psychiatry, 17*(4), 402-411. doi: 10.1038/mp.2011.10; 10.1038/mp.2011.10

Garcia-Segura, L. M. (2008). Aromatase in the brain: Not just for reproduction anymore. *Journal of Neuroendocrinology, 20*(6), 705-712. doi: 10.1111/j.1365-2826.2008.01713.x

Garcia-Segura, L. M., Veiga, S., Sierra, A., Melcangi, R. C., & Azcoitia, I. (2003). Aromatase: A neuroprotective enzyme. *Progress in Neurobiology, 71*(1), 31-41.

Ghaziuddin, M., & Butler, E. (1998). Clumsiness in autism and asperger syndrome: A further report. *Journal of Intellectual Disability Research : JIDR, 42 (Pt 1)*(Pt 1), 43-48.

Ghaziuddin, M., Ghaziuddin, N., & Greden, J. (2002). Depression in persons with autism: Implications for research and clinical care. *Journal of Autism and Developmental Disorders, 32*(4), 299-306.

Giguere, V., Beatty, B., Squire, J., Copeland, N. G., & Jenkins, N. A. (1995). The orphan nuclear receptor ROR alpha (RORA) maps to a conserved region of homology on human chromosome 15q21-q22 and mouse chromosome 9. *Genomics, 28*(3), 596-598. doi: 10.1006/geno.1995.1197

Giguere, V., Tini, M., Flock, G., Ong, E., Evans, R. M., & Otulakowski, G. (1994). Isoform-specific amino-terminal domains dictate DNA-binding properties of ROR alpha, a novel family of orphan hormone nuclear receptors. *Genes & Development, 8*(5), 538-553.

Gillberg, C. (1984). Infantile autism and other childhood psychoses in a swedish urban region. epidemiological aspects. *Journal of Child Psychology and Psychiatry, and Allied Disciplines, 25*(1), 35-43.

Gillberg, C. (2005). The epidemiology of autism. In M. Coleman (Ed.), *The neurology of autism* (pp. 119). New York, NY: Oxford University Press, Inc.

Gillberg, C., Cederlund, M., Lamberg, K., & Zeijlon, L. (2006). Brief report: "the autism epidemic". the registered prevalence of autism in a swedish urban area. *Journal of Autism and Developmental Disorders, 36*(3), 429-435. doi: 10.1007/s10803-006-0081-6

Gillberg, I. C., Gillberg, C., & Ahlsen, G. (1994). Autistic behaviour and attention deficits in tuberous sclerosis: A population-based study. *Developmental Medicine and Child Neurology, 36*(1), 50-56.

Giulivi, C., Zhang, Y. F., Omanska-Klusek, A., Ross-Inta, C., Wong, S., Hertz-Picciotto, I., . . . Pessah, I. N. (2010). Mitochondrial dysfunction in autism. *JAMA : The Journal of the American Medical Association, 304*(21), 2389-2396. doi: 10.1001/jama.2010.1706

Glass, C. K., & Rosenfeld, M. G. (2000). The coregulator exchange in transcriptional functions of nuclear receptors. *Genes & Development, 14*(2), 121-141.

Glessner, J. T., Wang, K., Cai, G., Korvatska, O., Kim, C. E., Wood, S., . . . Hakonarson, H. (2009). Autism genome-wide copy number variation reveals ubiquitin and neuronal genes. *Nature, 459*(7246), 569-573. doi: 10.1038/nature07953

Glickman, G. (2010). Circadian rhythms and sleep in children with autism. *Neuroscience and Biobehavioral Reviews, 34*(5), 755-768. doi: 10.1016/j.neubiorev.2009.11.017

Gold, D. A., Baek, S. H., Schork, N. J., Rose, D. W., Larsen, D. D., Sachs, B. D., . . . Hamilton, B. A. (2003). RORalpha coordinates reciprocal signaling in cerebellar development through sonic hedgehog and calcium-dependent pathways. *Neuron, 40*(6), 1119-1131.

Gold, D. A., Gent, P. M., & Hamilton, B. A. (2007). ROR alpha in genetic control of cerebellum development: 50 staggering years. *Brain Research, 1140*, 19-25. doi: 10.1016/j.brainres.2005.11.080

Goldowitz, D., & Hamre, K. (1998). The cells and molecules that make a cerebellum. *Trends in Neurosciences, 21*(9), 375-382.

Goldstein, S., & Schwebach, A. J. (2004). The comorbidity of pervasive developmental disorder and attention deficit hyperactivity disorder: Results of a retrospective chart review. *Journal of Autism and Developmental Disorders, 34*(3), 329-339.

Gomez, M. R. (1995). History of the tuberous sclerosis complex. *Brain & Development, 17 Suppl*, 55-57.

Gonzalez, M., Cabrera-Socorro, A., Perez-Garcia, C. G., Fraser, J. D., Lopez, F. J., Alonso, R., & Meyer, G. (2007). Distribution patterns of estrogen receptor alpha and beta in the human cortex and hippocampus during development and adulthood. *The Journal of Comparative Neurology, 503*(6), 790-802. doi: 10.1002/cne.21419

Goodall, G., & Gheusi, G. (1987). Abnormal patterns of maze patrolling in the mutant mouse staggerer. *Behavioral and Neural Biology, 47*(3), 307-320.

Greiner, E. F., Kirfel, J., Greschik, H., Huang, D., Becker, P., Kapfhammer, J. P., & Schule, R. (2000). Differential ligand-dependent protein-protein interactions between nuclear receptors and a neuronal-specific cofactor. *Proceedings of the National Academy of Sciences of the United States of America, 97*(13), 7160-7165.

Gu, F., Hsu, H. K., Hsu, P. Y., Wu, J., Ma, Y., Parvin, J., . . . Jin, V. X. (2010). Inference of hierarchical regulatory network of estrogen-dependent breast cancer through ChIP-based data. *BMC Systems Biology, 4*, 170. doi: 10.1186/1752-0509-4-170

Guastavino, J. M., Bertin, R., & Portet, R. (1991). Effects of the rearing temperature on the temporal feeding pattern of the staggerer mutant mouse. *Physiology & Behavior, 49*(2), 405-409.

Guastavino, J. M., Boufares, S., & Crusio, W. E. (2005). Ovarian abnormalities in the staggerer mutant mouse. *TheScientificWorldJournal, 5*, 661-664. doi: 10.1100/tsw.2005.87

Guastavino, J. M., & Larsson, K. (1992). The staggerer gene curtails the reproductive life span of females. *Behavior Genetics, 22*(1), 101-112.

Guastavino, J. M., Larsson, K., Allain, C., & Jaisson, P. (1993). Neonatal vestibular stimulation and mating in cerebellar mutants. *Behavior Genetics, 23*(3), 265-269.

Guastavino, J. M., Larsson, K., & Jaisson, P. (1992). Neurological murine mutants as models for single-gene effects on behavior. In D. Goldowitz, D. Wahlsten & R. E. Wimer (Eds.), *Techniques for the genetic analysis of brain and behavior: Focus on the mouse* (pp. 375). Amsterdam: Elsevier.

Hadj-Sahraoui, N., Frederic, F., Zanjani, H., Delhaye-Bouchaud, N., Herrup, K., & Mariani, J. (2001). Progressive atrophy of cerebellar purkinje cell dendrites during aging of the heterozygous staggerer mouse (rora(+/sg)). *Brain Research.Developmental Brain Research, 126*(2), 201-209.

Hamilton, B. A., Frankel, W. N., Kerrebrock, A. W., Hawkins, T. L., FitzHugh, W., Kusumi, K., . . . Lander, E. S. (1996). Disruption of the nuclear hormone receptor RORalpha in staggerer mice. *Nature, 379*(6567), 736-739. doi: 10.1038/379736a0

Harding, H. P., Atkins, G. B., Jaffe, A. B., Seo, W. J., & Lazar, M. A. (1997). Transcriptional activation and repression by RORalpha, an orphan nuclear receptor required for cerebellar development. *Molecular Endocrinology (Baltimore, Md.), 11*(11), 1737-1746.

Harris, J. M., Lau, P., Chen, S. L., & Muscat, G. E. (2002). Characterization of the retinoid orphan-related receptor-alpha coactivator binding interface: A structural basis for ligand-independent transcription. *Molecular Endocrinology (Baltimore, Md.), 16*(5), 998-1012.

Heh, C. W., Smith, R., Wu, J., Hazlett, E., Russell, A., Asarnow, R., . . . Buchsbaum, M. S. (1989). Positron emission tomography of the cerebellum in autism. *The American Journal of Psychiatry, 146*(2), 242-245.

Herbert, M. R. (2011). SHANK3, the synapse, and autism. *The New England Journal of Medicine, 365*(2), 173-175. doi: 10.1056/NEJMcibr1104261

Herrup, K., & Mullen, R. J. (1979). Staggerer chimeras: Intrinsic nature of purkinje cell defects and implications for normal cerebellar development. *Brain Research, 178*(2-3), 443-457.

Herrup, K., & Mullen, R. J. (1981). Role of the staggerer gene in determining purkinje cell number in the cerebellar cortex of mouse chimeras. *Brain Research, 227*(4), 475-485.

Hertz-Picciotto, I., & Delwiche, L. (2009). The rise in autism and the role of age at diagnosis. *Epidemiology (Cambridge, Mass.), 20*(1), 84-90. doi: 10.1097/EDE.0b013e3181902d15

Horlein, A. J., Naar, A. M., Heinzel, T., Torchia, J., Gloss, B., Kurokawa, R., . . . Glass, C. K. (1995). Ligand-independent repression by the thyroid hormone receptor

mediated by a nuclear receptor co-repressor. *Nature, 377*(6548), 397-404. doi: 10.1038/377397a0

Hornstra, I. K., Nelson, D. L., Warren, S. T., & Yang, T. P. (1993). High resolution methylation analysis of the FMR1 gene trinucleotide repeat region in fragile X syndrome. *Human Molecular Genetics, 2*(10), 1659-1665.

Hu, V. W., Frank, B. C., Heine, S., Lee, N. H., & Quackenbush, J. (2006). Gene expression profiling of lymphoblastoid cell lines from monozygotic twins discordant in severity of autism reveals differential regulation of neurologically relevant genes. *BMC Genomics, 7*, 118. doi: 10.1186/1471-2164-7-118

Hu, V. W., Nguyen, A., Kim, K. S., Steinberg, M. E., Sarachana, T., Scully, M. A., . . . Lee, N. H. (2009). Gene expression profiling of lymphoblasts from autistic and nonaffected sib pairs: Altered pathways in neuronal development and steroid biosynthesis. *PloS One, 4*(6), e5775. doi: 10.1371/journal.pone.0005775

Hu, V. W., Sarachana, T., Kim, K. S., Nguyen, A., Kulkarni, S., Steinberg, M. E., . . . Lee, N. H. (2009). Gene expression profiling differentiates autism case-controls and phenotypic variants of autism spectrum disorders: Evidence for circadian rhythm dysfunction in severe autism. *Autism Research : Official Journal of the International Society for Autism Research, 2*(2), 78-97. doi: 10.1002/aur.73

Hu, X., & Lazar, M. A. (2000). Transcriptional repression by nuclear hormone receptors. *Trends in Endocrinology and Metabolism: TEM, 11*(1), 6-10.

Hussman, J. P., Chung, R. H., Griswold, A. J., Jaworski, J. M., Salyakina, D., Ma, D., . . . Pericak-Vance, M. A. (2011). A noise-reduction GWAS analysis implicates altered regulation of neurite outgrowth and guidance in autism. *Molecular Autism, 2*(1), 1. doi: 10.1186/2040-2392-2-1

Ingudomnukul, E., Baron-Cohen, S., Wheelwright, S., & Knickmeyer, R. (2007). Elevated rates of testosterone-related disorders in women with autism spectrum conditions. *Hormones and Behavior, 51*(5), 597-604. doi: 10.1016/j.yhbeh.2007.02.001

Ino, H. (2004). Immunohistochemical characterization of the orphan nuclear receptor ROR alpha in the mouse nervous system. *The Journal of Histochemistry and Cytochemistry : Official Journal of the Histochemistry Society, 52*(3), 311-323.

International Molecular Genetic Study of Autism Consortium (IMGSAC). (1998). A full genome screen for autism with evidence for linkage to a region on chromosome 7q. *Human Molecular Genetics, 7*(3), 571-578.

International Molecular Genetic Study of Autism Consortium (IMGSAC). (2001). A genomewide screen for autism: Strong evidence for linkage to chromosomes 2q, 7q, and 16p. *American Journal of Human Genetics, 69*(3), 570-581. doi: 10.1086/323264

Ivanov, A. V., Peng, H., Yurchenko, V., Yap, K. L., Negorev, D. G., Schultz, D. C., . . . Rauscher, F. J.,3rd. (2007). PHD domain-mediated E3 ligase activity directs intramolecular sumoylation of an adjacent bromodomain required for gene silencing. *Molecular Cell, 28*(5), 823-837. doi: 10.1016/j.molcel.2007.11.012

James, S. J., Cutler, P., Melnyk, S., Jernigan, S., Janak, L., Gaylor, D. W., & Neubrander, J. A. (2004). Metabolic biomarkers of increased oxidative stress and impaired methylation capacity in children with autism. *The American Journal of Clinical Nutrition, 80*(6), 1611-1617.

Janmaat, S., Akwa, Y., Doulazmi, M., Bakouche, J., Gautheron, V., Liere, P., . . . Frederic, F. (2011). Age-related purkinje cell death is steroid dependent: RORalpha haplo-insufficiency impairs plasma and cerebellar steroids and purkinje cell survival. *Age (Dordrecht, Netherlands), 33*(4), 565-578. doi: 10.1007/s11357-010-9203-3

Janmaat, S., Frederic, F., Sjollema, K., Luiten, P., Mariani, J., & van der Want, J. (2009). Formation and maturation of parallel fiber-purkinje cell synapses in the staggerer cerebellum ex vivo. *The Journal of Comparative Neurology, 512*(4), 467-477. doi: 10.1002/cne.21910

Jetten, A. M. (2009). Retinoid-related orphan receptors (RORs): Critical roles in development, immunity, circadian rhythm, and cellular metabolism. *Nuclear Receptor Signaling, 7*, e003. doi: 10.1621/nrs.07003

Jetten, A. M., & Joo, J. H. (2006). Retinoid-related orphan receptors (RORs): Roles in cellular differentiation and development. *Advances in Developmental Biology (Amsterdam, Netherlands), 16*, 313-355. doi: 10.1016/S1574-3349(06)16010-X

Jiang, C., Ito, M., Piening, V., Bruck, K., Roeder, R. G., & Xiao, H. (2004). TIP30 interacts with an estrogen receptor alpha-interacting coactivator CIA and regulates c-

myc transcription. *The Journal of Biological Chemistry, 279*(26), 27781-27789. doi: 10.1074/jbc.M401809200

Johnson, E. S. (2004). Protein modification by SUMO. *Annual Review of Biochemistry, 73*, 355-382. doi: 10.1146/annurev.biochem.73.011303.074118

Jones, P. L., Veenstra, G. J., Wade, P. A., Vermaak, D., Kass, S. U., Landsberger, N., . . . Wolffe, A. P. (1998). Methylated DNA and MeCP2 recruit histone deacetylase to repress transcription. *Nature Genetics, 19*(2), 187-191. doi: 10.1038/561

Jones, V., & Prior, M. (1985). Motor imitation abilities and neurological signs in autistic children. *Journal of Autism and Developmental Disorders, 15*(1), 37-46.

Joo, J. H., Liao, G., Collins, J. B., Grissom, S. F., & Jetten, A. M. (2007). Farnesol-induced apoptosis in human lung carcinoma cells is coupled to the endoplasmic reticulum stress response. *Cancer Research, 67*(16), 7929-7936. doi: 10.1158/0008-5472.CAN-07-0931

Journiac, N., Jolly, S., Jarvis, C., Gautheron, V., Rogard, M., Trembleau, A., . . . Vernet-der Garabedian, B. (2009). The nuclear receptor ROR(alpha) exerts a bi-directional regulation of IL-6 in resting and reactive astrocytes. *Proceedings of the National Academy of Sciences of the United States of America, 106*(50), 21365-21370. doi: 10.1073/pnas.0911782106

Just, M. A., Cherkassky, V. L., Keller, T. A., Kana, R. K., & Minshew, N. J. (2007). Functional and anatomical cortical underconnectivity in autism: Evidence from an

FMRI study of an executive function task and corpus callosum morphometry. *Cerebral Cortex (New York, N.Y.: 1991), 17*(4), 951-961. doi: 10.1093/cercor/bhl006

Kallen, J., Schlaeppi, J. M., Bitsch, F., Delhon, I., & Fournier, B. (2004). Crystal structure of the human RORalpha ligand binding domain in complex with cholesterol sulfate at 2.2 A. *The Journal of Biological Chemistry, 279*(14), 14033-14038. doi: 10.1074/jbc.M400302200

Kallen, J. A., Schlaeppi, J. M., Bitsch, F., Geisse, S., Geiser, M., Delhon, I., & Fournier, B. (2002). X-ray structure of the hRORalpha LBD at 1.63 A: Structural and functional data that cholesterol or a cholesterol derivative is the natural ligand of RORalpha. *Structure (London, England : 1993), 10*(12), 1697-1707.

Kamphuis, W., Cailotto, C., Dijk, F., Bergen, A., & Buijs, R. M. (2005). Circadian expression of clock genes and clock-controlled genes in the rat retina. *Biochemical and Biophysical Research Communications, 330*(1), 18-26. doi: 10.1016/j.bbrc.2005.02.118

Kang, H. S., Okamoto, K., Takeda, Y., Beak, J. Y., Gerrish, K., Bortner, C. D., . . . Jetten, A. M. (2011). Transcriptional profiling reveals a role for RORalpha in regulating gene expression in obesity-associated inflammation and hepatic steatosis. *Physiological Genomics, 43*(13), 818-828. doi: 10.1152/physiolgenomics.00206.2010

Kanner, L. (1968). Autistic disturbances of affective contact. *Acta Paedopsychiatrica, 35*(4), 100-136.

Kelleher, R. J.,3rd, & Bear, M. F. (2008). The autistic neuron: Troubled translation? *Cell, 135*(3), 401-406. doi: 10.1016/j.cell.2008.10.017

Kemper, T. L., & Bauman, M. L. (1993a). The contribution of neuropathologic studies to the understanding of autism. *Neurologic Clinics, 11*(1), 175-187.

Kemper, T. L., & Bauman, M. L. (1993b). The contribution of neuropathologic studies to the understanding of autism. *Neurologic Clinics, 11*(1), 175-187.

Kern, J. K. (2003). Purkinje cell vulnerability and autism: A possible etiological connection. *Brain & Development, 25*(6), 377-382.

Kielinen, M., Rantala, H., Timonen, E., Linna, S. L., & Moilanen, I. (2004). Associated medical disorders and disabilities in children with autistic disorder: A population-based study. *Autism : The International Journal of Research and Practice, 8*(1), 49-60. doi: 10.1177/1362361304040638

Kim, H. G., Kishikawa, S., Higgins, A. W., Seong, I. S., Donovan, D. J., Shen, Y., . . . Gusella, J. F. (2008). Disruption of neurexin 1 associated with autism spectrum disorder. *American Journal of Human Genetics, 82*(1), 199-207. doi: 10.1016/j.ajhg.2007.09.011

Klauck, S. M., Munstermann, E., Bieber-Martig, B., Ruhl, D., Lisch, S., Schmotzer, G., . . . Poustka, F. (1997). Molecular genetic analysis of the FMR-1 gene in a large collection of autistic patients. *Human Genetics, 100*(2), 224-229.

Knickmeyer, R., Baron-Cohen, S., Fane, B. A., Wheelwright, S., Mathews, G. A., Conway, G. S., . . . Hines, M. (2006). Androgens and autistic traits: A study of individuals with congenital adrenal hyperplasia. *Hormones and Behavior, 50*(1), 148-153. doi: 10.1016/j.yhbeh.2006.02.006

Knickmeyer, R., Baron-Cohen, S., Raggatt, P., & Taylor, K. (2005). Foetal testosterone, social relationships, and restricted interests in children. *Journal of Child Psychology and Psychiatry, 46*(2), 198.

Konstantareas, M. M., & Hewitt, T. (2001). Autistic disorder and schizophrenia: Diagnostic overlaps. *Journal of Autism and Developmental Disorders, 31*(1), 19-28.

Kopmels, B., Mariani, J., Delhaye-Bouchaud, N., Audibert, F., Fradelizi, D., & Wollman, E. E. (1992). Evidence for a hyperexcitability state of staggerer mutant mice macrophages. *Journal of Neurochemistry, 58*(1), 192-199.

Kopmels, B., Mariani, J., Taupin, V., Delhaye-Bouchaud, N., & Wollman, E. E. (1991). Differential IL-6 mRNA expression by stimulated peripheral macrophages of staggerer and lurcher cerebellar mutant mice. *European Cytokine Network, 2*(5), 345-353.

Kopmels, B., Wollman, E. E., Guastavino, J. M., Delhaye-Bouchaud, N., Fradelizi, D., & Mariani, J. (1990). Interleukin-1 hyperproduction by in vitro activated peripheral macrophages from cerebellar mutant mice. *Journal of Neurochemistry, 55*(6), 1980-1985.

Kretz, O., Fester, L., Wehrenberg, U., Zhou, L., Brauckmann, S., Zhao, S., . . . Rune, G. M. (2004). Hippocampal synapses depend on hippocampal estrogen synthesis. *The Journal of Neuroscience : The Official Journal of the Society for Neuroscience, 24*(26), 5913-5921. doi: 10.1523/JNEUROSCI.5186-03.2004

Kulman, G., Lissoni, P., Rovelli, F., Roselli, M. G., Brivio, F., & Sequeri, P. (2000). Evidence of pineal endocrine hypofunction in autistic children. *Neuro Endocrinology Letters, 21*(1), 31-34.

Kuo, H. Y., Chang, C. C., Jeng, J. C., Hu, H. M., Lin, D. Y., Maul, G. G., . . . Shih, H. M. (2005). SUMO modification negatively modulates the transcriptional activity of CREB-binding protein via the recruitment of daxx. *Proceedings of the National Academy of Sciences of the United States of America, 102*(47), 16973-16978. doi: 10.1073/pnas.0504460102

Kurebayashi, S., Nakajima, T., Kim, S. C., Chang, C. Y., McDonnell, D. P., Renaud, J. P., & Jetten, A. M. (2004). Selective LXXLL peptides antagonize transcriptional activation by the retinoid-related orphan receptor RORgamma. *Biochemical and Biophysical Research Communications, 315*(4), 919-927. doi: 10.1016/j.bbrc.2004.01.131

Lalonde, R. (1987a). Exploration and spatial learning in staggerer mutant mice. *Journal of Neurogenetics, 4*(6), 285-291.

Lalonde, R. (1987b). Exploration and spatial learning in staggerer mutant mice. *Journal of Neurogenetics, 4*(6), 285-291.

Lalonde, R., Botez, M. I., & Boivin, D. (1987a). Object exploration in staggerer mutant mice. *Physiology & Behavior, 41*(2), 115-117.

Lalonde, R., Botez, M. I., & Boivin, D. (1987b). Object exploration in staggerer mutant mice. *Physiology & Behavior, 41*(2), 115-117.

Lalonde, R., Filali, M., Bensoula, A. N., Monnier, C., & Guastavino, J. M. (1996). Spatial learning in a Z-maze by cerebellar mutant mice. *Physiology & Behavior, 59*(1), 83-86.

Lalonde, R., Manseau, M., & Botez, M. I. (1988). Spontaneous alternation and exploration in staggerer mutant mice. *Behavioural Brain Research, 27*(3), 273-276.

Lalonde, R., & Strazielle, C. (2008). Discrimination learning in rora(sg) and Grid2(ho) mutant mice. *Neurobiology of Learning and Memory, 90*(2), 472-474. doi: 10.1016/j.nlm.2008.05.004

Lam, K. S., & Aman, M. G. (2007). The repetitive behavior scale-revised: Independent validation in individuals with autism spectrum disorders. *Journal of Autism and Developmental Disorders, 37*(5), 855-866. doi: 10.1007/s10803-006-0213-z

Landa, R. (2007). Early communication development and intervention for children with autism. *Mental Retardation and Developmental Disabilities Research Reviews, 13*(1), 16-25. doi: 10.1002/mrdd.20134

Landis, D. M., & Reese, T. S. (1977). Structure of the purkinje cell membrane in staggerer and weaver mutant mice. *The Journal of Comparative Neurology, 171*(2), 247-260. doi: 10.1002/cne.901710208

Landis, D. M., & Sidman, R. L. (1978). Electron microscopic analysis of postnatal histogenesis in the cerebellar cortex of staggerer mutant mice. *The Journal of Comparative Neurology, 179*(4), 831-863. doi: 10.1002/cne.901790408

Larsson, K., Guastavino, J. M., & Ly, A. K. (1986). Altered reproductive behaviour of the neurological mutant mouse staggerer. In J. Medioni, & G. Vaysse (Eds.), *Genetic approaches to behaviour* (pp. 69). Toulouse: Privat.

Lau, P., Bailey, P., Dowhan, D. H., & Muscat, G. E. (1999). Exogenous expression of a dominant negative RORalpha1 vector in muscle cells impairs differentiation: RORalpha1 directly interacts with p300 and myoD. *Nucleic Acids Research, 27*(2), 411-420.

Lau, P., Fitzsimmons, R. L., Raichur, S., Wang, S. C., Lechtken, A., & Muscat, G. E. (2008). The orphan nuclear receptor, RORalpha, regulates gene expression that controls lipid metabolism: Staggerer (SG/SG) mice are resistant to diet-induced obesity. *The Journal of Biological Chemistry, 283*(26), 18411-18421. doi: 10.1074/jbc.M710526200

Lauritsen, M. B., Als, T. D., Dahl, H. A., Flint, T. J., Wang, A. G., Vang, M., . . . Mors, O. (2006). A genome-wide search for alleles and haplotypes associated with autism

and related pervasive developmental disorders on the faroe islands. *Molecular Psychiatry, 11*(1), 37-46. doi: 10.1038/sj.mp.4001754

Lenski, C., Kooy, R. F., Reyniers, E., Loessner, D., Wanders, R. J., Winnepenninckx, B., . . . Ramser, J. (2007). The reduced expression of the HADH2 protein causes X-linked mental retardation, choreoathetosis, and abnormal behavior. *American Journal of Human Genetics, 80*(2), 372-377. doi: 10.1086/511527

Lepore, G., Gadau, S., Mura, A., Zedda, M., & Farina, V. (2009). Aromatase immunoreactivity in fetal ovine neuronal cell cultures exposed to oxidative injury. *European Journal of Histochemistry : EJH, 53*(4), 233-238.

Lepore, G., Gadau, S., Peruffo, A., Mura, A., Mura, E., Floris, A., . . . Farina, V. (2011). Aromatase expression in cultured fetal sheep astrocytes after nitrosative/oxidative damage. *Cell and Tissue Research, 344*(3), 407-413. doi: 10.1007/s00441-011-1160-3

Levy, D., Ronemus, M., Yamrom, B., Lee, Y. H., Leotta, A., Kendall, J., . . . Wigler, M. (2011). Rare de novo and transmitted copy-number variation in autistic spectrum disorders. *Neuron, 70*(5), 886-897. doi: 10.1016/j.neuron.2011.05.015

Lewis, J. D., Meehan, R. R., Henzel, W. J., Maurer-Fogy, I., Jeppesen, P., Klein, F., & Bird, A. (1992). Purification, sequence, and cellular localization of a novel chromosomal protein that binds to methylated DNA. *Cell, 69*(6), 905-914.

Lin, D. Y., Huang, Y. S., Jeng, J. C., Kuo, H. Y., Chang, C. C., Chao, T. T., . . . Shih, H. M. (2006). Role of SUMO-interacting motif in daxx SUMO modification, subnuclear localization, and repression of sumoylated transcription factors. *Molecular Cell, 24*(3), 341-354. doi: 10.1016/j.molcel.2006.10.019

Lise, M. F., & El-Husseini, A. (2006). The neuroligin and neurexin families: From structure to function at the synapse. *Cellular and Molecular Life Sciences : CMLS, 63*(16), 1833-1849. doi: 10.1007/s00018-006-6061-3

Liu, M., Hurn, P. D., Roselli, C. E., & Alkayed, N. J. (2007). Role of P450 aromatase in sex-specific astrocytic cell death. *Journal of Cerebral Blood Flow and Metabolism : Official Journal of the International Society of Cerebral Blood Flow and Metabolism, 27*(1), 135-141. doi: 10.1038/sj.jcbfm.9600331

Lutchmaya, S., Baron-Cohen, S., & Raggatt, P. (2002). Foetal testosterone and eye contact in 12-month-old human infants. *Infant Behavior and Development, 25*, 327.

Lutchmaya, S., & Baron-Cohen, S. (2002). Human sex differences in social and non-social looking preferences, at 12 months of age. *Infant Behavior and Development, 25*, 319.

Lutchmaya, S., Baron-Cohen, S., Raggatt, P., Knickmeyer, R., & Manning, J. T. (2004). 2nd to 4th digit ratios, fetal testosterone and estradiol. *Early Human Development, 77*(1-2), 23-28. doi: 10.1016/j.earlhumdev.2003.12.002

Manning, J. T., Baron-Cohen, S., Wheelwright, S., & Sanders, G. (2001). The 2nd to 4th digit ratio and autism. *Developmental Medicine and Child Neurology, 43*(3), 160-164.

Mariani, J. (1982). Extent of multiple innervation of purkinje cells by climbing fibers in the olivocerebellar system of weaver, reeler, and staggerer mutant mice. *Journal of Neurobiology, 13*(2), 119-126. doi: 10.1002/neu.480130204

Mariani, J., & Changeux, J. P. (1980). Multiple innervation of purkinje cells by climbing fibers in the cerebellum of the adult staggerer mutant mouse. *Journal of Neurobiology, 11*(1), 41-50. doi: 10.1002/neu.480110106

Martin, C. L., Duvall, J. A., Ilkin, Y., Simon, J. S., Arreaza, M. G., Wilkes, K., . . . Geschwind, D. H. (2007). Cytogenetic and molecular characterization of A2BP1/FOX1 as a candidate gene for autism. *American Journal of Medical Genetics.Part B, Neuropsychiatric Genetics : The Official Publication of the International Society of Psychiatric Genetics, 144B*(7), 869-876. doi: 10.1002/ajmg.b.30530

Mayes, S. D., & Calhoun, S. L. (2003). Ability profiles in children with autism: Influence of age and IQ. *Autism : The International Journal of Research and Practice, 7*(1), 65-80.

McCauley, J. L., Li, C., Jiang, L., Olson, L. M., Crockett, G., Gainer, K., . . . Sutcliffe, J. S. (2005). Genome-wide and ordered-subset linkage analyses provide support for

autism loci on 17q and 19p with evidence of phenotypic and interlocus genetic correlates. *BMC Medical Genetics, 6*, 1. doi: 10.1186/1471-2350-6-1

McGinnis, W. R. (2004). Oxidative stress in autism. *Alternative Therapies in Health and Medicine, 10*(6), 22-36; quiz 37, 92.

McKenna, N. J., & O'Malley, B. W. (2002). Minireview: Nuclear receptor coactivators--an update. *Endocrinology, 143*(7), 2461-2465.

Meehan, R. R., Lewis, J. D., & Bird, A. P. (1992). Characterization of MeCP2, a vertebrate DNA binding protein with affinity for methylated DNA. *Nucleic Acids Research, 20*(19), 5085-5092.

Messeguer, X., Escudero, R., Farre, D., Nunez, O., Martinez, J., & Alba, M. M. (2002). PROMO: Detection of known transcription regulatory elements using species-tailored searches. *Bioinformatics (Oxford, England), 18*(2), 333-334.

Michel, V., Monnier, Z., Guastavino, J. M., Propper, A., & Math, F. (2000). Functional alterations in the olfactory bulb of the staggerer mutant mouse. *Neuroscience Letters, 280*(1), 1-4.

Minshew, N. J., Sung, K., Jones, B. L., & Furman, J. M. (2004). Underdevelopment of the postural control system in autism. *Neurology, 63*(11), 2056-2061.

Misslin, R., Cigrang, M., & Guastavino, J. M. (1986). Responses to novelty in staggerer mutant mice. *Behavioural Processes, 12*(1), 51.

Moldin, S. O., & Rubenstein, J. L. R. (2006). *Understanding autism: From basic neuroscience to treatment*. Boca Raton: CRC/Taylor & Francis. Retrieved from http://opac.medlib.gwumc.edu/uhtbin/cgisirsi/0/0/0/5?searchdata1=0849327326{020}

Muller, J. M., Isele, U., Metzger, E., Rempel, A., Moser, M., Pscherer, A., . . . Schule, R. (2000). FHL2, a novel tissue-specific coactivator of the androgen receptor. *The EMBO Journal, 19*(3), 359-369. doi: 10.1093/emboj/19.3.359

Murakami, J. W., Courchesne, E., Press, G. A., Yeung-Courchesne, R., & Hesselink, J. R. (1989). Reduced cerebellar hemisphere size and its relationship to vermal hypoplasia in autism. *Archives of Neurology, 46*(6), 689-694.

Muris, P., Steerneman, P., Merckelbach, H., Holdrinet, I., & Meesters, C. (1998). Comorbid anxiety symptoms in children with pervasive developmental disorders. *Journal of Anxiety Disorders, 12*(4), 387-393.

Nagarajan, R. P., Hogart, A. R., Gwye, Y., Martin, M. R., & LaSalle, J. M. (2006). Reduced MeCP2 expression is frequent in autism frontal cortex and correlates with aberrant MECP2 promoter methylation. *Epigenetics : Official Journal of the DNA Methylation Society, 1*(4), e1-11.

Nagy, L., Kao, H. Y., Love, J. D., Li, C., Banayo, E., Gooch, J. T., . . . Schwabe, J. W. (1999). Mechanism of corepressor binding and release from nuclear hormone receptors. *Genes & Development, 13*(24), 3209-3216.

Nan, X., Ng, H. H., Johnson, C. A., Laherty, C. D., Turner, B. M., Eisenman, R. N., & Bird, A. (1998). Transcriptional repression by the methyl-CpG-binding protein MeCP2 involves a histone deacetylase complex. *Nature, 393*(6683), 386-389. doi: 10.1038/30764

Nguyen, A., Rauch, T. A., Pfeifer, G. P., & Hu, V. W. (2010). Global methylation profiling of lymphoblastoid cell lines reveals epigenetic contributions to autism spectrum disorders and a novel autism candidate gene, RORA, whose protein product is reduced in autistic brain. *FASEB Journal : Official Publication of the Federation of American Societies for Experimental Biology, 24*(8), 3036-3051. doi: 10.1096/fj.10-154484

Nir, I., Meir, D., Zilber, N., Knobler, H., Hadjez, J., & Lerner, Y. (1995). Brief report: Circadian melatonin, thyroid-stimulating hormone, prolactin, and cortisol levels in serum of young adults with autism. *Journal of Autism and Developmental Disorders, 25*(6), 641-654.

Noens, I., van Berckelaer-Onnes, I., Verpoorten, R., & van Duijn, G. (2006). The ComFor: An instrument for the indication of augmentative communication in people with autism and intellectual disability. *Journal of Intellectual Disability Research : JIDR, 50*(Pt 9), 621-632. doi: 10.1111/j.1365-2788.2006.00807.x

Odawara, H., Iwasaki, T., Horiguchi, J., Rokutanda, N., Hirooka, K., Miyazaki, W., . . . Koibuchi, N. (2009). Activation of aromatase expression by retinoic acid receptor-related orphan receptor (ROR) alpha in breast cancer cells: Identification of a novel

ROR response element. *The Journal of Biological Chemistry, 284*(26), 17711-17719. doi: 10.1074/jbc.M109.009241

Ofman, R., Ruiter, J. P., Feenstra, M., Duran, M., Poll-The, B. T., Zschocke, J., . . . Wanders, R. J. (2003). 2-methyl-3-hydroxybutyryl-CoA dehydrogenase deficiency is caused by mutations in the HADH2 gene. *American Journal of Human Genetics, 72*(5), 1300-1307.

Oliveira, G., Diogo, L., Grazina, M., Garcia, P., Ataide, A., Marques, C., . . . Oliveira, C. R. (2005). Mitochondrial dysfunction in autism spectrum disorders: A population-based study. *Developmental Medicine and Child Neurology, 47*(3), 185-189.

Olsson, I., Steffenburg, S., & Gillberg, C. (1988). Epilepsy in autism and autisticlike conditions. A population-based study. *Archives of Neurology, 45*(6), 666-668.

Ouyang, J., & Gill, G. (2009). SUMO engages multiple corepressors to regulate chromatin structure and transcription. *Epigenetics : Official Journal of the DNA Methylation Society, 4*(7), 440-444.

Ouyang, J., Shi, Y., Valin, A., Xuan, Y., & Gill, G. (2009). Direct binding of CoREST1 to SUMO-2/3 contributes to gene-specific repression by the LSD1/CoREST1/HDAC complex. *Molecular Cell, 34*(2), 145-154. doi: 10.1016/j.molcel.2009.03.013

Pardo, C. A., Vargas, D. L., & Zimmerman, A. W. (2005). Immunity, neuroglia and neuroinflammation in autism. *International Review of Psychiatry (Abingdon, England), 17*(6), 485-495. doi: 10.1080/02646830500381930

Pasca, S. P., Nemes, B., Vlase, L., Gagyi, C. E., Dronca, E., Miu, A. C., & Dronca, M. (2006). High levels of homocysteine and low serum paraoxonase 1 arylesterase activity in children with autism. *Life Sciences, 78*(19), 2244-2248. doi: 10.1016/j.lfs.2005.09.040

Philofsky, A., Hepburn, S. L., Hayes, A., Hagerman, R., & Rogers, S. J. (2004). Linguistic and cognitive functioning and autism symptoms in young children with fragile X syndrome. *American Journal of Mental Retardation : AJMR, 109*(3), 208-218. doi: 2

Pinto, D., Pagnamenta, A. T., Klei, L., Anney, R., Merico, D., Regan, R., . . . Betancur, C. (2010). Functional impact of global rare copy number variation in autism spectrum disorders. *Nature, 466*(7304), 368-372. doi: 10.1038/nature09146

Piven, J., Arndt, S., Bailey, J., & Andreasen, N. (1996). Regional brain enlargement in autism: A magnetic resonance imaging study. *Journal of the American Academy of Child and Adolescent Psychiatry, 35*(4), 530-536. doi: 10.1097/00004583-199604000-00020

Piven, J., Arndt, S., Bailey, J., Havercamp, S., Andreasen, N. C., & Palmer, P. (1995). An MRI study of brain size in autism. *The American Journal of Psychiatry, 152*(8), 1145-1149.

Piven, J., Gayle, J., Landa, R., Wzorek, M., & Folstein, S. (1991). The prevalence of fragile X in a sample of autistic individuals diagnosed using a standardized interview.

Journal of the American Academy of Child and Adolescent Psychiatry, 30(5), 825-830.

Poukka, H., Karvonen, U., Janne, O. A., & Palvimo, J. J. (2000). Covalent modification of the androgen receptor by small ubiquitin-like modifier 1 (SUMO-1). *Proceedings of the National Academy of Sciences of the United States of America, 97*(26), 14145-14150. doi: 10.1073/pnas.97.26.14145

Price, T., Aitken, J., & Simpson, E. R. (1992). Relative expression of aromatase cytochrome P450 in human fetal tissues as determined by competitive polymerase chain reaction amplification. *The Journal of Clinical Endocrinology and Metabolism, 74*(4), 879-883.

Purves, D., Augustine, G. J., Fitzpatrick, D., Hall, W. C., LaMantia, A., & White, L. E. (2012). Neuroscience. In D. Purves, G. J. Augustine, D. Fitzpatrick, W. C. Hall, A. LaMantia & L. E. White (Eds.), (5th ed., pp. 669-694). Sunderland, MA: Sinauer Associates, Inc.

Raichur, S., Fitzsimmons, R. L., Myers, S. A., Pearen, M. A., Lau, P., Eriksson, N., . . . Muscat, G. E. (2010). Identification and validation of the pathways and functions regulated by the orphan nuclear receptor, ROR alpha1, in skeletal muscle. *Nucleic Acids Research, 38*(13), 4296-4312. doi: 10.1093/nar/gkq180

Rapin, I., & Tuchman, R. F. (2008). Autism: Definition, neurobiology, screening, diagnosis. *Pediatric Clinics of North America, 55*(5), 1129-46, viii. doi: 10.1016/j.pcl.2008.07.005

Reyniers, E., Van Bogaert, P., Peeters, N., Vits, L., Pauly, F., Fransen, E., . . . Kooy, R. F. (1999). A new neurological syndrome with mental retardation, choreoathetosis, and abnormal behavior maps to chromosome Xp11. *American Journal of Human Genetics, 65*(5), 1406-1412. doi: 10.1086/302638

Ritvo, E. R., Freeman, B. J., Scheibel, A. B., Duong, T., Robinson, H., Guthrie, D., & Ritvo, A. (1986). Lower purkinje cell counts in the cerebella of four autistic subjects: Initial findings of the UCLA-NSAC autopsy research report. *The American Journal of Psychiatry, 143*(7), 862-866.

Rogers, S. J., Hepburn, S., & Wehner, E. (2003). Parent reports of sensory symptoms in toddlers with autism and those with other developmental disorders. *Journal of Autism and Developmental Disorders, 33*(6), 631-642.

Rozen, S., & Skaletsky, H. (2000). Primer3 on the WWW for general users and for biologist programmers. *Methods in Molecular Biology (Clifton, N.J.), 132*, 365-386.

Russell, A. J., Mataix-Cols, D., Anson, M., & Murphy, D. G. (2005). Obsessions and compulsions in asperger syndrome and high-functioning autism. *The British Journal of Psychiatry : The Journal of Mental Science, 186*, 525-528. doi: 10.1192/bjp.186.6.525

Ruta, L., Ingudomnukul, E., Taylor, K., Chakrabarti, B., & Baron-Cohen, S. (2011). Increased serum androstenedione in adults with autism spectrum conditions. *Psychoneuroendocrinology, 36*(8), 1154-1163. doi: 10.1016/j.psyneuen.2011.02.007

Rutter, M. (1970). Autistic children: Infancy to adulthood. *Seminars in Psychiatry, 2*(4), 435-450.

Rutter, M., Bailey, A., Bolton, P., & Le Couteur, A. (1994). Autism and known medical conditions: Myth and substance. *Journal of Child Psychology and Psychiatry, and Allied Disciplines, 35*(2), 311-322.

Saldanha, C. J., Duncan, K. A., & Walters, B. J. (2009). Neuroprotective actions of brain aromatase. *Frontiers in Neuroendocrinology, 30*(2), 106-118. doi: 10.1016/j.yfrne.2009.04.016

Sanders, S. J., Ercan-Sencicek, A. G., Hus, V., Luo, R., Murtha, M. T., Moreno-De-Luca, D., . . . State, M. W. (2011). Multiple recurrent de novo CNVs, including duplications of the 7q11.23 williams syndrome region, are strongly associated with autism. *Neuron, 70*(5), 863-885. doi: 10.1016/j.neuron.2011.05.002

Sarachana, T., Xu, M., Wu, R. C., & Hu, V. W. (2011). Sex hormones in autism: Androgens and estrogens differentially and reciprocally regulate RORA, a novel candidate gene for autism. *PloS One, 6*(2), e17116. doi: 10.1371/journal.pone.0017116

Sato, T. K., Panda, S., Miraglia, L. J., Reyes, T. M., Rudic, R. D., McNamara, P., . . . Hogenesch, J. B. (2004). A functional genomics strategy reveals rora as a component of the mammalian circadian clock. *Neuron, 43*(4), 527-537. doi: 10.1016/j.neuron.2004.07.018

Sauve, F., McBroom, L. D., Gallant, J., Moraitis, A. N., Labrie, F., & Giguere, V. (2001). CIA, a novel estrogen receptor coactivator with a bifunctional nuclear receptor interacting determinant. *Molecular and Cellular Biology, 21*(1), 343-353. doi: 10.1128/MCB.21.1.343-353.2001

Scheiffele, P., Fan, J., Choih, J., Fetter, R., & Serafini, T. (2000). Neuroligin expressed in nonneuronal cells triggers presynaptic development in contacting axons. *Cell, 101*(6), 657-669.

Schrader, M., Danielsson, C., Wiesenberg, I., & Carlberg, C. (1996). Identification of natural monomeric response elements of the nuclear receptor RZR/ROR. they also bind COUP-TF homodimers. *The Journal of Biological Chemistry, 271*(33), 19732-19736.

Sebat, J., Lakshmi, B., Malhotra, D., Troge, J., Lese-Martin, C., Walsh, T., . . . Wigler, M. (2007). Strong association of de novo copy number mutations with autism. *Science (New York, N.Y.), 316*(5823), 445-449. doi: 10.1126/science.1138659

Shmueli, O., Horn-Saban, S., Chalifa-Caspi, V., Shmoish, M., Ophir, R., Benjamin-Rodrig, H., . . . Lancet, D. (2003). GeneNote: Whole genome expression profiles in normal human tissues. *Comptes Rendus Biologies, 326*(10-11), 1067-1072.

Sidman, R. L., Lane, P. W., & Dickie, M. M. (1962). Staggerer, a new mutation in the mouse affecting the cerebellum. *Science (New York, N.Y.), 137*(3530), 610-612.

Sigman, M., Dijamco, A., Gratier, M., & Rozga, A. (2004). Early detection of core deficits in autism. *Mental Retardation and Developmental Disabilities Research Reviews, 10*(4), 221-233. doi: 10.1002/mrdd.20046

Smalley, S. L. (1998). Autism and tuberous sclerosis. *Journal of Autism and Developmental Disorders, 28*(5), 407-414.

Song, Y., Dang, C., Fu, Y., Lian, Y., Hottel, J., Li, X., . . . Fu, S. W. (2009). Genome-wide analysis of BP1 transcriptional targets in breast cancer cell line Hs578T. *International Journal of Biological Sciences, 5*(1), 1-12.

Spampinato, S. F., Molinaro, G., Merlo, S., Iacovelli, L., Caraci, F., Battaglia, G., . . . Sortino, M. A. (2012). Estrogen receptors and type 1 metabotropic glutamate receptors are interdependent in protecting cortical neurons against beta-amyloid toxicity. *Molecular Pharmacology, 81*(1), 12-20. doi: 10.1124/mol.111.074021

Sparagana, S. P., & Roach, E. S. (2000). Tuberous sclerosis complex. *Current Opinion in Neurology, 13*(2), 115-119.

Stahlberg, O., Soderstrom, H., Rastam, M., & Gillberg, C. (2004). Bipolar disorder, schizophrenia, and other psychotic disorders in adults with childhood onset AD/HD and/or autism spectrum disorders. *Journal of Neural Transmission (Vienna, Austria : 1996), 111*(7), 891-902. doi: 10.1007/s00702-004-0115-1

Stapleton, C. M., Jaradat, M., Dixon, D., Kang, H. S., Kim, S. C., Liao, G., . . . Jetten, A. M. (2005). Enhanced susceptibility of staggerer (RORalphasg/sg) mice to

lipopolysaccharide-induced lung inflammation. *American Journal of Physiology.Lung Cellular and Molecular Physiology, 289*(1), L144-52. doi: 10.1152/ajplung.00348.2004

Steffenburg, S., Gillberg, C., & Steffenburg, U. (1996). Psychiatric disorders in children and adolescents with mental retardation and active epilepsy. *Archives of Neurology, 53*(9), 904-912.

Steffenburg, S., Steffenburg, U., & Gillberg, C. (2003). Autism spectrum disorders in children with active epilepsy and learning disability: Comorbidity, pre- and perinatal background, and seizure characteristics. *Developmental Medicine and Child Neurology, 45*(11), 724-730.

Stehlin, C., Wurtz, J. M., Steinmetz, A., Greiner, E., Schule, R., Moras, D., & Renaud, J. P. (2001). X-ray structure of the orphan nuclear receptor RORbeta ligand-binding domain in the active conformation. *The EMBO Journal, 20*(21), 5822-5831. doi: 10.1093/emboj/20.21.5822

Stehlin-Gaon, C., Willmann, D., Zeyer, D., Sanglier, S., Van Dorsselaer, A., Renaud, J. P., . . . Schule, R. (2003). All-trans retinoic acid is a ligand for the orphan nuclear receptor ROR beta. *Nature Structural Biology, 10*(10), 820-825. doi: 10.1038/nsb979

Steinmayr, M., Andre, E., Conquet, F., Rondi-Reig, L., Delhaye-Bouchaud, N., Auclair, N., . . . Becker-Andre, M. (1998). Staggerer phenotype in retinoid-related orphan receptor alpha-deficient mice. *Proceedings of the National Academy of Sciences of the United States of America, 95*(7), 3960-3965.

Stielow, B., Sapetschnig, A., Kruger, I., Kunert, N., Brehm, A., Boutros, M., & Suske, G. (2008). Identification of SUMO-dependent chromatin-associated transcriptional repression components by a genome-wide RNAi screen. *Molecular Cell, 29*(6), 742-754. doi: 10.1016/j.molcel.2007.12.032

Su, A. I., Wiltshire, T., Batalov, S., Lapp, H., Ching, K. A., Block, D., . . . Hogenesch, J. B. (2004). A gene atlas of the mouse and human protein-encoding transcriptomes. *Proceedings of the National Academy of Sciences of the United States of America, 101*(16), 6062-6067. doi: 10.1073/pnas.0400782101

Sutcliffe, J. S., Nelson, D. L., Zhang, F., Pieretti, M., Caskey, C. T., Saxe, D., & Warren, S. T. (1992). DNA methylation represses FMR-1 transcription in fragile X syndrome. *Human Molecular Genetics, 1*(6), 397-400.

Suzuki, K., Matsuzaki, H., Iwata, K., Kameno, Y., Shimmura, C., Kawai, S., . . . Mori, N. (2011). Plasma cytokine profiles in subjects with high-functioning autism spectrum disorders. *PloS One, 6*(5), e20470. doi: 10.1371/journal.pone.0020470

Tager-Flusberg, H., & Caronna, E. (2007). Language disorders: Autism and other pervasive developmental disorders. *Pediatric Clinics of North America, 54*(3), 469-81, vi. doi: 10.1016/j.pcl.2007.02.011

Tordjman, S., Ferrari, P., Sulmont, V., Duyme, M., & Roubertoux, P. (1997). Androgenic activity in autism. *The American Journal of Psychiatry, 154*(11), 1626-1627.

Tosini, G., Davidson, A. J., Fukuhara, C., Kasamatsu, M., & Castanon-Cervantes, O. (2007). Localization of a circadian clock in mammalian photoreceptors. *FASEB Journal : Official Publication of the Federation of American Societies for Experimental Biology, 21*(14), 3866-3871. doi: 10.1096/fj.07-8371com

Treffert, D. A. (1970). Epidemiology of infantile autism. *Archives of General Psychiatry, 22*(5), 431-438.

Tsai, P. T., Hull, C., Chu, Y., Greene-Colozzi, E., Sadowski, A. R., Leech, J. M., . . . Sahin, M. (2012). Autistic-like behaviour and cerebellar dysfunction in purkinje cell Tsc1 mutant mice. *Nature,* doi: 10.1038/nature11310; 10.1038/nature11310

Tuchman, R., & Rapin, I. (2002). Epilepsy in autism. *Lancet Neurology, 1*(6), 352-358.

Ueda, E., Kurebayashi, S., Sakaue, M., Backlund, M., Koller, B., & Jetten, A. M. (2002). High incidence of T-cell lymphomas in mice deficient in the retinoid-related orphan receptor RORgamma. *Cancer Research, 62*(3), 901-909.

Vargas, D. L., Nascimbene, C., Krishnan, C., Zimmerman, A. W., & Pardo, C. A. (2005). Neuroglial activation and neuroinflammation in the brain of patients with autism. *Annals of Neurology, 57*(1), 67-81. doi: 10.1002/ana.20315

Vilensky, J. A., Damasio, A. R., & Maurer, R. G. (1981). Gait disturbances in patients with autistic behavior: A preliminary study. *Archives of Neurology, 38*(10), 646-649.

Vogel, M. W., Sinclair, M., Qiu, D., & Fan, H. (2000). Purkinje cell fate in staggerer mutants: Agenesis versus cell death. *Journal of Neurobiology, 42*(3), 323-337.

Voineagu, I., Wang, X., Johnston, P., Lowe, J. K., Tian, Y., Horvath, S., . . . Geschwind, D. H. (2011). Transcriptomic analysis of autistic brain reveals convergent molecular pathology. *Nature, 474*(7351), 380-384. doi: 10.1038/nature10110; 10.1038/nature10110

Volkmar, F., Chawarska, K., & Klin, A. (2005). Autism in infancy and early childhood. *Annual Review of Psychology, 56*, 315-336. doi: 10.1146/annurev.psych.56.091103.070159

Volkmar, F. R., & Chawarska, K. (2008). Autism in infants: An update. *World Psychiatry : Official Journal of the World Psychiatric Association (WPA), 7*(1), 19-21.

Volkmar, F. R., & Cohen, D. J. (1991). Comorbid association of autism and schizophrenia. *The American Journal of Psychiatry, 148*(12), 1705-1707.

Volkmar, F. R., Klin, A., Siegel, B., Szatmari, P., Lord, C., Campbell, M., . . . Kline, W. (1994). Field trial for autistic disorder in DSM-IV. *The American Journal of Psychiatry, 151*(9), 1361-1367.

Volkmar, F. R., & Nelson, D. S. (1990). Seizure disorders in autism. *Journal of the American Academy of Child and Adolescent Psychiatry, 29*(1), 127-129. doi: 10.1097/00004583-199001000-00020

Wada, T., Kang, H. S., Angers, M., Gong, H., Bhatia, S., Khadem, S., . . . Xie, W. (2008). Identification of oxysterol 7alpha-hydroxylase (Cyp7b1) as a novel retinoid-

related orphan receptor alpha (RORalpha) (NR1F1) target gene and a functional cross-talk between RORalpha and liver X receptor (NR1H3). *Molecular Pharmacology, 73*(3), 891-899. doi: 10.1124/mol.107.040741

Wassink, T. H., Piven, J., & Patil, S. R. (2001). Chromosomal abnormalities in a clinic sample of individuals with autistic disorder. *Psychiatric Genetics, 11*(2), 57-63.

Webb, D. W., Fryer, A. E., & Osborne, J. P. (1991). On the incidence of fits and mental retardation in tuberous sclerosis. *Journal of Medical Genetics, 28*(6), 395-397.

Wegiel, J., Kuchna, I., Nowicki, K., Imaki, H., Wegiel, J., Marchi, E., . . . Wisniewski, T. (2010). The neuropathology of autism: Defects of neurogenesis and neuronal migration, and dysplastic changes. *Acta Neuropathologica, 119*(6), 755-770. doi: 10.1007/s00401-010-0655-4

Wheelwright, S., Baron-Cohen, S., Goldenfeld, N., Delaney, J., Fine, D., Smith, R., . . . Wakabayashi, A. (2006). Predicting autism spectrum quotient (AQ) from the systemizing quotient-revised (SQ-R) and empathy quotient (EQ). *Brain Research, 1079*(1), 47-56. doi: 10.1016/j.brainres.2006.01.012

Williams, R. S., Hauser, S. L., Purpura, D. P., DeLong, G. R., & Swisher, C. N. (1980). Autism and mental retardation: Neuropathologic studies performed in four retarded persons with autistic behavior. *Archives of Neurology, 37*(12), 749-753.

Wisniewski, A. B. (1998). Sexually-dimorphic patterns of cortical asymmetry, and the role for sex steroid hormones in determining cortical patterns of lateralization. *Psychoneuroendocrinology, 23*(5), 519-547.

Wolf, I. M., Heitzer, M. D., Grubisha, M., & DeFranco, D. B. (2008). Coactivators and nuclear receptor transactivation. *Journal of Cellular Biochemistry, 104*(5), 1580-1586. doi: 10.1002/jcb.21755

Wozniak, J., Biederman, J., Faraone, S. V., Frazier, J., Kim, J., Millstein, R., . . . Snyder, J. B. (1997). Mania in children with pervasive developmental disorder revisited. *Journal of the American Academy of Child and Adolescent Psychiatry, 36*(11), 1552-9; discussion 1559-60. doi: 10.1016/S0890-8567(09)66564-3

Xiong, Z., Ding, L., Sun, J., Cao, J., Lin, J., Lu, Z., . . . Ye, Q. (2010). Synergistic repression of estrogen receptor transcriptional activity by FHL2 and Smad4 in breast cancer cells. *IUBMB Life, 62*(9), 669-676. doi: 10.1002/iub.367

Xu, W. (2005). Nuclear receptor coactivators: The key to unlock chromatin. *Biochemistry and Cell Biology = Biochimie Et Biologie Cellulaire, 83*(4), 418-428. doi: 10.1139/o05-057

Yanai, I., Benjamin, H., Shmoish, M., Chalifa-Caspi, V., Shklar, M., Ophir, R., . . . Shmueli, O. (2005). Genome-wide midrange transcription profiles reveal expression level relationships in human tissue specification. *Bioinformatics (Oxford, England), 21*(5), 650-659. doi: 10.1093/bioinformatics/bti042

Yang, X., Downes, M., Yu, R. T., Bookout, A. L., He, W., Straume, M., . . . Evans, R. M. (2006). Nuclear receptor expression links the circadian clock to metabolism. *Cell, 126*(4), 801-810. doi: 10.1016/j.cell.2006.06.050

Yang, X. O., Pappu, B. P., Nurieva, R., Akimzhanov, A., Kang, H. S., Chung, Y., . . . Dong, C. (2008). T helper 17 lineage differentiation is programmed by orphan nuclear receptors ROR alpha and ROR gamma. *Immunity, 28*(1), 29-39. doi: 10.1016/j.immuni.2007.11.016

Yang, Y., & Raine, A. (2009). Prefrontal structural and functional brain imaging findings in antisocial, violent, and psychopathic individuals: A meta-analysis. *Psychiatry Research, 174*(2), 81-88. doi: 10.1016/j.pscychresns.2009.03.012

Yi, S. S., Hwang, I. K., Shin, J. H., Baek, S. H., Yoon, Y. S., & Seong, J. K. (2010). Neuronal differentiation and developmental characteristics in the dentate gyrus of staggerer mutant mice. *BMB Reports, 43*(2), 122-126.

Ylisaukko-oja, T., Rehnstrom, K., Auranen, M., Vanhala, R., Alen, R., Kempas, E., . . . Jarvela, I. (2005). Analysis of four neuroligin genes as candidates for autism. *European Journal of Human Genetics : EJHG, 13*(12), 1285-1292. doi: 10.1038/sj.ejhg.5201474

Yoon, C. H. (1972). Developmental mechanism for changes in cerebellum of "staggerer" mouse, a neurological mutant of genetic origin. *Neurology, 22*(7), 743-754.

Yorbik, O., Sayal, A., Akay, C., Akbiyik, D. I., & Sohmen, T. (2002). Investigation of antioxidant enzymes in children with autistic disorder. *Prostaglandins, Leukotrienes, and Essential Fatty Acids, 67*(5), 341-343.

Young, A. M., Campbell, E., Lynch, S., Suckling, J., & Powis, S. J. (2011). Aberrant NF-kappaB expression in autism spectrum condition: A mechanism for neuroinflammation. *Frontiers in Psychiatry / Frontiers Research Foundation, 2*, 27. doi: 10.3389/fpsyt.2011.00027

Zanjani, H. S., Mariani, J., Delhaye-Bouchaud, N., & Herrup, K. (1992). Neuronal cell loss in heterozygous staggerer mutant mice: A model for genetic contributions to the aging process. *Brain Research.Developmental Brain Research, 67*(2), 153-160.

Zhang, F. P., Mikkonen, L., Toppari, J., Palvimo, J. J., Thesleff, I., & Janne, O. A. (2008). Sumo-1 function is dispensable in normal mouse development. *Molecular and Cellular Biology, 28*(17), 5381-5390. doi: 10.1128/MCB.00651-08

Zhou, L., Fester, L., von Blittersdorff, B., Hassu, B., Nogens, H., Prange-Kiel, J., . . . Rune, G. M. (2010). Aromatase inhibitors induce spine synapse loss in the hippocampus of ovariectomized mice. *Endocrinology, 151*(3), 1153-1160. doi: 10.1210/en.2009-0254

Zhu, Y., McAvoy, S., Kuhn, R., & Smith, D. I. (2006). RORA, a large common fragile site gene, is involved in cellular stress response. *Oncogene, 25*(20), 2901-2908. doi: 10.1038/sj.onc.1209314

Zimmerman, A. W., Jyonouchi, H., Comi, A. M., Connors, S. L., Milstien, S., Varsou, A., & Heyes, M. P. (2005). Cerebrospinal fluid and serum markers of inflammation in autism. *Pediatric Neurology, 33*(3), 195-201. doi: 10.1016/j.pediatrneurol.2005.03.014

Zoroglu, S. S., Armutcu, F., Ozen, S., Gurel, A., Sivasli, E., Yetkin, O., & Meram, I. (2004). Increased oxidative stress and altered activities of erythrocyte free radical scavenging enzymes in autism. *European Archives of Psychiatry and Clinical Neuroscience, 254*(3), 143-147. doi: 10.1007/s00406-004-0456-7

Appendices

Supplemental Table 1. List of frozen human brain tissue samples from the Autism Tissue Program.

Case#	Diagnosis	Gender	Age	PMI
5144	Autism	Male	20	23.7
5173	Autism	Male	30	20.3
6337	Autism	Male	22	25
5251	No Known Disorder	Male	19	18.58
5718	No Known Disorder	Male	22	21.47
5873	No Known Disorder	Male	28	23.25

Supplemental Table 2. List of antibodies, siRNAs, and shRNAs used in this dissertation.

Description	Species	Type	Catalog#
Antibodies			
AR (441)	mouse	monoclonal	SC-7305
CYP19A1 (C-16)	goat	polyclonal	SC-14245
ERα (D-12)	mouse	monoclonal	SC-8005
FHL2 (C-16)	goat	polyclonal	SC-13409
MAP2	mouse	monoclonal	13-1500
NCOA1 (C-20)	goat	polyclonal	SC-6096
NCOA5 (G-20)	goat	polyclonal	SC-86178
RORA (H-65)	rabbit	polyclonal	SC-28612
RORA1 (S-12)	goat	polyclonal	SC-26377
SUMO1 (N-19)	goat	polyclonal	SC-6376
normal goat IgG	goat		SC-2028
normal rabbit IgG	rabbit		SC-2027
normal mouse IgG	mouse		SC-2025
anti-mouse IgG-HRP	donkey		SC-2318
anti-rabbit IgG-HRP	donkey		SC-2317
anti-goat IgG-HRP	donkey		SC-2020
anti-mouse IgG-Alexa 488	donkey		A21202
anti-rabbit IgG-Alexa 647	donkey		A31573
anti-goat IgG-Alexa 546	donkey		A11056
siRNAs			
AR siRNA (h)			SC-29204
ERα siRNA (h)			SC-29305
SUMO1 siRNA (h)			SC-29498
NCOA5 siRNA (h)			SC-75885
shRNAs			
RORA1 shRNA			SC-38864-SH
Control shRNA Plasmid-A			SC-108060

Supplemental Table 3. List of primers for PCR cloning, qPCR, and RT-qPCR.

Analysis	Description	Forward primer (5' -> 3')	Reverse primer (5' -> 3')
PCR Cloning	RORApro(-10055 to -48)+SfiI RE sites	GGCCTAACTGGCC-GGCTATGCAGTGACACCCTTGCTATAATCTC	GGCCGCCGAGGCC-CCCTCTATCTTCTGTTTTCAGAGCAACTCTATGG
	RORApro(-6000 to -48)+SfiI RE sites	GGCCTAACTGGCC-TTGACCCTACCTCATTATTCAATCAATCTGTCAA	GGCCGCCGAGGCC-CCCTCTATCTTCTGTTTTCAGAGCAACTCTATGG
	RORApro(-2344 to -48)+SfiI RE sites	GGCCTAACTGGCC-GAGTTCCCAATTGTTTTAAATTGCAGAAGCAGTA	GGCCGCCGAGGCC-CCCTCTATCTTCTGTTTTCAGAGCAACTCTATGG
	RORApro(-1992 to -48)+SfiI RE sites	GGCCTAACTGGCC-AAATAAACATGAGGCAGCCAATGTATTCTGAGAT	GGCCGCCGAGGCC-CCCTCTATCTTCTGTTTTCAGAGCAACTCTATGG
ChIP-qPCR and ChIP-reChIP-qPCR	RORA_ERbsI	TGCTAGGCAGCATTTTTGTG	CAGGCATGATGGGTCAAAC
	RORA_ERbsII	TGCACAGGTGAACAAGTGAGA	TGGGTGAGATGAAGGGATGT
	RORA_ERbsIII	TTTTTGGAGCTGCGATCTTT	TTGGACCTTTAATGAGTTTCTTACTG
	RORA_ERbsIV	CACTGTCCCAGAGGAAGTTGTT	CCCATACGTGAAAGCACAGA
	RORA_ARbsI	AGGTGAAGCTGCTGGAAAAC	AGGGCATGAAGCAAGAAAGA
	RORA_ARbsII	TTTTTGGAGCTGCGATCTTT	TTGGACCTTTAATGAGTTTCTTACTG
	RORA_ARbsIII	CACTGTCCCAGAGGAAGTTGTT	CCCATACGTGAAAGCACAGA
	A2BP1_RORAbsI	TGAAGGTCACCTCCTTTCCA	GCTTGGAGAACCACTTCAGG
	A2BP1_RORAbsII	TTTCTCTTTTCCTCGATCTCTCA	CAAGGTTTTTATTTTCCCTTGCT
	A2BP1_RORAbsIII	GGTCATATAAACCTTCCGCAAAC	TCACCCAGCCAATTTTCTTC
	CYP19A1_RORAbsI	CTGCCAAGGACTAGTGTCCAG	TTTGGCTCTTTCTGCCTTGT
	CYP19A1_RORAbsII/III	GGGGAGACCAGGATGGATAG	AGTAGAGACGGGGTTTCACAG
	HSD17B10_RORAbsI	ACAAATTAGCGAGGCATGGT	TTGGGATTTTTCGAGACAGG
	HSD17B10_RORAbsII	CCTGAAGCCTCAACCTACCA	ACTCCAGACCACCATTCAGG
	HSD17B10_RORAbsIII	AAGCATGTCCCAAAGATTGC	GGTTTCATCATGTTGGTCAGG
	ITPR1_RORAbsI	GCAACTCCACTTTTTCCATGTC	TGCAGCATCTTGTTCTGCTC
	ITPR1_RORAbsII	GCTTGCTTTGGCAACAGAGT	CCTCCTTGGCGGTTTAGATAG
	ITPR1_RORAbsIII	AGGTCAAGCTGTCTTTGGCTAC	AAAACTGCATGGACTTCTGGTT
	NLGN1_RORAbsI	TTGATCATGAATTCTTGGGTTT	ACATTTCACTGGGCTATGACCT
	NLGN1_RORAbsII	CACCTAGAACACTCCATGACACA	GGACTCATTGACTCACACTGAAA
	NLGN1_RORAbsIII	TCCACAGGTCACTGGCATAA	AAGCCTTGACTGAACCAACAA
	NTRK2_RORAbsI	CAAATGCATCCCTTTCCAG	GGCATTCCATAAACCCACAG
	NTRK2_RORAbsII	TCCAGCAGAACAAGAAGTTGA	ATGGATGGATTGTGGTGATG
	NTRK2_RORAbsIII	AGTTGGCTGAACAGCTGAGA	CCTTCCCCAGCTAAACAAAA
RT-qPCR of SH-SY5Y cell line and human brain tissues	18S	CCGCAGCTAGGAATAATGGA	CCCTCTTAATCATGGCCTCA
	A2BP1	TACCACCACGCACTTGCTC	GCTTCCTTTCTCCCCACATT
	AR	TACCAGCTCACCAAGCTCCT	TGATCTCTGCCATCATTTCC
	CYP19A1	GCGCAAAGCCTTAGAAGATG	CAAAGCCAAATGGCTGAAAG
	ESR1 (ERalpha)	GCCAAGGAGACTCGCTACTG	ACTGGTTGGTGGCTGGAC
	FHL2	CAGTGCGTTCAGTGCAAAA	CAGGCAGTAGGCAAAGTCATC
	GAPDH	CCA GGT GGT CTC CTC TGA CT	TGC TGT AGC CAA ATT CGT TG

	HSD17B10	TTTGGCCGTGTGGATGTAG	TTGAAGGTGCCCATGAGATT
	ITPR1	CCA TGA AAC TTG TCA CGA ACC	GGG TTG ACA TTC ATG TGA GGA
	NCOA1	CAATGACCAAACCCACTCCT	ATAAGCCTGGCAACTGTGCT
	NCOA5	CCAGGCCCAGAAAGTCAGT	GCGTCTCTGGATTTCCTCAA
	NLGN1	TGTGATGCTGAGTGCAGTTGT	AACGGTTGGGTTTGGTATGA
	NTRK2	GTGGCGGAAAATCTTGTAGG	ACAGTGAATGGAATGCACCA
	RORA	TCATGGCTGCAAGAAAAGGT	GAGGAAAATGAAGTCGCACAA
	RORA1	CAGAGCTATTCCAGCACCAG	CCTGATGATTTGTCTCCACAG
	SUMO1	CATTGGACAGGATAGCAGTGA	TCTGACCCTCAAAGAGAAACC

Supplemental Table 4. Transcription factor binding sites in promoter regions of RORA and CYP19A1 genes.

Name	Sequence (5'-->3')	Genomic Location
RORA_ARbs-I	ATCAAAAGGAACATTTGCTG	chr15:59,314,304-59,314,323
RORA_ARbs-II	AGGAGAACAGTAAGAAACTC	chr15:59,310,855-59,310,874
RORA_ARbs-III	TGCATCAAGAACATTACTAA	chr15:59,310,557-59,310,576
RORA_ERbs-I	AAAGGAAGGTTTGACCCATC	chr15:59,318,256-59,318,275
RORA_ERbs-II	CGGTGGGGTCATAATGGGTC	chr15:59,314,497-59,314,516
RORA_ERbs-III	AATTGATTCAGGTCATTATG	chr15:59,310,925-59,310,944
RORA_ERbs-IV	AACAAGCTAGGTCAATTGCA	chr15:59,310,573-59,310,592
CYP19A1_RORAbsI	CTGCCTCGAGGGTCACTGTC	chr15:49,420,185-49,420,204
CYP19A1_RORAbsII	ATCTGATTGTGGGTCATAAG	chr15:49,418,286-49,418,305
CYP19A1_RORAbsIII	TTCCAGAGGAGGTCATGCCC	chr15:49,418,259-49,418,278

Supplemental Table 5. List of potential transcriptional targets of RORA identified by ChIP-on-chip analysis.

Gene Symbol	Description	p-value	log2 ratio
PPP2R2B	protein phosphatase 2 (formerly 2A), regulatory subunit B, beta isoform	0.000	0.752
DDX52	DEAD (Asp-Glu-Ala-Asp) box polypeptide 52	0.000	1.700
CBX3	similar to chromobox homolog 3; chromobox homolog 3 (HP1 gamma homolog, Drosophila)	0.001	0.592
UGT2B15	UDP glucuronosyltransferase 2 family, polypeptide B15	0.001	0.705
UGT2B17	UDP glucuronosyltransferase 2 family, polypeptide B17	0.001	0.641
CYP2R1	cytochrome P450, family 2, subfamily R, polypeptide 1	0.001	0.598
LYPLA1	lysophospholipase I	0.001	0.450
HSD17B10	hydroxysteroid (17-beta) dehydrogenase 10	0.001	0.698
ARPC4	tubulin tyrosine ligase-like family, member 3; actin related protein 2/3 complex, subunit 4, 20kDa	0.001	0.341
BCL11B	B-cell CLL/lymphoma 11B (zinc finger protein)	0.001	0.601
HK1	hexokinase 1	0.001	0.361
ABHD4	abhydrolase domain containing 4	0.001	0.535
PTPN11	protein tyrosine phosphatase, non-receptor type 11; similar to protein tyrosine phosphatase, non-receptor type 11	0.001	1.806
DGKH	diacylglycerol kinase, eta	0.001	4.309
KIF26B	kinesin family member 26B	0.002	0.442
UBE2Q1	ubiquitin-conjugating enzyme E2Q family member 1	0.002	0.389
ADRA1B	adrenergic, alpha-1B-, receptor	0.002	0.403
TMEM87B	transmembrane protein 87B	0.002	2.008
C7orf59	chromosome 7 open reading frame 59	0.002	1.044
GFRA2	similar to GDNF family receptor alpha 2; GDNF family receptor alpha 2	0.002	0.414
CAPRIN2	caprin family member 2	0.002	0.924
RAP1GAP	RAP1 GTPase activating protein	0.002	1.614
MTPN	myotrophin; leucine zipper protein 6	0.002	0.442
TM9SF2	transmembrane 9 superfamily member 2	0.002	0.397
KIF18A	kinesin family member 18A	0.002	0.386
LASS6	LAG1 homolog, ceramide synthase 6	0.002	0.364
LOC389332	hypothetical LOC389332	0.002	0.765
C9orf72	chromosome 9 open reading frame 72	0.002	0.418
IP6K3	inositol hexakisphosphate kinase 3	0.002	1.702
OR52K1	olfactory receptor, family 52, subfamily K, member 1	0.002	0.551
RUNDC3B	RUN domain containing 3B	0.002	0.363
MTNR1B	melatonin receptor 1B	0.002	0.617
GSDMB	gasdermin B	0.002	0.788
MLC1	megalencephalic leukoencephalopathy with subcortical cysts 1	0.003	3.155
CNKSR2	connector enhancer of kinase suppressor of Ras 2	0.003	0.352
SELI	selenoprotein I	0.003	0.594
TMPRSS7	transmembrane protease, serine 7	0.003	0.928
IFT20	intraflagellar transport 20 homolog (Chlamydomonas)	0.003	0.739
SLC3A1	solute carrier family 3 (cystine, dibasic and neutral amino acid transporters, activator of cystine, dibasic and neutral amino acid transport), member 1	0.003	1.534
RECK	reversion-inducing-cysteine-rich protein with kazal motifs	0.003	0.403
POLD2	polymerase (DNA directed), delta 2, regulatory subunit 50kDa	0.003	1.216

C9orf150	chromosome 9 open reading frame 150	0.003	0.446
CTXN3	cortexin 3	0.003	0.451
FAM13B	family with sequence similarity 13, member B	0.003	0.365
RASGRP3	RAS guanyl releasing protein 3 (calcium and DAG-regulated)	0.003	0.303
FAT1	FAT tumor suppressor homolog 1 (Drosophila)	0.003	0.462
EPHB4	EPH receptor B4	0.003	2.527
IL22RA2	interleukin 22 receptor, alpha 2	0.003	1.523
GLI2	GLI family zinc finger 2	0.003	0.315
DBNDD1	dysbindin (dystrobrevin binding protein 1) domain containing 1	0.003	0.788
ST20	suppressor of tumorigenicity 20	0.003	0.960
SSBP3	single stranded DNA binding protein 3; hypothetical LOC100131851	0.003	0.385
LOC728323	hypothetical LOC728323	0.003	0.355
AKNA	AT-hook transcription factor	0.003	0.504
CYLC2	cylicin, basic protein of sperm head cytoskeleton 2	0.003	1.170
LRRC15	leucine rich repeat containing 15	0.003	0.827
FERMT3	fermitin family homolog 3 (Drosophila)	0.003	0.550
ZC3H12B	zinc finger CCCH-type containing 12B	0.004	1.563
SERPINB13	serpin peptidase inhibitor, clade B (ovalbumin), member 13	0.004	0.450
ZNF546	zinc finger protein 546	0.004	0.748
THBS2	thrombospondin 2	0.004	0.432
IRF2BP2	interferon regulatory factor 2 binding protein 2	0.004	0.978
HBP1	HMG-box transcription factor 1	0.004	2.534
MKKS	McKusick-Kaufman syndrome	0.004	0.502
NCRNA00052	non-protein coding RNA 52	0.004	0.645
ABR	active BCR-related gene	0.004	1.321
CCL4L1	chemokine (C-C motif) ligand 4-like 1; chemokine (C-C motif) ligand 4-like 2	0.004	0.624
SLC5A4	solute carrier family 5 (low affinity glucose cotransporter), member 4	0.004	0.509
MAP2K3	mitogen-activated protein kinase kinase 3	0.004	0.349
SLC2A3	solute carrier family 2 (facilitated glucose transporter), member 3	0.004	2.198
C1QTNF1	C1q and tumor necrosis factor related protein 1	0.004	1.027
SLC22A13	solute carrier family 22 (organic anion transporter), member 13	0.004	0.836
RNF186	ring finger protein 186	0.004	1.148
C7orf10	chromosome 7 open reading frame 10	0.004	1.417
PIGR	polymeric immunoglobulin receptor	0.004	0.809
SH3BP4	SH3-domain binding protein 4	0.005	0.506
ABTB1	ankyrin repeat and BTB (POZ) domain containing 1	0.005	0.365
FAM71F2	family with sequence similarity 71, member F2	0.005	1.758
DSCAM	Down syndrome cell adhesion molecule	0.005	0.466
IGF2BP2	insulin-like growth factor 2 mRNA binding protein 2	0.005	0.637
CPNE9	copine family member IX	0.005	0.404
LMO1	LIM domain only 1 (rhombotin 1)	0.005	0.608
TUBB8	tubulin, beta 8	0.005	0.674
ITPR1	inositol 1,4,5-triphosphate receptor, type 1	0.005	0.370
APBA1	amyloid beta (A4) precursor protein-binding, family A, member 1	0.005	0.741
PPP1R9A	protein phosphatase 1, regulatory (inhibitor) subunit 9A	0.005	0.358
ZNF565	zinc finger protein 565	0.005	1.925
USP18	ubiquitin specific peptidase 18	0.005	0.999
SLAMF8	SLAM family member 8	0.005	1.058
CCDC70	coiled-coil domain containing 70	0.005	0.664

AKR1B10	aldo-keto reductase family 1, member B10 (aldose reductase); aldo-keto reductase family 1, member B10-like	0.005	1.717
PAPD5	PAP associated domain containing 5	0.005	1.131
ACADL	acyl-Coenzyme A dehydrogenase, long chain	0.005	0.347
FLJ45079	FLJ45079 protein	0.005	0.600
KCNIP2	Kv channel interacting protein 2	0.005	0.380
FOXF1	forkhead box F1	0.005	0.793
NCOR1	nuclear receptor co-repressor 1	0.006	0.418
C12orf65	chromosome 12 open reading frame 65	0.006	0.385
CA5BP	carbonic anhydrase VB pseudogene	0.006	0.957
ATP5J	ATP synthase, H+ transporting, mitochondrial F0 complex, subunit F6	0.006	0.438
SLC12A9	solute carrier family 12 (potassium/chloride transporters), member 9	0.006	0.628
PLSCR1	phospholipid scramblase 1	0.006	0.818
DNMT3A	DNA (cytosine-5-)-methyltransferase 3 alpha	0.006	0.330
ZMYND11	zinc finger, MYND domain containing 11	0.006	1.152
PCNXL2	pecanex-like 2 (Drosophila)	0.006	0.441
RBM44	RNA binding motif protein 44	0.006	0.559
POMP	proteasome maturation protein	0.006	0.594
FAM170A	family with sequence similarity 170, member A	0.006	1.131
FREQ	frequenin homolog (Drosophila)	0.006	0.318
PHYHIPL	phytanoyl-CoA 2-hydroxylase interacting protein-like	0.006	0.343
CCDC62	coiled-coil domain containing 62	0.006	2.982
MT1L	metallothionein 1L (gene/pseudogene); metallothionein 1E; metallothionein 1 pseudogene 3; metallothionein 1J (pseudogene)	0.006	0.591
SMN2	survival of motor neuron 1, telomeric; survival of motor neuron 2, centromeric	0.006	0.349
SLC7A2	solute carrier family 7 (cationic amino acid transporter, y+ system), member 2	0.006	0.700
SLC7A5P1	solute carrier family 7 (cationic amino acid transporter, y+ system), member 5 pseudogene 1	0.006	2.956
ZNF442	zinc finger protein 442	0.007	1.105
C16orf13	chromosome 16 open reading frame 13	0.007	0.301
LOC732275	similar to hCG1645603	0.007	0.532
SLAMF9	SLAM family member 9	0.007	1.037
TJP2	tight junction protein 2 (zona occludens 2)	0.007	1.016
CXCL5	chemokine (C-X-C motif) ligand 5	0.007	0.685
EIF2C2	eukaryotic translation initiation factor 2C, 2	0.007	0.554
ZNF167	zinc finger protein 852; zinc finger protein 167	0.007	2.387
MATR3	matrin 3	0.007	1.478
IKBKE	inhibitor of kappa light polypeptide gene enhancer in B-cells, kinase epsilon	0.007	0.778
DSP	desmoplakin	0.007	0.912
ATP4A	ATPase, H+/K+ exchanging, alpha polypeptide	0.007	1.939
CCDC19	coiled-coil domain containing 19	0.007	0.400
P2RX1	purinergic receptor P2X, ligand-gated ion channel, 1	0.007	0.393
HSD17B10	hydroxysteroid (17-beta) dehydrogenase 10	0.007	3.568
MACF1	microtubule-actin crosslinking factor 1	0.007	0.582
GMDS	GDP-mannose 4,6-dehydratase	0.007	1.142
SMCR7L	Smith-Magenis syndrome chromosome region, candidate 7-like	0.008	0.372
WFDC12	WAP four-disulfide core domain 12	0.008	0.919
TAS2R60	taste receptor, type 2, member 60	0.008	0.408
SCAMP3	secretory carrier membrane protein 3	0.008	3.926
TXLNA	taxilin alpha	0.008	0.679
SERPINA9	serpin peptidase inhibitor, clade A (alpha-1 antiproteinase, antitrypsin), member 9	0.008	0.481

HISPPD2A	histidine acid phosphatase domain containing 2A	0.008	0.707
WNT5B	wingless-type MMTV integration site family, member 5B	0.009	0.384
LOC728613	programmed cell death 6 pseudogene	0.009	1.230
C1orf107	chromosome 1 open reading frame 107	0.009	0.720
MS4A14	membrane-spanning 4-domains, subfamily A, member 14	0.009	0.480
RCHY1	ring finger and CHY zinc finger domain containing 1	0.009	0.358
SNTN	sentan, cilia apical structure protein	0.009	0.500
WDR13	WD repeat domain 13	0.009	0.581
ARFIP2	ADP-ribosylation factor interacting protein 2	0.009	0.401
AKAP1	A kinase (PRKA) anchor protein 1	0.009	0.951
ADAM21P	unknown	0.009	1.154
RSPH6A	radial spokehead-like 1	0.009	0.414
HIST2H2AB	histone cluster 2, H2ab	0.009	1.724
RGS14	regulator of G-protein signaling 14	0.009	0.846
EEA1	early endosome antigen 1	0.009	0.408
DAPK2	death-associated protein kinase 2	0.009	0.319
SMPD3	sphingomyelin phosphodiesterase 3, neutral membrane (neutral sphingomyelinase II)	0.009	0.333
CDH11	cadherin 11, type 2, OB-cadherin (osteoblast)	0.009	0.785
BTBD18	hypothetical protein LOC643376	0.009	0.469
TMEM143	transmembrane protein 143	0.009	0.315
PYY2	peptide YY, 2 (seminalplasmin)	0.009	0.497
PYGM	phosphorylase, glycogen, muscle	0.009	0.833
RAB2B	RAB2B, member RAS oncogene family	0.009	0.397
ZHX2	zinc fingers and homeoboxes 2	0.009	0.388
HFE	hemochromatosis	0.009	1.188
KLHL15	kelch-like 15 (Drosophila)	0.009	0.426
A2BP1	ataxin 2-binding protein 1	0.009	0.367
F11R	F11 receptor	0.009	0.576
CCDC112	coiled-coil domain containing 112	0.009	1.929
C15orf38	chromosome 15 open reading frame 38	0.009	0.548
RAPGEF5	Rap guanine nucleotide exchange factor (GEF) 5	0.009	1.010
RLN2	relaxin 2	0.009	0.595
OBSL1	obscurin-like 1	0.009	0.780
LNX1	ligand of numb-protein X 1	0.009	0.576
AP3B2	adaptor-related protein complex 3, beta 2 subunit	0.009	0.357
SSX4	synovial sarcoma, X breakpoint 4; synovial sarcoma, X breakpoint 4B	0.009	0.318
RPP25	ribonuclease P/MRP 25kDa subunit	0.009	1.377
HECW1	HECT, C2 and WW domain containing E3 ubiquitin protein ligase 1	0.009	0.728
RPS6KA5	ribosomal protein S6 kinase, 90kDa, polypeptide 5	0.009	0.974
SLC1A5	solute carrier family 1 (neutral amino acid transporter), member 5	0.009	1.463
ADARB1	adenosine deaminase, RNA-specific, B1 (RED1 homolog rat)	0.010	0.660
ZNF385D	zinc finger protein 385D	0.010	0.764
CDK5R1	cyclin-dependent kinase 5, regulatory subunit 1 (p35)	0.010	0.537
KATNB1	katanin p80 (WD repeat containing) subunit B 1	0.010	0.663
EIF4E	eukaryotic translation initiation factor 4E; similar to hCG1777996; similar to eukaryotic translation initiation factor 4E	0.010	0.685
COG2	component of oligomeric golgi complex 2	0.010	1.966
DYM	dymeclin	0.010	0.596
PTPN7	protein tyrosine phosphatase, non-receptor type 7	0.010	0.788
SCARNA18	small Cajal body-specific RNA 18	0.010	0.500

CNTN1	contactin 1	0.010	0.584
RAB20	RAB20, member RAS oncogene family	0.010	0.617
ROR2	receptor tyrosine kinase-like orphan receptor 2	0.010	0.790
ENKUR	enkurin, TRPC channel interacting protein	0.010	0.307
KIAA1383	KIAA1383	0.010	0.613
PEX26	peroxisomal biogenesis factor 26	0.010	1.527
LRRC56	leucine rich repeat containing 56	0.010	0.374
VGLL3	vestigial like 3 (Drosophila)	0.010	0.776
KCNS3	potassium voltage-gated channel, delayed-rectifier, subfamily S, member 3	0.010	0.510
LRRC16B	leucine rich repeat containing 16B	0.010	0.553
C6orf217	chromosome 6 open reading frame 217	0.010	0.397
MYL1	myosin, light chain 1, alkali; skeletal, fast	0.010	0.519
CFHR3	complement factor H-related 3	0.010	1.180
ZBTB12	zinc finger and BTB domain containing 12	0.010	0.454
SNRPD1	small nuclear ribonucleoprotein D1 polypeptide 16kDa; hypothetical protein LOC100129492	0.010	1.223
CUL2	cullin 2	0.010	0.576
PHLDB2	pleckstrin homology-like domain, family B, member 2; phosphatidylinositol-specific phospholipase C, X domain containing 2	0.011	0.329
FOLH1	folate hydrolase (prostate-specific membrane antigen) 1	0.011	0.340
C3orf59	chromosome 3 open reading frame 59	0.011	0.310
AWAT2	acyl-CoA wax alcohol acyltransferase 2	0.011	0.850
SPHKAP	SPHK1 interactor, AKAP domain containing	0.011	0.527
KRT16	keratin 16; keratin type 16-like	0.011	0.400
HLTF	helicase-like transcription factor	0.011	1.325
MGAT3	mannosyl (beta-1,4-)-glycoprotein beta-1,4-N-acetylglucosaminyltransferase	0.011	0.963
C4orf32	chromosome 4 open reading frame 32	0.011	0.738
PHF15	PHD finger protein 15	0.011	0.399
SOCS1	suppressor of cytokine signaling 1	0.011	0.608
PSME4	proteasome (prosome, macropain) activator subunit 4	0.011	0.791
PEBP4	phosphatidylethanolamine-binding protein 4	0.011	0.390
CABP1	calcium binding protein 1	0.011	3.967
OR7D2	olfactory receptor, family 7, subfamily D, member 2	0.011	1.513
MYEF2	myelin expression factor 2	0.011	0.338
DEFB104B	defensin, beta 104A; defensin, beta 104B	0.011	0.529
FAM134B	family with sequence similarity 134, member B	0.011	0.591
COL14A1	collagen, type XIV, alpha 1	0.011	0.744
RCN2	reticulocalbin 2, EF-hand calcium binding domain	0.011	1.087
PKD1L1	polycystic kidney disease 1 like 1	0.012	0.983
CBWD2	COBW domain containing 2	0.012	1.391
MUSTN1	transmembrane protein 110; musculoskeletal, embryonic nuclear protein 1	0.012	0.403
MAGI2	membrane associated guanylate kinase, WW and PDZ domain containing 2	0.012	0.315
CRELD1	cysteine-rich with EGF-like domains 1	0.012	0.680
CGNL1	cingulin-like 1	0.012	1.943
MSR1	macrophage scavenger receptor 1	0.012	0.322
PARS2	prolyl-tRNA synthetase 2, mitochondrial (putative)	0.012	0.811
SERPING1	serpin peptidase inhibitor, clade G (C1 inhibitor), member 1	0.012	0.856
MPPED1	metallophosphoesterase domain containing 1	0.012	0.721
RORC	RAR-related orphan receptor C	0.012	0.310
GOLGA4	golgi autoantigen, golgin subfamily a, 4	0.012	2.508
SIX2	SIX homeobox 2	0.012	1.235

TTC35	tetratricopeptide repeat domain 35	0.012	0.406
RTN1	reticulon 1	0.012	2.352
FADS6	fatty acid desaturase domain family, member 6	0.012	1.005
CDKAL1	CDK5 regulatory subunit associated protein 1-like 1	0.012	1.722
POLRMT	polymerase (RNA) mitochondrial (DNA directed)	0.012	0.463
GPR110	G protein-coupled receptor 110	0.012	0.917
VAMP8	vesicle-associated membrane protein 8 (endobrevin)	0.012	1.345
CHST6	carbohydrate (N-acetylglucosamine 6-O) sulfotransferase 6	0.012	0.730
MYCBP	c-myc binding protein	0.012	0.519
RFPL2	ret finger protein-like 2; ret finger protein-like 3	0.012	0.374
TCP10	t-complex 10-like 2 (mouse); t-complex 10 homolog (mouse)	0.012	0.363
MATN4	matrilin 4	0.012	0.702
LOC91316	glucuronidase, beta/ immunoglobulin lambda-like polypeptide 1 pseudogene	0.012	0.862
SLC22A4	solute carrier family 22 (organic cation/ergothioneine transporter), member 4	0.012	0.840
CAPS	calcyphosine	0.012	0.693
ARMC7	armadillo repeat containing 7	0.012	2.512
C14orf79	chromosome 14 open reading frame 79	0.012	1.415
PDIA3	protein disulfide isomerase family A, member 3	0.012	0.339
DPCR1	diffuse panbronchiolitis critical region 1	0.012	0.331
TMEM185B	transmembrane protein 185B (pseudogene)	0.012	0.369
CDKL1	cyclin-dependent kinase-like 1 (CDC2-related kinase)	0.013	0.842
SAMD4B	sterile alpha motif domain containing 4B	0.013	0.345
TMEM9B	TMEM9 domain family, member B	0.013	0.317
KRTAP10-7	keratin associated protein 10-7	0.013	0.431
GPR141	G protein-coupled receptor 141	0.013	0.814
NPL	N-acetylneuraminate pyruvate lyase (dihydrodipicolinate synthase)	0.013	1.062
COL18A1	collagen, type XVIII, alpha 1	0.013	0.442
MARCH6	membrane-associated ring finger (C3HC4) 6	0.013	0.307
MAGEA1	melanoma antigen family A, 1 (directs expression of antigen MZ2-E)	0.013	2.240
PLCH1	phospholipase C, eta 1	0.013	1.432
ADCY5	adenylate cyclase 5	0.013	1.063
CYP7B1	cytochrome P450, family 7, subfamily B, polypeptide 1	0.013	0.404
SGCA	sarcoglycan, alpha (50kDa dystrophin-associated glycoprotein)	0.013	0.578
CR1L	complement component (3b/4b) receptor 1-like	0.013	0.407
PXK	PX domain containing serine/threonine kinase	0.013	0.445
LMO2	LIM domain only 2 (rhombotin-like 1)	0.013	0.697
CHI3L1	chitinase 3-like 1 (cartilage glycoprotein-39)	0.013	0.681
PNRC1	proline-rich nuclear receptor coactivator 1	0.013	0.876
MATN2	matrilin 2	0.013	0.460
LAMA5	laminin, alpha 5	0.013	0.339
IDH1	isocitrate dehydrogenase 1 (NADP+), soluble	0.013	0.458
KCMF1	potassium channel modulatory factor 1	0.013	0.340
TMPRSS5	transmembrane protease, serine 5	0.013	0.401
CFP	complement factor properdin	0.013	0.455
PRDM7	PR domain containing 7	0.013	0.682
RAB7A	RAB7A, member RAS oncogene family	0.013	1.069
POTEH	POTE ankyrin domain family, member H	0.013	0.407
C3orf59	chromosome 3 open reading frame 59	0.013	0.751
SLC25A37	solute carrier family 25, member 37	0.013	0.352
TMCC2	transmembrane and coiled-coil domain family 2	0.013	0.453

KIF13A	kinesin family member 13A	0.013	0.495
APOBEC2	apolipoprotein B mRNA editing enzyme, catalytic polypeptide-like 2	0.014	0.433
ZNF837	zinc finger protein 837	0.014	0.398
CCND2	cyclin D2	0.014	0.306
ANKRD6	ankyrin repeat domain 6	0.014	0.373
PEX12	peroxisomal biogenesis factor 12	0.014	2.582
GLB1L	galactosidase, beta 1-like	0.014	1.941
OSGIN1	oxidative stress induced growth inhibitor 1	0.014	0.573
GPIHBP1	glycosylphosphatidylinositol anchored high density lipoprotein binding protein 1	0.014	0.443
ARPC5L	actin related protein 2/3 complex, subunit 5-like	0.014	2.901
ZBTB24	zinc finger and BTB domain containing 24	0.014	0.954
IKBKB	inhibitor of kappa light polypeptide gene enhancer in B-cells, kinase beta	0.014	0.444
TNFSF14	tumor necrosis factor (ligand) superfamily, member 14	0.014	0.916
SGPP2	sphingosine-1-phosphate phosphotase 2	0.015	0.412
CSF3R	colony stimulating factor 3 receptor (granulocyte)	0.015	1.473
ZNF573	zinc finger protein 573	0.015	0.643
C11orf2	chromosome 11 open reading frame2	0.015	1.005
SERPINA11	serpin peptidase inhibitor, clade A (alpha-1 antiproteinase, antitrypsin), member 11	0.015	0.946
BTBD11	BTB (POZ) domain containing 11	0.015	0.314
SNUPN	snurportin 1	0.015	0.459
LOC284009	hypothetical protein LOC284009	0.015	2.874
SSX4B	synovial sarcoma, X breakpoint 4; synovial sarcoma, X breakpoint 4B	0.015	0.454
GRB2	growth factor receptor-bound protein 2	0.015	0.961
AHNAK	AHNAK nucleoprotein	0.015	0.883
CORO2A	coronin, actin binding protein, 2A	0.015	0.668
CNOT10	CCR4-NOT transcription complex, subunit 10	0.015	0.358
PCGF2	polycomb group ring finger 2	0.015	0.356
MIER3	mesoderm induction early response 1, family member 3	0.015	0.592
FGF1	fibroblast growth factor 1 (acidic)	0.015	0.868
RLN2	relaxin 2	0.015	1.615
FGD2	FYVE, RhoGEF and PH domain containing 2	0.015	0.543
GUCA2B	guanylate cyclase activator 2B (uroguanylin)	0.015	0.339
LOC644538	hypothetical protein LOC644538	0.015	2.498
NTM	neurotrimin	0.015	0.529
SMARCD3	SWI/SNF related, matrix associated, actin dependent regulator of chromatin, subfamily d, member 3	0.015	0.336
SPTLC1	serine palmitoyltransferase, long chain base subunit 1	0.015	1.641
SMN2	survival of motor neuron 1, telomeric; survival of motor neuron 2, centromeric	0.015	0.632
ADRBK1	adrenergic, beta, receptor kinase 1	0.015	0.349
ACOT11	acyl-CoA thioesterase 11	0.015	0.472
ZNRF3	zinc and ring finger 3	0.015	0.829
PHF19	PHD finger protein 19	0.015	0.742
SDR16C5	short chain dehydrogenase/reductase family 16C, member 5	0.015	0.479
C21orf96	chromosome 21 open reading frame 96	0.015	0.429
GCNT2	glucosaminyl (N-acetyl) transferase 2, I-branching enzyme (I blood group)	0.015	0.307
C1QTNF3	C1q and tumor necrosis factor related protein 3; alpha-methylacyl-CoA racemase	0.015	2.367
KIAA1045	KIAA1045	0.016	0.368
C9orf170	chromosome 9 open reading frame 170	0.016	1.368
DVL2	dishevelled, dsh homolog 2 (Drosophila)	0.016	0.538
DCST1	DC-STAMP domain containing 1	0.016	1.742

CADM4	cell adhesion molecule 4	0.016	0.451
SSBP3	single stranded DNA binding protein 3; hypothetical LOC100131851	0.016	2.406
SLC45A3	solute carrier family 45, member 3	0.016	0.640
CBWD3	COBW domain containing 5; similar to COBW domain containing 1; COBW domain containing 7; COBW domain containing 3	0.016	1.019
LOC100287227	hypothetical protein LOC100287227	0.016	0.322
RPGRIP1	retinitis pigmentosa GTPase regulator interacting protein 1	0.016	0.471
CACNA1F	calcium channel, voltage-dependent, L type, alpha 1F subunit	0.016	0.355
C7orf72	Uncharacterized protein LOC340228	0.016	0.345
NR4A3	nuclear receptor subfamily 4, group A, member 3	0.016	0.428
CREB3L2	cAMP responsive element binding protein 3-like 2	0.016	1.284
HESX1	HESX homeobox 1	0.016	1.148
PDZK1	PDZ domain containing 1	0.016	1.413
ZFYVE21	zinc finger, FYVE domain containing 21	0.016	2.223
SH2D4B	SH2 domain containing 4B	0.016	0.374
FST	follistatin	0.016	0.320
FUT8	fucosyltransferase 8 (alpha (1,6) fucosyltransferase)	0.016	0.995
ZNF282	zinc finger protein 282	0.016	0.555
SMPD1	sphingomyelin phosphodiesterase 1, acid lysosomal	0.016	0.850
SERP2	stress-associated endoplasmic reticulum protein family member 2	0.016	0.566
TMEM90A	transmembrane protein 90A	0.016	0.314
C22orf34	chromosome 22 open reading frame 34	0.016	1.117
CCDC11	coiled-coil domain containing 11	0.016	1.066
HOPX	HOP homeobox	0.016	0.465
FABP1	fatty acid binding protein 1, liver	0.016	0.599
SFRP1	secreted frizzled-related protein 1	0.016	0.351
ARHGAP28	Rho GTPase activating protein 28	0.016	0.316
RGPD3	RANBP2-like and GRIP domain containing 5; RANBP2-like and GRIP domain containing 4; RANBP2-like and GRIP domain containing 3; RANBP2-like and GRIP domain containing 8; RANBP2-like and GRIP domain containing 7; RANBP2-like and GRIP domain containing 6	0.016	1.483
TSPAN18	tetraspanin 18	0.016	1.247
GYPC	glycophorin C (Gerbich blood group)	0.016	0.973
SSX3	synovial sarcoma, X breakpoint 3	0.016	0.431
ELOVL7	ELOVL family member 7, elongation of long chain fatty acids (yeast)	0.016	0.760
DAP	death-associated protein	0.016	0.589
HAUS7	three prime repair exonuclease 2; HAUS augmin-like complex, subunit 7	0.016	0.375
MFSD7	major facilitator superfamily domain containing 7	0.016	0.551
ACSL1	acyl-CoA synthetase long-chain family member 1	0.016	0.471
IRF3	interferon regulatory factor 3	0.016	0.446
ZNF442	zinc finger protein 442	0.017	1.429
SOD1	superoxide dismutase 1, soluble	0.017	1.703
GSTA3	glutathione S-transferase alpha 3	0.017	0.556
USP7	ubiquitin specific peptidase 7 (herpes virus-associated)	0.017	1.290
FAM49B	family with sequence similarity 49, member B	0.017	0.533
TMEM128	transmembrane protein 128	0.017	0.750
TRPM8	transient receptor potential cation channel, subfamily M, member 8	0.017	1.780
TRIP13	thyroid hormone receptor interactor 13	0.017	0.372
LOC407835	mitogen-activated protein kinase kinase 2 pseudogene; mitogen-activated protein kinase kinase 2	0.017	0.869
TRPV3	transient receptor potential cation channel, subfamily V, member 3	0.017	0.410

SPEF1	sperm flagellar 1	0.017	1.244
EIF4E3	eukaryotic translation initiation factor 4E family member 3	0.017	0.437
RNF145	ring finger protein 145	0.018	0.303
MLXIP	MLX interacting protein	0.018	0.319
PMS2	PMS2 postmeiotic segregation increased 2 (S. cerevisiae)	0.018	0.421
DTX2	deltex homolog 2 (Drosophila)	0.018	1.451
B4GALT4	UDP-Gal:betaGlcNAc beta 1,4- galactosyltransferase, polypeptide 4	0.018	1.194
GALNTL2	UDP-N-acetyl-alpha-D-galactosamine:polypeptide N-acetylgalactosaminyltransferase-like 2	0.018	0.395
ABCC5	ATP-binding cassette, sub-family C (CFTR/MRP), member 5	0.018	0.745
ALDH3A1	aldehyde dehydrogenase 3 family, memberA1	0.018	1.069
MGMT	O-6-methylguanine-DNA methyltransferase	0.018	0.559
NAT12	N-acetyltransferase 12	0.018	1.101
GDF5	growth differentiation factor 5	0.018	0.462
NXF5	nuclear RNA export factor 5	0.018	0.655
PAQR5	progestin and adipoQ receptor family member V	0.018	0.317
C10orf47	chromosome 10 open reading frame 47	0.019	0.574
OR5J2	olfactory receptor, family 5, subfamily J, member 2	0.019	0.363
SELL	selectin L	0.019	0.602
STAB2	stabilin 2	0.019	0.311
LRRC49	leucine rich repeat containing 49; similar to leucine rich repeat containing 49	0.019	0.565
SLC7A6OS	solute carrier family 7, member 6 opposite strand	0.019	0.658
RNF207	ring finger protein 207	0.019	2.098
GTDC1	glycosyltransferase-like domain containing 1	0.019	0.307
RAB8B	RAB8B, member RAS oncogene family	0.019	1.694
TTC25	tetratricopeptide repeat domain 25	0.019	0.329
TMPRSS4	transmembrane protease, serine 4	0.019	0.908
ZNF70	zinc finger protein 70	0.019	0.327
TUBA4B	tubulin, alpha 4b (pseudogene)	0.019	1.019
CC2D2B	coiled-coil and C2 domain containing 2B	0.019	0.320
ZFP41	zinc finger protein 41 homolog (mouse)	0.019	1.064
TCP10L	t-complex 10 (mouse)-like	0.019	0.525
C8orf55	chromosome 8 open reading frame 55	0.019	0.485
BDKRB2	bradykinin receptor B2	0.019	1.315
ALKBH4	alkB, alkylation repair homolog 4 (E. coli)	0.019	0.663
SHC3	SHC (Src homology 2 domain containing) transforming protein 3	0.019	0.334
C10orf105	chromosome 10 open reading frame 105	0.019	0.422
TIAM2	T-cell lymphoma invasion and metastasis 2	0.019	0.375
TRO	trophinin	0.019	0.323
MPZL1	myelin protein zero-like 1	0.019	0.360
THOC6	THO complex 6 homolog (Drosophila)	0.020	0.327
ABCA3	ATP-binding cassette, sub-family A (ABC1), member 3	0.020	0.532
FAM38A	family with sequence similarity 38, member A	0.020	0.301
ZNF83	zinc finger protein 83	0.020	0.615
TES	testis derived transcript (3 LIM domains)	0.020	0.887
KCTD16	potassium channel tetramerisation domain containing 16	0.020	0.392
IL16	interleukin 16 (lymphocyte chemoattractant factor)	0.020	0.405
SLFN13	schlafen family member 13	0.020	2.189
P2RX1	purinergic receptor P2X, ligand-gated ion channel, 1	0.020	0.780
BID	BH3 interacting domain death agonist	0.020	0.343

TFAM	transcription factor A, mitochondrial	0.020	0.721
LOC84931	hypothetical LOC84931	0.020	0.464
RNASEH2C	ribonuclease H2, subunit C	0.020	0.422
NDUFS8	NADH dehydrogenase (ubiquinone) Fe-S protein 8, 23kDa (NADH-coenzyme Q reductase)	0.020	0.591
DOCK10	dedicator of cytokinesis 10	0.020	0.352
USP13	ubiquitin specific peptidase 13 (isopeptidase T-3)	0.020	0.452
NOVA1	neuro-oncological ventral antigen 1	0.020	0.436
HCFC1	host cell factor C1 (VP16-accessory protein)	0.020	0.387
MARK2	MAP/microtubule affinity-regulating kinase 2	0.020	1.161
TMEM39A	transmembrane protein 39A	0.020	0.338
FGL1	fibrinogen-like 1	0.020	0.735
SDHAP1	succinate dehydrogenase complex, subunit A, flavoprotein pseudogene 1	0.020	0.981
DDX31	DEAD (Asp-Glu-Ala-Asp) box polypeptide 31	0.020	0.426
RG9MTD1	RNA (guanine-9-) methyltransferase domain containing 1	0.020	1.307
FNTB	farnesyltransferase, CAAX box, beta	0.020	1.489
VWA3A	von Willebrand factor A domain containing 3A	0.020	0.826
SSH1	slingshot homolog 1 (Drosophila)	0.020	0.536
KLHL29	kelch-like 29 (Drosophila)	0.020	0.536
ACVR1B	activin A receptor, type IB	0.020	0.981
ADO	2-aminoethanethiol (cysteamine) dioxygenase	0.020	0.444
HEMGN	hemogen	0.020	0.416
FOLH1	folate hydrolase (prostate-specific membrane antigen) 1	0.020	2.130
NCAPG2	non-SMC condensin II complex, subunit G2	0.020	1.237
SAMSN1	SAM domain, SH3 domain and nuclear localization signals 1	0.020	0.694
C9orf116	chromosome 9 open reading frame 116	0.020	0.328
TRIM4	tripartite motif-containing 4	0.021	1.234
DEFB104A	defensin, beta 104A; defensin, beta 104B	0.021	0.351
LOC400891	chromosome 14 open reading frame 166B pseudogene	0.021	1.424
ITGB5	integrin, beta 5	0.021	0.444
PGBD5	piggyBac transposable element derived 5	0.021	1.399
DHX33	DEAH (Asp-Glu-Ala-His) box polypeptide 33	0.021	0.584
C20orf95	chromosome 20 open reading frame 95	0.021	0.356
GUCA1A	guanylate cyclase activator 1A (retina)	0.021	0.574
SNED1	sushi, nidogen and EGF-like domains 1	0.021	0.550
CAMKK1	calcium/calmodulin-dependent protein kinase kinase 1, alpha	0.021	0.444
MIR1973	microRNA 1973	0.021	0.660
CSNK2B	lymphocyte antigen 6 complex, locus G5B; casein kinase 2, beta polypeptide	0.021	0.478
JAM3	junctional adhesion molecule 3	0.021	0.333
ETV3	ets variant 3	0.021	0.323
CD1A	CD1a molecule	0.021	1.037
SPAG4L	sperm associated antigen 4-like	0.021	0.521
DHX16	DEAH (Asp-Glu-Ala-His) box polypeptide 16	0.021	0.488
TSSK2	testis-specific serine kinase 2	0.021	0.313
RGSL1	regulator of G-protein signaling like 1	0.021	0.805
LYZL6	lysozyme-like 6	0.021	0.633
GPR88	G protein-coupled receptor 88	0.021	0.504
ACPT	acid phosphatase, testicular	0.021	0.528
DEFA5	defensin, alpha 5, Paneth cell-specific	0.021	1.726
SMC3	structural maintenance of chromosomes 3	0.021	0.701

GFI1B	growth factor independent 1B transcription repressor	0.021	0.750
ACSL4	acyl-CoA synthetase long-chain family member 4	0.021	0.391
EML2	echinoderm microtubule associated protein like 2	0.021	0.355
MDGA1	MAM domain containing glycosylphosphatidylinositol anchor 1	0.021	0.518
MRGPRE	MAS-related GPR, member E	0.021	0.377
PAQR5	progestin and adipoQ receptor family member V	0.021	0.433
SCRN2	secernin 2	0.021	0.476
FOXD1	forkhead box D1	0.021	0.369
GPR25	G protein-coupled receptor 25	0.021	0.363
ZMYND8	zinc finger, MYND-type containing 8	0.021	0.982
FAM155B	family with sequence similarity 155, member B	0.021	0.489
CYP26A1	cytochrome P450, family 26, subfamily A, polypeptide 1	0.021	0.352
C16orf74	chromosome 16 open reading frame 74	0.021	0.989
PSMC2	proteasome (prosome, macropain) 26S subunit, ATPase, 2	0.021	0.673
B4GALT2	UDP-Gal:betaGlcNAc beta 1,4- galactosyltransferase, polypeptide 2	0.021	0.499
SLC39A11	solute carrier family 39 (metal ion transporter), member 11	0.021	0.470
TOB2	transducer of ERBB2, 2	0.021	0.599
BPIL3	bactericidal/permeability-increasing protein-like 3	0.021	0.948
TMEM205	transmembrane protein 205	0.021	1.278
FOXJ2	forkhead box J2	0.021	0.347
GPD1L	glycerol-3-phosphate dehydrogenase 1-like	0.021	1.318
STARD8	StAR-related lipid transfer (START) domain containing 8	0.021	0.353
GAR1	GAR1 ribonucleoprotein homolog (yeast)	0.022	0.855
C1orf210	chromosome 1 open reading frame 210	0.022	0.370
ZNF738	zinc finger protein 738	0.022	1.790
C1orf27	chromosome 1 open reading frame 27	0.022	0.345
LOC151009	hypothetical LOC151009	0.023	0.306
MKNK1	MAP kinase interacting serine/threonine kinase 1	0.023	0.735
KIAA1109	KIAA1109	0.023	0.350
DIRAS3	DIRAS family, GTP-binding RAS-like 3	0.023	0.307
LAIR2	leukocyte-associated immunoglobulin-like receptor 2	0.023	1.478
TDRD7	tudor domain containing 7	0.023	0.364
PIK3C2G	phosphoinositide-3-kinase, class 2, gamma polypeptide	0.023	0.401
ESPL1	extra spindle pole bodies homolog 1 (S. cerevisiae)	0.023	0.360
XRCC3	X-ray repair complementing defective repair in Chinese hamster cells 3	0.023	1.078
SLC20A2	solute carrier family 20 (phosphate transporter), member 2	0.023	1.400
ASB1	ankyrin repeat and SOCS box-containing 1	0.023	0.394
SPSB1	splA/ryanodine receptor domain and SOCS box containing 1	0.023	0.699
FBXO11	F-box protein 11	0.023	1.464
STAMBPL1	STAM binding protein-like 1	0.023	0.967
MIR639	microRNA 639	0.024	1.197
DCHS1	dachsous 1 (Drosophila)	0.024	0.689
DSEL	dermatan sulfate epimerase-like	0.024	0.535
FAM3D	family with sequence similarity 3, member D	0.024	0.426
INHBC	inhibin, beta C	0.024	0.349
RHOG	ras homolog gene family, member G (rho G)	0.024	0.328
PYDC1	PYD (pyrin domain) containing 1	0.024	0.697
RPS27L	ribosomal protein S27-like	0.024	0.625
GLIPR2	GLI pathogenesis-related 2	0.024	0.507
NFATC2	nuclear factor of activated T-cells, cytoplasmic, calcineurin-dependent 2	0.024	0.350

CD44	CD44 molecule (Indian blood group)	0.024	0.404
ST3GAL6	ST3 beta-galactoside alpha-2,3-sialyltransferase 6	0.024	0.555
PPAP2B	phosphatidic acid phosphatase type 2B	0.024	0.349
PCSK6	proprotein convertase subtilisin/kexin type 6	0.024	0.636
LHCGR	luteinizing hormone/choriogonadotropin receptor	0.024	0.336
SLC5A6	solute carrier family 5 (sodium-dependent vitamin transporter), member 6	0.024	0.387
MTMR11	myotubularin related protein 11	0.025	0.371
KDM6B	lysine (K)-specific demethylase 6B	0.025	0.736
TMEM104	transmembrane protein 104	0.025	0.489
ARHGEF18	Rho/Rac guanine nucleotide exchange factor (GEF) 18	0.025	0.639
MAP2K3	mitogen-activated protein kinase kinase 3	0.025	0.466
MAP3K3	mitogen-activated protein kinase kinase kinase 3	0.025	0.553
NT5E	5'-nucleotidase, ecto (CD73)	0.025	0.376
CACNA1D	calcium channel, voltage-dependent, L type, alpha 1D subunit	0.025	0.495
XKR7	XK, Kell blood group complex subunit-related family, member 7	0.025	0.330
ASB16	ankyrin repeat and SOCS box-containing 16	0.025	1.109
MRPL42	mitochondrial ribosomal protein L42	0.025	0.995
DEFB123	defensin, beta 123	0.025	0.452
RAI2	retinoic acid induced 2	0.025	0.607
DAOA	D-amino acid oxidase activator	0.025	0.566
GPR4	G protein-coupled receptor 4	0.025	0.530
ERC2	ELKS/RAB6-interacting/CAST family member 2	0.025	0.514
MEIS2	Meis homeobox 2	0.025	0.327
DNAH9	dynein, axonemal, heavy chain 9	0.025	0.461
NDUFV2	NADH dehydrogenase (ubiquinone) flavoprotein 2, 24kDa	0.025	0.709
KERA	keratocan	0.025	0.440
RPS21	ribosomal protein S21	0.025	0.314
FAM115A	family with sequence similarity 115, member A; family with sequence similarity 115, member B (pseudogene)	0.025	0.547
ANKRD30A	ankyrin repeat domain 30A	0.025	0.661
DOCK6	dedicator of cytokinesis 6	0.025	0.415
PTHLH	parathyroid hormone-like hormone	0.025	0.356
UTP6	UTP6, small subunit (SSU) processome component, homolog (yeast)	0.025	0.396
PLEKHB1	pleckstrin homology domain containing, family B (evectins) member 1	0.025	0.349
DUSP23	dual specificity phosphatase 23	0.026	0.369
PAMR1	peptidase domain containing associated with muscle regeneration 1	0.026	0.849
KDR	kinase insert domain receptor (a type III receptor tyrosine kinase)	0.026	0.355
CRISP3	cysteine-rich secretory protein 3	0.026	0.536
ABTB1	ankyrin repeat and BTB (POZ) domain containing 1	0.026	0.375
GP1BA	glycoprotein Ib (platelet), alpha polypeptide	0.026	0.385
TTLL13	tubulin tyrosine ligase-like family, member 13	0.026	0.693
RIMS2	regulating synaptic membrane exocytosis 2	0.026	0.420
ITGAE	integrin, alpha E (antigen CD103, human mucosal lymphocyte antigen 1; alpha polypeptide)	0.026	1.156
MCRS1	microspherule protein 1	0.026	0.389
CDYL2	chromodomain protein, Y-like 2	0.026	0.385
LASS1	growth differentiation factor 1; LAG1 homolog, ceramide synthase 1	0.026	0.457
PMS2CL	PMS2 C-terminal like pseudogene	0.026	0.373
E2F2	E2F transcription factor 2	0.026	2.100
P4HB	prolyl 4-hydroxylase, beta polypeptide	0.026	1.735
C1orf43	chromosome 1 open reading frame 43	0.026	0.308

MATN3	matrilin 3	0.026	0.657
MALAT1	metastasis associated lung adenocarcinoma transcript 1 (non-protein coding)	0.026	2.354
RPAP3	RNA polymerase II associated protein 3	0.026	0.392
NEK6	NIMA (never in mitosis gene a)-related kinase 6	0.026	2.394
SIP1	survival of motor neuron protein interacting protein 1	0.026	0.671
SLCO2B1	solute carrier organic anion transporter family, member 2B1	0.026	0.440
DGCR6L	DiGeorge syndrome critical region gene 6-like	0.026	1.029
SDCBP2	syndecan binding protein (syntenin) 2	0.026	0.745
PRPS1	phosphoribosyl pyrophosphate synthetase 1; phosphoribosyl pyrophosphate synthetase 1-like 1	0.026	0.950
SPDEF	SAM pointed domain containing ets transcription factor	0.026	0.388
SEC1	secretory blood group 1	0.026	0.369
IL17RE	interleukin 17 receptor E	0.026	0.394
POLR2C	polymerase (RNA) II (DNA directed) polypeptide C, 33kDa	0.027	0.929
MLN	motilin	0.027	0.384
CCDC36	coiled-coil domain containing 36	0.027	0.755
GSTM2	glutathione S-transferase mu 2 (muscle)	0.027	0.438
MYO18B	myosin XVIIIB	0.027	0.448
SLAMF6	SLAM family member 6	0.027	0.441
MEI1	meiosis inhibitor 1	0.027	1.181
RNF115	ring finger protein 115	0.027	0.828
FUCA2	fucosidase, alpha-L- 2, plasma	0.027	2.107
C7orf68	chromosome 7 open reading frame 68	0.027	1.460
SART1	squamous cell carcinoma antigen recognized by T cells	0.027	0.634
GOLGA6A	golgi autoantigen, golgin subfamily a, 6C; golgi autoantigen, golgin subfamily a, 6 pseudogene; golgi autoantigen, golgin subfamily a, 6D; golgi autoantigen, golgin subfamily a, 6	0.027	0.590
TRPC4AP	transient receptor potential cation channel, subfamily C, member 4 associated protein	0.027	0.427
NTSR1	neurotensin receptor 1 (high affinity)	0.027	0.400
RABL2A	RAB, member of RAS oncogene family-like 2A	0.027	0.331
C3orf26	chromosome 3 open reading frame 26	0.027	1.114
RASGRP3	RAS guanyl releasing protein 3 (calcium and DAG-regulated)	0.027	2.827
KDM2A	lysine (K)-specific demethylase 2A	0.027	0.442
FAM27C	family with sequence similarity 27, member C; family with sequence similarity 27, member A; family with sequence similarity 27, member B	0.027	1.774
CLEC2L	C-type lectin domain family 2, member L	0.027	0.849
LOC728323	hypothetical LOC728323	0.027	1.715
ZNF354A	zinc finger protein 354A	0.027	0.435
BAHCC1	BAH domain and coiled-coil containing 1	0.027	0.337
OR10H2	olfactory receptor, family 10, subfamily H, member 2	0.027	2.050
DPEP1	dipeptidase 1 (renal)	0.027	0.438
SLC25A37	solute carrier family 25, member 37	0.027	1.131
C4orf41	chromosome 4 open reading frame 41	0.027	0.631
SLPI	secretory leukocyte peptidase inhibitor	0.027	0.523
GPHB5	glycoprotein hormone beta 5	0.027	0.308
KIAA0087	KIAA0087	0.028	0.706
ARAP2	ArfGAP with RhoGAP domain, ankyrin repeat and PH domain 2	0.028	0.489
STRADB	STE20-related kinase adaptor beta	0.028	0.383
MCHR2	melanin-concentrating hormone receptor 2	0.028	1.355
NDOR1	NADPH dependent diflavin oxidoreductase 1	0.028	0.302

PDK4	pyruvate dehydrogenase kinase, isozyme 4	0.028	0.441
CLDN2	claudin 2	0.028	0.310
BBS9	Bardet-Biedl syndrome 9	0.028	0.493
ARL14	ADP-ribosylation factor-like 14	0.028	0.312
C14orf1	chromosome 14 open reading frame 1	0.028	0.553
CAMP	cathelicidin antimicrobial peptide	0.028	0.328
FUT6	fucosyltransferase 6 (alpha (1,3) fucosyltransferase)	0.028	0.494
OR5M9	olfactory receptor, family 5, subfamily M, member 9	0.028	0.350
TBCCD1	TBCC domain containing 1	0.028	1.330
ASGR1	asialoglycoprotein receptor 1	0.028	0.432
LIMS1	LIM and senescent cell antigen-like domains 1	0.028	0.498
CNTN3	contactin 3 (plasmacytoma associated)	0.028	0.635
SLC39A4	solute carrier family 39 (zinc transporter), member 4	0.028	0.313
SSTR2	somatostatin receptor 2	0.028	2.278
NEIL3	nei endonuclease VIII-like 3 (E. coli)	0.028	0.334
RHOXF1	Rhox homeobox family, member 1	0.028	0.330
RPS26P11	ribosomal protein S26 pseudogene 11	0.028	0.563
DOCK7	dedicator of cytokinesis 7	0.028	1.529
ACTR10	actin-related protein 10 homolog (S. cerevisiae)	0.028	0.523
DCHS1	dachsous 1 (Drosophila)	0.028	0.782
EDN2	endothelin 2	0.028	0.447
FOXF2	forkhead box F2	0.028	0.443
CCDC88B	coiled-coil domain containing 88B	0.028	0.404
LOC728927	unknown	0.028	0.560
SGPL1	sphingosine-1-phosphate lyase 1	0.028	0.334
FBXL5	F-box and leucine-rich repeat protein 5	0.028	0.300
PPEF1	protein phosphatase, EF-hand calcium binding domain 1	0.028	0.484
C6orf10	chromosome 6 open reading frame 10	0.028	0.458
TUB	tubby homolog (mouse)	0.028	0.304
RGS22	regulator of G-protein signaling 22	0.028	0.381
IL1A	interleukin 1, alpha	0.028	0.338
FOXH1	forkhead box H1	0.028	0.331
SNX25	sorting nexin 25	0.028	0.795
MAP3K2	mitogen-activated protein kinase kinase kinase 2	0.028	0.900
XKR7	XK, Kell blood group complex subunit-related family, member 7	0.028	0.669
MC2R	melanocortin 2 receptor (adrenocorticotropic hormone)	0.028	0.407
AANAT	arylalkylamine N-acetyltransferase	0.028	0.575
PRDXDD1P	non-protein coding RNA 117	0.028	0.372
MYO9B	myosin IXB	0.028	0.677
PTP4A2	protein tyrosine phosphatase type IVA, member 2	0.028	0.418
FLJ10213	hypothetical protein FLJ10213	0.028	0.375
C8orf34	chromosome 8 open reading frame 34	0.028	0.307
INTS1	integrator complex subunit 1	0.028	0.418
MRO	maestro	0.028	0.367
EMR4P	egf-like module containing, mucin-like, hormone receptor-like 4 pseudogene	0.028	0.930
UROS	uroporphyrinogen III synthase	0.028	1.229
GCNT4	glucosaminyl (N-acetyl) transferase 4, core 2 (beta-1,6-N-acetylglucosaminyltransferase)	0.028	0.618
NEGR1	neuronal growth regulator 1	0.028	0.529
MTSS1	metastasis suppressor 1	0.028	0.462

NUDT14	nudix (nucleoside diphosphate linked moiety X)-type motif 14	0.028	1.121
FCN1	ficolin (collagen/fibrinogen domain containing) 1	0.028	0.334
ST3GAL1	ST3 beta-galactoside alpha-2,3-sialyltransferase 1	0.028	0.563
ANKH	ankylosis, progressive homolog (mouse)	0.028	0.628
ZNF180	zinc finger protein 180	0.028	0.582
DHX29	DEAH (Asp-Glu-Ala-His) box polypeptide 29	0.028	0.811
RNF20	ring finger protein 20	0.029	1.417
CLCA1	chloride channel accessory 1	0.029	1.641
ZNF599	zinc finger protein 599	0.029	0.568
AKTIP	AKT interacting protein; similar to AKT interacting protein	0.029	0.319
CS	citrate synthase	0.029	3.285
CYP19A1	cytochrome P450, family 19, subfamily A, polypeptide 1	0.029	0.575
TMEM84	transmembrane protein 84	0.029	0.341
CMIP	c-Maf-inducing protein	0.029	2.542
PTPN3	protein tyrosine phosphatase, non-receptor type 3	0.029	0.374
IL1R2	interleukin 1 receptor, type II	0.029	0.342
DEFB129	defensin, beta 129	0.029	0.745
ACTN1	actinin, alpha 1	0.029	0.327
C16orf57	chromosome 16 open reading frame 57	0.029	0.579
RHOBTB1	Rho-related BTB domain containing 1	0.029	0.356
NCF1	neutrophil cytosolic factor 1; neutrophil cytosolic factor 1C pseudogene	0.029	0.334
HIGD2A	HIG1 hypoxia inducible domain family, member 2A	0.029	1.157
CDC42BPB	CDC42 binding protein kinase beta (DMPK-like)	0.029	0.906
NCOR2	nuclear receptor co-repressor 2	0.029	0.354
AKD1	adenylate kinase domain containing 1	0.029	0.307
TPK1	thiamin pyrophosphokinase 1	0.029	0.436
LOC220729	succinate dehydrogenase complex, subunit A, flavoprotein pseudogene	0.029	1.233
PIAS2	protein inhibitor of activated STAT, 2	0.029	0.746
ZNF397	zinc finger protein 397	0.029	0.322
FER1L6	fer-1-like 6 (C. elegans)	0.029	0.399
EIF2C2	eukaryotic translation initiation factor 2C, 2	0.030	1.691
SELENBP1	selenium binding protein 1	0.030	0.537
ANXA7	annexin A7	0.030	1.030
NDN	necdin homolog (mouse)	0.030	0.357
REP15	RAB15 effector protein	0.030	0.579
OTOL1	Otolin-1	0.030	1.051
DLG5	discs, large homolog 5 (Drosophila)	0.030	0.449
NRBF2	nuclear receptor binding factor 2	0.030	0.303
CNTN4	contactin 4	0.030	0.419
ZNF727	zinc finger protein 727	0.030	0.823
ATF1	activating transcription factor 1	0.030	0.538
ARPC4	tubulin tyrosine ligase-like family, member 3; actin related protein 2/3 complex, subunit 4, 20kDa	0.030	0.647
C1QA	complement component 1, q subcomponent, A chain	0.030	1.713
NCOA7	nuclear receptor coactivator 7	0.030	0.388
ITGAD	integrin, alpha D	0.030	0.532
ANK2	ankyrin 2, neuronal	0.030	0.627
GFRA2	similar to GDNF family receptor alpha 2; GDNF family receptor alpha 2	0.030	0.533
CCDC79	coiled-coil domain containing 79	0.030	0.413
LOC100128191	hypothetical protein LOC100128191	0.030	3.240

TUBA8	tubulin, alpha 8	0.030	0.869
C16orf57	chromosome 16 open reading frame 57	0.030	0.591
SPIN2A	spindlin family, member 2A	0.031	0.418
MYOZ2	myozenin 2	0.031	0.389
POLR2B	polymerase (RNA) II (DNA directed) polypeptide B, 140kDa	0.031	2.122
TFE3	transcription factor binding to IGHM enhancer 3	0.031	0.739
ZNF165	zinc finger protein 165	0.031	1.033
SDC4	syndecan 4	0.031	0.470
TBC1D22A	TBC1 domain family, member 22A	0.031	0.719
FREM2	FRAS1 related extracellular matrix protein 2	0.031	0.314
ADH5	alcohol dehydrogenase 5 (class III), chi polypeptide, pseudogene 4; alcohol dehydrogenase 5 (class III), chi polypeptide	0.032	0.328
KLHL23	kelch-like 23 (Drosophila)	0.032	0.358
RAB20	RAB20, member RAS oncogene family	0.032	1.826
ARHGEF10L	Rho guanine nucleotide exchange factor (GEF) 10-like	0.032	0.788
ZNF558	zinc finger protein 558	0.032	0.412
TCEB3B	transcription elongation factor B polypeptide 3B (elongin A2)	0.032	0.349
ZNF704	zinc finger protein 704	0.032	0.685
GUCY2G	guanylate cyclase 2G	0.032	0.514
LPCAT3	lysophosphatidylcholine acyltransferase 3	0.032	0.539
C5orf36	chromosome 5 open reading frame 36	0.032	0.440
POLR3K	polymerase (RNA) III (DNA directed) polypeptide K, 12.3 kDa	0.032	0.425
CIRH1A	cirrhosis, autosomal recessive 1A (cirhin)	0.032	0.381
CHRNG	cholinergic receptor, nicotinic, gamma	0.032	1.716
C9orf71	chromosome 9 open reading frame 71	0.032	0.431
ZNF629	zinc finger protein 629	0.033	0.458
FRMPD2	FERM and PDZ domain containing 2; FERM and PDZ domain containing 2 like 2; FERM and PDZ domain containing 2 like 1	0.033	0.329
SERPING1	serpin peptidase inhibitor, clade G (C1 inhibitor), member 1	0.033	0.896
PYY2	peptide YY, 2 (seminalplasmin)	0.033	3.409
RCN1	reticulocalbin 1, EF-hand calcium binding domain	0.033	0.344
PHF8	PHD finger protein 8	0.033	1.552
KLC2	kinesin light chain 2	0.033	0.473
PECAM1	platelet/endothelial cell adhesion molecule	0.033	1.377
PSMD7	proteasome (prosome, macropain) 26S subunit, non-ATPase, 7	0.033	1.613
HOXB1	homeobox B1	0.033	1.144
NUP107	nucleoporin 107kDa	0.033	0.509
LRRK1	leucine-rich repeat kinase 1	0.033	2.126
CDR2	cerebellar degeneration-related protein 2, 62kDa	0.033	1.059
MAPK7	mitogen-activated protein kinase 7	0.033	0.777
CXCL3	chemokine (C-X-C motif) ligand 3	0.033	0.443
NTNG1	netrin G1	0.033	0.528
ADORA3	adenosine A3 receptor	0.033	0.552
SNAPC1	small nuclear RNA activating complex, polypeptide 1, 43kDa	0.033	0.684
KRTAP5-11	keratin associated protein 5-11	0.033	0.448
ADAMTS13	ADAM metallopeptidase with thrombospondin type 1 motif, 13	0.033	0.316
TMEM141	KIAA1984; transmembrane protein 141	0.033	0.311
HMGN4	high mobility group nucleosomal binding domain 4	0.033	0.481
OVOL1	ovo-like 1(Drosophila)	0.033	0.308
SH2B1	SH2B adaptor protein 1	0.034	0.426
EEA1	early endosome antigen 1	0.034	1.789

KANK3	KN motif and ankyrin repeat domains 3	0.034	0.430
MAP3K7	mitogen-activated protein kinase kinase kinase 7	0.034	0.876
RAB36	RAB36, member RAS oncogene family	0.034	0.901
ISCA1L	unknown	0.034	0.576
FBXO38	F-box protein 38	0.034	0.308
STX6	syntaxin 6	0.034	0.937
NTNG2	netrin G2	0.034	0.666
DSEL	dermatan sulfate epimerase-like	0.034	0.561
FOXA2	forkhead box A2	0.034	0.503
BLOC1S2	biogenesis of lysosomal organelles complex-1, subunit 2	0.034	0.451
SIAH1	seven in absentia homolog 1 (Drosophila)	0.034	0.337
EXOC6B	exocyst complex component 6B	0.034	1.186
OR51E1	olfactory receptor, family 51, subfamily E, member 1	0.034	0.430
IRF8	interferon regulatory factor 8	0.034	0.385
UBE2G1	ubiquitin-conjugating enzyme E2G 1 (UBC7 homolog, yeast)	0.034	1.869
LOC256880	hypothetical LOC256880	0.034	0.391
C12orf5	chromosome 12 open reading frame 5	0.034	1.369
RPS17	ribosomal protein S17	0.034	0.318
DIABLO	diablo homolog (Drosophila)	0.034	0.462
RND1	Rho family GTPase 1	0.034	0.471
MAOB	monoamine oxidase B	0.034	0.305
TM4SF20	transmembrane 4 L six family member 20	0.035	1.365
TNS1	tensin 1	0.035	0.354
FAM178A	family with sequence similarity 178, member A	0.035	0.332
MAB21L2	mab-21-like 2 (C. elegans)	0.035	0.305
PLEKHA7	pleckstrin homology domain containing, family A member 7	0.035	0.623
HTR5A	5-hydroxytryptamine (serotonin) receptor 5A	0.035	0.316
XAF1	XIAP associated factor 1	0.035	0.502
CITED4	Cbp/p300-interacting transactivator, with Glu/Asp-rich carboxy-terminal domain, 4	0.035	0.496
APOA4	apolipoprotein A-IV	0.035	0.380
TLR3	toll-like receptor 3	0.035	0.896
SCP2	sterol carrier protein 2	0.035	0.641
FAM107B	family with sequence similarity 107, member B	0.035	0.500
EPHB1	EPH receptor B1	0.035	0.358
C1QL2	complement component 1, q subcomponent-like 2	0.035	0.317
ARFRP1	ADP-ribosylation factor related protein 1	0.035	0.334
CCL4L1	chemokine (C-C motif) ligand 4-like 1; chemokine (C-C motif) ligand 4-like 2	0.035	0.711
PCDHB19P	protocadherin beta 19 pseudogene	0.035	0.593
ZNF267	zinc finger protein 267	0.035	0.485
LOC100129716	hypothetical LOC100129716	0.035	0.417
LIMD1	LIM domains containing 1	0.035	0.314
FBXO30	F-box protein 30	0.035	0.319
THRB	thyroid hormone receptor, beta (erythroblastic leukemia viral (v-erb-a) oncogene homolog 2, avian)	0.035	0.328
C6orf195	chromosome 6 open reading frame 195	0.035	0.405
PARD6B	par-6 partitioning defective 6 homolog beta (C. elegans)	0.035	0.735
LBR	lamin B receptor	0.035	0.374
CCNY	cyclin Y	0.035	0.414
PRELID2	PRELI domain containing 2	0.035	0.781
CLCN4	chloride channel 4	0.035	0.962

FAM84B	family with sequence similarity 84, member B	0.035	0.564
OR4E2	olfactory receptor, family 4, subfamily E, member 2	0.035	1.801
CD8B	CD8b molecule	0.035	1.209
FRMD4B	FERM domain containing 4B	0.035	0.533
ADAMTS12	ADAM metallopeptidase with thrombospondin type 1 motif, 12	0.035	0.382
OSBPL5	oxysterol binding protein-like 5	0.035	0.382
C9orf130	chromosome 9 open reading frame 130	0.035	0.661
MTM1	myotubularin 1	0.035	1.215
PDRG1	p53 and DNA-damage regulated 1	0.035	0.843
ATRN	attractin	0.035	0.517
CYP2B6	cytochrome P450, family 2, subfamily B, polypeptide 6	0.035	0.865
SLC19A3	solute carrier family 19, member 3	0.035	0.579
LOC100134368	similar to hCG1644121	0.035	0.569
LOC144438	hypothetical LOC144438	0.035	0.857
RAB6A	RAB6C, member RAS oncogene family; RAB6A, member RAS oncogene family; hypothetical LOC100130819; RAB6C-like	0.035	0.484
LGMN	legumain	0.036	0.367
MYO1C	myosin IC	0.036	0.443
KIF26B	kinesin family member 26B	0.036	2.617
FER1L6	fer-1-like 6 (C. elegans)	0.036	0.598
BMP3	bone morphogenetic protein 3	0.036	0.881
SAMD7	sterile alpha motif domain containing 7	0.036	0.418
NINJ1	ninjurin 1	0.036	0.301
LOC651250	hypothetical LOC651250	0.036	1.243
NLGN1	neuroligin 1	0.036	1.708
DPEP1	dipeptidase 1 (renal)	0.036	0.781
SLC5A9	solute carrier family 5 (sodium/glucose cotransporter), member 9	0.036	0.378
RBM47	RNA binding motif protein 47	0.036	0.709
MC4R	melanocortin 4 receptor	0.036	0.560
OR7E5P	olfactory receptor, family 7, subfamily E, member 5 pseudogene	0.036	0.450
NBEAL2	neurobeachin-like 2	0.036	0.304
TCF3	transcription factor 3 (E2A immunoglobulin enhancer binding factors E12/E47)	0.036	0.789
CTRC	chymotrypsin C (caldecrin)	0.036	0.678
FLJ35776	hypothetical LOC649446	0.036	0.386
OPN1SW	opsin 1 (cone pigments), short-wave-sensitive	0.036	0.557
COX10	COX10 homolog, cytochrome c oxidase assembly protein, heme A: farnesyltransferase (yeast)	0.036	0.406
SEPT8	septin 8	0.036	0.746
LOC440040	glutamate receptor, metabotropic 5 pseudogene	0.036	0.530
PNPLA8	patatin-like phospholipase domain containing 8	0.036	0.900
AAA1	CHLREDRAFT_195230	0.036	0.305
SMAD1	SMAD family member 1	0.036	0.679
TAGAP	T-cell activation RhoGTPase activating protein	0.036	0.503
ARMCX5	armadillo repeat containing, X-linked 5	0.036	0.348
RGN	regucalcin (senescence marker protein-30)	0.036	1.494
MARK4	MAP/microtubule affinity-regulating kinase 4	0.036	1.672
ASS1	argininosuccinate synthetase 1	0.036	0.334
FLJ31306	hypothetical LOC379025	0.036	0.406
SIRPA	signal-regulatory protein alpha	0.036	0.663
GPSM2	G-protein signaling modulator 2 (AGS3-like, C. elegans)	0.036	0.426
NFAT5	nuclear factor of activated T-cells 5, tonicity-responsive	0.036	0.405

LTF	lactotransferrin	0.036	0.311
GJC2	gap junction protein, gamma 2, 47kDa	0.036	0.727
PLK1	polo-like kinase 1 (Drosophila)	0.036	0.640
KIAA0513	KIAA0513	0.036	0.712
WWC1	WW and C2 domain containing 1	0.037	0.516
PHF3	PHD finger protein 3	0.037	2.328
DPT	dermatopontin	0.037	0.852
CUBN	cubilin (intrinsic factor-cobalamin receptor)	0.037	0.574
PVRL3	poliovirus receptor-related 3	0.037	0.464
CNTN4	contactin 4	0.037	0.437
ZBTB3	zinc finger and BTB domain containing 3	0.037	0.347
CRHR2	corticotropin releasing hormone receptor 2	0.037	0.331
MIA	melanoma inhibitory activity	0.037	0.349
CLDN7	claudin 7	0.037	1.458
TXNL4B	thioredoxin-like 4B	0.037	0.400
PCGF2	polycomb group ring finger 2	0.037	0.400
MMP28	matrix metallopeptidase 28	0.037	0.356
CNGA1	cyclic nucleotide gated channel alpha 1	0.037	0.474
GLT8D2	glycosyltransferase 8 domain containing 2	0.037	0.499
STX3	syntaxin 3	0.037	0.486
TEX101	testis expressed 101	0.037	0.379
ATN1	atrophin 1	0.037	0.429
ACAT1	acetyl-Coenzyme A acetyltransferase 1	0.037	0.578
TIAM2	T-cell lymphoma invasion and metastasis 2	0.037	0.458
C7orf16	chromosome 7 open reading frame 16	0.037	0.305
EOMES	eomesodermin homolog (Xenopus laevis)	0.037	1.145
SNX15	sorting nexin 15	0.037	1.182
GLRX3	glutaredoxin 3	0.037	0.488
MEIS1	Meis homeobox 1	0.037	0.357
MED30	mediator complex subunit 30	0.037	0.305
NF2	neurofibromin 2 (merlin)	0.037	0.584
MICA	MHC class I polypeptide-related sequence A	0.037	0.533
C4orf12	chromosome 4 open reading frame 12	0.037	0.617
UGT1A8	UDP glucuronosyltransferase 1 family, polypeptide A3; UDP glucuronosyltransferase 1 family, polypeptide A5; UDP glucuronosyltransferase 1 family, polypeptide A4; UDP glucuronosyltransferase 1 family, polypeptide A7; UDP glucuronosyltransferase 1 family, p	0.037	0.544
FCRL2	Fc receptor-like 2	0.037	0.346
C12orf66	chromosome 12 open reading frame 66	0.037	0.310
OR2S2	olfactory receptor, family 2, subfamily S, member 2	0.037	0.541
CDK10	cyclin-dependent kinase 10	0.037	0.484
FAM190A	KIAA1680 protein	0.037	0.641
OGT	O-linked N-acetylglucosamine (GlcNAc) transferase (UDP-N-acetylglucosamine:polypeptide-N-acetylglucosaminyl transferase)	0.037	0.445
GSDMB	gasdermin B	0.037	2.131
ZDHHC3	zinc finger, DHHC-type containing 3	0.037	0.624
TXLNA	taxilin alpha	0.037	1.219
MVK	mevalonate kinase	0.037	0.699
LPIN3	lipin 3	0.037	0.577
KCTD3	potassium channel tetramerisation domain containing 3	0.037	0.333
ECH1	enoyl Coenzyme A hydratase 1, peroxisomal	0.037	0.571

RAPGEF1	Rap guanine nucleotide exchange factor (GEF) 1	0.037	1.975
GLDN	gliomedin	0.037	0.366
GPR65	G protein-coupled receptor 65	0.037	0.350
CCBE1	collagen and calcium binding EGF domains 1	0.037	0.345
PLEKHA6	pleckstrin homology domain containing, family A member 6	0.037	0.475
KCNN1	potassium intermediate/small conductance calcium-activated channel, subfamily N, member 1	0.037	0.543
RBMY2FP	RNA binding motif protein, Y-linked, family 2, member F pseudogene	0.037	0.467
DUSP26	dual specificity phosphatase 26 (putative)	0.037	0.980
MBD5	methyl-CpG binding domain protein 5	0.037	0.347
ATP6V0D1	ATPase, H+ transporting, lysosomal 38kDa, V0 subunit d1	0.037	1.050
RPTOR	regulatory associated protein of MTOR, complex 1	0.037	0.859
C4orf27	chromosome 4 open reading frame 27	0.037	0.552
POM121L8P	POM121 membrane glycoprotein-like 8 (rat) pseudogene	0.037	1.480
PHLDB2	pleckstrin homology-like domain, family B, member 2; phosphatidylinositol-specific phospholipase C, X domain containing 2	0.037	1.044
TMEM171	transmembrane protein 171	0.037	0.541
FBXO9	F-box protein 9	0.037	0.388
IGLL3	immunoglobulin lambda-like polypeptide 3	0.037	0.673
AQP5	aquaporin 5	0.037	0.316
MXRA8	matrix-remodelling associated 8	0.037	0.894
PTPRE	protein tyrosine phosphatase, receptor type, E	0.037	1.522
NAPA	N-ethylmaleimide-sensitive factor attachment protein, alpha	0.037	1.370
SLC12A8	solute carrier family 12 (potassium/chloride transporters), member 8	0.037	0.554
JAM2	junctional adhesion molecule 2	0.037	0.977
NEURL1B	neuralized homolog 1B (Drosophila)	0.037	0.311
SEC1	secretory blood group 1	0.037	0.657
SH3D19	SH3 domain containing 19	0.037	0.311
GRB10	growth factor receptor-bound protein 10	0.037	0.914
PAQR7	progestin and adipoQ receptor family member VII	0.038	0.970
HRCT1	histidine rich carboxyl terminus 1	0.038	0.313
GALNT10	UDP-N-acetyl-alpha-D-galactosamine:polypeptide N-acetylgalactosaminyltransferase 10 (GalNAc-T10)	0.038	0.698
LOC349408	hypothetical protein LOC349408	0.038	1.102
AMBRA1	autophagy/beclin-1 regulator 1	0.038	0.553
ZNF362	zinc finger protein 362	0.038	1.423
SLC31A1	solute carrier family 31 (copper transporters), member 1	0.038	0.482
FBXO18	F-box protein, helicase, 18	0.038	0.432
FLJ40504	hypothetical protein FLJ40504	0.038	0.364
LOC100133469	hypothetical LOC100133469	0.038	0.405
SCGB2A1	secretoglobin, family 2A, member 1	0.038	0.885
TBC1D7	TBC1 domain family, member 7	0.038	0.341
TCEAL1	transcription elongation factor A (SII)-like 1	0.038	0.486
NLRP2	NLR family, pyrin domain containing 2	0.038	0.858
LARP1	La ribonucleoprotein domain family, member 1	0.038	0.575
NACAD	NAC alpha domain containing	0.038	0.635
OR4K15	olfactory receptor, family 4, subfamily K, member 15	0.038	0.356
RAB11FIP3	RAB11 family interacting protein 3 (class II)	0.038	0.309
SERPINB9	serpin peptidase inhibitor, clade B (ovalbumin), member 9	0.038	1.280
HABP2	hyaluronan binding protein 2	0.038	0.717
ACTL6B	actin-like 6B	0.038	0.378

KRTAP5-7	keratin associated protein 5-7	0.038	0.361
LMNB1	lamin B1	0.038	0.303
KRTAP10-6	keratin associated protein 10-6	0.038	0.516
NCRNA00200	chromosome 10 open reading frame 139	0.038	0.435
C18orf19	chromosome 18 open reading frame 19	0.038	0.330
BCR	breakpoint cluster region	0.038	1.238
RASSF2	Ras association (RalGDS/AF-6) domain family member 2	0.038	0.887
CYP2A7	cytochrome P450, family 2, subfamily A, polypeptide 7	0.038	1.964
FYB	FYN binding protein (FYB-120/130)	0.038	0.350
TPD52L2	tumor protein D52-like 2	0.038	0.464
TPM4	tropomyosin 4	0.038	0.637
HIST2H2BE	histone cluster 2, H2be	0.038	0.478
NACC1	nucleus accumbens associated 1, BEN and BTB (POZ) domain containing	0.038	0.434
PDIA5	protein disulfide isomerase family A, member 5	0.038	0.708
MYL2	myosin, light chain 2, regulatory, cardiac, slow	0.038	0.545
FAM27L	family with sequence similarity 27-like	0.038	0.638
FKBP4	FK506 binding protein 4, 59kDa	0.038	0.359
ATG10	ATG10 autophagy related 10 homolog (S. cerevisiae)	0.038	0.584
UBAP2L	ubiquitin associated protein 2-like	0.038	0.388
SOX4	SRY (sex determining region Y)-box 4	0.038	0.405
ARL9	ADP-ribosylation factor-like 9	0.038	0.404
LIMK2	LIM domain kinase 2	0.038	0.357
PPP1R9B	protein phosphatase 1, regulatory (inhibitor) subunit 9B	0.038	0.336
APBA2	amyloid beta (A4) precursor protein-binding, family A, member 2	0.038	0.305
ACAT2	acetyl-Coenzyme A acetyltransferase 2	0.038	0.521
DCUN1D1	DCN1, defective in cullin neddylation 1, domain containing 1 (S. cerevisiae)	0.038	0.719
NCAM2	neural cell adhesion molecule 2	0.038	0.375
GCAT	glycine C-acetyltransferase (2-amino-3-ketobutyrate coenzyme A ligase)	0.038	0.304
GPR155	G protein-coupled receptor 155	0.038	0.574
LAMB2	laminin, beta 2 (laminin S)	0.038	0.453
SPAG11B	sperm associated antigen 11A; sperm associated antigen 11B	0.038	0.531
CD300LG	CD300 molecule-like family member g	0.039	0.696
UBE2L6	ubiquitin-conjugating enzyme E2L 6	0.039	0.609
C15orf26	chromosome 15 open reading frame 26	0.039	0.458
DTX4	deltex homolog 4 (Drosophila)	0.039	0.338
SLC7A8	solute carrier family 7 (cationic amino acid transporter, y+ system), member 8	0.039	0.738
PUS1	pseudouridylate synthase 1	0.039	0.725
CHRDL2	chordin-like 2	0.039	0.309
DLG5	discs, large homolog 5 (Drosophila)	0.039	0.531
CDSN	corneodesmosin	0.039	0.401
DLG5	discs, large homolog 5 (Drosophila)	0.039	0.696
RNF215	ring finger protein 215	0.039	0.310
OR2L13	olfactory receptor, family 2, subfamily L, member 13	0.039	0.476
SMAD1	SMAD family member 1	0.039	0.820
FLNC	filamin C, gamma (actin binding protein 280)	0.039	0.377
SOD2	superoxide dismutase 2, mitochondrial	0.039	0.583
CYP4A22	cytochrome P450, family 4, subfamily A, polypeptide 22	0.039	0.389
ZNF628	zinc finger protein 628	0.039	0.578
GLCCI1	glucocorticoid induced transcript 1	0.039	0.312
PSME4	proteasome (prosome, macropain) activator subunit 4	0.039	0.975

HKDC1	hexokinase domain containing 1	0.039	0.621
RIPPLY2	chromosome 6 open reading frame 59; ripply2 homolog (zebrafish)	0.039	0.608
C15orf26	chromosome 15 open reading frame 26	0.039	0.572
EFHD2	EF-hand domain family, member D2	0.039	1.115
MESDC1	mesoderm development candidate 1	0.039	0.989
ITGAL	integrin, alpha L (antigen CD11A (p180), lymphocyte function-associated antigen 1; alpha polypeptide)	0.039	0.436
KIAA1731	KIAA1731	0.039	0.349
GOLGA8D	unknown	0.039	0.390
CD300LD	CD300 molecule-like family member d	0.039	0.438
CXCL17	chemokine (C-X-C motif) ligand 17	0.039	0.385
CD101	immunoglobulin superfamily, member 2	0.039	0.649
LRRC66	leucine rich repeat containing 66	0.039	0.341
ST3GAL1	ST3 beta-galactoside alpha-2,3-sialyltransferase 1	0.039	1.194
RFXAP	regulatory factor X-associated protein	0.039	0.388
C19orf75	hypothetical protein FLJ40235	0.039	0.357
MIA3	melanoma inhibitory activity family, member 3	0.039	0.309
DCAF4	WD repeat domain 21A	0.039	0.765
FAM192A	NEFA-interacting nuclear protein NIP30	0.039	0.723
TGM7	transglutaminase 7	0.039	0.497
LAPTM4A	lysosomal protein transmembrane 4 alpha	0.039	0.491
FNBP4	formin binding protein 4	0.039	0.700
OR56B4	olfactory receptor, family 56, subfamily B, member 4	0.039	0.439
BRUNOL4	bruno-like 4, RNA binding protein (Drosophila)	0.039	0.832
VIPR2	vasoactive intestinal peptide receptor 2	0.039	1.142
PSMF1	proteasome (prosome, macropain) inhibitor subunit 1 (PI31)	0.039	0.790
CD302	CD302 molecule; lymphocyte antigen 75	0.039	0.855
CTHRC1	collagen triple helix repeat containing 1	0.039	0.334
FIP1L1	FIP1 like 1 (S. cerevisiae)	0.039	0.844
C7orf28B	chromosome 7 open reading frame 28A; similar to Chromosome 7 open reading frame 28B; chromosome 7 open reading frame 28B	0.039	0.611
MRPL47	mitochondrial ribosomal protein L47	0.039	0.876
MARCH5	membrane-associated ring finger (C3HC4) 5	0.039	0.408
TACC2	transforming, acidic coiled-coil containing protein 2	0.039	0.399
CD40LG	CD40 ligand	0.039	0.334
THSD1	thrombospondin, type I, domain containing 1	0.039	0.522
VPS8	vacuolar protein sorting 8 homolog (S. cerevisiae)	0.039	0.324
ERH	enhancer of rudimentary homolog (Drosophila)	0.039	0.868
HINT2	histidine triad nucleotide binding protein 2	0.039	0.321
EGFLAM	EGF-like, fibronectin type III and laminin G domains	0.039	0.431
ANKRD10	ankyrin repeat domain 10	0.039	0.321
LSG1	large subunit GTPase 1 homolog (S. cerevisiae)	0.039	0.307
ELOF1	elongation factor 1 homolog (S. cerevisiae)	0.039	0.392
BCLAF1	similar to Bcl-2-associated transcription factor 1 (Btf); BCL2-associated transcription factor 1	0.039	0.395
C8orf40	chromosome 8 open reading frame 40	0.040	0.670
ASPG	asparaginase homolog (S. cerevisiae)	0.040	0.469
IFNAR2	interferon (alpha, beta and omega) receptor 2	0.040	0.396
HSBP1	heat shock factor binding protein 1	0.040	1.379
C11orf86	chromosome 11 open reading frame 86	0.040	0.828
PTK2	PTK2 protein tyrosine kinase 2	0.040	0.513

STRC	stereocilin; stereocilin pseudogene	0.040	0.516
MIR1284	microRNA 1284	0.040	1.002
CAPN5	calpain 5	0.040	0.348
FOXD1	forkhead box D1	0.040	0.746
TBC1D16	TBC1 domain family, member 16	0.040	0.479
NUP133	nucleoporin 133kDa	0.040	0.412
RCOR3	REST corepressor 3	0.040	0.364
CDAN1	congenital dyserythropoietic anemia, type I	0.040	0.332
RERE	arginine-glutamic acid dipeptide (RE) repeats	0.040	0.770
CYP19A1	cytochrome P450, family 19, subfamily A, polypeptide 1	0.040	0.691
SH3GL2	SH3-domain GRB2-like 2	0.040	0.390
ENPP6	ectonucleotide pyrophosphatase/phosphodiesterase 6	0.040	0.815
NUP205	nucleoporin 205kDa	0.040	0.582
CTNND2	catenin (cadherin-associated protein), delta 2 (neural plakophilin-related arm-repeat protein)	0.040	0.410
LOC284805	unknown	0.040	0.523
HMOX1	heme oxygenase (decycling) 1	0.040	1.221
PIK3R6	phosphoinositide-3-kinase, regulatory subunit 6	0.040	0.346
CAMKK2	calcium/calmodulin-dependent protein kinase kinase 2, beta	0.040	1.031
EFHC1	EF-hand domain (C-terminal) containing 1	0.040	0.390
SDF2	stromal cell-derived factor 2	0.040	1.879
SERPINE2	serpin peptidase inhibitor, clade E (nexin, plasminogen activator inhibitor type 1), member 2	0.040	0.573
BTBD16	BTB (POZ) domain containing 16	0.040	0.544
HIST1H3J	histone cluster 1, H3j; histone cluster 1, H3i; histone cluster 1, H3h; histone cluster 1, H3g; histone cluster 1, H3f; histone cluster 1, H3e; histone cluster 1, H3d; histone cluster 1, H3c; histone cluster 1, H3b; histone cluster 1, H3a; histone cluster	0.040	0.396
LRTOMT	leucine rich transmembrane and 0-methyltransferase domain containing	0.040	1.019
ZNF670	zinc finger protein 670	0.040	0.556
NCRNA00094	non-protein coding RNA 94	0.040	0.547
TTR	transthyretin	0.040	0.433
ADCYAP1R1	adenylate cyclase activating polypeptide 1 (pituitary) receptor type I	0.040	0.537
PAQR5	progestin and adipoQ receptor family member V	0.040	0.653
UFD1L	ubiquitin fusion degradation 1 like (yeast)	0.040	0.480
PI4K2B	phosphatidylinositol 4-kinase type 2 beta	0.040	0.625
CUX1	cut-like homeobox 1	0.040	0.734
INPP5K	inositol polyphosphate-5-phosphatase K	0.040	0.373
CCL17	chemokine (C-C motif) ligand 17	0.040	0.362
PPIG	peptidylprolyl isomerase G (cyclophilin G)	0.040	0.489
ARHGAP30	Rho GTPase activating protein 30	0.040	0.404
NFKBIE	nuclear factor of kappa light polypeptide gene enhancer in B-cells inhibitor, epsilon	0.040	0.374
C2orf77	chromosome 2 open reading frame 77	0.040	0.337
E2F1	E2F transcription factor 1	0.040	0.561
MIR548H2	unknown	0.040	0.850
RBM19	RNA binding motif protein 19	0.040	0.464
ZNF682	zinc finger protein 682	0.040	0.517
FRY	furry homolog (Drosophila)	0.040	0.328
DHX33	DEAH (Asp-Glu-Ala-His) box polypeptide 33	0.041	0.787
C11orf60	chromosome 11 open reading frame 60	0.041	0.313
FAM58A	family with sequence similarity 58, member A; hypothetical gene supported by NM_152274	0.041	0.970

RNF216	ring finger protein 216	0.041	1.351
GRAP2	GRB2-related adaptor protein 2	0.041	0.327
SAP130	Sin3A-associated protein, 130kDa	0.041	0.302
FAM120B	family with sequence similarity 120B	0.041	1.825
RORC	RAR-related orphan receptor C	0.041	0.438
NETO2	neuropilin (NRP) and tolloid (TLL)-like 2	0.041	0.378
C19orf40	chromosome 19 open reading frame 40	0.041	0.412
TOMM40	translocase of outer mitochondrial membrane 40 homolog (yeast)	0.041	0.545
CATSPER2	cation channel, sperm associated 2	0.041	0.403
SYT8	synaptotagmin VIII	0.041	0.603
CBFB	core-binding factor, beta subunit	0.041	0.465
CLDN12	claudin 12	0.042	0.600
ESCO1	establishment of cohesion 1 homolog 1 (S. cerevisiae)	0.042	0.415
NFYB	nuclear transcription factor Y, beta	0.042	0.410
IL3RA	interleukin 3 receptor, alpha (low affinity)	0.042	0.981
GTSF1	gametocyte specific factor 1	0.042	1.076
RPS3A	ribosomal protein S3A pseudogene 5; ribosomal protein S3a pseudogene 47; ribosomal protein S3a pseudogene 49; ribosomal protein S3A; hypothetical LOC100131699; hypothetical LOC100130107	0.042	0.464
DDX47	DEAD (Asp-Glu-Ala-Asp) box polypeptide 47	0.042	1.792
SP6	Sp6 transcription factor	0.042	0.730
HSD17B3	hydroxysteroid (17-beta) dehydrogenase 3	0.042	1.216
COPS7A	COP9 constitutive photomorphogenic homolog subunit 7A (Arabidopsis)	0.042	0.431
NEDD8	neural precursor cell expressed, developmentally down-regulated 8; similar to neural precursor cell expressed, developmentally down-regulated gene 8	0.042	0.846
CACNA1C	hypothetical protein LOC100131098; calcium channel, voltage-dependent, L type, alpha 1C subunit	0.042	0.351
SH3D19	SH3 domain containing 19	0.042	0.864
GGTA1	glycoprotein, alpha-galactosyltransferase 1	0.042	0.397
SEPT3	septin 3	0.042	0.770
ACSM4	acyl-CoA synthetase medium-chain family member 4	0.042	0.385
WISP2	WNT1 inducible signaling pathway protein 2	0.043	0.415
TRIM3	tripartite motif-containing 3	0.043	1.259
DAZAP2	DAZ associated protein 2	0.043	0.887
NLN	neurolysin (metallopeptidase M3 family)	0.043	0.342
NEDD4L	neural precursor cell expressed, developmentally down-regulated 4-like	0.043	0.426
RASSF4	Ras association (RalGDS/AF-6) domain family member 4	0.043	0.734
ZBTB8B	zinc finger and BTB domain containing 8B	0.043	0.648
HNRNPA3P1	heterogeneous nuclear ribonucleoprotein A3 pseudogene 1	0.043	0.391
ZNF829	zinc finger protein 829	0.043	0.345
CRKL	v-crk sarcoma virus CT10 oncogene homolog (avian)-like	0.043	1.134
SMU1	smu-1 suppressor of mec-8 and unc-52 homolog (C. elegans)	0.044	0.444
CTAGE4	CTAGE family, member 5 pseudogene; CTAGE family member; CTAGE family, member 4; CTAGE family, member 5	0.044	0.387
PNLIPRP1	pancreatic lipase-related protein 1	0.044	0.329
KRT78	keratin 78	0.044	1.091
CENPJ	centromere protein J	0.044	0.881
PDLIM2	PDZ and LIM domain 2 (mystique)	0.044	2.236
IL1B	interleukin 1, beta	0.044	0.436
PEAR1	platelet endothelial aggregation receptor 1	0.044	0.379
PMAIP1	phorbol-12-myristate-13-acetate-induced protein 1	0.044	0.469

MCM6	minichromosome maintenance complex component 6	0.044	0.467
HHLA3	HERV-H LTR-associating 3	0.044	1.873
MFNG	MFNG O-fucosylpeptide 3-beta-N-acetylglucosaminyltransferase	0.044	0.345
PRPF4B	similar to hCG1820375; PRP4 pre-mRNA processing factor 4 homolog B (yeast)	0.044	0.390
GLDC	glycine dehydrogenase (decarboxylating)	0.044	1.579
NTRK2	neurotrophic tyrosine kinase, receptor, type 2	0.044	1.115
LOC100128640	hypothetical protein LOC100128640	0.044	0.380
HIST2H3C	histone cluster 1, H3j; histone cluster 1, H3i; histone cluster 1, H3h; histone cluster 1, H3g; histone cluster 1, H3f; histone cluster 1, H3e; histone cluster 1, H3d; histone cluster 1, H3c; histone cluster 1, H3b; histone cluster 1, H3a; histone cluster	0.044	0.343
CDH8	cadherin 8, type 2	0.044	0.934
MTUS1	mitochondrial tumor suppressor 1	0.044	0.493
CYP4F3	cytochrome P450, family 4, subfamily F, polypeptide 3	0.044	0.327
FBXW7	F-box and WD repeat domain containing 7	0.044	0.634
PEX6	peroxisomal biogenesis factor 6	0.045	0.511
ZNF790	zinc finger protein 790	0.045	2.799
CCDC7	coiled-coil domain containing 7	0.045	0.657
RFX5	regulatory factor X, 5 (influences HLA class II expression)	0.045	0.422
ZNF346	zinc finger protein 346	0.045	0.516
WDR20	WD repeat domain 20	0.045	0.470
CPEB2	cytoplasmic polyadenylation element binding protein 2	0.045	0.383
RBMS1	RNA binding motif, single stranded interacting protein 1	0.045	0.314
MRS2	MRS2 magnesium homeostasis factor homolog (S. cerevisiae)	0.045	0.304
ARHGEF19	Rho guanine nucleotide exchange factor (GEF) 19	0.045	0.396
TTTY18	testis-specific transcript, Y-linked 18	0.045	0.503
AGXT2	alanine-glyoxylate aminotransferase 2	0.045	0.416
VN1R4	similar to Vomeronasal type-1 receptor 4; vomeronasal 1 receptor 4	0.045	0.414
PTP4A1	protein tyrosine phosphatase type IVA, member 1	0.045	0.379
ZNF32	zinc finger protein 32	0.045	0.472
OR6F1	olfactory receptor, family 6, subfamily F, member 1	0.045	0.330
HIGD1B	HIG1 hypoxia inducible domain family, member 1B	0.045	0.757
PLOD2	procollagen-lysine, 2-oxoglutarate 5-dioxygenase 2	0.045	0.353
NCRNA00173	hypothetical protein LOC100287569	0.045	0.718
FSCB	fibrous sheath CABYR binding protein	0.045	0.527
POFUT1	protein O-fucosyltransferase 1	0.045	0.316
DLL4	delta-like 4 (Drosophila)	0.045	0.540
CRHR2	corticotropin releasing hormone receptor 2	0.045	0.438
SPHKAP	SPHK1 interactor, AKAP domain containing	0.045	0.872
NOL12	nucleolar protein 12	0.045	0.561
BAHCC1	BAH domain and coiled-coil containing 1	0.046	0.640
SGK196	protein kinase-like protein SgK196	0.046	0.391
STARD8	StAR-related lipid transfer (START) domain containing 8	0.046	0.725
IBTK	inhibitor of Bruton agammaglobulinemia tyrosine kinase	0.046	0.427
PION	pigeon homolog (Drosophila)	0.046	0.325
SLC25A28	solute carrier family 25, member 28	0.046	0.715
EIF4E1B	eukaryotic translation initiation factor 4E family member 1B	0.046	1.488
CILP	cartilage intermediate layer protein, nucleotide pyrophosphohydrolase	0.046	0.316
C11orf80	chromosome 11 open reading frame 80	0.046	0.779
CHST9	carbohydrate (N-acetylgalactosamine 4-0) sulfotransferase 9	0.046	0.424
DGKK	diacylglycerol kinase, kappa	0.046	0.335
ATP2B2	ATPase, Ca++ transporting, plasma membrane 2	0.046	0.623

C20orf123	chromosome 20 open reading frame 123	0.046	0.317
BOK	BCL2-related ovarian killer	0.046	0.396
MOSPD3	motile sperm domain containing 3	0.046	0.613
FAM156B	family with sequence similarity 156, member A; family with sequence similarity 156, member B	0.046	0.519
NBPF1	neuroblastoma breakpoint family, member 15; neuroblastoma breakpoint family, member 14; neuroblastoma breakpoint family, member 9; neuroblastoma breakpoint family, member 11; neuroblastoma breakpoint family, member 11-like; neuroblastoma breakpoint family	0.046	0.378
SLC38A7	solute carrier family 38, member 7	0.046	0.409
LPPR5	phosphatidic acid phosphatase type 2	0.046	0.362
MAD2L2	MAD2 mitotic arrest deficient-like 2 (yeast)	0.046	0.394
ACAP1	ArfGAP with coiled-coil, ankyrin repeat and PH domains 1	0.046	0.375
FBXO25	F-box protein 25	0.046	0.509
C18orf45	chromosome 18 open reading frame 45	0.046	0.382
UBXN6	UBX domain protein 6	0.046	1.615
PRHOXNB	parahox cluster neighbor	0.046	0.747
PAQR8	progestin and adipoQ receptor family member VIII	0.046	0.523
RAVER1	ribonucleoprotein, PTB-binding 1	0.046	0.364
ZNF324B	zinc finger protein 324B	0.046	0.519
MKI67IP	MKI67 (FHA domain) interacting nucleolar phosphoprotein	0.046	0.364
MSX2P1	msh homeobox 2 pseudogene 1	0.046	0.577
IRX2	iroquois homeobox 2	0.047	0.339
TSPAN16	tetraspanin 16	0.047	1.899
NTM	neurotrimin	0.047	0.734
MARCH9	membrane-associated ring finger (C3HC4) 9	0.047	0.301
TRPV2	transient receptor potential cation channel, subfamily V, member 2	0.047	0.818
RNFT2	ring finger protein, transmembrane 2	0.047	1.430
NCRNA00174	non-protein coding RNA 174	0.047	0.311
C12orf11	chromosome 12 open reading frame 11	0.047	2.201
TULP2	tubby like protein 2	0.047	0.570
MERTK	c-mer proto-oncogene tyrosine kinase	0.047	0.349
PEX10	peroxisomal biogenesis factor 10	0.047	0.892
RAB39	RAB39, member RAS oncogene family	0.047	0.786
CSMD2	CUB and Sushi multiple domains 2	0.047	0.407
ANG	angiogenin, ribonuclease, RNase A family, 5	0.047	0.340
IGBP1	chromosome 14 open reading frame 19; immunoglobulin (CD79A) binding protein 1	0.047	0.478
ELAC1	elaC homolog 1 (E. coli)	0.047	0.388
SOST	sclerosteosis	0.047	0.388
VAMP3	vesicle-associated membrane protein 3 (cellubrevin)	0.047	1.486
C1orf210	chromosome 1 open reading frame 210	0.047	1.243
C8orf38	chromosome 8 open reading frame 38	0.047	0.905
PLAT	plasminogen activator, tissue	0.047	0.653
CCL24	chemokine (C-C motif) ligand 24	0.047	0.730
C1QTNF6	C1q and tumor necrosis factor related protein 6	0.047	0.637
DTNB	dystrobrevin, beta	0.047	0.452
PPP1R14A	protein phosphatase 1, regulatory (inhibitor) subunit 14A	0.047	0.749
CCDC134	coiled-coil domain containing 134	0.047	0.349
WWC1	WW and C2 domain containing 1	0.047	0.623
ARHGEF10	Rho guanine nucleotide exchange factor (GEF) 10	0.047	0.549

HNRNPD	heterogeneous nuclear ribonucleoprotein D (AU-rich element RNA binding protein 1, 37kDa)	0.048	0.322
LRRK2	leucine-rich repeat kinase 2	0.048	0.744
CPNE5	copine V	0.048	0.528
OPRD1	opioid receptor, delta 1	0.048	1.323
TRIM64	tripartite motif-containing 64	0.048	0.324
EYA2	eyes absent homolog 2 (Drosophila)	0.048	0.392
PDGFD	platelet derived growth factor D	0.048	0.901
OR13C9	olfactory receptor, family 13, subfamily C, member 9	0.048	0.738
ADPGK	ADP-dependent glucokinase	0.048	0.851
GOLGA6B	golgi autoantigen, golgin subfamily a, 6B	0.048	0.552
ZDHHC19	zinc finger, DHHC-type containing 19	0.048	0.509
NACC2	NACC family member 2, BEN and BTB (POZ) domain containing	0.048	0.384
INTS3	integrator complex subunit 3	0.048	0.699
KCNE1	potassium voltage-gated channel, Isk-related family, member 1	0.048	0.523
C10orf71	chromosome 10 open reading frame 71; similar to hCG1996658	0.048	0.448
ZNF2	zinc finger protein 2	0.048	0.379
ARHGAP6	Rho GTPase activating protein 6	0.048	0.308
STAB2	stabilin 2	0.048	0.630
SVIL	supervillin	0.048	0.441
VEZF1	vascular endothelial zinc finger 1	0.048	0.460
ZNF706	zinc finger protein 706	0.048	0.962
CSRNP2	cysteine-serine-rich nuclear protein 2	0.048	0.532
GADD45A	growth arrest and DNA-damage-inducible, alpha	0.048	0.323
EXT2	exostoses (multiple) 2	0.048	0.528
XKRY2	XK, Kell blood group complex subunit-related, Y-linked; XK, Kell blood group complex subunit-related, Y-linked 2	0.048	0.413
DPF3	D4, zinc and double PHD fingers, family 3	0.048	0.320
ILDR2	immunoglobulin-like domain containing receptor 2	0.048	0.405
TESK1	testis-specific kinase 1	0.048	0.390
PAX3	paired box 3	0.048	0.754
IQCH	IQ motif containing H	0.048	0.581
EEA1	early endosome antigen 1	0.048	1.921
TOP1MT	topoisomerase (DNA) I, mitochondrial	0.048	0.802
NSF	N-ethylmaleimide-sensitive factor	0.048	3.373
HSPA12B	heat shock 70kD protein 12B	0.048	0.408
USH1C	Usher syndrome 1C (autosomal recessive, severe)	0.049	0.358
FRY	furry homolog (Drosophila)	0.049	0.605
VCL	vinculin	0.049	1.094
CEACAM8	carcinoembryonic antigen-related cell adhesion molecule 8	0.049	0.396
KBTBD11	kelch repeat and BTB (POZ) domain containing 11	0.049	0.394
METTL1	methyltransferase like 1	0.049	0.338
CKMT1A	creatine kinase, mitochondrial 1A; creatine kinase, mitochondrial 1B	0.049	0.446
SVEP1	sushi, von Willebrand factor type A, EGF and pentraxin domain containing 1	0.049	0.541
FAT3	FAT tumor suppressor homolog 3 (Drosophila)	0.049	0.437
CAMK1G	calcium/calmodulin-dependent protein kinase IG	0.049	0.384
NAV2	neuron navigator 2	0.049	0.424
IDI1	isopentenyl-diphosphate delta isomerase 1	0.049	2.157
USH1C	Usher syndrome 1C (autosomal recessive, severe)	0.049	1.129
STIM1	stromal interaction molecule 1	0.049	0.562
PSMA8	proteasome (prosome, macropain) subunit, alpha type, 8	0.049	1.334

C19orf69	chromosome 19 open reading frame 69	0.049	0.579
TENC1	tensin like C1 domain containing phosphatase (tensin 2)	0.049	0.348
PLCE1	phospholipase C, epsilon 1	0.049	0.358
OR2T29	olfactory receptor, family 2, subfamily T, member 29	0.049	0.351
VPS24	vacuolar protein sorting 24 homolog (S. cerevisiae); ring finger protein 103	0.049	0.502
DTNB	dystrobrevin, beta	0.049	0.462
EPHA3	EPH receptor A3	0.049	0.340
RIMS3	regulating synaptic membrane exocytosis 3	0.049	0.566
C14orf43	chromosome 14 open reading frame 43	0.049	0.314
GEMIN7	gem (nuclear organelle) associated protein 7	0.049	0.395
ZNF197	zinc finger protein 197	0.049	0.700
OR1C1	olfactory receptor, family 1, subfamily C, member 1	0.049	0.618
GNG5	guanine nucleotide binding protein (G protein), gamma 5	0.049	0.716
MRVI1	murine retrovirus integration site 1 homolog	0.049	0.361
PAQR8	progestin and adipoQ receptor family member VIII	0.049	0.823
RFT1	RFT1 homolog (S. cerevisiae)	0.049	0.487
DKFZp686O24166	hypothetical protein DKFZp686O24166	0.049	0.320
MAST3	microtubule associated serine/threonine kinase 3	0.049	0.580
TEX264	testis expressed 264	0.049	0.449
SNUPN	snurportin 1	0.049	0.739
STYX	serine/threonine/tyrosine interacting protein	0.049	0.389
ANKLE1	ankyrin repeat and LEM domain containing 1	0.049	0.347
CSNK1E	casein kinase 1, epsilon	0.050	0.317
ZNF479	zinc finger protein 479; zinc finger protein 733	0.050	0.679
SRGAP1	SLIT-ROBO Rho GTPase activating protein 1	0.050	0.362
GLIPR2	GLI pathogenesis-related 2	0.050	1.004
SNORA70C	small nucleolar RNA, H/ACA box 70C (retrotransposed); small nucleolar RNA, H/ACA box 70; small nucleolar RNA, H/ACA box 70B (retrotransposed)	0.050	0.421
PTPRR	protein tyrosine phosphatase, receptor type, R	0.050	0.389
LSM1	LSM1 homolog, U6 small nuclear RNA associated (S. cerevisiae)	0.050	0.382
LRFN2	leucine rich repeat and fibronectin type III domain containing 2	0.050	0.320
SPR	sepiapterin reductase (7,8-dihydrobiopterin:NADP+ oxidoreductase)	0.050	1.166
KCNH4	potassium voltage-gated channel, subfamily H (eag-related), member 4	0.050	0.415
YTHDF1	YTH domain family, member 1	0.050	0.386
IL1RAPL2	interleukin 1 receptor accessory protein-like 2	0.050	0.358
FNDC1	fibronectin type III domain containing 1	0.050	0.420
TMCC2	transmembrane and coiled-coil domain family 2	0.050	0.835
TUBB4Q	tubulin, beta polypeptide 4, member Q	0.050	0.584
HRH4	histamine receptor H4	0.050	1.184
LONP1	lon peptidase 1, mitochondrial	0.050	0.389
NCAPG	non-SMC condensin I complex, subunit G	0.050	0.310